Phylogenomic systematics, bioacoustics, and morphology of frogs from Madagascar reveals that background noise drives the evolution of high frequency acoustic signaling

By

Carl Richard Hutter

Submitted to the graduate degree program in Ecology and Evolutionary Biology and the Graduate Faculty of the University of Kansas in partial fulfillment of the requirements for the degree of Doctor of Philosophy.

_____

Co-Chair: Richard Glor

_____

Co-Chair: Rafe Brown

_____

Mark Holder

_____

Paulyn Cartwright

_____

Stuart Macdonald

Date Defended: 30 July 2019

The dissertation committee for Carl Richard Hutter certifies that this is the approved version of the following dissertation:

Phylogenomic systematics, bioacoustics, and morphology of frogs from Madagascar reveals that background noise drives the evolution of high frequency acoustic signaling

_____

Co-Chair: Richard Glor

_____

Co-Chair: Rafe Brown

Date Approved: 30 July 2019

ABSTRACT

Madagascar is considered a globally important biodiversity hotspot, having some of the highest rates of species endemism in the world and has been the focus of substantial effort from researchers to understand the evolution of its distinctive biota. This is especially true for frogs, where the microcontinent hosts an impressively diverse amphibian fauna totaling over 500 species, where a large amount of this diversity has only been described relatively recently. Much of this accelerated taxonomic progress can be attributed to the combination of DNA barcoding and the widespread application of bioacoustics enabling more efficient species identification and characterization of new lineages. The availability of bioacoustic data for the majority of species has revealed the incredible diversity of acoustic signals in Malagasy frogs; despite the incredible acoustic diversity in Madagascar, explanations for the evolution of distinct advertisement calls have been little explored.

Acoustic signaling is important to frogs because it is the primary mechanism of communication and mate selection and therefore it is expected that acoustic communication and factors that drive variation in acoustic signals should be under strong selection. Frogs from the most species-rich genus *Boophis* from the family Mantellidae in Madagascar communicate acoustically during a rainy and short breeding season and aggregate around water bodies in high abundance making *Boophis* an ideal model system to address the evolution of advertisement calls. A potential explanation for signal diversity is the acoustic adaptation hypothesis, which predicts that natural and sexual selection drive optimization of signal transmission and perception across different habitats. In many organisms, the efficiency of acoustic signal transmission can be affected by habitat structure or background noise. One prediction of the

acoustic adaptation hypothesis is that environmental ambient noise, which is the background level of sound in the environment, will drive signal evolution if the noise is sufficiently similar and lessens the receiver's perception of the signal. Because *Boophis* reproduce near water bodies and most often in stream habitats that might be noisy from the sound of rushing water, they present an excellent system to address acoustic interference.

In Chapter 1, I describe a new species of *Boophis* that is morphologically cryptic with its sister species but differs remarkably in advertisement call, which underlines the importance of call variation in the genus. To contribute to the taxonomic progress and integration of bioacoustic data, I describe a new species of *Boophis* by using these multiple lines of evidence and also suggesting future research to understand the evolution of advertisement calls in the genus. I also develop the acoustic analysis pipeline used for acquiring frequency traits from thousands of calls rapidly, where these methods will be used in Chapter 5. In this study, I also suggest that reproductive character displacement could be driving divergence in advertisement calls and that other important factors from the environment could lead to broad patterns in the evolution of advertisement calls.

In Chapter 2, to understand signal evolution across a broad range of taxa, a strongly supported phylogenetic hypothesis is needed and I estimate a new multi-locus phylogeny using Sanger sequencing. The systematics of frogs from the family Mantellidae have had a long and turbulent history where Mantellidae was considered a family relatively recently. In *Boophis* tree frogs, early researchers considered them as belonging to the Asian genus *Rhacophorus* because of their strong similarities and breeding habitat in water bodies. Furthermore, despite the numerous works that contributed to understanding the molecular phylogeny of *Boophis* many aspects of their evolutionary relationships remain insufficiently supported and a complete Sanger

multi-locus phylogeny had not been estimated. For understanding the relationships among *Boophis* frogs, I estimated a multi-locus phylogeny from eight Sanger markers that includes as much diversity as possible. Despite these efforts, I could not adequately support the phylogenetic relationships among Boophis taxa and adding additional Sanger markers would not be likely to resolve these relationships.

In Chapter 3 I aim to expand upon this dataset and develop a new sequencing technology to obtain thousands of markers affordably. The widespread use of high-throughput sequencing technologies to sequence large portions of organisms' genome has led to new and exciting challenges and questions that can be addressed with the massive increase in sequence data these new methods provide. The objective of sequence capture is to sequence genomic regions typically through hybridization-based capture from a previously designed set of known markers and benefits from the potential to acquire markers that are useful at all evolutionary time-scales. Therefore, I developed a sequence capture probe set called FrogCap to sequence ~15,000 genomic markers that can be used across the entire frog radiation. I compare the efficacy of the probe set on six phylogenetic scales and quantify the number of markers sequenced, depth of coverage, missing data, and parsimony informative sites, and I also compared differences between these measures across different types of data. The results from this chapter show that FrogCap is a very promising new sequence capture probe set that can be used across all frogs.

In Chapter 4 I test the effectiveness of FrogCap by addressing the systematics of frogs from the family Mantellidae, by comparing the FrogCap sequence capture results to those from transcriptomes. The phylogeny of Mantellidae remains unresolved and contentious, where the phylogenetic relationships among subfamilies and genera are not well delimited. Prior to this it was thought the different groups in Madagascar were non-monophyletic and were thought to be

from several different families. I address the weak phylogenetic support and also test the FrogCap probe set on Mantellidae frogs, comparing the probe set to transcriptomic sequencing of samples from the same groups. I find that both FrogCap and transcriptomes work similarly well for resolving these difficult and contentious relationships. FrogCap sequence capture also provided several advantages over the transcriptomic data; FrogCap sequences non-protein coding markers from across the genome, such that these other types of markers could be useful by providing sequence data from potentially neutrally evolving genomic regions and also can serve as another line of phylogenetic evidence when compared to other data types. Transcriptomes also provide advantages through a larger amount of sequence data and lesser gene discordance because the transcriptomes are much longer and thus providing more resolution than shorter markers. I find that the FrogCap probe set is an effective tool at disentangling difficult phylogenetic problems, and that transcriptomic sequencing is less effective for phylogenetics.

In Chapter 5, I estimate a new phylogeny for *Boophis* tree frogs using the FrogCap probe set and address whether acoustic interference leads to the evolution of higher frequency advertisement calls in *Boophis* frogs. I integrate an unprecedented dataset incorporating data collected from all previous chapters which includes a massive dataset of 300+ acoustic recordings from nearly every species in the genus, a new *Boophis* time-calibrated phylogeny using a backbone of ~15,000 genomic markers acquired from the sequence capture data combined with the data from Chapter 2 for full species sampling and used soft tissue computed tomography on 28 species to acquire detailed morphological information from the larynges of males. After finding that the sequence capture dataset provides strong statistical support for nearly every node in the tree, I time-calibrate the phylogeny and test the acoustic adaptation hypothesis. I find that *Boophis* tree frogs are evolving higher frequency acoustic signals in loud

stream habitats, which is supported after correcting for body size. These results are further evidenced by laryngeal measurements from the CT Scans, where I find that loud stream frog laryngeal morphology is decoupled from the predicted relationship to body size that is found in quiet stream frogs.

ACKNOWLEDGEMENTS

I would like to thank the Biodiversity Institute (KUBI) and Department of Ecology and Evolutionary Biology (EEB) for providing me with the opportunity and support for my PhD. I would like to thank the Director of the KUBI Dr. Leonard Krishtalka, the previous Chair of EEB Dr. Christopher Haufler and current chair Dr. Maria Orive, the EEB Graduate Coordinator Aagje Ashe, Lori Schlenker, Jamie Keeler, and Emily Emke at the KUBI for their time, patience and assistance. I would also like to thank KU Graduate Studies, National Science Foundation (Graduate Research Fellowship), the American Philosophical Society, and the Society for the Study of Evolution for funding and financial support for this research.

I would especially like to thank my PhD advisors Dr. Richard Glor and Dr. Rafe Brown who have provided an invaluable guidance and support. I would also like to thank my committee members Drs. Paulyn Cartwright, Mark Holder, Stuart Macdonald, and Leo Smith who have provided advice and support. Furthermore, I would also like to thank Dr. John Wiens who without his mentorship during my master's degree at Stony Brook University, my graduate career would have never began. I would like to thank past and present graduate students, investigators, and friends — within and outside of KU — who have assisted and supported me in various ways: Robin Abraham, Alana Alexander, Katie Allen, Kyle Atkins-Weltman, Tashitso Anamza, Matt Buehler, Kevin Chovanec, Kerry Cobb, Bill Duellman, Frank Glaw, Jesse Grismer, Shea Lambert, Mark Herr, Paul Hime, Justin Jacobs, Luke Mahler, Pietro de Mello, Carl Oliveros, Karen Olson, Chan Kin Onn, Mark Scherz, Emma Tuschhoff, Walter Tapondjou, Javier Torres, Scott Travers, Linda Trueb, Miguel Vences, Jeff Weinell, Luke Welton, and Perry Wood Jr. Finally, and most importantly, I would like to thank my wife and best friend Zo Faniry

Andriampenomana for her unwavering love and moral support; she brought happiness and camaraderie when life was challenging.

In the field I would like to thank the following for logistics and field assistance: the Malagasy authorities for approving research permits and the organizations MICET and Centro ValBio for logistics assistance with permits and in the field. I am also grateful to James P. Herrera, Devin Edmonds, John Cadle, and Patricia Wright for their invaluable assistance while in Madagascar; Solo Justin, Ginah Tsiorisoa Andrianasolo, Jary Harinarivo, Ralaivao Jean Fulgence, Emile Rajeriarison, Asa Conover, and Vincente Primmel for their assistance in the field.

CONTENTS

Chapter 2. Molecular phylogeny and diversification of Malagasy bright-eyed tree frogs (Mantellidae: *Boophis*)

INTRODUCTION

Madagascar is considered a globally important biodiversity hotspot, having some of the highest rates of species endemism in the world (Myers *et al.* 2000), and has been the focus of substantial effort from researchers to understand the evolution of its distinctive biota. Madagascar has been an important biome in many different organisms for the study of species richness patterns (Wollenberg *et al.* 2008; Rakotoarinivo *et al.* 2013; Brown *et al.* 2014), adaptive radiation (Moore *et al.* 2012; Reddy *et al.* 2012), biogeography (Yoder *et al.* 2006; Pearson & Raxworthy 2009; Wilmé *et al.* 2006), and understanding diversification (Raxworthy *et al.* 2008; Vences *et al.* 2009; Blair *et al.* 2013).

This is especially true for frogs, where the microcontinent hosts an impressively diverse amphibian fauna, composed of up to five independent endemic radiations that contains 363 currently described frogs (Perl *et al.* 2014; AmphibiaWeb 2019). A large amount of this diversity has only been described relatively recently, and greater than 241 lineages have provisionally been identified as candidate species and require formal taxonomic description (Vieites *et al.* 2009; Perl *et al.* 2014). Much of this accelerated taxonomic progress can be attributed to the combination of DNA barcoding and the widespread application of bioacoustics enabling more efficient species identification and characterization of new lineages (e.g. Andreone 1993, 1994, 1996; Glaw & Thiesmeier 1993; Glaw *et al.* 2001; Glaw & Vences 2002; Vences & Glaw 2002; Köhler *et al.* 2007, 2008; Wollenberg *et al.* 2008; Glaw *et al.* 2010; Vences *et al.* 2010; Penny *et al.* 2014; Lambert *et al.* 2016; Rakotoarison *et al.* 2017). The availability of bioacoustic data for the majority of species has revealed the incredible diversity of acoustic signals in Malagasy frogs and presents an exciting opportunity to understand the evolution of acoustic signals and to supplement these basic data with more substantial sampling.

Despite the incredible acoustic diversity in Madagascar, explanations for the evolution of distinct advertisement calls have been little explored. Acoustic signaling is important to frogs because it is the primary mechanism of communication and mate selection (Morton 1975; Wilkins *et al.* 2013), and therefore it is expected that acoustic communication and factors that drive variation in acoustic signals should be under strong selection (Morton 1975; Marten & Marler 1977; Wiley & Richards 1978; Endler 1992; Ey & Fischer 2009). In particular, frogs from the most species-rich genus *Boophis* from the family Mantellidae in Madagascar communicate acoustically during a rainy and short breeding season and aggregate around water bodies in high abundance (Glaw & Vences 2007), making *Boophis* an ideal model system to address the evolution of advertisement calls. Furthermore, *Boophis* have a large variety of different sounding advertisement calls, which have often been used to distinguish new species (e.g. Köhler *et al.* 2007, 2008; Wollenberg *et al.* 2008; Glaw *et al.* 2010; Vences *et al.* 2010; Penny *et al.* 2014). Despite this recent increase in taxonomic progress, a robustly-sampled and multi-locus nuclear phylogeny is not yet available for this genus, hindering many potential comparative analyses.

The systematics of frogs from the family Mantellidae have had a long and turbulent history. Mantellidae was considered a family relatively recently, with some of the first molecular systematic studies concluding that mantellid frogs are a well-supported monophyletic group (Vences *et al.* 2000; Glaw & Vences 2006). Prior to this it was thought that many different groups in Madagascar were non-monophyletic and were considered as part of several different families (e.g. Ranidae, Tomopterna, Rhacophoridae). In *Boophis* tree frogs, our focal clade, early researchers considered them as belonging to the Asian genus *Rhacophorus* because of their strong similarities and breeding habitat in water bodies (Blommers-Schlösser 1979).

Furthermore, despite the numerous works that contributed to understanding the molecular phylogeny of *Boophis* (e.g., Richards *et al.* 2000; Vences *et al.* 2002; Glaw & Vences 2006; Frost *et al.* 2006; Kurabayashi *et al.* 2008; Wollenberg *et al.* 2008, 2011; Pyron & Wiens 2011), many aspects of their evolutionary relationships remain insufficiently supported and a complete Sanger multi-locus phylogeny has not been estimated. For understanding the relationships among *Boophis* frogs, a multi-locus phylogeny should first be estimated that includes as much diversity as possible, and if these data cannot provide strong statistical support for phylogenetic relationships, an alternative approach such as using high-throughput sequencing would be necessary.

The widespread use of high-throughput sequencing technologies to sequence large portions of organisms' genome has led to new and exciting challenges and questions that can be addressed with the massive increase in sequence data these new methods provide. The objective of sequence capture is to sequence genomic regions typically through hybridization-based capture from a previously designed set of known markers (e.g. Faircloth *et al.* 2012; Hancock-Hanser *et al.* 2013; Jones & Good 2016). Sequence capture benefits from the potential to acquire markers that are useful at all evolutionary time-scales. Disadvantages of sequence capture are that target markers need to be known before probe design which requires genomes and/or transcriptomes of a related species. Phylogenomics from sequence capture have helped resolve numerous uncertain relationships at very deep to shallow time scales (Johnson *et al.* 2013; Prum *et al.* 2015; Gentekaki *et al.* 2017). Therefore, sequence capture is a suitable methodology to addressing difficult phylogenetic relationships that are difficult or impossible to provide statistical confidence using few Sanger markers.

A potential explanation for signal diversity is the acoustic adaptation hypothesis, which predicts that natural and sexual selection drive optimization of signal transmission and perception across different habitats (Morton 1975; Marten & Marler 1977; Wiley & Richards 1978; Endler 1992; Ryan & Kime 2003; Ey & Fischer 2009). In many organisms, the efficiency of acoustic signal transmission can be affected by habitat structure or background noise (Morton 1975; Bee & Swanson 2007; Boeckle *et al.* 2009; Erdtmann & Lima 2013; Cunnington & Fahrig 2010; Goutte *et al.* 2016). One prediction of the acoustic adaptation hypothesis is that environmental ambient noise, which is the background level of sound in the environment, will drive signal evolution if the noise is sufficiently similar and lessens the receiver's perception of the signal (Fig. 1; Boonman & Kurniati 2011; Cardoso & Atwell 2011; Both & Grant 2012; Goodwin & Podos 2013). Because *Boophis* reproduce near water bodies and most often in stream habitats that might be noisy from the sound of rushing water, they present an excellent system to address acoustic interference.

Despite the potential significance of the acoustic adaptation hypothesis, it has proven challenging to test because of potentially confounded variables, such as call plasticity due to temperature and body size, and sampling deficiencies (e.g. Gerhardt 1978; Gayou 1984; Narins *et al.* 2006; Gingras *et al.* 2013; Rohr *et al.* 2016). For example, body size in frogs is predicted to have a negative relationship with acoustic signal dominant frequency (i.e. the pitch of the signal) such that smaller bodied frogs have higher pitched calls (Narins *et al.* 2006; Wells 2007). Adding to this challenge is that most frog phylogenies are not fully sampled and call data are difficult to acquire, so studies have focused on single species or very small groups when addressing acoustic signal optimization (Ryan & Rand 1993; Cocroft & Ryan 1995; Cannatella *et al.* 1998; Robillard *et al.* 2006; Goicoechea *et al.* 2010). The importance of broad-scale phylogenetic analyses is not

often considered, but shared ancestry could be an alternative explanation to signal optimization for some patterns of signal diversity.

Here in this dissertation, I aim to elucidate how acoustic interference plays a critical role in driving the evolution of variation in acoustic signals using frogs from the genus *Boophis* in Madagascar, which is outlined as follows: **Chapter 1** — To contribute to the taxonomic progress and integration of bioacoustic data, I describe a new species of *Boophis* that is morphologically identical to several related species but can easily be distinguished using bioacoustic evidence. Here I also develop the acoustic analysis pipeline used in Chapter 5 for acquiring frequency traits from thousands of calls rapidly. **Chapter 2** — The genus *Boophis* has been lacking in multi-locus phylogenetic studies, and I perform the first study of this kind in the genus. While the dataset was enough to draw some systematic conclusions and provide some biogeographic insights on *Boophis* speciation, the phylogenetic results did not provide strong statistical support for most of the nodes in the tree. **Chapter 3** — I developed a sequence capture probe set called FrogCap to sequence ~15,000 genomic markers that can be used across the entire frog radiation. The results from this chapter show that FrogCap is a very promising new sequence capture probe set that can be used across all frogs. **Chapter 4** — The phylogeny of Mantellidae remains unresolved and contentious, where the phylogenetic relationships among subfamilies and genera are not well delimited. I address the weak phylogenetic support and also test the FrogCap probe set on Mantellidae frogs, comparing the probe set to transcriptomic sequencing of samples from the same groups. **Chapter 5** — To address whether acoustic interference leads to the evolution of higher frequency advertisement calls, I integrate an unprecedented dataset incorporating data from all previous chapters that includes: (1) a massive dataset of 300+ acoustic recordings from nearly every species in the genus; (2) a new *Boophis* time-calibrated phylogeny using a backbone

of ~15,000 genomic markers for half the genus acquired from sequence capture combined with GenBank data from Chapter 2 for full species sampling; and (3) used soft tissue computed tomography (CT scanning) on 28 species to acquire detailed morphological information from the larynges of males with associated acoustic recordings using Diffusible Iodine-based Contrast-enhanced Computed Tomography (DiceCT). I used these data to test the acoustic adaptation hypothesis and to understand the morphological basis underlying acoustic signal diversity.

CHAPTER 1

A new species of bright-eyed treefrog (Mantellidae) from Madagascar, with comments on call evolution and patterns of syntopy in the *Boophis ankaratra* complex

Hutter C.R., Lambert S.M., Cobb K.A., Andriampenomanana Z.F., and Vences M. (2015). A new species of bright-eyed treefrog (Mantellidae) from Madagascar, with comments on call evolution and patterns of syntopy in the *Boophis ankaratra* complex. *Zootaxa* 4034(3): 531–555. http://dx.doi.org/10.11646/zootaxa.4034.3.6

1.1 Introduction

Madagascar hosts an impressively diverse amphibian fauna comprised of five anuran clades: the family Mantellidae, the microhylid subfamilies Dyscophinae, Scaphiophryninae and Cophylinae, the hyperoliid genus *Heterixalus*, and the most recent arrival, a single species of the African genus *Ptychadena* (Crottini *et al.* 2012). The vast majority of Madagascar's 305 currently described frogs (Perl *et al.* 2014; Penny *et al.* 2014; AmphibiaWeb 2015) are endemic to this 'microcontinent'. Recently, this unique biota has been the focus of intensive field surveys (e.g. overviews: Goodman & Benstead 2003; D'Cruze *et al.* 2009), phylogenetic and biogeographic studies (e.g. Wollenberg *et al.* 2011; Brown *et al.* 2014), and conservation assessments (e.g. Andreone *et al.* 2005; Kremen *et al.* 2008). Many of Madagascar's amphibians are remarkably well known, with adult and larval morphology, advertisement calls, and phylogeographic differentiation of the majority of the described species being at least partially characterized. However, this knowledge base includes a large number of lineages that have only provisionally been identified as candidate species and require formal taxonomic description. Vieites *et al.* (2009) listed 221 such provisional taxonomic units and Perl *et al.* (2014) increased this number to 241.

The genus *Boophis* Tschudi, 1838 constitutes an excellent model of this taxonomic progress. The genus contains a large number of arboreal frogs with 76 described species (AmphibiaWeb 2015) and 13 additional candidate taxonomic units (Perl *et al.* 2014). *Boophis* treefrogs mostly inhabit the eastern rainforest biome in Madagascar (Cadle 2003). Frequently, low variation in external morphology and skin pigments that fade after preservation have contributed to a severe historical underestimation of species diversity in this genus (e.g. Vieites *et al.* 2009; Glaw *et al.* 2010). This is especially true for eye coloration, which is an important

diagnostic trait in *Boophis* (e.g. Glaw & Vences 2007), but typically is not reliably recognizable in preserved specimens. Most importantly, the advertisement calls of most *Boophis* species are loud and characteristic, and have shown to be more taxonomically informative than external morphology or skin pigment (Vences *et al.* 2008).

Bioacoustic comparisons of Malagasy anurans started with the pioneering work of Blommers-Schlösser (1979), and have substantially accelerated the rate of species discovery in this genus (Köhler *et al.* 2005; Glaw *et al.* 2010). After the widespread application of bioacoustics, species identification and characterization in these frogs has outpaced other Malagasy anuran groups (e.g. Andreone 1993, 1994, 1996; Glaw & Thiesmeier 1993; Glaw & Vences 2002; Vences & Glaw 2002; Köhler *et al.* 2007, 2008; Wollenberg *et al.* 2008; Glaw *et al.* 2010; Vences *et al.* 2010; Penny *et al.* 2014). While Blommers-Schlösser & Blanc (1991) listed only five species of green-colored *Boophis*, the latest accounts identify 34 or more species in the *B. albilabris* group, *B. albipunctatus* group, *B. luteus* group, *B. mandraka* group, *B. rappiodes* group, and *B. ulftunni* group (Glaw & Vences 2006; Vieites *et al.* 2009; Glaw *et al.* 2010; Perl *et al.* 2014; Penny *et al.* 2014).

Herein, we describe a new species belonging to the *Boophis albipunctatus* group. The new species is a member of a sub-clade in this group we define as the *Boophis ankaratra* complex, containing five species (*B. ankaratra, B. haingana, B. miadana, B. schuboeae,* and the new species). The *Boophis ankaratra* complex lacks a well-distinguished dorsal white-dotted pattern present in the second sub-clade *(B. albipunctatus, B. sibilans, B. luciae)*, except for the new species, which often has similar yellowish-white spots. The new species occurs at Ranomafana National Park (RNP) and the surrounding area in the southern central east of Madagascar (Fig. 1). Ranomafana is one of the most intensively surveyed areas of amphibian

diversity in Madagascar with over 120 species and candidate species known from the reserve and surrounding sites (Vieites *et al.* 2009), including 36 species of *Boophis*. Additionally, the newly described taxon has been previously characterized as a candidate species based on its molecular differentiation and advertisement calls (Vieites *et al.* 2009).

1.2 Materials and Methods

1.2.1 Terminology

We follow the unified concept of species (i.e. general lineage concept), which defines a species as a separately evolving lineage within a temporal segment of a population (Simpson 1961; Wiley 1978; de Queiroz 1998, 2005, 2007). However, we stress that the new species described herein likely represents a species even if conservative species criteria are applied (e.g. biological species criterion), as it occurs syntopically with close relatives with no evidence of genetic admixture. Importantly, all species in the *Boophis ankaratra* complex differ in advertisement call, suggesting they are reproductively isolated (see Vences & Wake 2007).

We use an integrative taxonomic approach in assessing species boundaries, combining data from morphology, phylogenetics, bioacoustics, and biogeography (Dayrat 2005; Padial *et al.* 2010; Vences *et al.* 2013). This evidence is then weighted equally and used as support for the hypothesis that a given population is an independently evolving lineage and thus a distinct species. Family and generic names follow the taxonomy proposed by Glaw & Vences (2006). Geographic regions for biogeographic analyses are defined according to Glaw & Vences (2007). According to this zonation, RNP is within a region named the southern central east of Madagascar.

1.2.2 Morphology

Specimens were collected at night by opportunistic searching or by locating males through their conspicuous advertisement calls. Specimens were sacrificed using 20% benzocaine, fixed in ~10% formalin (buffered with sodium phosphate to ~7.0 pH) for 24 hours and then stored in 70% ethanol for long-term preservation. We deposited and examined alcohol-preserved specimens from the amphibian collections at the Biodiversity Institute of the University of Kansas (KU) and Département de Biologie Animale, Antananarivo (UADBA) (Appendix I). Additional collection acronyms used herein are FAZC, ZCMV, FGZC, and LR (field number series of F. Andreone, M. Vences, F. Glaw, and L. Raharivololoniaina respectively), FGMV (field number series shared between M. Vences and F. Glaw), and ZSM (Zoologische Staatssammlung München, Germany).

Morphological measurements were taken by K.A. Cobb with a digital caliper (precision 0.01 mm) to the nearest 0.1 mm. Terminology and measurements largely follow Glaw *et al.* (2001) and we used the following: (1) snout-vent length (SVL); (2) head width at the greatest point (HW); (3) head length (=rostrum) from snout tip to maxillary commissure (HL); (4) horizontal eye diameter (ED); (5) interorbital distance (IOD); (6) eye-snout tip distance (ESD); (7) eye-nostril distance (END); (8) nostril-snout tip distance (NSD); (9) nostril-nostril distance (NND); (10) horizontal tympanum diameter (TD); (11) forelimb (=radioulna) length from humerus-radioulna articulation point to carpal-metacarpal articulation (FORL); (12) hand length from carpal-metacarpal articulation to tip of longest finger (HAL); (13) Finger I length from outer margin of palmar tubercle to tip of Finger I (FIL); (14) Finger II length from outer margin of palmar tubercle to tip of Finger II (FIIL); (15) femur length from cloaca to the femur-tibia articulation (FEML); (16) tibia length measured along the shank (TIBL); (17) foot length from

tarsal-metatarsal articulation to tip of longest toe (FOL); (18) foot+tarsus length from the tibiotarsal articulation to tip of longest toe (FOTL); and (19) relative hindlimb length to SVL by (FEML + TIBL)/SVL (RHL). We note that RHL is typically measured by adpressing the hindlimb along the body and noting the point the tibiotarsal articulation reaches (e.g. eye center, beyond snout tip; Glaw *et al.* 2010); however, we were unable to measure this character with formalin preserved specimens as this would damage the specimen. Sexual maturity was determined by male calling activity (all males collected were calling) and by the presence of eggs in females. Description of eye coloration follows Glaw & Vences (1997) and webbing formulae follow Blommers-Schlösser (1979).

1.2.3 Phylogenetics

Following euthanasia, we extracted whole livers and left hind limb muscles and stored the tissues in 95% ethanol. We obtained new genetic data for 10 specimens (nine from the newly described species, and one from *Boophis ankaratra*). Sequences were deposited in GenBank and their associated voucher specimens and accession numbers are provided in Appendix II.

Genomic DNA was extracted from the tissue using proteinase K (final concentration 20 mg/ml) and a standard salt-based Guanidine Thiocyanate Extraction extraction protocol (Esselstyn *et al.* 2008). We amplified a ~1400bp segment of mitochondrial DNA, corresponding to the almost complete large ribosomal subunit (16S rRNA) using polymerase chain reaction (PCR). The forward and reverse primers used were LX12SN1 and LX16S1R (Zhang *et al.* 2013). PCR reactions were performed using the following procedure: 1.5 µL genomic DNA, 0.2 µM of each primer, 200 µM of dNTPs, 1.25 U of OneTaq® DNA polymerase, and 5 µL OneTaq® Standard Reaction Buffer (20mM Tris-HCl, 22mM NH_4Cl, 22mM KCl, 1.8mM

$MgCl_2$, 0.06% IGEPAL® CA-630, and 0.05% Tween® 20). The final volume was brought to 25 µL with nuclease-free water. We visualized amplification success using 2 µL of PCR product on 1.5% agarose gel. Additionally, a ~900bp segment of the nuclear gene 'dynein axonemal heavy chain 3' (DNAH-3) was amplified using the primers and PCR protocol from Shen *et al.* (2013).

PCR products were purified of excess dNTPs and primers using Shrimp Alkaline Phosphatase (1U/µL) and Exonuclease I (20U/µL). We used the remaining 23 µL of PCR product and added 0.025 µL Exonuclease I, 0.250 µL Shrimp Alkaline Phosphatase and 9.725 µL nuclease-free water for a final volume of 32 µL per reaction. Next, we incubated the samples at 37ºC for 30 minutes and then 95ºC for 5 minutes in a thermocycler. For cycle sequencing, we conducted two separate reactions for the target 5' and 3' end DNA strands per purified PCR product. We prepared a 7 µL sequencing reaction that included 2 µL of the purified PCR product, 1.5 µL of 5X sequencing buffer, 0.5 µL of the forward or reverse primer (separately), 0.5 µL of BigDye Terminator® (version 3.1 sequencing standard, Applied Biosystems) and 2.5 µL of water. The sequence reaction began with 1 cycle at 95ºC for 60 s, and 30 cycles of 95ºC for 15 s, 50ºC for 15 s, and 60ºC for 240 s. In preparation for sequencing, we purified the reaction product of BigDye Terminator® by filtering the product through Sephadex® G-50 in a spin column centrifuged at 850 rcf for 5 min. We collected and visualized sequence data on an Applied Biosystems 3130 automated sequencer. After sequencing, DNA data were manually edited for quality in Geneious R8 (Biomatters 2015).

Initially, we used uncorrected p-distances in a commonly used region of the 16S rRNA marker as a preliminary assessment of genetic differentiation (Vieites *et al.* 2009). However, we did not consider an absolute threshold of genetic distance (e.g. 2.5%–3.0%) as primary criterion to delimit species because this approach might be misleading due to introgression, incomplete

lineage sorting, low genetic variability of markers, or recently evolved reproductive isolation. This consideration is supported by other recently described *Boophis* species of low genetic divergence to their sister species (e.g. *B. narinsi* vs. *B. majori;* and other species in the *B. ankaratra* complex; Glaw *et al.* 2010; Vences *et al.* 2012). To more directly address whether a species is a separately evolving lineage, we test for strongly supported reciprocal monophyly in mitochondrial genetic data using phylogenetic analyses (Avise 2000).

We supplemented newly generated mitochondrial data with published sequences of the 16S rRNA marker of *Boophis* specimens we obtained from GenBank (Appendix III). We selected a subset of closely related nominal taxa, using the tree available from Vieites *et al.* (2009) and data from Glaw *et al.* (2010) as guides. For examination of genetic distances, we selected data from a ~600bp fragment of 16S which is commonly used for distance comparisons in Malagasy frogs (Vieites *et al.* 2009). To test for reciprocal monophyly, we included another ~650bp fragment of 16S, spanned by our primer pair and available on GenBank for most, but not all species of the *B. ankaratra* complex. Whenever possible, we selected multiple individuals from each selected species to test for reciprocal monophyly of the new species using mitochondrial data.

We included the distantly related *Boophis periegetes* (for mtDNA) as an outgroup based on previous phylogenetic studies (Vieites *et al.* 2009). Our final mtDNA matrices included 43 individuals of seven species of the *B. albipunctatus* group spanning 1,229bp for phylogenetic analysis, and 50 individuals from the same species spanning 583bp for examination of genetic distances. All matrices were aligned in Geneious using MAFFT v7 (Katoh & Standley 2013) and manually inspected for accuracy.

For maximum likelihood (ML) estimation of phylogenetic relationships using 16S, we used RAxML 8.1.17 (Stamatakis 2014). We used the GTR + G model (Generalized Time–Reversible + Gamma) of nucleotide substitution, which accounts for variable base frequencies and includes a gamma-shaped distribution for rates across sites. Next, we performed 100 tree searches and assessed node support using 1000 bootstrap replicates, using the standard, non-rapid bootstrap procedure.

For Bayesian Inference analyses (BA) of 16S, we used MrBayes 3.2.4 (Ronquist *et al.* 2012). First, we used JModelTest 2.0 (Posada 2008) to select the model of sequence evolution that best fits the data, using the Bayesian information criterion (BIC; Schwarz 1978). We chose not to evaluate models that include both gamma-distributed rate variation across sites (G) and a proportion of invariant sites (I) because their joint estimation can be compromised by correlation between parameters (Yang 2006, p. 114). The best-fit model for the 16S alignment was TRNef+G. We then conducted analyses for 10 million generations (sampling every 1000) with four Markov chains. All parameters were left at default settings unless otherwise noted. We ran four replicate analyses to ensure convergence to a consistent optimum between independent analyses. To assess convergence we examined the standard deviation of split frequencies to ensure values were below a conservative value of 0.005, and plots of –lnL per generation to evaluate stationarity. We discarded the first 25% of generations as 'burn-in' for evaluation of convergence and computation of clade credibility trees.

Finally, we assessed if the putative new species was reciprocally monophyletic in reference to all other species of the complex, using the estimated phylogeny. Statistical support for this hypothesis is given through a conservative and high bootstrap support (BS > 90%) in ML

analyses and high posterior probability support (PP > 0.95) in BA analyses for the monophyly of *Boophis boppa*.

As an additional step to determine the evolutionary independence of the new species we examined haplotypes of the nuclear exon DNAH-3. We chose to represent the DNAH-3 sequence data using a minimum-spanning haplotype network because initial phylogenetic trees were weakly resolved. This lack of resolution could be due to insufficient variability of the marker and/or limited taxon sampling for the *Boophis ankaratra* complex (4 individuals of *B. boppa*, 1 of *B. miadana*, 1 of *B. haingana*, 2 of *B. ankaratra*). Our final nDNA matrix included 11 individuals from 8 species and spans 747bp. After manual editing in Geneious, sequences were first unphased using PHASE v2.1 (Stephens *et al.* 2001; Stephens & Donelly 2003). Next, the data was analyzed and visualized using the minimum-spanning algorithm (Bandelt *et al.* 1999) implemented in PopART v1.7 (http://popart.otago.ac.vz).

1.2.4 Bioacoustics

Calling males were located in streams and recorded in the field at less than 2 m distance from the calling individual. As species of *Boophis* call frequently and simultaneously, we ensured that the male being recorded was the same captured through visual inspection of vocal sac movement under a red light. Calling males were observed for extended periods and in varying conditions to ensure that the call being recorded was the advertisement call and not an alternative call type. While the advertisement call is typically the most frequently emitted call type, males might engage each other in territorial behavior using an alternative call type (e.g. Wells 2007; Glaw *et al.* 2010). We observed this behavior infrequently, but were unable to

obtain recordings due to the reduced volume of the alternative call type and its unpredictable occurrence.

Calls were recorded with an Olympus LS-10 Linear PCM Field Recorder and a Sennheiser K6-ME 66 unidirectional microphone. The calls were recorded in uncompressed WAV format at a sampling rate of 44.1 kHz and 16 bits resolution. We recorded the air temperature following each call using an analog thermometer. Comparative calls used from the *Boophis ankaratra* complex are the same audio recordings described in Glaw *et al.* (2010).

We follow Duellman & Trueb (1994) in defining a call as the entire assemblage of acoustic signals produced in a given sequence. Under this definition, and following previous call descriptions for the *Boophis ankaratra* complex (Glaw & Vences 2002, 2007; Glaw *et al.* 2010), we define a series of notes as a call, where notes are temporally distinct segments separated by a return to the background noise between each note. We acknowledge that an alternative approach would be defining each note as a single-noted call and a series of notes could be considered a series of calls. Pulsed notes are those having one or more clear amplitude peaks while tonal notes have relatively constant amplitude throughout the call.

Following Hutter & Guayasamin (2012; Figure 3), Hutter *et al.* (2013; Table 1) and Glaw *et al.* (2010), we chose the following call variables: (1) note amplitude type (tonal or pulsed); (2) call arrangement type (notes singular or in a series); (3) number of notes per call; (4) call duration (s); (5) note duration (ms); (6) inter-note interval duration (ms); (7) note repetition rate within call (notes/s); (8) pulse rate (/s); (9) note envelope shape (time at peak amplitude / call duration); (10) dominant frequency, measured at peak amplitude (Hz); (11) lower fundamental frequency limit (=fundamental frequency) (Hz); (12) upper fundamental frequency limit (Hz);

and (13) 1st harmonic frequency (Hz). Measures are reported as the range followed by the mean ± two standard deviations from the mean.

The parameters above were measured using the R package SEEWAVE (Sueur *et al.* 2008; R Development Core Team 2015). The analysis of calls was automated using a custom script (available upon request), following Hutter & Guayasamin (2015). To test the accuracy of this method, we reanalysed the same audio files used for manual measurements in Glaw *et al.* (2010) and found the results to be generally the same to that of automated measurements. For example, we compared the following for *Boophis ankaratra* between automated and manual measurements from Glaw *et al.* (2010), respectively: (1) dominant frequency, 2756–3015 vs. 2750–3000 Hz; (2) note duration, 134 ± 10.6 vs. 125 ± 4 ms; (3) note repetition rate, 2.5 vs. 2.5 (/s); and (4) inter-note interval duration, 269 ± 37 vs. 257 ± 4 ms (compare Table 2 vs. Glaw *et al.* 2010, Table 1)**.** We also emphasize that we examined each analysed call visually to ensure it was not another species, background noise, or artefact. Digital recordings are deposited at the University of Kansas Biodiversity Institute and are available upon request.

Finally, we evaluated the amount of bioacoustic differences between species following Vieites *et al.* (2009). We considered differences in general call structure (e.g. pulsed/tonal notes, consistent note arrangements, amplitude envelope shape; Ryan & Rand 1990) and such temporal variables that are putatively less influenced by temperature, body size, and behavior (e.g. note duration, pulse rate; Gerhardt *et al.* 2000) to be important traits for distinguishing species. We did not correct for temperature as all calls recorded were within a degree of each other, except those of *Boophis schuboeae* (see below for justification).

1.3 Taxonomic Results and Description

***Boophis boppa* sp. nov.**

Suggested common English name. Boppa's Bright-eyed treefrog

Suggested common Malagasy name. Fity maso hazo Sahona ny Boppa

Remarks. Previously referred to as *Boophis* sp. 1 (aff. *ankaratra*) (Andreone *et al.* 2007), *Boophis* aff. *ankaratra* 'Antoetra slow' (Glaw & Vences, 2007), and *Boophis* sp. Ca18 (Vieites *et al.* 2009).

Holotype (Figs. 2–3A). KU 336824, an adult male collected by Carl R. Hutter and Zo F. Andriampenomanana on 18 January 2014, at Maharira within Ranomafana National Park (21°20'06.3"S, 047°24'28.31"E; 1233 m, above sea level [a.s.l.]), Fianarantsoa province, Madagascar.

Paratypes. Adult female KU 336829 and adult male KU 336826 collected on 21 January 2013 by Carl R. Hutter and Shea M. Lambert with same locality data as holotype. Adult males KU 336828, KU 336825, KU 336827, with same collection data as holotype.

Referred specimens. UADBA-Uncatalogued (CRH 080), UADBA-Uncatalogued (CRH 168), UADBA-Uncatalogued (CRH 178) with same collection data as holotype.

Diagnosis. Boophis boppa (Fig. 4) is placed in the family Mantellidae, subfamily Boophinae, and genus *Boophis*, as diagnosed by Glaw & Vences (2006). The new species shares the following combination of morphological traits with all other *Boophis*: presence of intercalary element between ultimate and penultimate phalanges of fingers and toes; presence of nuptial pads and absence of femoral glands in males; absence of gular glands in males; terminal discs of fingers and toes enlarged; lateral metatarsalia separated by webbing; and absence of outer metatarsal tubercle. Furthermore, phylogenetic analyses support the placement of the new species in the genus *Boophis*.

Boophis boppa is placed in the *Boophis albipunctatus* group as supported by the phylogenetic analyses. Additionally, the following combination of characters provide additional evidence for the inferred phylogenetic relationships: small body size (male SVL < 27 mm); tubercles or flaps on heel and elbow absent; webbing between fingers present; canthus rostralis indistinct; distinct white tarsal folds present; dorsal coloration translucent green in life and cream-colored in preservative; ventral skin partially transparent in life; red ventral coloration absent; single subgular vocal sac; and vomerine teeth present.

Boophis boppa is a member of the monophyletic *B. ankaratra* complex and cannot easily be distinguished morphologically from other closely related species in the group, which includes *B. ankaratra, B. haingana*, *B. miadana*, and *B. schuboeae* (Fig. 5). Species in this complex lack a dense and regular white-spotted pattern that is present in other members of the *B. albipunctatus* group; however, most individuals of the new species show some light yellow and white spotting. *Boophis boppa* differs from syntopic *B. ankaratra* by lacking a yellow parietal peritoneum, which was present in all live photographs and examined live individuals from two different populations for *B. ankaratra* (e.g. Fig. 3B and Fig. 5A). *Boophis boppa* differs from allopatric *B.*

miadana and *B. haingana* by having the smallest, non-overlapping body size among these three species (adult male SVL: *B. boppa* = 20.3–24.4 mm; *B. miadana* = 25.5–26.8 mm; *B. haingana* 24.8–29.0 mm). However, we could not discern any morphological differences between the new species and *B. schuboeae*, which occurs sympatrically at Ranomafana National Park, but has not been observed syntopic with *B. boppa*, instead occurring at lower elevations. While we find discernable morphological differences in life, our observations generally agree with previous studies suggesting that reliable morphological differentiation among specimens of these species is difficult (Glaw *et al.* 2010). Despite this difficulty, these species all can be easily diagnosed by advertisement call and/or molecular phylogenetics.

Bioacoustically, *Boophis boppa* can easily be distinguished from all other species in this group by having the longest note duration (Fig. 6) and longest intervals between notes and thus the slowest note repetition rate within calls (Fig. 7; Table 2). The most similar species in call is *B. miadana* (Fig. 6B; Fig. 7B), which has the second longest note duration and inter-note interval in the group, but does not overlap with the new species in these values. All other species in this complex have much shorter advertisement calls. Additionally, these differences cannot be attributed to temperature, which fall within 1ºC across the recordings of *B. miadana* and *B. boppa*. We did not correct the call of *B. schuboeae* for temperature (it was ~5ºC warmer), as it has dramatically shorter note and inter-note interval durations (4-fold and 7-fold shorter, respectively) and a much faster note repetition rate than *B. boppa*, which are differences not likely due to this amount of temperature change. Furthermore, motivation of the calling male was unlikely a factor as the temporal differences remained consistent across hundreds of calls and a variety of motivational states and weather conditions.

Phylogenetically, *Boophis boppa* is reciprocally monophyletic to all other species in the complex with strong support based on DNA sequences of the mitochondrial marker 16S (Fig. 8). The new species also shares no haplotypes of the nuclear exon DNAH-3 with other related species (Fig. 9). Importantly, *B. ankaratra* is also monophyletic, which includes individuals from the southern parts of its range and a specimen from Ranomafana National Park that was syntopic with *B. boppa*. Although the sister group of *B. boppa* cannot be determined from the analyses undertaken here, close phylogenetic affinity is suggested with *B. ankaratra*, *B. schuboeae*, or *B. miadana*. Additionally, the low genetic distance among individuals within *B. boppa* and its monophyly is strong evidence that no genetic admixture is occurring with other species of the *B. ankaratra* complex. Notably, *B. boppa* and *B. ankaratra* occur syntopically and can commonly be found calling within a meter distance from each other, with consistent and strong call differences (Figs. 6–7). *Boophis boppa* also occurs sympatrically with *B. schuboeae* (although calling males have thus far not been found together in syntopy) and the calls of these species are highly distinct (Figs. 6–7). Finally, *B. miadana* is distributed allopatrically and has a genetic distance of 3.5–4.5% compared to *B. boppa*.

Description of the holotype (Fig. 2). Adult male, SVL 23.4 mm. Body moderately slender; head wider than body, HW 36.3% of SVL; head slightly shorter than wide, HL 33.8% of SVL; snout of moderate length, ESD 15.8% of SVL; snout rounded in dorsal and lateral view; nostrils directed dorsolaterally, nearer to eye than to tip of snout; ED larger than END; cranial crests absent; canthus rostralis indistinct, loreal region slightly concave; single subgular vocal sac; gular glands absent. Tympanic annulus distinct, round, TD 48.0% of ED; supratympanic fold barely distinct, tympanic membrane transparent. Vomerine odontophores distinct, well separated

in two elongated patches, positioned posteromedial to choanae; choanae medium-sized, rounded. Tongue longer than wide; ovoid in shape, posteriorly bifid, free. Arms slender; subarticular tubercles single, round; metacarpal tubercles not recognizable. Nuptial pad on inner finger 1, barely distinguishable; not pigmented, slightly lighter than ground color; fingers moderately webbed and with lateral dermal fringes; webbing formula 1(1.5), 2i(1.5), 2e(1), 3i(2), 3e(1.5), 4(1); relative length of fingers 1<2<4<3, finger 2 distinctly shorter than finger 4, finger 1 slightly shorter than finger 2; finger discs enlarged. Hind limbs slender; femoral glands absent; white tarsal folds distinct; TIBL 52.6% of SVL; FOL 46.6% of SVL; lateral metatarsalia separated by webbing; inner metatarsal tubercle small, distinct, elongated; no outer metatarsal tubercle; toes broadly webbed; webbing formula 1(0.5), 2i(0.75), 2e(0.25), 3i(1), 3e(0.25), 4i(1.25), 4e(1.5), 5(0.5); relative length of toes 1<2<3<5<4; toe discs enlarged. Skin smooth on dorsal surfaces, finely granular on throat and chest, coarsely granular on belly and ventral surfaces of thighs. Enlarged tubercles absent in cloacal region. Muscle from right thigh and liver removed for tissue samples; abdominal cavity of right side opened.

After one year in preservative (Fig. 2), body coloration uniform cream-yellow. Dark pigments are present around nostrils. Dark pigmented spots are present on upper eyelids and along the dorsum. In life (Figs. 3A–4), dorsum lime green with numerous white-yellow flecks, dark brown spots present, skin translucent especially on limbs, groin turquoise; upper 3/4 visceral peritoneum white, lower peritoneum and flanks transparent; underside of limbs translucent green, joints turquoise. Pupil black; iris coloration reddish-brown around the pupil and outer edges lighter in color, non-uniform; iris outlined in black; iris periphery blue, posterior edges black; eye periphery black. Color sequence from pupil to eye periphery: black, reddish-brown, yellowish-brown, black, blue, and black.

Morphometry of type series. Measurements of the holotype and paratypes are shown in Table 1.

Variation (Figs. 10–11). In life, dorsal coloration is lime to a light-lime green, with a white venter that is transparent posteriorly and along the flanks. Some individuals of this species have a white spotting pattern, with some spots being light yellow upon closer examination. Given this, the morphological distinction between the *Boophis ankaratra* complex and other species in the *B. albipunctatus* group is weakened; however, these spots can be useful in distinguishing *B. boppa* when present. Brown dorsal spots are also variable, as some individuals may have dense, dark patches, several spots, or none at all (Fig. 10). Additionally, the intensity of the iris coloration is variable (Fig. 11).

Bioacoustics (Figs. 6A–7A; Table 2). We recorded and analyzed 171 notes from six individuals of *Boophis boppa* and 209 notes from two individuals *B. ankaratra* in syntopy with *B. boppa*. All individuals are adult males recorded at night with mist or light rain at a temperature of 16.9–18.2°C. The males were calling on the upper surfaces of leaves 2–4 m above the ground and were recorded 1 m or less from the male. The advertisement call of this species sounds like a long 'groan' to the human observer, emitted frequently in slow-paced succession. We define each groan as a note (Fig. 6A), which are arranged in series (each series we consider a call) of 5–16 notes separated by extended periods of silence.

Each note in the call of *Boophis boppa* is strongly amplitude modulated, with the peak amplitude occurring in the last 50% of the note. The notes are strongly pulsed, with a rate of 135–263 (187 ± 31) pulses / s. The note duration is 379–526 (451.6 ± 42.4) ms with an inter-note

interval of 989–1659 (1192 ± 167) ms. The dominant frequency measured at peak amplitude is 2929–3531 (3205 ± 139) Hz. The dominant frequency is within the fundamental frequency, which has a lower limit of 2500–2594 (2702 ± 101) Hz and an upper limit of 3001–3431 (3165 ± 91.8) Hz. The first harmonic is 5768–6384 (6073 ± 148) Hz. See Table 2 for a comparison among all identified species in the *B. ankaratra* complex.

Phylogenetics (Figs. 8–9). The phylogenetic results support the morphological diagnosis by placing *Boophis boppa* in the genus *Boophis* within the *B. albipunctatus* group. At the species level, *B. boppa* is monophyletic with strong support in all analyses (BS > 90%; PP > 0.95; Fig. 8). Uncorrected p-distances using the 16S fragment indicate that *B. ankaratra* has the lowest distance to the new species, at 1.9–3.7%. Additionally, we find that variation in genetic distance among *B. boppa* and *B. ankaratra* is not related to geographic proximity. The lowest distance of 1.9% (Imaitso Forest; FMGV 1697) does not correspond to proximate localities and the highest distance of 3.7% is from Ranomafana National Park (Ranomena; ZCMV 5989). This variability in distances is likely a result of varying amounts of sequence overlap being compared. Overall, these results provide strong evidence that the species is a separately evolving lineage and does not reproduce with other species in the complex.

Distribution (Fig. 1). Boophis boppa is known from Ranomafana National Park (RNP), but has only been found at high elevation sites (~1046–1312 m, a.s.l.). In addition to the type locality of Maharira, DNA sequences also confirm that specimens FAZC 11454, 11462, and 11480 collected from Farihimazava forest near Antoetra (20°50'06"S, 47°19'57"E, 1380–1420 m, a.s.l.; ca. 55 km north west of the type locality; see Andreone *et al.* 2007) are conspecific.

Additionally, tadpoles ZCMV 9739 collected at Imaloka (RNP: 21°14'32"S, 47°27'55"E, 1020 m, a.s.l.) and ZSM 1164/2007 from Sakaroa (RNP: 21°15'00.1"S, 47°24'53.6"E) belong to *Boophis boppa*. The species has a known elevational distribution of ca. 1020–1400 m, a.s.l.

Natural History (Fig. 12). Boophis boppa was locally abundant but thus far only found in undisturbed, primary forests along fast moving streams and were occasionally found along slow flowing tributaries adjacent to fast streams. Males of the species typically were calling at night from the surfaces of vegetation less than three meters in height (Fig. 12A–B). Females of *B. boppa* were rarely encountered and were only observed while in amplexus (Fig. 12C). We also confirm that *Boophis boppa* is syntopic with *Boophis ankaratra* at Maharira and that the two species can be found calling less than a meter apart. This is also consistent with Andreone *et al.* (2007), which found *B. boppa* (i.e. *Boophis* aff. *ankaratra*) and *B. ankaratra* to occur sympatrically. Other syntopic species of *Boophis* at Maharira include: *B. madagascariensis, B. majori, B.* aff. *marojezensis, B.* aff. *picturatus*, *B. popi,* and *B. reticulatus*.

Conservation status. The new species is known from Ranomafana National Park and its vicinity, extending into the Antoetra area. While it is known from a geographic area less than ~5,000 km^2, there are no known immediate threats, reductions in quality or extent of habitat, or observed declines as the species is well protected within Ranomafana National Park. Therefore, the new species meets only criterion (B1), and could become endangered in the future if the situation changes at Ranomafana, for instance through an outbreak of chytridiomycosis, which has been detected in the park (Bletz *et al.* 2015). We recommend a conservation status of Near Threatened, following IUCN (2001) criteria.

1.4 Discussion

The sequence data presented here were insufficient to resolve the phylogenetic relationships among species of the *Boophis ankaratra* complex with high confidence. Wollenberg *et al.* (2011), based on sequences of three mitochondrial genes (16S, cytochrome *b*, cytochrome oxidase subunit I), obtained statistical support for a relationship in agreement with advertisement call structure, placing species characterized by slower note repetition rates (*B. ankaratra* with *B. miadana*), and species with faster note repetition rates (*B. haingana* and *B. schuboeae*) as sister taxa, respectively. However, this study did not include *B. boppa* for which the 16S data suggest a possible sister relationships with *B. miadana, B. schuboeae,* or *B. ankaratra.*

Boophis boppa provides an additional example of syntopic occurrence of closely related species of mantellid frogs (also see Andreone *et al.* 2007). Previous examples include the sister species pairs *Gephyromantis eiselti / G. thelenae* (Wollenberg *et al.* 2011), and *Boophis majori* / *B. narinsi* (Vences *et al.* 2012). Instances of syntopic occurrence between species of the *B. ankaratra* complex (*B. miadana* / *B. haingana* in Andohahela and *B. boppa* / *B. ankaratra* in Ranomafana) are restricted to species with highly distinct advertisement calls. Conversely, allopatric species pairs (*B. haingana* / *B schuboeae* and *B. miadana* / *B. boppa*) have somewhat more similar advertisement calls. The bioacoustic and distributional patterns of these closely related species suggest the possibility of mating signal divergence owing to selection for enhanced pre-mating reproductive isolation, a process known as reinforcement (*sensu* Howard 1993). This phenomenon would be expected if there were a fitness cost to inter-specific mating or courtship resulting from imperfect species recognition. We note that some authors (e.g. Butlin

1987; Coyne & Orr 2004) restrict the term 'reinforcement' to instances where post-zygotic reproductive isolation is incomplete. Instead, we here follow a definition that extends to cases with complete post-zygotic reproductive isolation, as have other authors (e.g. Howard 1993; Hoskin & Higgie 2010; Lambert *et al.* 2013). However, the observed patterns are merely suggestive, and future research should include more evidence from species co-occurrences, advertisement calls, and female preference to properly assess such a hypothesis.

Phylogeny should allow for basic inferences about call evolution and biogeography that could be informative about evolutionary processes. However, without a well-supported resolution of the relationships between members of the *Boophis ankaratra* complex, it is difficult to use phylogeny to assess the likelihood of particular evolutionary scenarios. Nevertheless, it may be useful to consider two polarized alternatives. First, as found in Wollenberg *et al.* (2011), it is possible that species with similar advertisement call are also most closely related (thus *B. boppa* would be most closely related to *B. miadana*, the species with the second slowest note repetition rate). Such a scenario would suggest conservatism in call evolution and allo- or parapatric speciation between northern and southern lineages. An alternative would find *B. boppa* phylogenetically most closely related to *B. schuboeae* or *B. ankaratra*. This scenario would suggest more recent call evolution occurring in currently syntopic species, a pattern consistent with a hypothesis of mating signal evolution through reinforcement. The placement of *B. schuboeae, B. boppa, B. miadana,* and *B. ankaratra* in a polytomy in our analyses suggests at least some call divergence occurring between closely related and geographically overlapping species. It is worth noting that this polytomy could either a soft polytomy (i.e. caused by insufficient phylogenetic resolution) or a hard polytomy (i.e. caused by essentially simultaneous

divergence between the species). However, even with perfect phylogenetic knowledge, reinforcement cannot be demonstrated through phylogenetic evidence alone.

More substantial evidence for reinforcement would be demonstration of the 'classic pattern' of reproductive character displacement (*sensu* Brown & Wilson 1956), where reproductive traits and corresponding preferences are more different in areas of sympatry than in areas of allopatry. This pattern is consistent with the idea that selection for enhanced species recognition is concentrated where species are syntopic, although it could result from processes other than reinforcement (e.g. competition for signal space; Hoskin & Higgie 2010). Preliminary bioacoustic results suggest that the dominant frequency of the call of *Boophis ankaratra* overlaps with *B. boppa* in allopatric populations, but is non-overlapping when they are found sympatrically. However, additional evidence on community composition and advertisement call variation is needed to confirm these observations, which might also be related to body size differences between these species. Future work should document the call and female preference variation of *B. ankaratra* and *B. boppa* in sympatric and allopatric populations to look for evidence of reproductive character displacement.

1.5 Tables

Table 1. Morphometric measurements (in mm) of the holotype (KU 336824) and selected paratypes of *Boophis boppa*.

	Specimen					
Measure	KU 336824	KU 336825	KU 336826	KU 336827	KU 336828	KU 336829
Sex	Male	Male	Male	Male	Male	Female
SVL	23.4	23.4	22.0	24.4	20.3	32.2
HW	8.5	9.3	8.2	9.1	8.1	12.3
HL	7.9	8.4	7.7	8.4	6.3	10.6
ED	2.5	2.6	2.8	2.8	2.0	3.4
IOD	3.5	3.9	4.0	3.6	3.6	5.9
ESD	3.7	3.1	3.7	3.9	3.2	5.5
END	1.4	1.7	1.7	1.7	1.7	2.8
NSD	2.1	2.1	1.6	1.9	1.8	2.1
NND	2.6	2.7	2.5	3.1	2.5	3.5
TD	1.2	1.2	1.2	1.2	1.2	2.1
FORL	5.3	5.2	4.7	5.1	4.4	6.5
HAL	6.8	6.9	6.2	7.3	6.3	7.5
FIL	3.2	3.4	3.3	3.2	2.6	5.0
FIIL	3.6	3.6	3.3	3.7	3.2	5.2
FEML	12.6	11.5	11.2	11.9	11.0	16.8
TIBL	12.2	12.1	11.0	11.8	10.7	17.2
FOL	10.9	10.7	9.3	11.5	9.3	16.0
FOTL	16.9	16.9	15.8	16.9	15.8	25.2
RHL	1.05	1.01	1.01	0.97	1.07	1.06

Table 2. Comparisons of advertisement calls recorded for the *Boophis ankaratra* species complex. Calls used for comparison are from Glaw *et al.* (2010). Calls were recorded from males calling at night and were subsequently collected as vouchers. Note envelope is the ratio of the time of peak amplitude to note duration. RNP is an abbreviation for Ranomafana National Park. Data are the range and then the mean ± two standard deviations in parentheses, when appropriate.

	Species					
Parameter	*B. boppa*	*B. ankaratra*	*B. ankaratra*	*B. haingana*	*B. miadana*	*B. schuboeae*
Locality	Maharira, RNP	Maharira, RNP	Manjakatompo	Andohahela	Andohahela	Vohipara, RNP
Temp. (C°)	16.9–18.2	17.9	18.0	17.6	17.6	23.0
n – individuals	6	2	1	2	2	2
n – calls (note series)	26	4	1	2	2	2
n– notes	171	209	66	150	144	108
Call duration (s)	3.9–22.12 (10.2 ± 3.9)	13.5–27.1 (19.7 ± 6.5)	25.8	16.4–28.4 (22.4 ± 8.5)	12.8–13.1 (13.0 ± 0.2)	13.9–14.8 (14.3 ± 0.6)
Note duration (ms)	379.0–526.0 (451.6 ± 42.4)	104.56–130 (110.5 ± 8.076)	111.5–153.7 (134 ± 10.6)	46.6–85.8 (61.7 ± 12.7)	208.3–316.4 (249.7 ± 29.8)	73.17–169.3 (124.3 ± 20.9)
Inter-note interval (ms)	989–1659 (1192 ± 167)	204–341 (269 ± 3)	222–318 (259 ± 37)	232–352 (238 ± 86)	591–910 (675 ± 102)	114–248 (162 ± 42)
Note repetition rate (/s)	0.4–0.8	2.6–2.8	2.5	2.6–3.0	1.0–1.2	3.4
Note envelope shape	0.582–0.954 (0.779 ± 0.087)	0.550–0.881 (0.746 ± 0.072)	0.539–0.864 (0.72 ± 0.078)	0.173–0.259 (0.216 ± 0.061)	0.417–0.807 (0.635 ± 0.094)	0.542–0.915 (0.752 ± 0.079)
Pulse rate (/s)	135-263 (187 ± 31)	147-323 (212 ± 29)	110-169 (143 ± 11)	155-173 (164 ± 13)	76-203 (120 ± 39)	35-234 (119 ± 46)
Dominant frequency (Hz)	2929–3531 (3205 ± 139)	2584–2756 (2671 ± 68)	2756–3015 (2905 ± 72)	2929	2756–3015 (2893 ± 71)	3359–3531 (3403 ± 45)
Lower fundamental	2500-2972 (2702 +/- 101.046)	2329-2525 (2435 +/-	2509-2746 (2659 +/- 48.378)	2700-2733 (2716 +/-	2438-2563 (2506 +/- 29.911)	3200-3281 (3248 +/- 18.165)

frequency (Hz)		55.698)		22.988)		
Higher fundamental frequency (Hz)	3001-3431 (3165 +/- 91.79)	2636-2839 (2757 +/- 48.063)	2802-3028 (2960 +/- 43.895)	2936-2955 (2946 +/- 12.989)	2818-2967 (2902 +/- 47.896)	3289-3350 (3318 +/- 12.698)
First harmonic (Hz)	5768-6384 (6073 +/- 148.285)	5930-7074 (6322 +/- 295.493)	5843-6229 (5996 +/- 83.465)	6172-6337 (6254 +/- 117.035)	6128-6415 (6268 +/- 78.665)	6054-6573 (6437 +/- 90.211)

1.6 Figures

Figure 1. The distribution of species in the *Boophis albipunctatus* group in southeastern Madagascar. The black dotted line shows the boundaries of Ranomafana National Park (RNP), and partially colored circles indicate syntopy of their corresponding species. The numbered localities are as follows (species occurring at each locality abbreviated as BA, *B. ankaratra*; BB, *B. boppa*, BL, *B. luciae*; BS, *B. schuboeae*): Within RNP: (1) Maharira (BA, BB; type locality of BB); (2) Valohoaka (BL); (3) Vohiparara (BS); (4) Andranoroa river (BA, BB); (5) Sakaroa (BB); (6) Ambatolahy (BL, BS); (7–8) Imaloka (BB, BL); and (9) Andemaka (BB, BL). Outside RNP: (10) Ambohitsara-Ranomafana (BL); (11) Farihimazava (BA, BB); (12) Soamazaka (BA, BB); and (13) Vohisokina (BA, BB). Note that at Ambohitsara, records also exist for another species of the group (*B. albipunctatus*) that is not discussed herein.

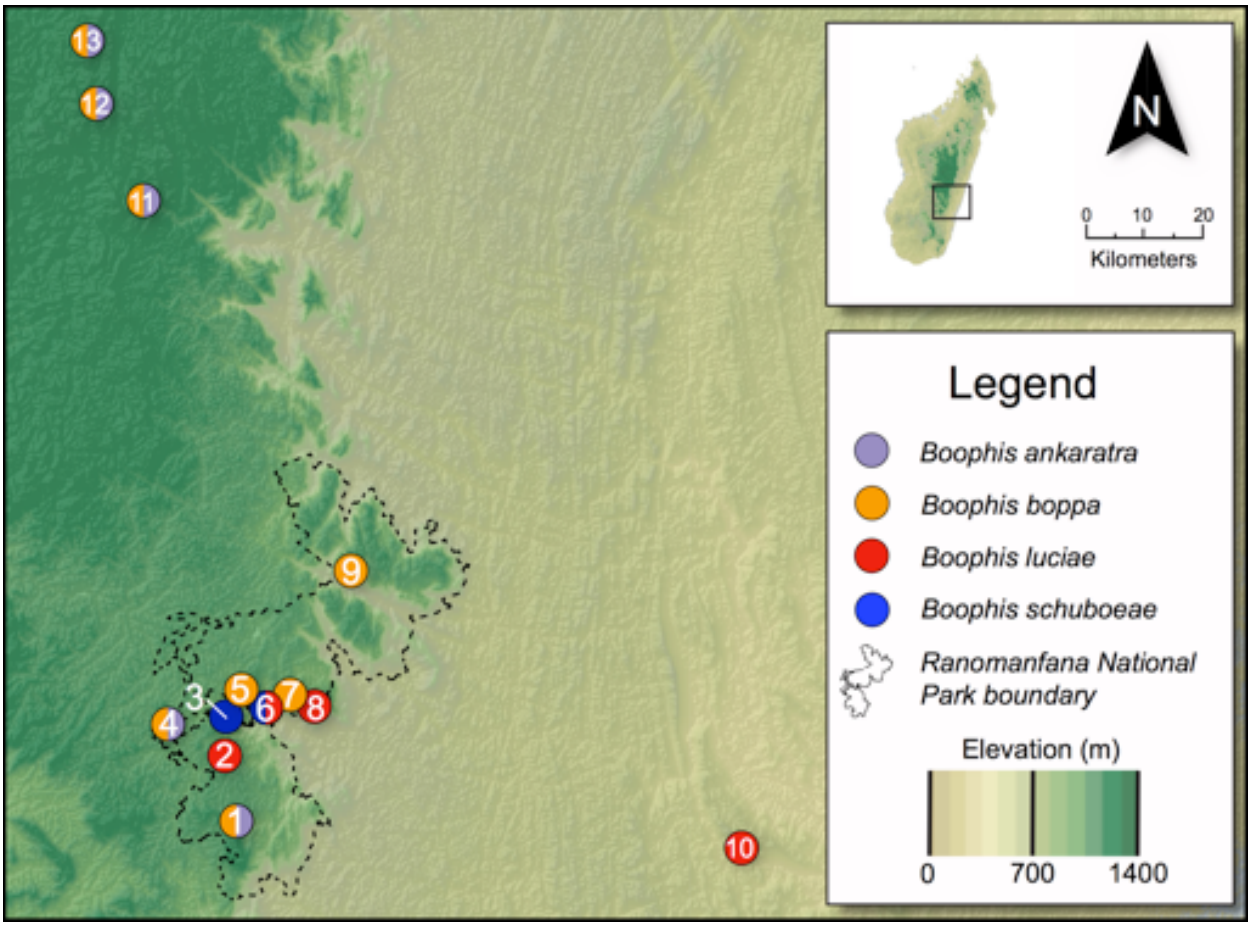

Figure 2. Dorsal view (right) and ventral view (left) of the *Boophis boppa* holotype (KU 336824) in preservative.

Figure 3. *Ex-situ* dorsal and ventral photographs of (**A**) *Boophis boppa* (holotype, KU 336824) and (**B**) *Boophis ankaratra* (KU 336830) in life.

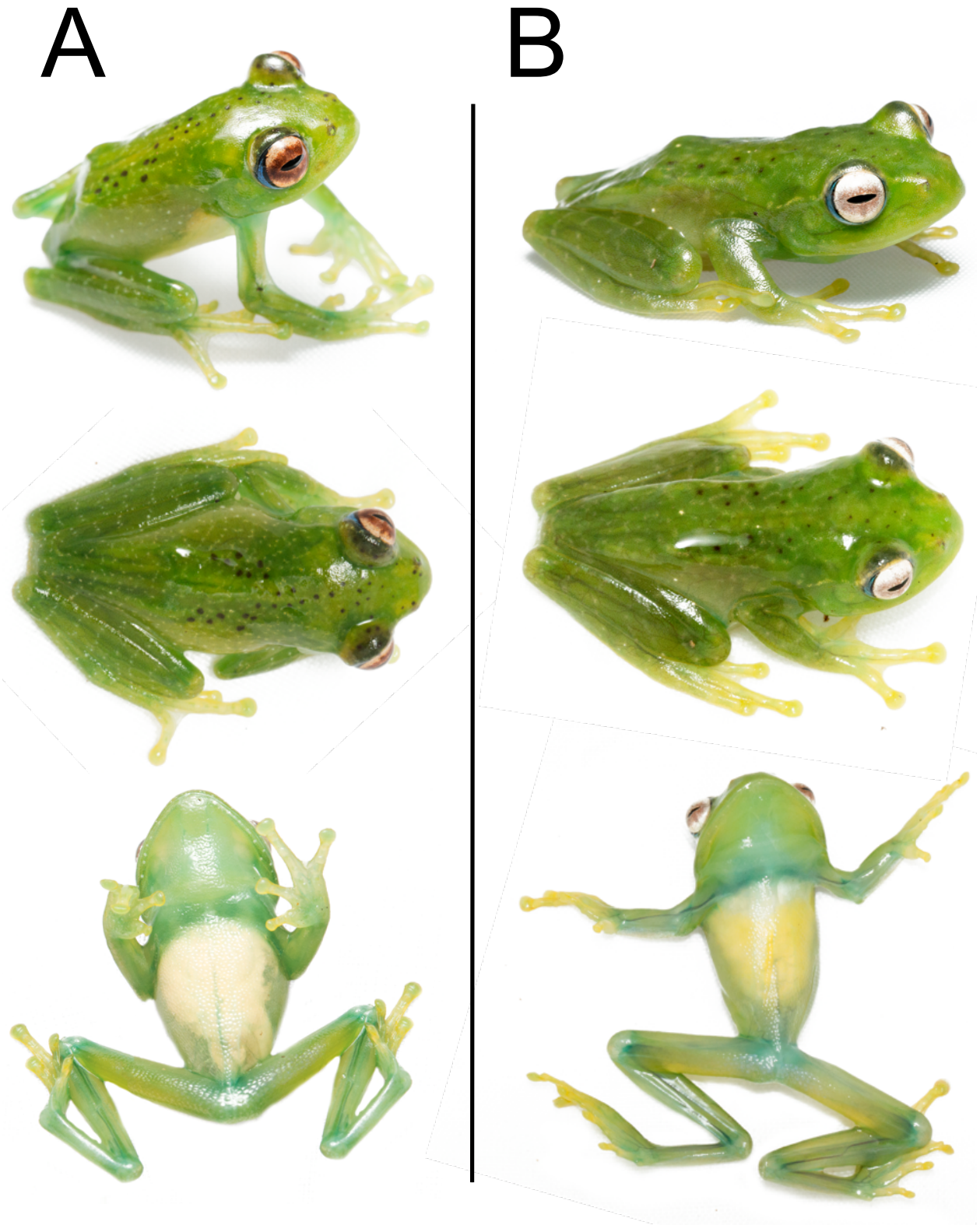

Figure 4. *In-situ* photograph of *Boophis boppa*. (**A**) *in-situ,* specimen not collected. (**B**) close-up view of the eyes from the same individual.

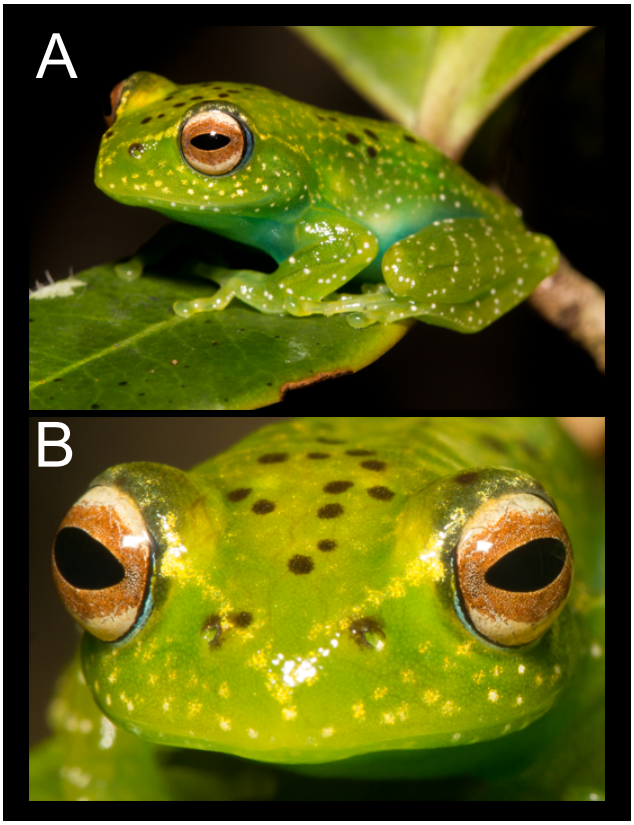

Figure 5. Comparative photographs of members of the *Boophis ankaratra* complex. (**A**) *Boophis ankaratra*; (**B**) *Boophis haingana*; (**C**) *Boophis miadana*; and (**D**) *Boophis schuboeae*.

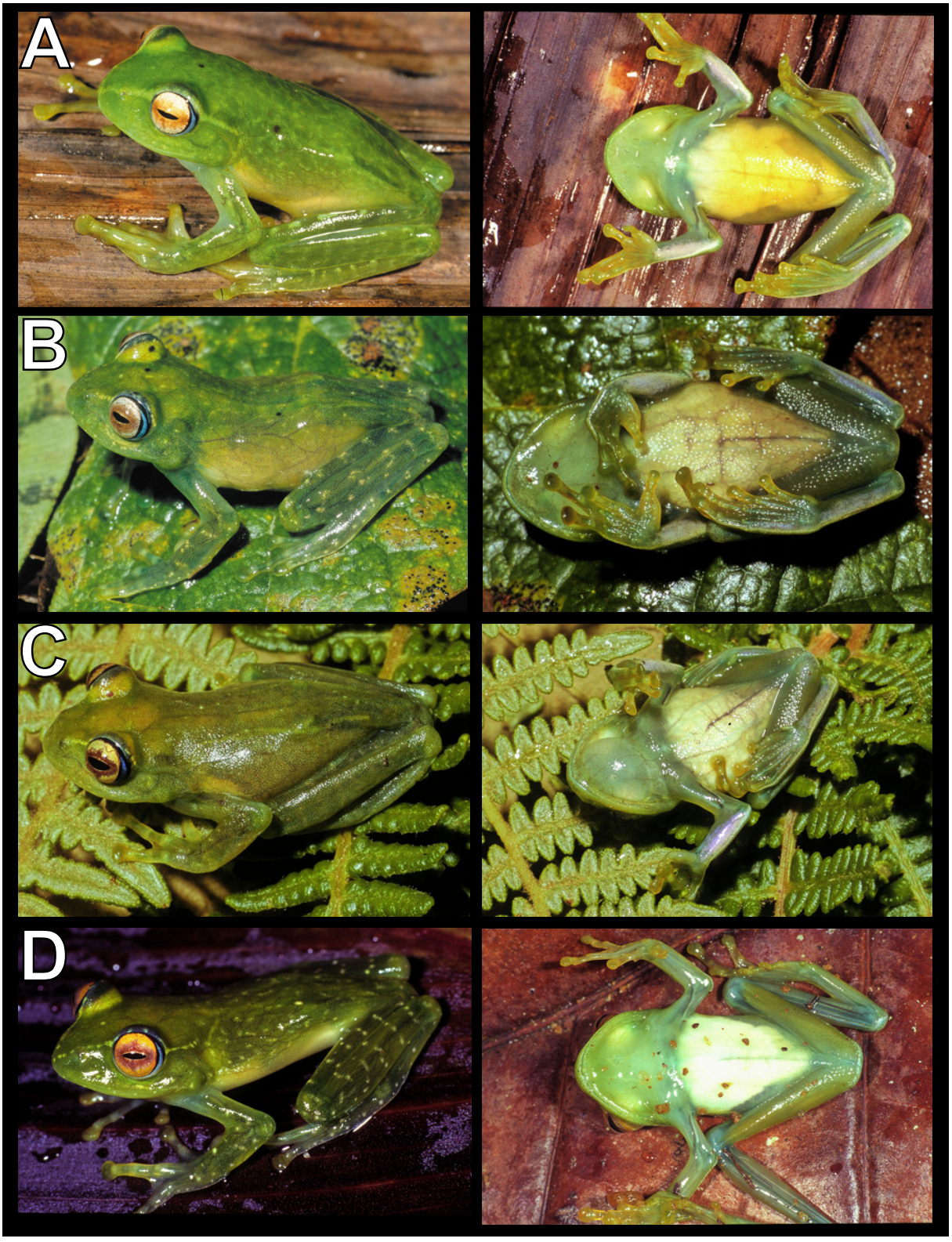

Figure 6. Comparative oscillograms (top) and corresponding spectrograms (bottom) of single notes of the advertisement calls on the same time scale in the *Boophis ankaratra* complex. Species shown are: (**A**) *B. boppa* (Maharira); (**B**) *B. miadana* (Andohahela)*;* (**C**) *B. ankaratra* (Maharira); (**D**) *B. schuboeae* (Ambatolahy); and (**E**) *B. haingana* (Andohahela).

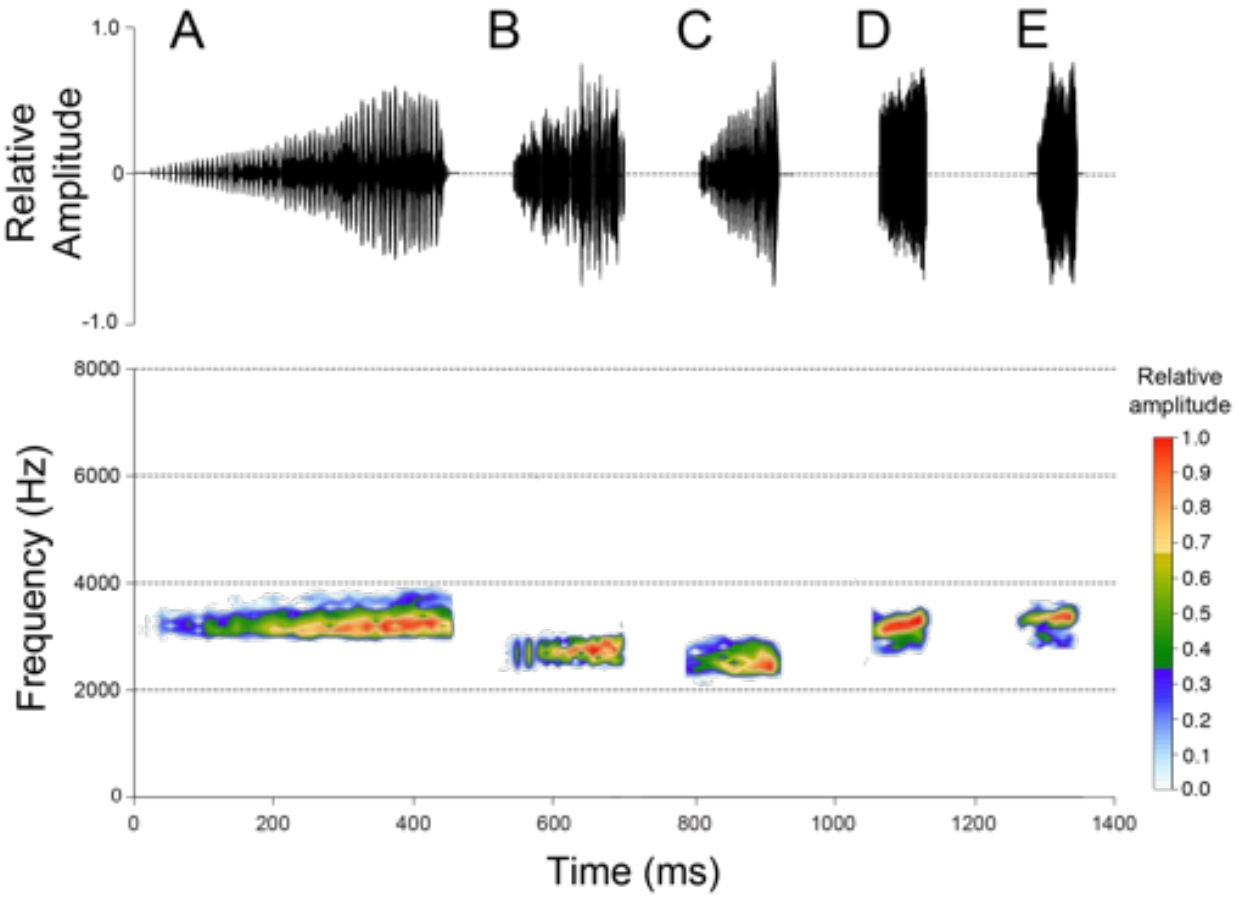

Figure 7. Advertisement call comparative oscillograms of five-second sections in the *Boophis ankaratra* complex. Species shown are: (**A**) *B. boppa*; (**B**) *B. miadana;* (**C**) *B. ankaratra*; (**D**) *B. schuboeae*; and (**E**) *B. haingana*. The localities are the same as Fig. 6.

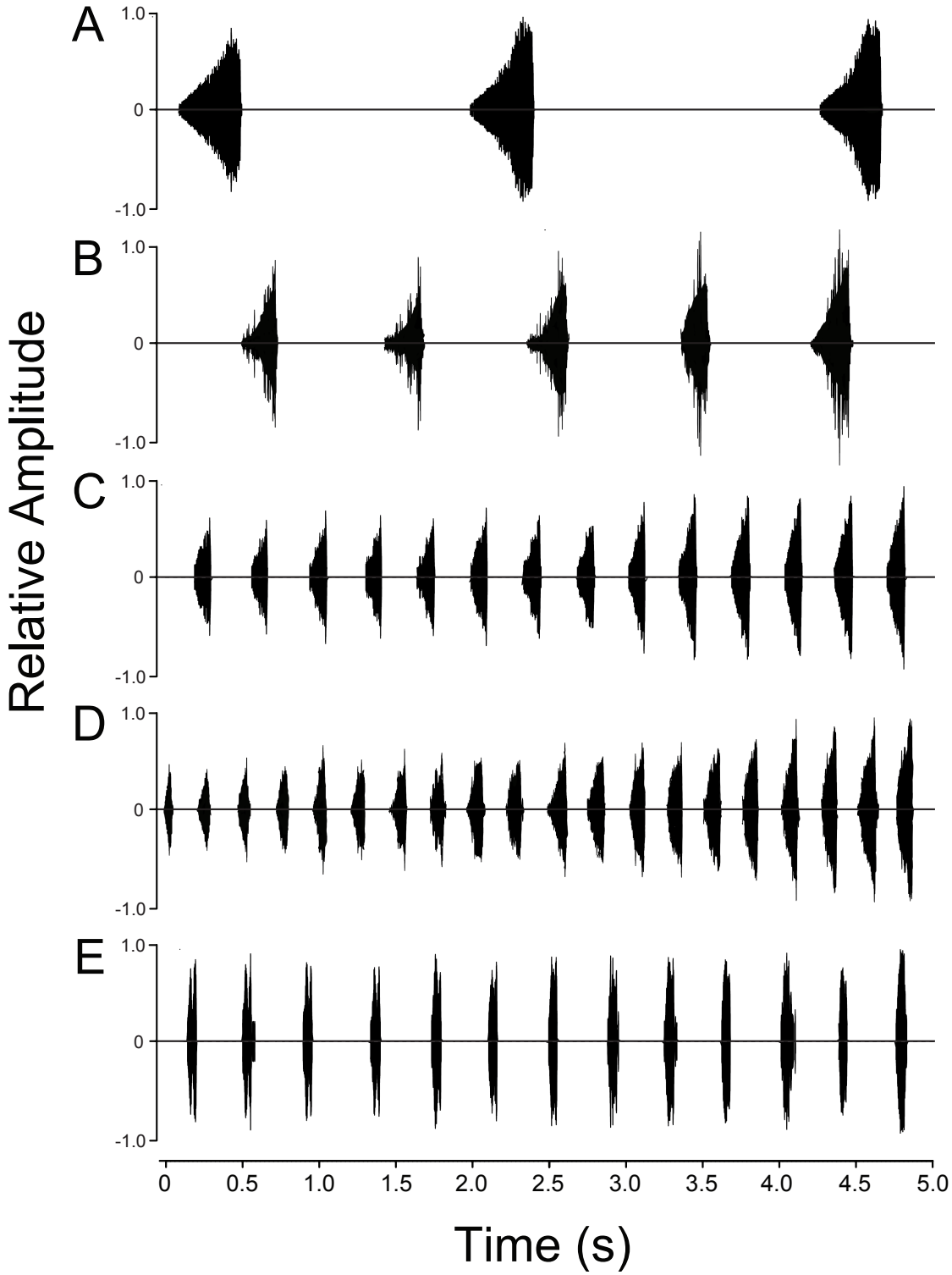

Figure 8. Results of phylogenetic analysis of the concatenated 16S alignment for maximum likelihood (ML) and Bayesian (BA) analyses. Topology is a consensus tree from MrBayes. Significant support for ML and BA analyses are indicated by the black circles at the nodes (analyses were completely consistent). Note that *Boophis boppa* is strongly supported as reciprocally monophyletic with respect to all other species of the *B. ankaratra* species group.

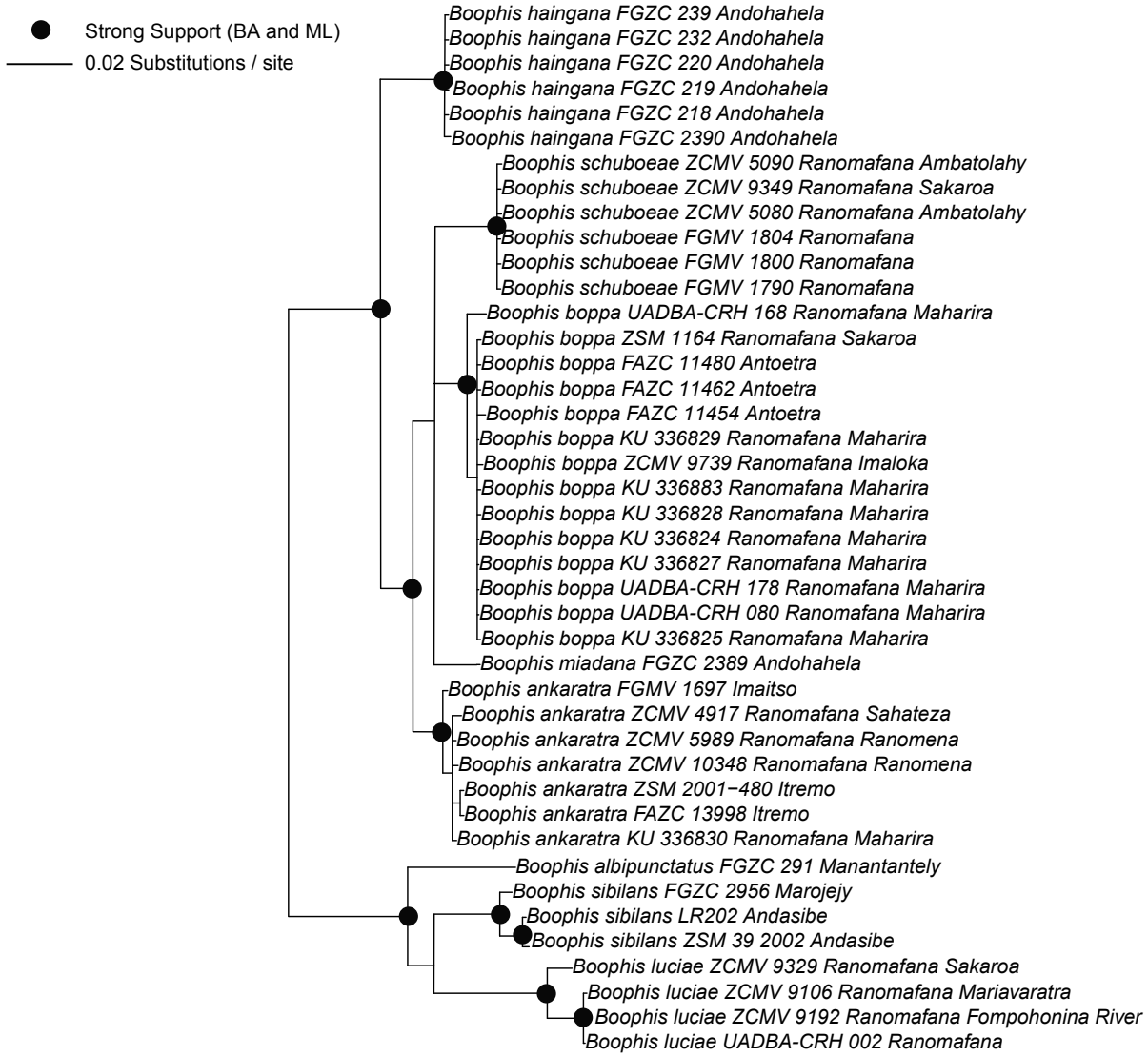

Figure 9. Minimum-spanning haplotype network for the nuclear exon DNAH-3 in the *B. albipunctatus* group. Ticks on branches represent single nucleotide changes. Branch lengths are not meaningful.

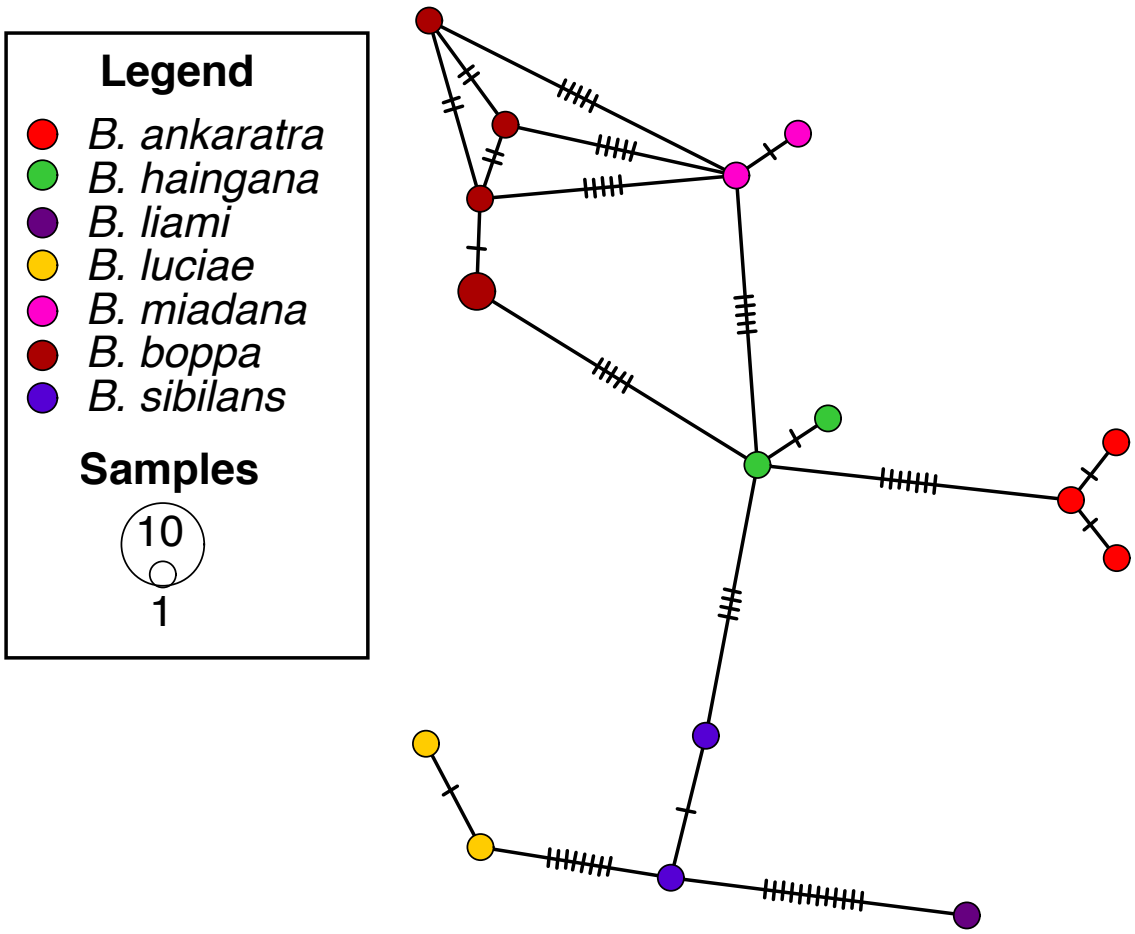

Figure 10. Dorsal pattern and color variation of six living specimens of *Boophis boppa*.

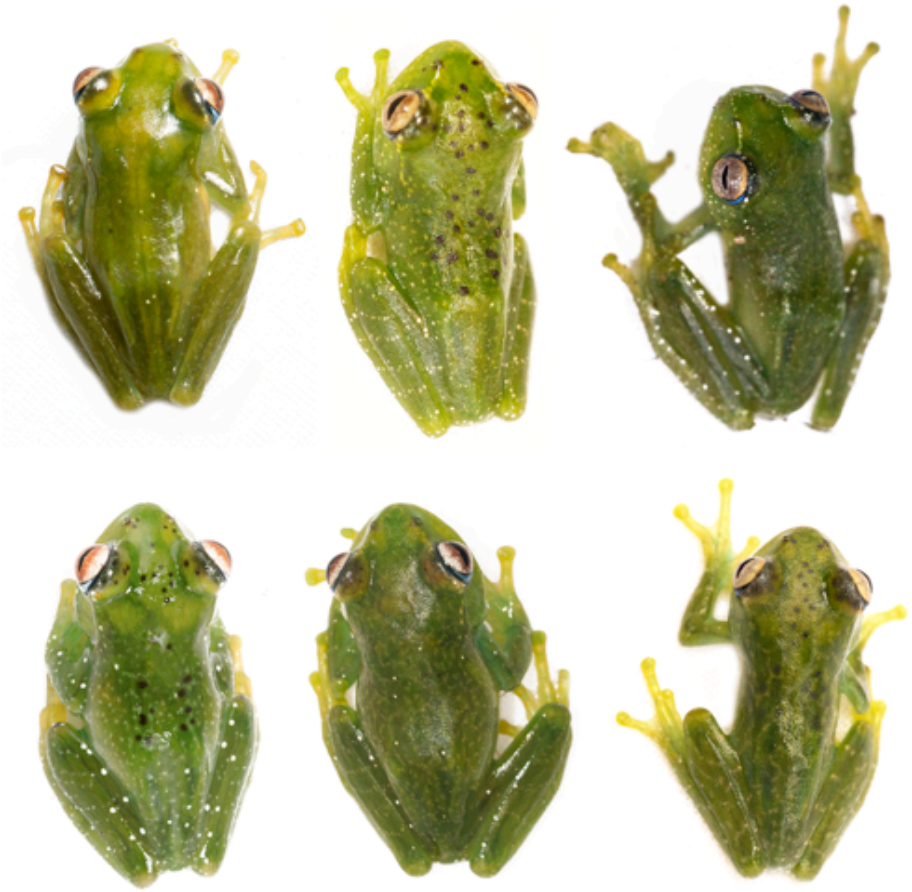

Figure 11. Close-up photographs of different living specimens of *Boophis boppa* showing variation in eye color.

Figure 12. Reproductive behavior of species of the *B. ankaratra* complex. (**A**) A typical perch of a male *B. boppa* preparing to call; (**B**) a male *B. boppa* during emission of advertisement call; and (**C**) amplexus, male not collected, female KU 336829 of *B. boppa*.

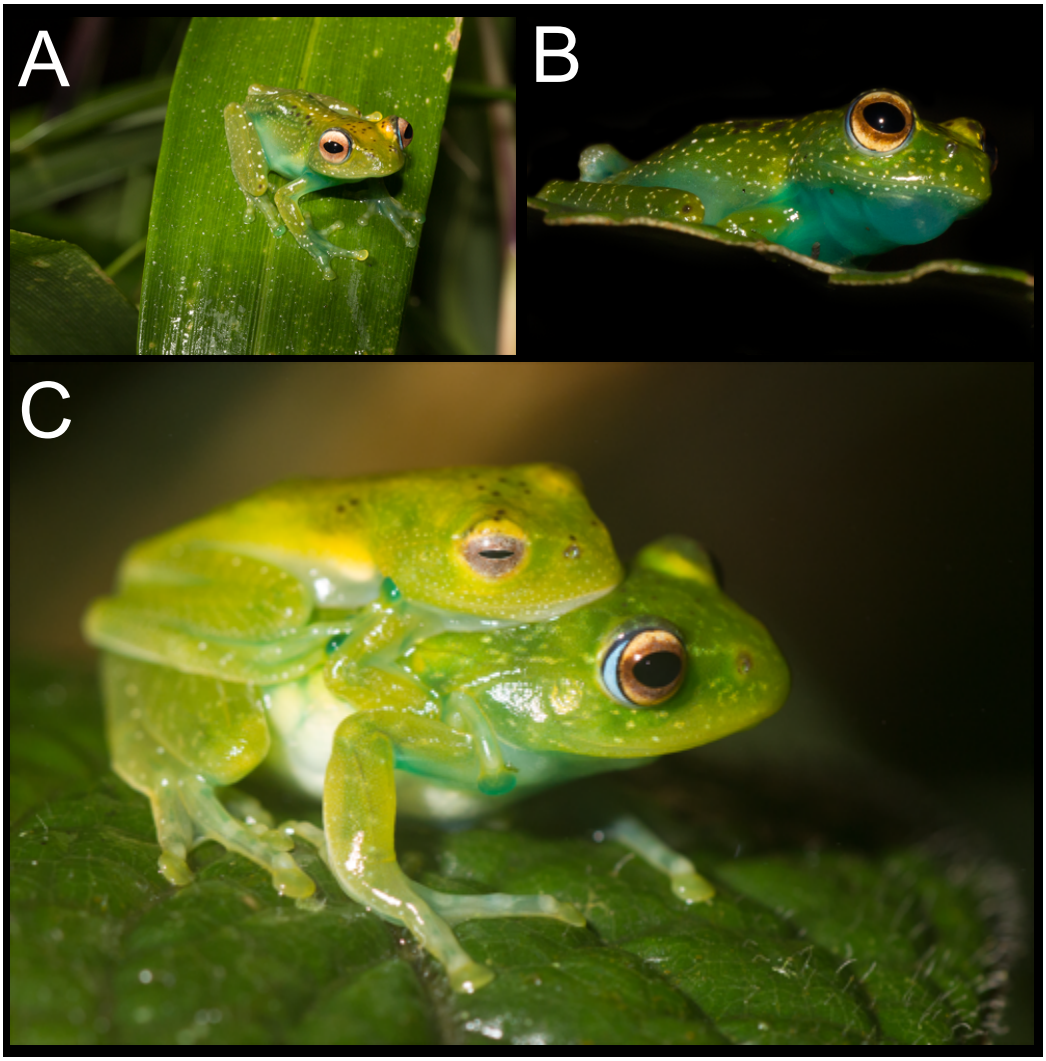

CHAPTER 2

Molecular phylogeny and diversification of Malagasy bright-eyed tree frogs (Mantellidae: *Boophis*)

Hutter C.R., Lambert S.M., Andriampenomanana Z.F., Glaw F., and Vences M. (2018). Molecular systematics and diversification of Malagasy bright-eyed tree frogs (Mantellidae: *Boophis*). *Molecular Phylogenetics and Evolution* 127: 568–578. https://doi.org/10.1016/j.ympev.2018.05.027

2.1 Introduction

Madagascar harbors among the highest rates of amphibian endemism in the world, with exceptionally high species richness relative to land area (Myers *et al.* 2000). Most species belong to the family Mantellidae, and the genus *Boophis* Tschudi, 1838 is the most species-rich genus in the family (AmphibiaWeb 2017). The genus contains mostly arboreal frogs (Cadle 2003), with 77 currently recognized species (AmphibiaWeb 2017) and >30 additional "candidate" species, which are genetically divergent lineages that require formal taxonomic revision (Vieites *et al.* 2009; Perl *et al.* 2014). The relatively recent integration of DNA barcoding and bioacoustic analyses with *Boophis* systematics has revealed numerous such genetically divergent lineages, many of which are morphologically cryptic. This led to the descriptions of 34 new species since 2001 (e. g. Glaw *et al.* 2001; Glaw & Vences 2002; Vences & Glaw 2002; Köhler *et al.* 2007, 2008; Wollenberg *et al.* 2008; Glaw *et al.* 2010; Vences *et al.* 2012; Penny *et al.* 2014; Hutter *et al.* 2015). Despite this recent taxonomic progress, a well-sampled and multi-locus nuclear phylogeny is not yet available for this genus, hindering many potential comparative and biogeographic analyses.

Boophis have previously been divided into two sub-generic monophyletic groups: *Sahona* Glaw & Vences 2006, which includes species that breed in ponds, and *Boophis* Tschudi, 1838, which are predominantly stream-breeding specialists (Glaw & Vences 2006). *Sahona* species are distributed mainly in the lowland rainforests and also in the arid regions of western and southern Madagascar, while species in the subgenus *Boophis* are generally found in rainforests or montane habitats in eastern and northern Madagascar (Glaw & Vences 2006; Glaw *et al.* 2006). In some early phylogenetic analyses, Vences *et al.* (2002) suggested that species now placed in *Sahona* may not form a clade; however, the addition of more taxa and molecular markers in later studies

strongly supported *Sahona* as monophyletic (Glaw & Vences,2006; Glaw *et al.* 2006). The subgenus *Boophis* has greater species richness than *Sahona* (68 vs. 9 species), and contains eight named species groups. Within mantellids, *Boophis* are characterized by a conserved external morphology of adults (Wollenberg Valero *et al.* 2017) and rather uniform karyotypes (Aprea *et al.* 2004), whereas the larvae of these frogs have evolved a remarkable ecomorphological diversity (e.g., Blommers-Schlösser 1979; Blommers-Schlösser & Blanc 1991; Altig & McDiarmid 2006; Randrianiaina *et al.* 2009, 2012; Grosjean *et al.* 2011; Wollenberg Valero *et al.* 2017).

While early researchers placed *Boophis* in the Asian genus *Rhacophorus* (e.g., Guibé 1978), its species were recognized as distinct by Blommers-Schlösser (1979) mostly by their reproductive traits, in particular the absence of foam nesting. This author diagnosed seven species groups within the genus based on morphology and bioacoustics. Several of these groups (*B. opisthodon* group, *B. pauliani* group, and *B. rhodoscelis* group) were later abandoned based on morphology (Blommers-Schlösser & Blanc 1991), and on molecular phylogenetic evidence (Glaw & Vences 2006). Additionally, Glaw & Vences (2006) newly defined the *B. mandraka* group and *B. albipunctatus* group, and transferred the *B. tephraeomystax* group to the subgenus *Sahona* using molecular phylogenetic evidence. The current eight species groups of *Boophis* are: *Boophis albilabris* group, *B. albipunctatus* group, *B. goudotii* group, *B. luteus* group, *B. majori* group, *B. mandraka* group, *B. microtympanum* group (Glaw & Vences 2006), and the recently proposed *B. ulftunni* group (Wollenberg *et al.* 2008; Köhler *et al.* 2008). Despite the numerous works that contributed to understanding the molecular phylogeny of *Boophis* (e.g., Richards *et al.* 2000; Vences & Glaw 2001; Vences *et al.* 2002; Glaw & Vences 2006; Frost *et al.* 2006; Kurabayashi *et al.* 2008; Wollenberg *et al.* 2008, 2011; Pyron & Wiens 2011), many facets of

their evolutionary relationships remain insufficiently supported. More reliably resolving the deep and shallow relationships among species of *Boophis* is a prerequisite for understanding the origin of morphological adaptations in adults and tadpoles (Wollenberg Valero *et al.* 2017), as well as evolution of color pattern (Wollenberg *et al.* 2008) and advertisement calls (Hutter *et al.* 2015).

We here construct a multi-locus phylogeny using Bayesian and maximum likelihood approaches, sampling a total of five mitochondrial and five nuclear genes across all nominal *Boophis* species and 35 candidate species. We use the resulting phylogeny to revisit prior species-group definitions and to test their monophyly. We also discuss subgeneric classification, illustrate repeated evolution of dorsal and ventral coloration, and address the biogeographic history and broad patterns of species diversification in the genus.

2.2 Materials and Methods

2.2.1 Taxon sampling and sequencing

We collected data for 10 genetic markers from 77 nominal *Boophis* species and 35 candidate species through new sequencing and previously published sequences from GenBank (112 total terminals; Table S1). We obtained 365 new sequences and added 338 sequences from GenBank, doubling the amount of molecular data for *Boophis*. We increased the molecular sampling from 10 to 82 species compared to the (mitochondrial + nuclear) multi-locus dataset of Wollenberg *et al.* (2011) and added four additional nuclear markers. Whenever possible, we used a single individual for all markers. In some species, we combined sequences from multiple individuals, but only in situations where sequences of the *16S* rRNA gene were available for all individuals and they were identical or very similar (<1% uncorrected p-distance) in this marker (Table S1). Each marker had varying levels of completeness, and the mean marker completeness

(species sampled per marker) was 74% for recognized species (decreasing to 58% when including all candidate species; see Table 1 for complete summary statistics). All markers had 75% species sampling or greater for recognized species, except rhodopsin, which did not show much genetic variation, so we only included data from past studies. Additionally, we added genetic data for outgroup taxa available in GenBank (Table S1), choosing the species from each genus with the most relevant genetic data available. We included 26 outgroup species from all other genera in Mantellidae and five species from Rhacophoridae.

We extracted genomic DNA from ethanol-preserved tissues using proteinase K (final concentration 20 mg/ml) and a standard phenol-chloroform protocol. We amplified 10 mitochondrial and nuclear markers (Table 1) using polymerase chain reaction (PCR; markers and primers are included in Table S2).

PCR reactions were performed using the following procedure: 1–2 µl genomic DNA, 0.2 µM of each primer, 200 µM of dNTPs, 1.25 U of OneTaq® DNA polymerase, and 5 µl OneTaq® Standard Reaction Buffer (20 mM Tris-HCl, 22 mM NH_4Cl, 22 mM KCl, 1.8 mM $MgCl_2$, 0.06% IGEPAL® CA-630, and 0.05% Tween® 20). The final volume was brought to 25 µl with nuclease-free water. We visualized amplification success using 2 µl of PCR product on 1.5 x agarose gel.

PCR products were purified of excess dNTPs and primers using Shrimp Alkaline Phosphatase (1U/µl) and Exonuclease I (20U/µl). We used the remaining 22 µl of PCR product and added 0.025 µl Exonuclease I, 0.250 µl Shrimp Alkaline Phosphatase and 9.725 µl nuclease-free water for a final volume of 32 µl per reaction. Next, we incubated the samples at 37ºC for 30 minutes and then 95ºC for 5 minutes in a thermocycler. For cycle sequencing, we conducted two separate reactions for the target 5’ and 3’ end DNA strands per purified PCR product. We

prepared a 7 µl sequencing reaction that included 2 µl of the purified PCR product, 1.5 µl of 5X sequencing buffer, 0.5 µl of the forward or reverse primer (separately), 0.5 µl of BigDye Terminator® (version 3.1 sequencing standard, Applied Biosystems) and 2.5 µl of water. The sequence reaction began with 1 cycle at 95ºC for 60 s, and 30 cycles of 95ºC for 15 s, 50ºC for 15 s, and 60ºC for 240 s. In preparation for sequencing, we purified the reaction product of BigDye Terminator® by filtering the product through Sephadex® G-50 in a spin column centrifuged at 850 rcf for 5 min. We collected and visualized sequence data on an Applied Biosystems 3130 automated sequencer. DNA sequences were then manually edited in Geneious R9 (Biomatters, 2016) to trim poor-quality stretches, correct obvious base-calling errors, and identify heterozygous positions.

2.2.2 Phylogenetic analyses and divergence dating

DNA sequences were aligned in Geneious R9 (Biomatters 2016) using MAFFT v7 (Katoh & Standley 2013) and alignments manually inspected for accuracy. The *12S* and *16S* rRNA data were aligned using the Q-INS-I algorithm in MAFFT that considers RNA secondary structure in alignment. We did not remove hyper-variable regions in the *12S* and *16S* alignment for the main analyses since these might be informative to reconstruct relationships among closely related species; however, we also tested the effect of removal using GBLOCKS (Talavera & Castresana 2007) and found no changes in the topology (results not shown). All other genetic markers were protein coding and were manually inspected to ensure an open reading frame was maintained.

Prior to conducting our phylogenetic analyses, we selected optimal partitioning schemes and best-fitting models of sequence evolution for the dataset using PartitionFinder2 (Lanfear *et*

al. 2017). We provided PartitionFinder2 with initially defined data blocks corresponding to three codon positions for each protein-coding gene, and we partitioned *12S* into one partition and *16S* into two partitions based on the two fragments sequenced previously for these taxa. To select a partitioning scheme for tree searches under Maximum Likelihood (ML) optimality criterion to be used in RAxML v8.2.9 (Stamatakis, 2014), we considered only the GTR+G model of substitution, as only one model type can be used for a given RAxML analysis, and used the sample-size corrected Akaike information criterion (AICc) to compare partitioning schemes in PartitionFinder2. To select models and an optimal partitioning scheme for Bayesian Inference (BI) analyses, we considered all the models available in BEAST2 (Bouckaert *et al.* 2014), except for models including a parameter for the proportion of invariant sites ("I") and a parameter for among-site rate variation ("G"; based on the gamma distribution). We avoided such models, as correlation between the "I" and "G" parameters can potentially hinder parameter estimation (Sullivan *et al.* 1999; Yang 2006). We used the Bayesian information criterion (BIC; Schwarz 1978) in PartitionFinder2 to compare model schemes for our BI analyses. The optimized partitioning schemes, and associated models are provided in Table S3.

We ran ML phylogenetic analyses using RAxML v8.2.9. We specified in RAxML the partitions selected by PartitionFinder2 using the -q flag and applied the GTR+G model of evolution to all partitions using the -m flag. We used the -f flag to search for the best-scoring maximum likelihood tree and ran 1000 rapid bootstraps for assessment of support.

For BI phylogenetic analyses and divergence dating, we used BEAST2.4.5. We linked and specified site models according to the optimal scheme selected by PartitionFinder2. We used a single uncorrelated lognormal relaxed clock prior linked across all partitions. Following the recommendations of the BEAST2 authors (https://www.beast2.org/tag/clock-rates), we estimated

relative substitution rates for each partition, with the mean substitution rate fixed to 1, and estimated the relaxed clock rate using an initial value of 1e-9 and a broad prior (in our case, a gamma distribution with a shape parameter of 0.001 and scale parameter of 1000). We used a Yule (speciation) process for the tree prior and ran Markov chain Monte Carlo (MCMC) searches for a total of 100 million generations, sampling every 10000 generations. All BEAST2 analyses were run using the CIPRES Science Gateway v3.3 (Miller *et al.* 2010).

To calibrate our relaxed-clock BI analysis, we tested two different approaches. First, we used a secondary calibration point for the root of Mantellidae. We applied the 95% confidence intervals of the age estimated from Feng *et al.* (2017) as a normal distribution with a mean of 42.5 Myr (35.9–48.9 Myr). Feng *et al.* (2017) includes the largest molecular dataset for frogs and also a robust selection of fossils verified through cladistic analyses. Second, instead of the secondary calibration point, we used the fossil *Indorana prasadi* (Folie *et al.* 2013) to calibrate the age of the most recent common ancestor of Rhacophoridae, the sister group to Mantellidae, which has previously been used for divergence-dating for Rhacophoridae (Li *et al.* 2013). As the minimum age of the *Indorana* fossil is 45 Mya, we used a lognormal prior offset at 45 Mya, with a standard deviation of 1 and a mean of 15, applied to the most recent common ancestor of all of our sampled rhacophorids (which include *Buergeria*, the sister taxon to all other rhacophorids).

For both analyses, we also used a geographic calibration point of the colonization of the island Mayotte by *Boophis* sp. Ca01. Mayotte is a volcanic, oceanic island in the Comoros that has no previous land connections to Madagascar (Audru *et al.* 2010; but see: Hawlitschek *et al.* 2016). The estimated age of the formation of Mayotte is 10–15 Mya (Audru *et al.* 2010); therefore, we assumed that *B.* sp. Ca01 has not split from its extant sister lineages before this time (considering the hypothesis of extinction of these generalized frogs in Madagascar as

unlikely). We set the age of this colonization event at 15 Mya or before, using a broad uniform prior from 15 Ma to the present. Past studies have either calibrated the split between *B.* sp. Ca01 and *B. doulioti* (Wollenberg *et al.* 2011) or *B. tephraeomystax* and *B. doulioti* (Li *et al.* 2013). Given the uncertain results from our maximum-likelihood and Bayesian analyses, we find a strongly supported clade comprising *B.* sp. Ca01 + *B. doulioti* + *B. tephraeomystax,* but no strong support for the relationships among these three species within the clade (see Results for details). Therefore, we apply this calibration to the most recent common ancestor of *B.* sp. Ca01*, B. doulioti,* and *B. tephraeomystax*. Additionally, we used the same calibration for the most recent common ancestor between *Blommersia wittei* and *B.* sp. Ca04, which is endemic to Mayotte island.

We assessed convergence of our MCMC chain using Tracer 1.6 (Drummond *et al.* 2012) checking for acceptably high effective sample sizes for all parameters ('ESS', values of >200 considered acceptable; Drummond *et al.* 2012). We used TreeAnnotator (Drummond *et al.* 2012) to generate a maximum clade credibility tree after discarding the first 25% of generations as burn-in.

2.2.3 Correlated evolution of body coloration

We performed ancestral character reconstruction on the *Boophis* phylogeny to address the evolution of ventral transparency and dorsal coloration. The characters for these two separate analyses were coded as binary, discrete characters as follows: (1) we coded presence of ventral transparency as either fully or partially transparent and opaque coloration as an absence; and (2) we coded the presence of green dorsal coloration as one state and absence of green coloration was coded for all other dorsal colors, which was mostly brown (coding data available in Table

S4). We next used these character states and reconstructed ancestral states using the Mk2 model, which fits the Pagel (1999) model using maximum likelihood to estimate the parameters.

2.2.4 Ancestral range reconstruction

To perform ancestral area reconstructions on the *Boophis* phylogeny, we used the package BioGeoBEARS (BioGeography with Bayesian Evolutionary Analysis in R Scripts; Matzke 2014; R Development Core Team 2017). BioGeoBEARS estimates the ancestral ranges at internal nodes using maximum likelihood, modeling the transitions between geographic ranges along branches as a function of time. The program implements three widely-used biogeographic models: (1) the LaGrange DEC model ("Dispersal-Extinction-Cladogenesis"), which is a probabilistic approach where geographic range is allowed to change along the phylogeny through dispersal or extinction (Ree & Smith 2008); (2) a likelihood version of the Dispersal-Vicariance Analysis ("DIVA-like"), which reconstructs ancestral biogeographic areas using parsimony (Ronquist 1997); and (3) a likelihood version of the range evolution model of the Bayesian Binary Model ("BayArea-like"), which is similar to the DEC model except that it assumes no range changes at cladogenesis (Landis *et al.* 2013). BioGeoBEARS also implements a free parameter (+J) to model founder-event speciation; however, we did not include these models, as founder-event speciation would only apply in situations with an *a priori* hypothesis on such events, for example those hypothesized within island systems (Matzke 2014). We compared the three biogeographic models described above using the Akaike Information Criterion (AIC).

We code geographic regions following Boumans *et al.* (2007), who proposed a scheme based on centers of endemism derived from the watershed hypothesis of Wilmé *et al.* (2006). These regions were: (A) Sambirano; (B) North; (C) North East; (D) Northern Central East; (E)

Southern Central East; (F) South East; (G) South; (H) Central; (I) West; and (J) North West (see Table S5 for species' regions). We also considered a second analysis with a more simplified regional coding, generally based on distribution gaps and centers of endemism (Brown *et al.* 2016): (A) North = Sambirano, North, North West, and North East; (B) North East = Northern Central East; (C) South = South, South-East, and Southern Central East; and (D) Central = West and Central regions (see Table S6 for species region coding). We constrained the analysis to prevent species from occurring in non-adjacent regions (e.g. North and South). Locality information was obtained from a curated database of locality data (Glaw & Vences 2007; updated in Brown *et al.* 2014).

To reconstruct generalized ancestral elevational distributions in BioGeoBEARS, we coded the elevational distributions of species as discrete traits ("Highland" vs. "Lowland" vs. "Both Highland and Lowland"), which should capture the general distribution of each species. For elevation-based analyses, we assumed that we were estimating the general habitats of ancestral species and the organismal traits (e.g. physiology, behavioral habitat selection) underlying these distributions rather than their exact ancestral elevations, which likely changed throughout past climatic changes. We also assumed that these traits are phylogenetically heritable, which is supported by strong phylogenetic signal in the elevational distributions of these species (using the midpoint of their elevational range; Pagel's lambda = 0.992). We obtained elevational distributions for each species by extracting the elevations from the locality dataset (Brown *et al.* 2014) using the R package RASTER (Hijmans & van Etten 2012). We categorized lowland species as those occurring below 700 m and highland species as above 700 m. Species that span across both the lowlands and highland regions were coded as both (coding data available in Table S4).

2.2.5 Diversification rate analyses

We assessed the influence of geographic regions (occurring in highland versus lowland habitats) on diversification rates using the Geographic and Quantitative State Speciation and Extinction likelihood approach (Goldberg *et al.* 2011). We coded the elevational distributions of species as discrete traits following the coding scheme above. We did not use a proportion of species sampled for each state because our phylogeny has complete sampling of nominal species and known candidate species.

We evaluated the influence of elevational distributions on diversification rates across the phylogeny with GeoSSE using the R package DIVERSITREE (v. 0.9–3; FitzJohn 2012). We compared eight different models that constrained speciation, extinction, and dispersal to be different or equal between regions in different combinations. We compared these models to another subset of the same eight models that constrain between-region speciation to zero (i.e. for species in the "both" category). We tested this constraint because between-region speciation may not be important and could result in model over-parameterization. Finally, we compared the log-likelihoods of these models using the Akaike Information Criterion (AIC). AIC differences ≥4 were considered strong support for a given model (Burnham & Anderson 1998).

2.3 Results

2.3.1 *Boophis* systematics

Analyses of the concatenated dataset of the five mitochondrial and five nuclear markers indicate well supported relationships across the tree. Node support for relationships among

species groups differed between ML and BI, with generally weaker support in ML (Fig. 1). These analyses also strongly support monophyly of the two *Boophis* subgenera: *Sahona* and *Boophis,* and most of the previously defined species groups: *Boophis albilabris* group, *B. albipunctatus* group, *B. goudotii* group, *B. luteus* group, *B. mandraka* group, *B. microtympanum* group, and the *B. rappiodes* group. However, the *B. majori* group and the *B. ulftunni* group were found to be non-monophyletic, with some members of the *B. majori* group forming the sister clade to the *B. mandraka* group, and the *B. ulftunni* group nested within the *B. majori* group. Additionally, the *B. ulftunni* group was not monophyletic in any individual gene analysis, and always nested within the *B. majori* group (Fig. 1; Supplemental Tree Files). The *B. majori* group has been noted to be paraphyletic in previous molecular analyses (Glaw *et al.* 2010; Wollenberg *et al.* 2011; Vences *et al.* 2012).

The phylogenetic results also suggest several striking instances of repeated evolution in morphology: (1) ventral transparency occurs in the unrelated *B. mandraka* and *B. rappiodes* groups, and additionally to a lower degree in the *B. albipunctatus* group and *B. pauliani*; (2) small body size combined with broad and short heads, slender limbs, and brown body coloration occurs in the two non-sister clades of the *B. majori* group and a new group defined below; and (3) small-bodied frogs with smooth and uniform green body coloration without ventral transparency characterize some species of the *B. luteus* group and the paraphyletic "*B. ulftunni"* group (Fig. 2). Other frogs from the *B. albilabris* group, *B. microtympanum* group, and *B. pauliani* have green body coloration, but differ through larger body size, non-uniform green body coloration, or have a tuberculate dorsum. Given the difficulty in assigning ancestral or derived states for these observations, we use ancestral reconstruction methods described above to address patterns of potential repeated evolution in morphology.

2.3.2 Diagnosis of the newly proposed *B. blommersae* group

Frogs of the *B. blommersae* group are characterized by: (1) small size (adult male snout-vent length 20–27 mm); (2) usually brown dorsal ground coloration (rarely greenish in *B. blommersae*); (3) white to cream colored venters (not transparent); (4) complete absence of red coloration ventrally, dorsally or on the webbing, both in in life and in preservative; (5) hindlimbs with (sometimes indistinct) dark crossbands; (6) vomerine teeth present; (7) single subgular vocal sac in calling males; (8) webbing between external fingers present; (9) no dermal flaps or tubercles on heels; (10) dorsal integument of breeding males not more granular than of females; (11) egg deposition and larval development in fast flowing streams; and (12) tadpoles with suctorial mouthparts, including a large oral disc without any dorsal gap of papillae and with many labial tooth rows and papillae.

Frogs of the *B. blommersae* group differ from most brown species of the phenotypically similar *B. majori* group by complete absence of red pigment and generally reproduce in slower moving streams. Their tadpoles differ by having suctorial mouthparts, whereas tadpoles in the *B. majori* group (as far as is known) have generalized to strong reductions of their keratinized mouthparts (Randrianiaina *et al.* 2012).

Frogs of the *B. blommersae* group differ from the phylogenetically closely related species of the *Boophis mandraka* group by brown ground coloration (versus green) and by non-transparent ventral skin (versus transparent). Their tadpoles differ by having an oral disk without dorsal gap of papillae (versus oral disk with dorsal gap in the *B. mandraka* group).

2.3.3 Revised diagnosis of the *Boophis majori* group

The newly defined *Boophis majori* group is characterized by: (1) small size (adult male snout-vent length 18–33 mm); (2) brown or green dorsal ground coloration; (3) white to cream colored venters (not transparent); (4) presence in many brown species of red coloration ventrally, dorsally or on the webbing, both in in life and in preservative; (5) hindlimbs with or without dark crossbands; (6) vomerine teeth present or indistinct; (7) single subgular vocal sac in calling males; (8) webbing between external fingers present; (9) no dermal flaps or tubercles on heels; (10) dorsal integument of breeding males not more granular than of females; (11) egg deposition and larval development usually in slowly flowing streams; and (12) tadpoles with generalized or reduced keratinized mouthparts.

2.3.4 Divergence dating

Testing the two different node calibrations resulted in somewhat different mean ages for the two chronograms. The chronogram that used the secondary calibration from Feng *et al.* (2017) gave an age of ~45 Myr for Mantellidae and ~35 Myr for *Boophis.* In contrast, the inclusion of the Rhacophoridae fossil on the second chronogram gave an older age of ~55 Myr for Mantellidae and ~45 Myr for *Boophis* (Table 2). The difference shown here is a ~20% difference in ages, which is also observed across other clades in the tree (Table 2).

Earlier mitochondrial DNA studies revealed a different relationship among *Boophis* sp. Ca01*, B. doulioti,* and *B. tephraeomystax* (e.g. Wollenberg *et al.* 2011), which are taxa important in the application of a geographic calibration point in divergence dating (Wollenberg *et al.* 2011; Li *et al.* 2013). Here we find that *B.* sp. Ca01, *B. doulioti,* and *B. tephraeomystax* form a strongly supported clade in both analyses; however, our ML vs. BI analyses yield two different topologies

for this clade (Supplemental Tree Files). Maximum Likelihood groups *B.* sp. Ca01 and *B. doulioti,* while BI groups *B. doulioti* + *B. tephraeomystax.* Therefore, the geographic calibration of the colonization of Mayotte by *B.* sp. Ca01 is uncertain, and we calibrate it using the strongly supported node representing the most recent common ancestor of the three species.

2.3.5 Correlated evolution of body coloration

Ancestral reconstructions support the independent evolution of ventral and partial ventral transparency four times in *Boophis*: the *B. rappiodes* group, the *B. mandraka* group, and as partial transparency in the *B. albipunctatus* group and in *B. pauliani* from the subgenus *Sahona* (Fig. 2). Additionally, the ancestral reconstructions support the opaque ventral coloration as the ancestral state whereas transparent venters are supported as derived characters. The reconstructions also support an ancestrally green dorsal coloration whereas the brown coloration is supported as the derived state, evolving four times independently. The presence of green dorsal coloration in extant *Boophis* is more widespread than ventral transparency, with ventral transparency evolving independently within clades of dorsally green *Boophis* (Fig. 2).

2.3.6 Ancestral range reconstruction

The BioGeoBEARS analysis supported the DIVALIKE model, with an AIC difference of 5 from the BAYAREALIKE model (Table 3). The biogeographic reconstructions from the DIVALIKE model of 10 areas suggest a Southern Central East initial diversification of the genus *Boophis* (Fig. S1), while the four-area analysis suggests a North East (North Central East) initial diversification (Fig. 3; see Fig. S2 for pie chart-based marginal probabilities at each node). Most species groups were also found to have originated in these two areas, depending on the analysis.

In contrast, the *B. blommersae* group and *B. albilabris* group originated in Northern regions in both analyses. Finally, the subgenus *Sahona* was found to have originated in the Southern Central East region, with multiple dispersals into the arid Western and Central regions (Fig. 3).

Biogeographic reconstructions of lowland and highland habitats place most species groups originating in highland areas. The subgenus *Sahona*, the *B. luteus* species group, and the *B. albilabris* species group are exceptions, having originated in the lowlands. There was also a later colonization of highland areas by *Sahona* and a recolonization of highland regions within the *B. luteus* species group (Fig. 3). These results also indicate at least for the subgenus *Boophis* that after the initial diversification of *Boophis* in highland regions, some subgroups of these frogs dispersed more recently into the lowlands.

2.3.7 Diversification rate analyses

The comparison of the eight different diversification models from GeoSSE supports four models within an AIC difference of four from the lowest AIC model (Table S7; similar results for the alternative chronogram in Table S8). The best-fitting model constrains equal extinction among highland and lowland lineages, while in the other supported models the extinction rate is near zero. Importantly, all of the supported models suggest higher diversification rates for highland lineages when compared to lowland lineages and are more strongly supported than minimal models with speciation rates constrained to be equal (Table S7). Higher highland speciation rates are also supported by confidence intervals estimated from posterior probability distributions from the full GeoSSE model, while lowland and both regions have larger uncertainty and are non-overlapping (Fig. 4). Finally, these models support a higher dispersal rate of lineages from the highlands to lowlands.

2.4 Discussion

2.4.1 *Boophis* systematics

Previous molecular analyses have suggested that the *B. majori* group is non-monophyletic, with species similar to *B. marojezensis* being more closely related to other clades (e.g., Glaw & Vences 2006; Wollenberg *et al.* 2011). Despite extreme similarity in external morphology of adults, drastic differences in tadpole morphology also suggest non-monophyly of the group (Raharivololoniaina *et al.* 2006; Randrianiaina *et al.* 2009, 2012). However, previous molecular analyses of *Boophis* were limited by the number of included taxa (e.g. Glaw & Vences 2006; Wollenberg *et al.* 2011), or were based on single mitochondrial markers (Vences *et al.* 2002; Vieites *et al.* 2009; Perl *et al.* 2014). Our study expands upon these previous studies with a large increase in sampled species and molecular markers, confirming previous observations of non-monophyly of the *B. majori* group. In particular, the species *Boophis marojezensis*, *B. vittatus*, and *B. blommersae* and associated candidate species, characterized by suctorial tadpole morphology (Raharivololoniaina *et al.* 2006; Randrianiaina *et al.* 2012), form a strongly supported sister clade to the *B. mandraka* group (Fig. 1). Given the dissimilarity of these species to those of the *B. mandraka* group in adult morphology, we propose a new species group, the *B. blommersae* group, to accommodate *B. marojezensis*, *B. blommersae*, *B. vittatus,* and all related candidate species (see Appendix A for a diagnosis of the *B. blommersae* group).

We also recover the *Boophis ulftunni* group as paraphyletic (*B. lilianae* placed separately from the *B. baetkei* + *B. ulftunni* clade). All three species are nested within the *B. majori* group in all combined and single-gene analyses (Supplemental Tree Files), and the clade comprising the species of the *B. ulftunni* + *B. majori* groups is strongly supported in BI and ML analyses (Fig. 1). Therefore, we propose to dissolve the *B. ulftunni* group and to transfer the species *B.*

baetkei, *B. lilianae*, and *B. ulftunni* to the *B. majori* group (see Appendix B for an updated diagnosis for the *B. majori* group).

2.4.2 Divergence dating

We estimated divergence dates for *Boophis* using two calibration points not yet used for the genus and Mantellidae specifically, and find an overall agreement of the resulting chronograms in placing the early divergence of these frogs during the Eocene. Our first analysis used a secondary calibration for the root of Mantellidae from Feng *et al.* (2017), where our results estimated an age for *Boophis* of ~35 Mya. Our second analysis used a newly available, but little tested fossil calibration (*Indorana prasadi*; used in Li *et al.* 2013 and Lv *et al.* 2018), giving a set of ages that are ~20% older across different clades in the chronogram (Table 2). The *I. prasadi* fossil might be a problematic calibration, as the original description of the fossil expressed uncertainty that the species should be included in Rhacophoridae (Folie *et al.* 2013). In addition, the fossil has not been evaluated in a phylogenetic analysis, and it might not conclusively place the fossil as it is a small fragment with few characters (Folie *et al.* 2013). Furthermore, one recent divergence dating study (Lv *et al.* 2018) uses this fossil, but a response to this work suggests that the ages are significantly overestimated and lead to biogeographically implausible scenarios (Ali 2018). Previous studies have warned that different applications of calibrations could potentially lead to large differences in age estimates (Ho & Phillips 2009; Parham *et al.* 2011), yet it is encouraging that in our case, the differences were comparatively moderate. The ages estimated in Feng *et al.* (2017) were based on the largest molecular dataset for frogs and also a robust selection of fossils verified through cladistic analyses, and the obtained divergence dates agree with other studies on Malagasy frogs, e.g., the *Boophis* crown

age (~35 Mya) agrees with Wollenberg *et al.* (2011), and the calibration itself (mantellid root at 45 Mya) roughly agrees with Crottini *et al.* (2012) who estimated this node at 51 Mya. In any case, the biogeographic and diversification analyses carried out herein had the same results for our two alternative chronograms, and the different ages had little impact because we were not attempting to address absolute ages. Considering the uncertainty in the phylogenetic relationships of the *I. prasadi* fossil, the criticism of Lv *et al.* (2018) by Ali (2018), and our results, we caution against using this fossil calibration for future divergence dating in frogs.

2.4.3 Correlated evolution of body coloration

Our results show that ventral transparency is a derived state that has evolved four separate times in *Boophis*, whereas green body coloration is reconstructed as an ancestral state that gave rise to other body colorations (i.e. shades of brown) four separate times in the genus (Fig. 2). These results are surprising because the derived transparent ventral state is found in only frogs with green dorsal coloration, and the idea of both green dorsal color and ventral transparency being derived states might be more intuitive. Instead, our results support the idea that the evolution of green body coloration precedes the evolution of ventral transparency, and they did not evolve at the same time in ancestral species (Fig. 2). A validation of this hypothesis would require a more comprehensive phylogenetic sampling of Mantellidae; while green color is rare in many mantellid genera, it also occurs in the relict species *Tsingymantis antitra* (see photos in Glaw & Vences 2007), a species splitting basally in Mantellidae (Wollenberg *et al.* 2011), increasing the plausibility of a dorsally green ancestor of *Boophis*.

The evolution of ventral transparency can be observed multiple times in other distantly related frogs, especially in the Neotropical glassfrogs, family Centrolenidae (Guayasamin *et al.*

2009), but also in single lineages of other families such as the African reed frogs, family Hyperoliidae (Dehling 2012). However, this study is the first to report multiple origins of this trait in sympatric clades of a single genus of frogs. Although the precise adaptive value of the transparent ventral skin is still unknown, it is relevant to note that in all known cases, the "glassfrog morphotype" with full ventral transparency evolved in small-sized arboreal treefrogs of predominantly green dorsal color and bluish-green colored bones.

2.4.4 *Boophis* diversification

We find an initial diversification of *Boophis* frogs generally in the Eastern highland forest regions (i.e. Southern Central East or North Central East) of Madagascar, which also has the highest species richness for this genus (Brown *et al.* 2014; Brown *et al.* 2016) and for mantellids in general (Colwell and Lees, 2000). This pattern differs from other organisms in Madagascar, where previous studies have suggested a Northern origin (cophyline frogs: Andreone *et al.* 2005, Wollenberg *et al.* 2008; *Gephyromantis* frogs: Kaffenberger *et al.* 2012; *Brookesia* leaf chameleons: Townsend *et al.* 2009). Additionally, the biogeographic analysis of ancestral elevational areas revealed most *Boophis* diversifying in highland regions ~20 Mya, and then later dispersing to the lowlands (the subgenus *Sahona, B. albilabris* species group, and *B. luteus* species group being exceptions). This hypothesis applies to the subgenus *Boophis* clade; whether the ancestor of the whole genus would be highland or lowland is less obvious, given that other mantellid clades splitting from basal nodes (*Tsingymantis* and the laliostomines) are predominantly lowland frogs. Independent from this restriction, our diversification analyses provide support for higher diversification rates of *Boophis* in highland regions, with a high dispersal rate from highland to lowland regions, supporting these prior reconstructions (Fig. 4).

This supports the montane museum hypothesis, previously suggested as playing a partial role in influencing species richness patterns of *Boophis* (Brown *et al.* 2014), and supported in explaining high mid-elevation richness in many organisms globally (e.g., Tibetan fish: Li *et al.* 2009; Appalachian salamanders: Kozak & Wiens 2010; Andean frogs: Hutter *et al.* 2017). Together these results suggest that mountain regions might have been important centers of *Boophis* diversification with a rapid accumulation of species richness relative to other regions, and also as a source of diversity through recent dispersals into lowlands.

Most of the stream-breeding species groups of *Boophis* originated 30–40 Myr ago, and many of them diversified within the highlands ~20–25 Myr ago (Fig. 3). These diversification events also correspond to the formation of the Indian Ocean Monsoon season around the upper Oligocene, early Miocene boundary (Prell & Kutzbach 1992). These rapid environmental changes have previously been hypothesized to be important for initiating strong selection and rapid diversification of morphology for adults and tadpoles across Mantellidae frogs (Wollenberg Valero *et al.* 2017). It is of relevance that virtually all of these species are stream breeders, whereas only the relatively species-poor subgenus *Sahona* contains pond-breeding species (Vences *et al.* 2002). This differs from the situation in other treefrog clades such as rhacophorids, hyperoliids, and many groups of hylids, where most species breed in lentic water bodies (Wells 2007); glassfrogs (Centrolenidae) are another of the few examples of species-rich treefrog clades reproducing predominantly or exclusively in lotic environments. We speculate that the scarceness or absence of fishes in tributary streams in Malagasy rainforests, especially in the highlands, contributes to the high species richness and individual densities of tadpoles in these water bodies (Strauß *et al.* 2013), and the same factor might also have favored speciation and radiation of stream-breeding *Boophis*. A further relevant factor is Madagascar's topography,

including a central mountain chain from north to south, which leads to substantial and regular relief rainfall along the east coast. Additionally, the eastern rainforest areas are characterized by a rather steep, heterogeneous topography with few flat areas and consequently few lentic water bodies. A comparative study of synecological factors such as density of aquatic predators, topographic factors influencing habitat availability, and palaeoclimatic factors, across different continents, could help explain why frog ecomorphs differ in their relative diversity across continents.

2.5 Tables

Table 1. Summary of sampling for genetic markers for *Boophis*. Includes all 77 described species and 35 candidate species (112 total *Boophis* terminals).

Marker	Length (bp)	Number of (ingroup) species sampled	Parsimony-informative sites (with outgroups)	Parsimony-informative sites (without outgroups)
12S	618	69 (63%)	296	250
16S (part 1)	792	76 (69%)	373	288
16S (part 2)	634	107 (97%)	252	206
CO1	625	86 (78%)	272	256
Cyt-b	535	75 (68%)	328	295
ND1	1151	61 (55%)	634	590
DNAH3	909	41 (37%)	90	90
POMC	512	45 (54%)	123	64
RAG1	726	61 (41%)	171	105
RAG2	626	64 (58%)	220	129
Rhod	316	18 (16%)	46	16
Summary	7444 bp	Mean = 58%	2805	2289

Table 2. Summary of the comparison between two different node-based calibrations we used for divergence-dating in *Boophis*. The secondary calibration point was used from the ages estimated for Anura in Feng *et al.* (2017), while the fossil calibration was from *Indorana prasadi* (Folie *et al.* 2013). The ages are compared for important clades and species groups between the two trees, and ancestral biogeographic area reconstruction was identical between trees.

Clade	Secondary calibration age (Myr)	Fossil calibration age (Myr)	Ancestral Biogeographic Area
Rhacophoridae	42.2	51.5	-
Mantellidae	44.4	56.2	-
Boophis	35.1	44.3	South East
B. tephraeomystax	31.5	39.7	South East
B. albilabris	9.5	12.0	North Central East + South East
B. goudotii	21.3	26.8	South East
B. blommersae	13.3	16.9	North + North Central East
B. mandraka	15.0	18.9	North Central East
B. albipunctatus	15.7	19.9	South East
B. luteus	17.6	22.2	North + North Central East
B. rappiodes	15.5	19.6	South East
B. microtympanum	12.8	16.0	South East
B. majori	16.6	21.1	South East

Table 3. Summary of the results from BioGeoBEARS. The most strongly supported model from each set of models is bolded, selected using the Akaike Information Criterion (AIC).

Analysis	Model	Log Likelihood	Parameters	Dispersal	Extinction	AIC
10 Regions	DEC	-356.2	2	0.007	0.007	716.5
	DIVALIKE	**-342.7**	**2**	**0.008**	**0**	**689.4**
	BAYAREALIKE	-345.7	2	0.005	0.053	695.5
4 Regions						
	DEC	-279.6	2	0.022	0.012	563.1
	DIVALIKE	**-223.3**	**2**	**0.015**	**0**	**524.0**
	BAYAREALIKE	-284.3	2	0.009	0.049	572.5
2 Regions	DEC	-110.6	2	0.035	0	225.4
Elevations	**DIVALIKE**	**-107.9**	**2**	**0.038**	**0**	**219.9**
	BAYAREALIKE	-128.5	2	0.031	0	261.1

2.6 Figures

Figure 1. Consensus ultrametric phylogeny of the genus *Boophis* obtained from Bayesian Inference (BI) with BEAST, combined with support values from the Maximum Likelihood (ML) analysis from RAxML. We used five mitochondrial and five nuclear markers, totaling 7444 bp of concatenated DNA for these analyses. Circles at nodes represent support values, with the top circle indicating BI posterior probability (PP) support and the bottom circle showing the ML bootstrap (BS) support. Colored branches represent species groups as labelled at nodes, with a photo of a representative species from each species group. The *B. majori* group includes species formerly included in the *B. ulftunni* group (*B. baetkei*, *B. lilianae*, and *B. ulftunni*). Additionally, the *B. blommersae* group is described for the first time in this study. Photographs by CR Hutter.

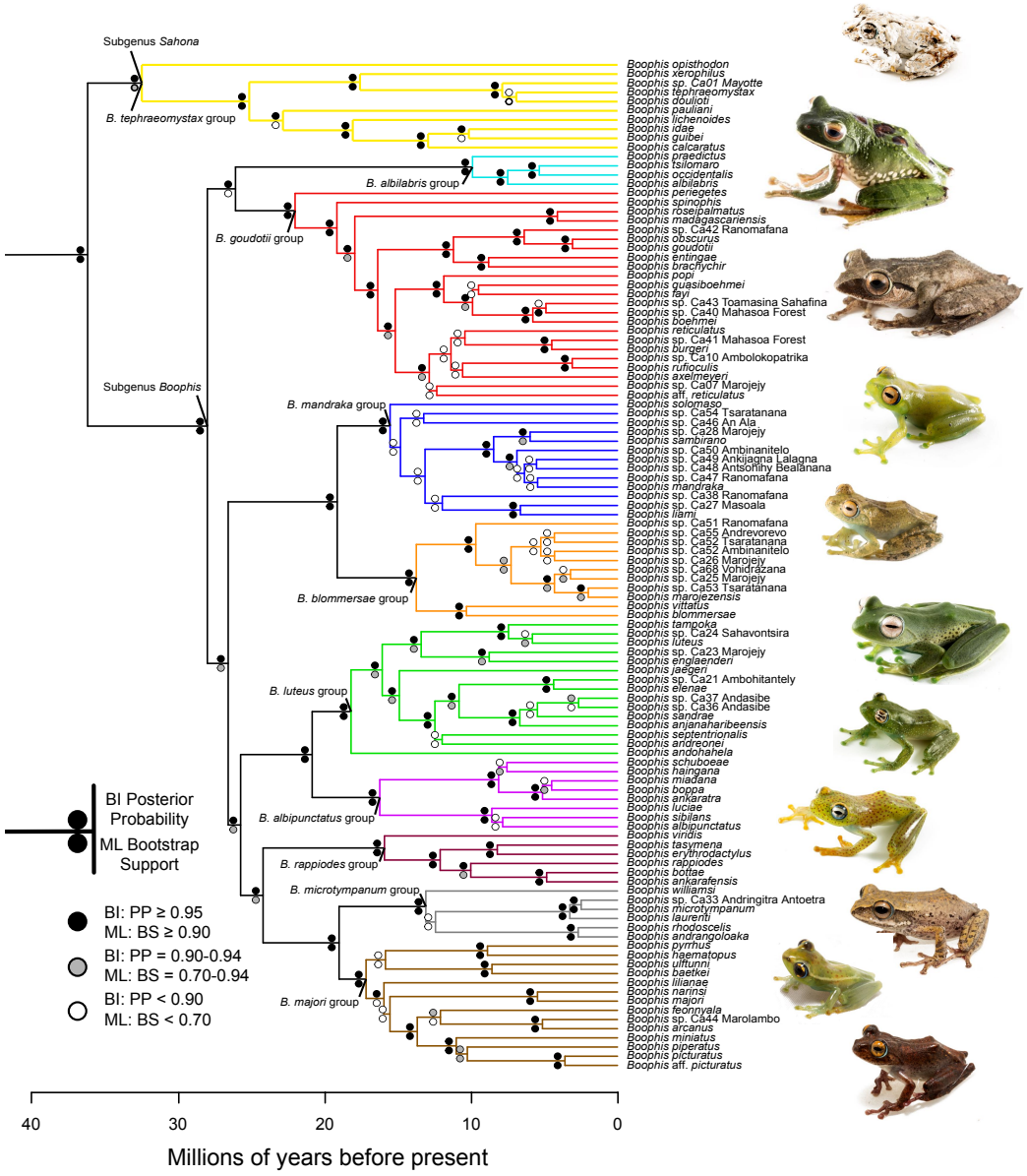

Figure 2. Ancestral reconstructions of ventral transparency (on the left) and dorsal coloration (on the right) in *Boophis*. These reconstructions show that transparent venters are the derived state and also illustrate striking examples of repeated evolution of ventral transparency in the *B. mandraka* group, *B. albipunctatus* group, *B. rappiodes* group, and to a lesser extent in *B. pauliani*. Additionally, ancestral reconstructions of dorsal coloration show that green dorsal coloration is the ancestral state while brown dorsal coloration has repeatedly evolved in *Sahona*, the *B. goudotii* group, the *B. blommersae* group, and *B. majori* group. Together these results suggest that green dorsal coloration is a precursor to the evolution of transparent venters.

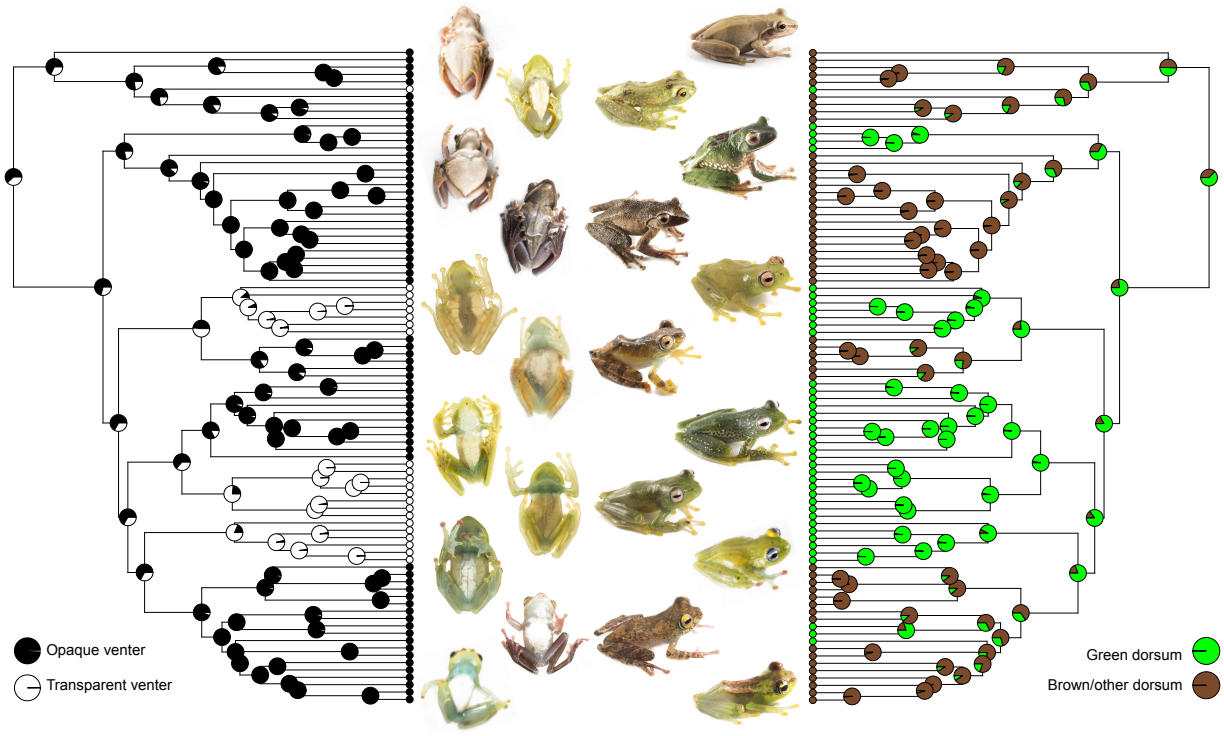

Figure 3. Biogeographic and elevational ancestral reconstructions for *Boophis* frogs in Madagascar. The colored circles at each node show the region and elevational zone (lowlands < 700 m and highlands > 700 m) with the greatest marginal probability. The dotted line on the map shows the approximate boundary between the lowlands and highlands. These results show an early diversification of *Boophis* in the highlands of the Eastern rainforests (i.e. North East and South regions). The four-state analysis is shown for simplicity, which is similar to the 10-state model (Fig. S1). Pie charts with the relative marginal probability for each node are in Fig. S2.

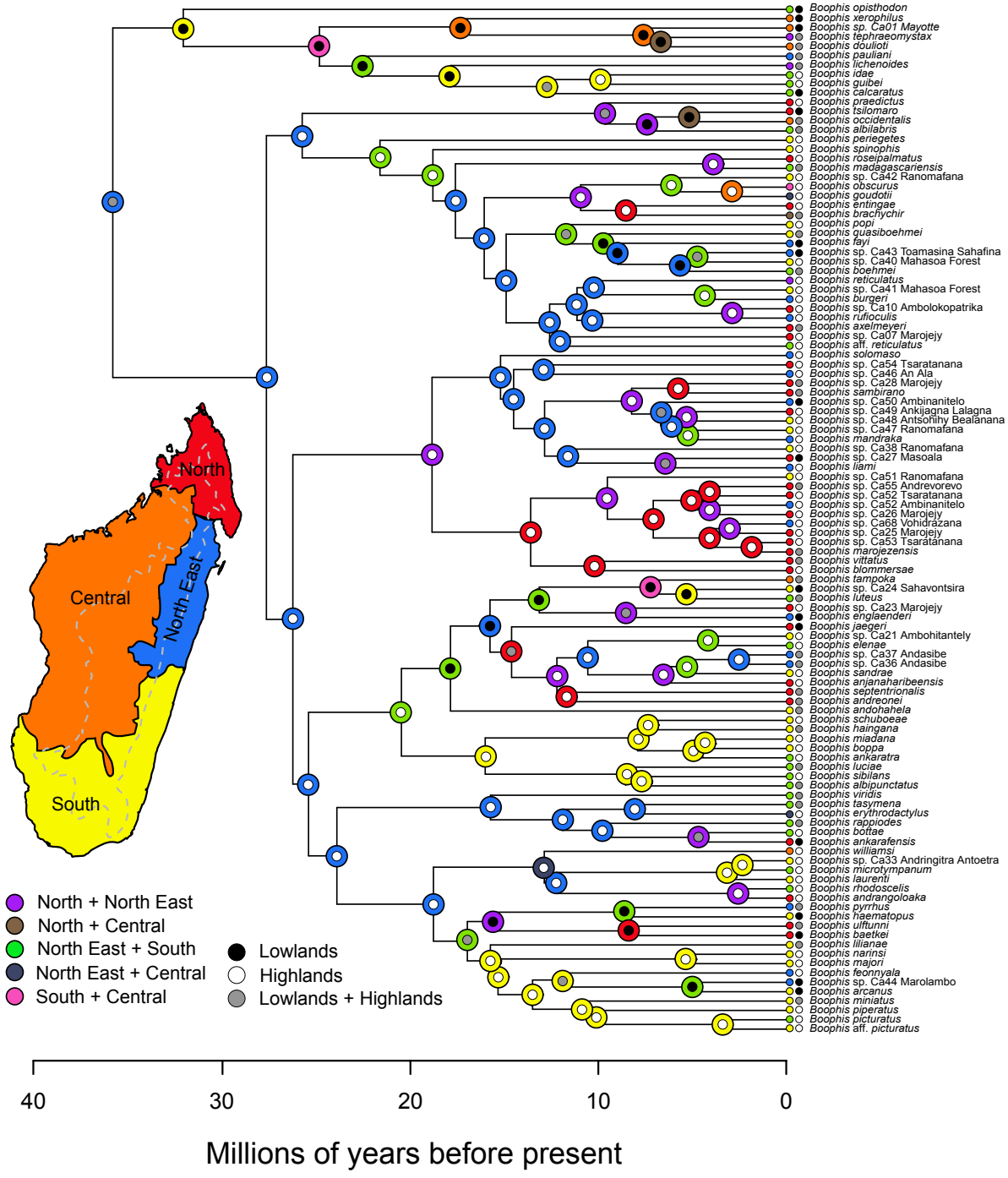

Figure 4. Posterior probability distributions for the speciation (A) and dispersal rate (B) parameters calculated from GeoSSE. True values are indicated by the solid vertical lines and the shaded areas correspond to the 95% credibility intervals. Parameters were taken from the most strongly supported model, where extinction rates were constrained to be equal. Posterior density is the relative probability that the parameter value would equal a random sample of values.

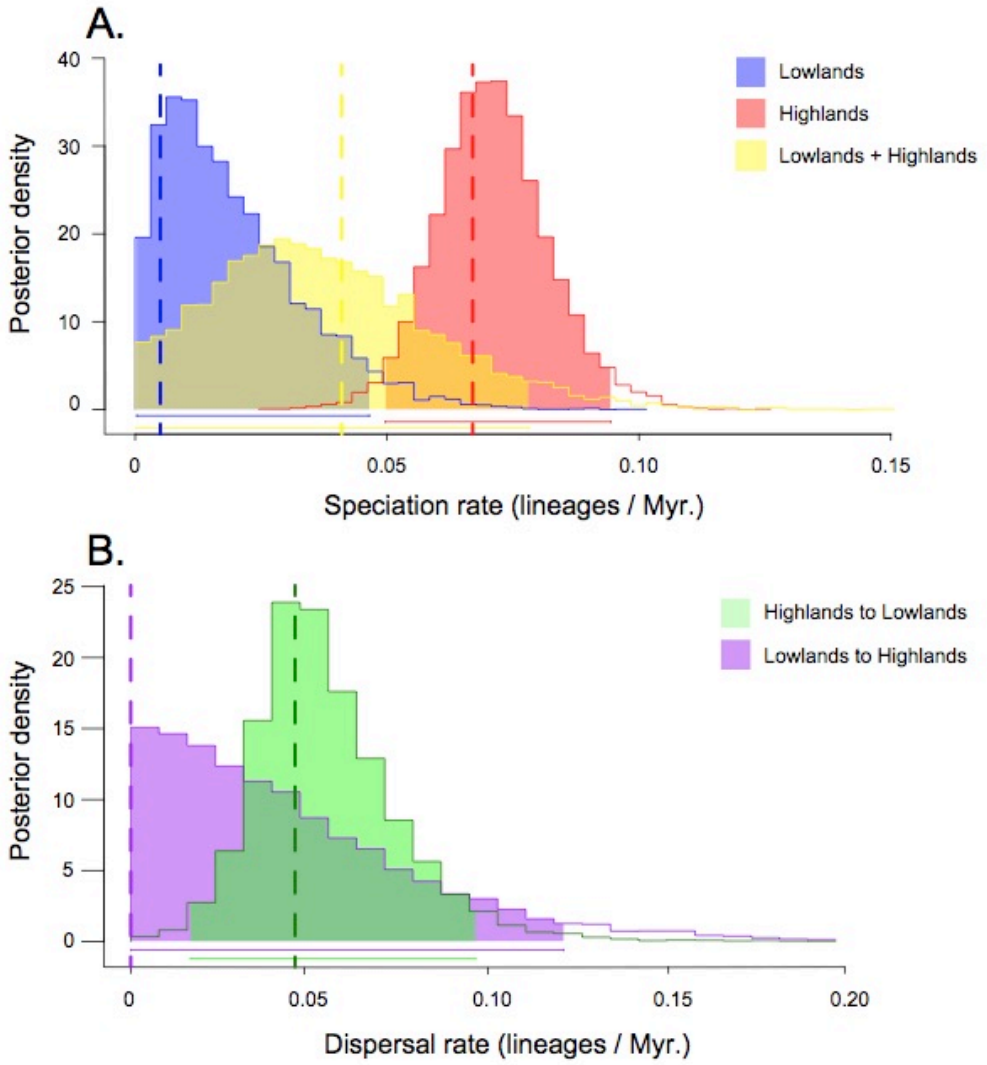

CHAPTER 3

FrogCap: a modular sequence capture probe set for phylogenomics and population genetics for all frogs, assessed across multiple phylogenetic scales

Hutter CR, Cobb KA, Portik DM, Travers S, and Brown RM; Not yet published.

3.1 Introduction

The widespread use of high-throughput sequencing technologies has led to new challenges for ecologists and evolutionary biologists designing projects and selecting methods for sequencing reduced portions of the genome (Shendure & Ji 2008; Kircher & Kelso 2010). While genome sequencing for non-model organisms remains costly, high throughput sequencing of targeted genomic regions has enabled numerous approaches for creating reduced genomic representation datasets at a lower financial cost per nucleotide (Kircher & Kelso 2010; Rohland & Reich 2012). These reduced genome representation approaches aim to affordably sequence reduced portions of the genome and reduce costs by allowing more individuals and/or species to be sampled simultaneously (Rohland & Reich 2012). Of particular interest to researchers are technologies that target genomic regions that remain orthologous and can be sequenced across moderate to deep time-scales (Sulonen *et al.* 2011), so a compatible method would be needed to meet this goal.

There are now many approaches for sampling subsets of an organism's genome for sequencing, and distinguishing among the many alternatives can largely depend on the hypothesis being tested. The most common methods for obtaining subsets of genome-wide sequence data include: (1) Restriction-associated digestion methods (RADseq) targets markers adjacent to restriction enzyme sites (Miller *et al.* 2007); (2) targeted sequence capture (HybSeq) targets genomic regions through hybridization-based sequence capture (Hancock-Hanser *et al.* 2013; Jones & Good 2016); and (3) transcriptome sequencing (RNASeq) targets the expressed exome of a given tissue type (Wang *et al.* 2009). These three methods have been used in addressing phylogenetic and population genetic questions and have different advantages and disadvantages. In RADseq, the markers are highly variable and therefore extremely useful at

addressing population level questions; however, the probability of obtaining markers decreases with phylogenetic distance from the focal taxon and obtains much fewer homologous markers when used at moderate amounts of species relatedness (e.g. genus, family level; Rubin *et al.* 2012; Cariou *et al.* 2013; Manthey *et al.* 2016). Conversely, HybSeq targets conserved genomic regions to capture markers from tens to hundreds of millions of years of divergence, and therefore offer less variability than RADSeq markers (Manthey *et al.* 2016; Portik *et al.* 2016). Finally, RNASeq excels at obtaining portions of the exome expressed in a given tissue type, thus enabling sequencing of a large part of the exome and hypothesis testing not possible with other methods; however, the method is costly and requires fresh tissue that is not commonly available (e.g. Romero *et al.* 2014; Sudmant *et al.* 2015) and may not be practical for testing hypotheses in phylogenetics and systematics where the majority of DNA tissue samples are incompatible with current RNASeq technology (Wang *et al.* 2009).

Targeted capture is widely used by the phylogenetics community and has been dominated by targeting and sequencing conserved elements through two main approaches: anchored hybrid enrichment (AHE; Lemmon *et al.* 2012), ultra-conserved elements (UCEs; Faircloth *et al.* 2012) or long ultra-conserved exons (RELIC; Karin *et al.* 2019). These two approaches identify regions of the genome that are conserved across distantly related taxa and probes are designed for these conserved regions, which are used in hybridization-based target capture. The two methods differ in that AHE targets ~400 long exons (>500bp) that are moderately divergent but still conserved enough to capture regions across hundreds of millions of years, and have a dense tiling density of probes (i.e. more probes per target region) which allegedly enable a higher chance of capture at the cost of fewer exons (Lemmon *et al.* 2012; Hime *et al.* 2019). Meanwhile, UCEs target ~5600 ultra-conserved regions (~120 bp long) with the goal of obtaining highly variable flanking

regions adjacent to the conserved regions (Bejerano *et al.* 2004; Faircloth *et al.* 2012). Both AHE and UCEs are now widely used in inferring phylogenies across broad and shallow phylogenetic scales (Crawford *et al.* 2012; Smith *et al.* 2013; Brandley *et al.* 2015; Prum *et al.* 2015; Streicher *et al.* 2018).

For amphibians, the performance of targeted sequence capture remains largely unexplored (but see Hedtke *et al.* 2013; Portik *et al.* 2016). Several studies have used UCEs (Alexander *et al.* 2016; Streicher *et al.* 2018) and others have used AHE markers (Peloso *et al.* 2016; Heinicke *et al.* 2018; Yuan *et al.* 2018; Hime *et al.* 2019), whereas one additional study created a customized probe set for Afrobatrachia, a clade of several African families (Portik *et al.* 2016). While UCEs have been used in frogs, they are problematic because they were designed for amniotes (frogs are not member of this group), and because of the phylogenetic distance of frogs from amniotes, only about half the target UCEs are typically captured (~2350/5600 UCEs; Streicher *et al.* 2018). Additionally, UCE markers have received criticism in the literature for several reasons, including their unknown function (Alexander *et al.* 2010), the fact that many UCEs are uninformative due to low variability (McCormack *et al.* 2012), and the high variability of flanking regions leads to difficulty in aligning these regions among distantly related taxa (Singhal *et al.* 2017; Streicher *et al.* 2018). For the AHE probe set, the main advantage is longer exons and possibly less missing data because of the tiling density. Conversely, because of the higher tiling density, the AHE marker set contains fewer total exons because more probes are dedicated to each exon when increasing density; AHE markers could also bias phylogenetic results due to natural selection because AHE targets only exons (Bragg *et al.* 2016; Singhal *et al.* 2017). Furthermore, the AHE probe set is proprietary and has only recently become publicly available after nearly a decade of use by a single laboratory (Yuan *et al.* 2018; Hime *et al.* 2019).

Despite the widespread use of high-throughput sequencing in non-model organisms and the increasing number of studies in frogs, a publicly available probe set for a substantial amount of diversity across the global radiation of frogs has not yet been published.

Herewith, we introduce FrogCap, a publicly available sequence capture probe set and data analysis pipeline for all frogs. We provide a modular, large, and flexible set of probes corresponding to ~15,000 markers that unifies all previous sequencing work on frogs through the inclusion of "legacy" loci previously used in phylogenetic studies (Figure 1; Pyron & Wiens 2011; Feng *et al.* 2017) and also successful UCEs from past studies in frogs (Alexander *et al.* 2016; Streicher *et al.* 2018). Additionally, we describe a novel approach for creating a sequence capture probe set of orthologous markers that functions well across divergent taxa within across the two main Superfamilies of frogs (Hyloidea + Archaeobatrachia and Ranoidea), by creating two complimentary probe sets that allows markers to be combined across these two superfamilies (Feng *et al.* 2017). The FrogCap probe set is designed to be modular, such that subsets of the markers can be selected based on the probe set size, type of research question and taxonomic scale being addressed. We also provide a new pipeline in R to analyze sequence capture data by processing them from raw reads into cleaned alignments. Finally, using 105 test samples, we evaluate our sequence capture results from the Hyloidea and Ranoidea probe sets, and test the modularity of the probe set with a reduced version of the Ranoidea set and also six different phylogenetic scales. For the probe sets we measure the number of loci captured per taxa, the sensitivity and specificity of the sequence capture, levels of missing data, and the resulting depth of coverage. Using alignments from six different phylogenetic scales, we assess number of markers and base pairs of data, the proportion of informative sites, missing data at

different phylogenetic scales, and tested the effects of phylogenetic relatedness from the reference genome.

3.2 Materials and Methods

3.2.1 Data availability

A major goal in disseminating these resources is to provide the probe set described and tested here as a freely available and open access resource. The probe set and other resources are licensed under a Creative Commons Attribution 3.0 United States (https://creativecommons.org/licenses/by/3.0/us/legalcode).

All raw sequencing reads will be made available in the GenBank SRA. All alignments analyzed and materials for replicating analyses will be made available on the Open Science Framework (https://osf.io/gvbr5/) following manuscript acceptance. Finally, the data analysis pipeline and scripts for all analyses here, the probe set and marker files, and data for several outgroups for other researchers to use are now available on Carl R. Hutter's GitHub (https://github.com/chutter/FrogCap-Sequence-Capture).

3.2.2 Sequence capture probe design

Published "legacy" marker selection. To maintain compatibility with previously published datasets, we assessed 40 commonly used nuclear markers for phylogenetic studies in frogs (e.g. Frost *et al.* 2006; Pyron & Wiens 2011). No mitochondrial markers are included because the relative abundance of mitochondrial DNA is higher and would be more likely to be sequenced than the nuclear target markers and mitochondrial DNA is sequence incidentally and can be mined from the raw reads. The selected legacy markers were matched to the *Xenopus* and

Nanorana genomes, ensuring that none were paralogs or had portions matching to multiple genomic regions. We selected 36 markers from this assessment; this set of legacy markers were used in the Ranoidea V1 probe set (Figure 1).

To include markers from a more recent study in the Hyloidea and Ranoidea-reduced probe sets, we assessed the 95 set of markers from Feng *et al.* (2017). We removed any duplicates overlapping with the previous legacy marker set (36 markers) and assessing each marker for potential duplicate genomic matches resulting in a final set of 86 legacy markers. Final marker sequences were designed from the consensus sequences across the multiple sequence alignments from Feng *et al.* (2017) to be used for probe design.

Ultra-conserved elements have been previously used in frogs, with ~50% success capture rate (e.g. Streicher *et al.* 2018). For this study, we selected a subset of the orthologous UCEs previously sequenced from *Kaloula* (Microhylidae: Alexander *et al.* 2016). We selected a subset of UCEs that had greater than 10% parsimony informative sites, which was 651 UCEs to be used in the initial Ranoidea probe set, using the stock UCE probe sequences. Improving upon this for the Hyloidea set, we included the 2360 successfully captured UCEs from Streicher *et al.* (2018), which contains the 651 UCEs selected above. For these UCEs, we redesigned the sequences used for probes by creating consensus sequences across the multiple sequence alignments for each UCE from Streicher *et al.* (2018).

Transcriptome assembly. Twenty-five transcriptomes were obtained from published studies from the NCBI transcriptome assembly database (https://www.ncbi.nlm.nih.gov/genbank/TSA; Table S1). Methods for assembling three additional transcriptomes follows (Portik *et al.* 2016). After acquiring the assembly, isoforms, alternatively

spliced sequences, and other redundancies were removed using CD-HIT-EST at a similarity threshold of 95%, keeping the longest transcript. (Li & Godzik 2006). These reduced-redundancy transcriptomes were used in all following analyses.

Ranoidea genome-based probe design. To target new exons for sequence capture, we designed the probe set by locating orthologous, protein-coding exons that were well represented across frogs from the Ranoidea superfamily. We used the *Nanorana parkeri* genome (Sun *et al.* 2015), and the genomic annotations therein to determine the genomic coordinates of predicted exons in the genome (Genome and annotations available at GigaScience: dx.doi.org/10.5524/100132). We conducted all data processing and other analyses in R (RDCT 2018), using customized scripts with the following R packages: GENOMICRANGES (Lawrence *et al.* 2013), SEQINR (Charif & Lobry 2008), APE (v5.0; Paradis & Schliep 2019).

First, we used the program BLAT (Kent 2002) to match each assembled frog transcriptome to the *Nanorana parkeri* genome using 75% as the similarity threshold. Second, we used a custom R script to evaluate each transcript to genome match, where we combined the match dataset for each species into a single dataset so that orthologous matches could be more easily clustered together (this resulted in 2.7 million match records). Third, we filtered out matches that were less than 50 bp and matched to multiple locations in the genome to remove potential paralogs (removed ~2 million of the aggregated matches; 749,821 matches remained). Fourth, matches were clustered together when they overlapped within a predicted exon from the *N. parkeri* genome (removed ~500,000 matches; 228,960 matches remained). After these initial filtration steps of the matches, a final candidate marker set of 94,293 exons remained.

The sequence data for each candidate exon match above were collected from each transcriptome and aligned together with the *N. parkeri* genome exon sequence using MAFFT v7.312 (Katoh & Stanley 2013). To assist in exon selection, each multiple species alignment was assessed and filtered through the following criteria: (1) greater than 5% parsimony informative sites; (2) GC content between 30-50%, as these types of sequences are inefficient for sequence capture (Gnirke *et al.* 2009); (3) exons shorter than 100bp and greater than 5000bp were removed; (4) exons were kept only if they were found in at least 50% of the species transcriptomes; and (5) potential paralogs were removed by using BLAT to detect multiple hits across the *N. parkeri* genome. After exon assessment and removal, 18,505 exons remained in the final candidate exon dataset.

The candidate exon dataset was used to design a MYbaits-2 (40,040 baits) custom bait library (MYcroarray, now Arbor Biosciences), using 120mer baits to best capture sequences with greater than 5% divergence from the probes. We used the already published 120mer UCE Amniote probes from Faircloth *et al.* 2012 (https://www.ultraconserved.org) and did not redesign them because they have already been tested. To design the probes, the finalized set of markers were separated into probe sequences following a 2x tiling scheme, starting 20bp behind the start codon of the locus and tiling 120bp probes every 60bp until 20bp past the stop codon for exons (total 61,939 baits). Next, we filtered individual probes using these criteria: (1) excluded probes that matched to multiple locations in the *Nanorana parkeri* genome using BLAT with a 70% similarity; (2) GC content between 30–50%; (3) no repetitive sequences based off the *Nanorana parkeri* RepeatMasker annotations (Sun *et al.* 2015); and (4) no matches with BLAT to other probes with a 70% similarity. After filtration 51,344 baits remained; markers and their baits were randomly selected to drop 11,304 baits from the dataset to fit into the 40,040 bait limit resulting

in 12,934 exons. The final probe set included 13,621 markers that totaled 3,983,022 base pairs (final configuration: Legacy = 36; UCE = 651; exons = 12,934; Table 1; Figure 1).

Hyloidea transcriptome-based probe design. To design probes from orthologous markers for frogs from the Hyloidea superfamily, a different approach was required because there was no available genome for this group. We began with the Ranoidea exons designed above and matched each exon to the six transcriptomes available from Hyloidea using BLAT. We clustered together matches, created multiple sequence alignments, and filtered as described above for the genome-based probe design. After these steps, the candidate dataset included 7,627 exons. Next, we generated new exon sequences from these data by creating consensus sequences from all the matching transcriptomes from each exon (ambiguous sites were replaced with the base that would maintain an optimal GC content).

To add additional exons to this dataset, we used VSEARCH (Rognes *et al.* 2016) to cluster together transcripts from the Hyloidea transcriptomes to find orthologous clusters (18,949 cluster were found). We obtained the consensus sequence for each cluster and matched it back to each transcriptome resulting in 101,863 matches. Next, we generated 18,949 sequence alignments for each cluster and filtered the alignments as described for the Ranoidea probe set resulting in 16,511 transcript alignments. Before designing probes, we created the final set of markers to be used in probe design by generating consensus sequences from each filtered transcript alignment. Finally, we designed and filtered probes as described above for the Ranoidea set using the MyBaits-2 kit of 40,040 baits, resulting in a final set of 8,788 exons. After combining with the legacy Sanger and UCE data, the final probe set targeted 2,926,956 bp

from 10,633 markers (Final configuration: Legacy = 86; UCEs = 2360; exons = 8,788; Table 1; Figure 1).

Reduced-Ranoidea marker selection. To test the modularity and customization potential of FrogCap, we selected a reduced set of markers from the 40,040-bait kit to be used in the smaller 20,020-bait kit. For this probe set, we also tested additional markers that could be incorporated into future customized kits. We included the 86 Feng *et al.* (2017) markers described above that were included in the Hyloidea but not Ranoidea probe set. We also included ~47 ultra-long exons (>5000bp) previously excluded from the Ranoidea probe set.

The Reduced-Ranoidea probe set was designed after the 40K Ranoidea probe set had been tested, which enabled the selection of markers that were captured successfully across the entire superfamily. To select markers that had already been tested, we began with alignments from the the 24 sample Ranoidea probe set evaluated below, and reduced the probe set to markers successfully captured across 75% or greater of the samples, which was 10,274 markers. Next, we filtered the markers as follows: (1) UCEs were excluded; (2) the largest exon within 100,000 bp of another exon on the *Nanorana parkeri* genome was kept reducing potential genetic linkage; and (3) all the exons greater than 500bp in size were included. This final candidate set included ~4,312 exons and exons were randomly deleted until the 20,020 bait limit was reached, which was 3,161 exons. After combining the 86 Legacy markers, the final marker set included 3,247 markers targeting 1,519,233 bp of data (Table 1; Figure 1).

3.2.3 Sequencing

Taxonomic sampling strategy. To test these new sequence capture probe sets, we aimed to explore their efficiency across seven different datasets from five phylogenetic scales. We selected 105 samples for this study and we assessed the following phylogenetic scales: (1) Order: we included 48 samples including samples using the Ranoidea and Hyloidea probe sets; (2) Superfamily: we assess the Ranoidea and Hyloidea superfamilies independently, including 24 samples from each superfamily (the same samples used in the Anura assessment); (3) Family: we included 8 samples from the family Mantellidae, which include a single representative for each genus; (4) Genus: we included 24 samples from a completely taxon sampled clade in the genus *Cornufer* (Ceratobatrachidae); and (5) Species: we include 16 samples from within a single species, from four different populations. We also evaluated the Reduced-Ranoidea probe set using 30 samples from the genus *Occidozyga*, (Dicroglossidae) where this dataset is comparable to the Genus dataset. See Table S2 for a list of all samples sequenced and their datasets.

Library preparation and sequencing. Genomic DNA was extracted from the 105 tissue samples using either a standard phenol-chloroform extraction or through the use of a PROMEGA Maxwell bead extraction robot. The resultant DNA was quantified using Qubit DNA Broad-range assay (Life Technologies). Approximately 500 ng total DNA was acquired and set to a volume of 50 ul through dilution (with H_20) or concentration (using a vacuum centrifuge) of the extraction when necessary.

The genomic libraries for the samples were prepared by MYcroarray library preparation service. Prior to library preparation, the genomic DNA samples were quantified with fluorescence and up to 4 ug was then taken to sonication with a QSonica Q800R instrument.

After sonication and SPRI bead-based size-selection to modal lengths of roughly 300 nt, up to 500 ng of each sheared DNA sample were taken to Illumina Truseq-style sticky-end library preparation. Following adapter ligation and fill-in, each library was amplified for 6 cycles using unique combinations of i7 and i5 indexing primers, and then quantified with fluorescence. For each capture reaction, 125 ng of 8 libraries were pooled, and subsequently enriched for targets using the MYbaits v 3.1 protocol. Following enrichment, library pools were amplified for 10 cycles using universal primers and subsequently pooled in equimolar amounts for sequencing. Samples were sequenced on an Illumina HiSeq 3000 with 150bp paired-end reads.

3.2.4 Data processing and alignment

Data processing pipeline. A bioinformatics pipeline for filtering adapter contamination, assembling contigs, and exporting alignments is scripted in R and available at (https://github.com/chutter/FrogCap-Sequence-Capture). Prior to processing raw reads, Illumina sequence data was de-multiplexed using the Illumina software bcl2fastq. Next, the raw reads were cleaned of adapter contamination, low complexity sequences, and other sequencing artifacts using the program FASTP (default settings; Chen *et al.* 2018). Adapter-cleaned reads were then matched to the UNIVEC database of bacterial and other genomes to ensure that no contamination was in the final dataset (https://www.ncbi.nlm.nih.gov/tools/vecscreen/univec/). We decontaminated the adapter-cleaned reads with the program BBMAP from BBTools (https://jgi.doe.gov/data-and-tools/bbtools/), where we matched the cleaned reads to each reference contaminant genome and removed if they matched >95 percent similarity. After this step, these reads were saved separated as “cleaned-reads”, which are processed as needed for later variant calling.

Prior to assembly, the "cleaned-reads" were further processed to decrease computational load and increase accuracy. We merged paired-end reads using BBMerge (Bushnell *et al.* 2017) from BBTools. BBMerge also fills in missing gaps between non-overlapping paired-end reads by assembling the missing data from the other paired-end reads using the "Tadpole" program. Next, exact duplicates were removed when both read pairs were duplicated using "dedupe" from BBTools. Additionally, duplicates from the set of merged paired-end contigs were removed if they were exact duplicates or were contained within another merged contig.

The merged singletons and paired-end reads were next *de novo* assembled using the program SPADES v.3.12 (Bankevich *et al.* 2012), which runs BAYESHAMMER (Nikolenko *et al.* 2013) error correction on the reads internally. Data were assembled using several different k-mer values (21, 33, 55, 77, 99, 127), where orthologous contigs resulting from the different k-mer assemblies were merged. We used the DIPSPADES (Sofanova *et al.* 2015) function from this program to better assemble contigs that were polymorphic by generating a consensus sequence from both haplotypes from orthologous regions where polymorphic sites were resolved randomly.

The consensus haplotype contigs were then matched against reference marker sequences used to design the probes separately for the three probe sets with BLAST (*dc-megablast*). Contigs were discarded if they did not match to at least 30 percent of the reference marker and contig matches less than 50 bp were removed. Contigs matches to a given reference marker were discarded if more than one contig matched to the marker and they were overlapping. For non-overlapping matches to the same reference marker, we merged the contigs by joining them together with Ns based on their match position within the marker. The final set of matching

contigs were named with the name of the marker followed by the sample name in a single file to be parsed out separately for multiple sequence alignment in the next step.

Alignment and trimming. The final set of matching markers was next aligned on a marker-by-marker basis using MAFFT local pair alignment (settings: max iterations = 1000; ep = 0.123; op = 3; --adjust-direction). We screened each alignment for samples that were greater than 40 percent divergent from the consensus sequence, which are almost always incorrectly assigned contigs. Alignments were kept if they had greater than 4 taxa, had more than 100 base pair length, and a mean sample specificity (i.e. the "breadth of coverage" of the sample; see below) of greater than 50 percent across the alignment (to prevent non-overlapping segments of the alignment). We next separated the alignments into two initial datasets: (1) "exons-only", which included only exon contigs that had the intronic region trimmed from each alignment using the reference exon as a guide; and (2) "all-markers", which included the entire matching contig to the reference marker and includes the UCE markers. These two sets of alignments were only externally trimmed, where at least 50 percent of the samples have sequence data at the two alignment ends. These alignments have not been internally trimmed and should not be used until further processing (see next step).

Final Sequence Alignments. The exons-only and all-markers sets of alignments were further trimmed into usable datasets for phylogenetic analyses and data type comparisons: (1) exons, each exons-only alignment was adjusted to be in an open-reading frame in multiples of three bases and trimmed to the largest reading frame that accommodated >90% of the sequences; (2) introns, a consensus sequence of the exon previously delimited was aligned to the all-markers

dataset and the aligning region was removed leaving only the two intron ends, which were concatenated; (3) UCEs, were separately saved and not modified; (4) legacy, markers from prior studies (excluding UCEs) were saved separately for ease of access and comparison; (5) gene, exons from the dataset above were concatenated and grouped together if they were found from the same predicted gene from the *Nanorana parkeri* and *Xenopus tropicalis* genomes because these exons are likely to be strongly linked genetically (the exons could also be unlinked because of long introns so both datasets should be considered). Finally, the introns and UCE datasets were internally trimmed using TRIMAL (automatic1 function; Capella-Gutiérrez *et al.* 2009). These five trimmed datasets are ready for phylogenetic analyses and are saved as Phylip formatted files.

3.2.5 Sequence capture evaluation

Sequence capture sensitivity. We evaluated the "sensitivity" of the sequence capture results, where sensitivity (also termed "breadth of coverage") is defined as the percent of bases from each target marker covered by post-assembly contigs. To calculate sensitivity, we used the collection of target markers from probe design and compared them to the matching contig for each of the sequenced samples using BLAST (*dc-megablast*). We did not evaluate introns, as they were not specifically targeted, but assess intron length separately below. After matching with BLAST, for each sample we calculated the percent sensitivity per target marker by divided the total base-pair length of the target marker sequence by the length of the matching portions of the sample contig.

To predict whether phylogenetic distance is important to sensitivity rather than stochastic factors or sequencing effort, we test for positive relationship between sensitivity (%) and

phylogenetic distance (%) from the design markers. We compared the genome-designed Ranoidea probe set and transcriptome-based consensus sequence design from the Hyloidea probe set. Phylogenetic distance was calculated using an uncorrected pairwise distance; in Ranoidea the distance was calculated from the *Nanorana parkeri* genome sequence used in creating probe sequences while in Hyloidea the distance was calculated from the consensus sequences created for the target markers using available sequence from the Hyloidea transcriptomes. A significant negative relationship would suggest that lower sensitivity is driven by higher sample genetic distance from the design markers.

Sequence capture specificity. "Specificity" refers to the percentage of cleaned reads (from the cleaned-reads-snp folder) that can be mapped back to the target markers. We assessed specificity across the six phylogenetic scale datasets as well as within the Hyloidea (24), Ranoidea (24), and Reduced-Ranoidea (30) probe set samples. First, we created a reference from the markers targeted with the probe set and mapped cleaned reads from each sample to the target markers using the program BWA v0.712 (Li & Durbin 2009). Each reference was indexed (function: *bwa index*) and reads were mapped to each reference (function: *bwa mem*), using SAMTOOLS (Li *et al.* 2009) to convert between file-types (functions: *view* and *fastq*). Finally, we counted the number of cleaned reads that mapped back to the reference markers to calculate the specificity (number mapped reads / total cleaned reads).

Similar to specificity, phylogenetic distance or sequencing effort could influence sensitivity, so we test for positive relationship between sensitivity (%) and phylogenetic distance (%) from the design markers. We compared the genome-designed Ranoidea probe set and transcriptome-based consensus sequence design from the Hyloidea probe set. Phylogenetic

distance was calculated using an uncorrected pairwise distance as described above. A significant negative relationship would suggest that sample dissimilarity from the design markers leads to a lower specificity and fewer of the sequenced reads mapping to the target markers.

Sequence capture missing data. To understand potential causes of missing data, we investigate how phylogenetic or genetic distance of samples from the design markers could lead to variation in missing data, measured from the filtered all-markers trimmed dataset. Missing data could be described in two important ways: (1) missing data at the base pair level refers to targeted base pairs that are missing from a sample in an alignment (called "missing base pair data" throughout; also the inverse of sensitivity from above); and (2) missing data at the marker level (called "missing marker data" throughout) refers to targeted markers that were not adequately captured for a sample after applying the standard alignment filtering from above. To calculate missing base pair data, we counted the number of base pairs for each sample for each alignment and divided by the total length of the alignment. To calculate missing marker data, we used the final set of marker alignments after the post-processing filtration steps described above (all-markers trimmed dataset) and calculated missing marker data as the percent of markers not included in the final set of alignments for each sample. Genetic distance was calculated as described for sensitivity and specificity analyses above. Finally, we tested for a relationship between percent of missing base pair and marker data and genetic distance for the three probe sets, where a significant positive relationship would suggest that sample dissimilarity to the design markers leads to missing data.

Marker depth of coverage. The "depth of coverage" or "depth" for targeted sequence capture data was calculated, where depth refers to the number of bases from the cleaned reads that overlap a given assembled base or bin of bases from each of the target markers, which is often notated as "X". We first created a reference for each samples' set of post assembly contigs that were targeted with the probe set and next mapped cleaned reads to these contigs using BWA ("bwa-mem" function). We next removed exact duplicate reads using PICARD TOOLS (http://broadinstitute.github.io/picard/). To calculate a per-base overlap of cleaned reads to contig base pairs, the 'depth' function was used from SAMTOOLS. Depth was calculated across all targeted markers and samples for every base pair and was binned into 1% sized bins.

To describe the variation in depth among samples and markers separately, we calculated two metrics: (1) sample depth: the median depth of markers calculated for each sample; and (2) the marker depth: for each marker, the median depth of samples with data for that marker is calculated. We used the median because individual depth measurements are not centered on zero and have a positive skew where few samples / markers have extremely high depth values, biasing towards much higher mean values that don't accurately describe the data. Additionally, we also calculated the marker depth separately for the exon and intron across markers. Finally, we used a Student's two-sample *t*-test to test for a significant difference between the depth of coverage from the Reduced-Ranoidea 20K set and the Ranoidea 40K set. We transformed values to fit a normal distribution and when that assumption could not be met, we used the Mann-Whitney U test which does not assume a normal distribution. Statistical tests were performed in R.

Suitability for phylogenetics. We evaluated the all-marker, exon, intron, UCE and gene datasets for their utility in use for phylogenetics. We calculated statistics for each marker, which

included: number of taxa, alignment length, percentage of missing base pair data described as percent of missing bases across the alignment, percentage of missing marker data described as number of missing taxa from the alignment, the number of informative sites, and percent of informative sites. We did not estimate phylogenies for these clades because this is beyond the scope of this work. The species relationships will be addressed in future publications with increased species sampling.

Suitability for population genetics. To test whether these data could be used for population genetics, we aimed to locate variants and SNPs that are high quality and have sufficient depth of coverage. We note that these statistics depend entirely on the output from the sequencing platform being used, number of samples multiplexed per lane, and number of markers from the probe set included during hybridization enrichment. We used GATK v4.1 (McKenna *et al.* 2010) and followed the recommended best practices when discovering and calling variants (Van der Auwera *et al.* 2011).

To discover potential variant data (e.g. SNPs, InDels), we used a consensus sequence from each alignment from the target group as a reference and mapped the cleaned reads back to the reference markers from each sample. We used BWA ("bwa mem" function) to map cleaned reads (cleaned-reads dataset explained above) to the reference markers, adding the read group information (e.g. Flowcell, Lane, Library) obtained from the fastq header files. We next used SAMTOOLS to convert the mapped reads SAM file to a cleaned BAM file, and merged the BAM file with the unmapped reads as required to be used in downstream analyses. We used the program PICARD to mark exact duplicate reads that may have resulted from optical and PCR artifacts and reformatted the dataset for variant calling. To locate variant and invariant sites, we

used GATK4 to generate a preliminary variant dataset using the GATK program *HaplotypeCaller* to call haplotypes in the GVCF format for each sample individually.

After processing each sample, we used the GATK *GenomicsDBImport* program to aggregate the samples from the separate datasets into their own combined database. Using these databases, we used the *GenotypeGVCF* function to genotype the combined sample datasets and output separate ".vcf" files for each marker that contains variant data from all the samples for final filtration. The preliminary variant set was filtered into four datasets: (1) All variants: variants are kept after moderate filtering to remove probable errors filtered at a quality score > 5; (2) High quality variants: variants included SNPs, MNPs, and indels filtered at a quality > 20; (3) SNPs: the number of SNPs after high-quality filtering (quality > 20); and (4) unique markers: the number of unique markers from the probe sets that contain at least one high quality SNP.

3.3 Results

3.3.1 Sequence capture evaluation

We sequenced 105 samples, which resulted in a mean base pair yield of 1,234.0 ± 577.9 mega base pairs (Mbp; range: 466.7–4,321.8 Mb) and a mean 8,172,461 ± 3,827,207 (range: 3,090,636–28,621,450) paired reads for each sample (Figure 2). Raw reads were then filtered to remove exact duplicates, low complexity and poor-quality bases, adapter and contamination from other non-target organisms; filtering resulted in a mean 84.5% ± 11% of reads (range: 27–96%) passing the quality filtration steps (mean: 1,041.5 ± 544.3 Mbp; range: 233.8–3,900.2 Mbp). After merging paired-end reads and reducing redundancy (removing duplicate and containment reads), there we recovered a mean of 443,032 ± 275,084 (range: 159,958–2,123,190) merged paired-end reads and singletons used as input for assembly. After assembly,

the samples yielded a mean of 15,832 ± 5,575.9 (range: 6,968–43,113) contigs, which had a mean length of 860.9 ± 92.2 (range: 128–24,355) base pairs (Figure 2; Figure S1).

The assembled contigs were next matched to the target markers from each of the three probe sets (Hyloidea, Ranoidea, Reduced-Ranoidea). For the Hyloidea probe set a mean 7443.1 ± 2,022.7 (range: 616–9570) contigs were matched uniquely to the target markers (mean marker proportion: 0.701 ± 0.199; range: 0.058–0.901). When matching contigs to the Ranoidea probe set, a mean 10,304.6 ± 1645.6 (range: 5050–12,235) contigs matched uniquely to the target marker set (mean marker proportion: 0.757 ± 0.121; range: 0.371–0.898). Finally, when matching the sample contigs to the target markers from the Reduced-Ranoidea probe set, a mean 2847.2 ± 123.2 (range: 2,299–2,983) unique contig matches were found (mean marker proportion: 0.877 ± 0.038; range: 0.708–0.919). See Table S2 for individual sample statistics.

3.3.2 Sequence capture sensitivity

The sequence capture "sensitivity" was measured across the three probe sets (Hyloidea, Ranoidea, Reduced-Ranoidea); sensitivity refers to the percent of bases of target markers (exons and UCEs) that are covered by post-assembly contigs. The mean sensitivity across in exons from samples in the Hyloidea probe set was 70.3 ± 20 % (*n* = 24; range: 5.7–89.9%), the Ranoidea probe set was 70.6 ± 19 % (*n* = 24; range: 36.9–93.1%), and the Reduced-Ranoidea probe set was 89.1 ± 4 % (*n* = 30; range: 71.6–93.5%; Table 2; Figure 3A). In UCEs, the mean sensitivity from samples in the Hyloidea probe set was 87.1% ± 16.9% (*n* = 24; range: 15.5–96.6%) and the Ranoidea probe set was 85.7 ± 8 % (*n* = 24; range: 62.2–94.6%), and the Reduced-Ranoidea probe set did not include UCEs.

To understand how the difference in the genome-based Ranoidea and consensus sequences from transcriptomes in the Hyloidea probe sequences might lead to different sensitivity in sequence capture, we used linear regression to test for a relationship between sensitivity and phylogenetic distance within the 48 samples from the two superfamily datasets (Table 3). We found a strong negative relationship ($R^2 = 0.746$; $P < 0.001$) within the genome-designed Ranoidea samples (Figure 3A). In addition, we found a weak but significant relationship within the Hyloidea consensus sequence samples ($R^2=0.350$; $P = 0.002$; Figure 3A). The Reduced-Ranoidea samples were not tested because all of the samples are from the same genus with very similar genetic distances; therefore, phylogenetic distance from the design sequences would not be relevant.

3.3.3 Sequence capture specificity

Specificity refers to the percentage of cleaned reads that can be mapped back to the target markers. We assessed specificity within the Hyloidea, Ranoidea, and Reduced-Ranoidea probe sets. The Hyloidea set had a mean specificity of 47.9 ± 13.8 % ($n = 24$; range: 1.7–68.3%). In the Ranoidea set, the mean specificity is the highest at 71.1 ± 12.8 % ($n = 24$; range: 47.3–90.5%). Surprisingly, the specificity was the lowest in the Reduce-Ranoidea set with a mean of 35.7 ± 3.3 % ($n = 30$; range: 24.5–40.0%; Table 2; Figure 3B).

To test whether specificity is related to phylogenetic distance, we used linear regression to test for a relationship between specificity and phylogenetic distance for each of the three probe sets. We found a strong negative relationship ($R^2 = 0.632$; $P < 0.001$) within the genome-designed Ranoidea samples (Figure 3B). Conversely, we found a weak and insignificant relationship within the Hyloidea consensus sequence samples ($R^2=0.121$; $P = 0.095$; Figure 3B).

The Reduced-Ranoidea samples were not tested because phylogenetic distance from the design sequences would not be relevant for samples from a single genus.

3.3.4 Sequence capture missing data

We assessed the amount of missing data for the three probe sets (Hyloidea, Ranoidea, Reduced-Ranoidea) by calculating the percent of missing markers out of the number of target markers for each sample. The Hyloidea set had a mean percent of missing markers of 21.9 ± 22.7 % (n = 24; range: 0–95.0%), which a much larger range and variation because of the inclusion of divergent clades (Archaeobatrachian frogs and Salamanders). In the Ranoidea set, the mean percent of missing markers is the highest at 22.7 ± 21.2 % (n = 24; range: 0–59.7%). Finally, the percent of missing markers in the Reduce-Ranoidea set was the lowest with a mean of 4.5 ± 4.2 % (n = 30; range: 0–23.2%; Table 2; Figure 4A-B).

To understand if increased divergence from the target marker sequence leads to more missing data, we tested for a relationship between percent of missing markers and genetic distance for the three probe sets. We found a strong positive relationship (R^2 = 0.769; P < 0.001) within the genome-designed Ranoidea samples (Figure 4C). In the consensus-designed Hyloidea samples, we found a weak but significant positive relationship (R^2=0.377; P = 0.001; Figure 4D). However, the relationship is not significant when three samples outside the scope of the Hyloidea design are removed (n = 21; R^2=0.041; P = 0.379), suggesting that the high genetic divergence from the non-target samples leads to the high number of missing markers. Conversely, the nonsignificant relationship for the target samples suggests that marker missing data for consensus-based marker designs is random or based upon another factor other than

genetic distance. Finally, the Reduced-Ranoidea samples were not tested because genetic distance from the design sequences would not be relevant for samples from a single genus.

3.3.5 Marker depth of coverage

We assessed depth of coverage across markers and also separately for exons and introns, where the exon was targeted with probes and the intron is incidentally sequenced. Depth was calculated from median number of cleaned-read base pairs that overlapped with the sample sequenced region per 1 percent bin. We compared depth using two different metrics: (1) we calculated the sample depth which is the median depth of all markers for each sample (Figure 5A); (2) the marker depth which is the median depth of all samples within each marker (Figure 5B); and (3) the marker depth for the exon and intron separately from all samples within each marker (Figure 5C).

In the Hyloidea probe set, we found a median sample depth of 19.7 ± 6.9 X (n = 24; range: 5.1-34.1 X; Figure 5A). For the Ranoidea probe set, we found a median sample depth of 22.1 ± 8.5 X (n = 24; range: 4.2-39.2 X; Figure 5A). Finally, the Reduced-Ranoidea probe set had a median sample depth of 26.8 ± 5.5 X (n = 30; range: 14.2-34.7 X; Figure 5A). Because of the small sample size and the distributions were severely non-normal, we used a Mann-Whitney U test and found a significant difference in the mean ranks of the median sample depth between the Reduced-Ranoidea 20K and Ranoidea 40K probe sets (U = 236; P = 0.031).

We next assessed the median depth across markers in the Hyloidea probe set which had a median marker depth of 16.6 ± 13.5 X (n = 24; range: 1.8–87.0 X; Figure 5B, D). The Ranoidea probe set had a median marker depth of 21.9 ± 14.0 X (n = 24; range: 3–115 X; Figure 5B, E). Finally, the Reduced-Ranoidea probe set had a median marker depth of 27.1 ± 16.0 X (n = 30;

range: 2–100.7 X; Figure 5B, F), which was 5 X higher than the Ranoidea 40K set. Using a Student's two-sample *t*-test, we found a significant difference in the distribution of median depth of markers between the Reduced-Ranoidea 20K and the Ranoidea 40K probe set (*ln* transformed*;* $T = -9.346$; $df = 4464.6$; $P < 0.001$). It is possible that the unshared markers between the 20K and 40K sets led to this difference, so we test only markers shared between the two sets (3054 markers); we still found a significant difference in depth of coverage between the median depth of markers (*ln* transformed; $T = 4.8$; $df = 6105.2$; $P < 0.001$); unexpectedly, the 40K had a higher median depth than the 20K across shared markers, but the overall median difference was small (Ranoidea = 26.9 X; Reduced = 26.5 X).

To evaluate exons and introns separately, we measured the same parameters as above across all the samples. When measuring depth in the Hyloidea dataset, we found a median depth of 40.4 ± 29.3 X ($n = 24$; range: 2.3–129.8 X) for exons and a much smaller median depth of 13.8 ± 10.7 X ($n = 24$; range: 1.3–72.9 X) for introns (Figure 5C). In the Ranoidea dataset, we found a median exon depth of 43.6 ± 29.6 X ($n = 24$; range: 2.7–147.7 X) and a much smaller median intron depth of 13.2 ± 9.7 X ($n = 24$; range: 1.5–96.2 X; Figure 5C). Finally, when using the 20K Reduced-Ranoidea we found a median depth of 48.1 ± 25.7 X ($n = 30$; range: 2.3–117.6 X) for exons and a smaller median depth of 15.8 ± 8.9 X ($n = 30$; range: 1.4–64.6 X) for introns (Figure 5C). Within the whole contig (Figure 5D–F), depth is generally highest near the center of the sequence and decreased towards the two ends of the contig. When binning the contigs in 1 percent bins, the distance from the either edge of the contig to the start of the exon is ~32–37 percent of the contig (Figure 5D–F). Interestingly, only ~25 percent of the contig is targeted exon sequence while ~75 percent is intron sequence, showing that the incidental capture is 3 X

higher than the targeted areas. These also results show that when considering the exon separately from the intron, the median depth between the 20K and 40K probe sets are nearly the same.

3.3.6 Population genetics

To understand whether FrogCap markers could be used for population genetics, we used GATK4 to discover genetic variants and SNPs across samples within the six phylogenetic scales. Generally, we find a pattern of decreasing variants from higher to lower phylogenetic scales, with greater than 20,000 variants at the species level after high quality filtering (Figure 8). This pattern remains for SNPs only, with greater than 10,000 SNPs found at the species level after aggressive filtering (Figure 8). Finally, when the independence of the SNP is required, we find that there is at least one strongly supported SNP (and often numerous more) on each individual marker permitting thousands of unlinked SNPs even at the species level (Figure 8). The results here only apply to our specific study configuration (number of markers and probes, sequencing platform, multiplexing strategy, taxonomic groups), but should provide a general set of expectations for variant discovery.

3.4 Discussion

We introduce FrogCap, a new and freely available set of configurable sequence capture markers for all frogs, representing a remarkably powerful new resource to be used for phylogenomics, systematics and population genetics. FrogCap is modular and provides numerous options for marker selection and analyses, which can easily be modified and adapted to different study questions. We assessed FrogCap using 105 samples across three differently designed probe sets and five phylogenetic scales. FrogCap is designed with a novel approach that located

orthologous markers from frog genomes and transcriptomes and uses two complementary probe sets (with 40,040 baits) to capture the same markers across the major clades within frogs: Ranoidea and Hyloidea. We also test a reduced version of the Ranoidea probe set (Reduced-Ranoidea with 20,020 baits) and address the advantages and disadvantages of different bait kit sizes, including the effects on depth of coverage and missing data. We compared our sequence capture results within the three probe sets (Hyloidea, Ranoidea, Reduced-Ranoidea) and calculate the sensitivity and specificity, quantify missing marker data, and address the depth of coverage. Furthermore, after processing, filtration, and alignment, we used five phylogenetic scales and four data types to compare the number of high-quality markers, missing marker data, quantity of sequence data, marker length, parsimony informative sites, and variants and SNPs discovered from the datasets. Importantly, we demonstrate the success of the FrogCap probe set and offer recommendations for its use for different phylogenetic scales and data types. The findings here will also be generally important for sequence capture study design and the applicability of different data types (e.g. exons, introns, UCEs) across organisms.

3.4.1 Bait kit size

One of the first decisions in sequence capture study design is selecting the size of the bait kit, which have important implications for the number of target markers and depth of coverage. Although larger sized bait kits are advantageous by targeting more markers, they could be disadvantageous if the sequencing effort is not adequate, resulting in higher amounts of missing data. Additionally, a smaller set of markers that contain fewer baits than a larger set would be expected to have a higher sequencing depth and thus greater depth because fewer genomic areas are being targeted for sequencing. We compared the 20,020 and 40,040 bait kits (20K and 40K

respectively; MyBaits kits from Arbor Biosciences), using the same number of samples and samples per pool sequenced on the same sequencing platform. The Ranoidea and Reduced-Ranoidea sets were compared here because the Reduced-Ranoidea set uses a subset of the same bait sequences from the Ranoidea set.

Our results suggest that there might be an advantage to using the 20K bait set when compared to the 40K set, where using a smaller bait set could result in a higher capture success from higher sensitivity and less missing data. Our results show that the 20K bait set had a higher sensitivity (~89% versus ~70% in the 40K; Figure 3) and much fewer missing marker data overall (~5% vs ~22% in the 40K; Figure 4). When capture success is not related to sequencing effort, we would expect no relationship between genetic distance and sensitivity / missing data; here we found significant relationships between genetic distance of samples from design markers and missing marker data / sensitivity in the Ranoidea 40K bait set. These results suggest that the 40K set had adequate sequencing depth to sequence most of the markers, ruling out a potential advantage of the 20K set.

Despite the potential advantages regarding capture success and missing data, depth of coverage is another important factor that could benefit the 20K reduced probe set. While the depth was significantly different between the samples and markers in 20K and 40K sets, we did not find a much larger depth in the 20K set (40K = ~24X; 20K = ~26X; Figure 5). Additionally, when comparing only shared markers, unexpectedly, the 40K set had a significantly higher depth than the 20K set, but the actual median difference was marginal (20K = ~26.5X; 40K = ~26.9X). This probably occurred from less variation in depth from the 20K set because all the samples were from the same genus and had similar depth, where the 40K had more variation because we sampled from many different families. Our expectation was twice the depth because the 20K

used half the number of baits and therefore more sequencing effort should be placed on this half-sized set. Overall our study suggests that the 20K offers a small advantage over the 40K, but we recommend using the 40K because it results in thousands more sequenced markers despite the higher capture success and slighter higher depth of the 20K set. One possibility to take advantage of 20K reduced sets is to multiplex and include more samples, possibly even twice the number of samples, to optimize the sequencing depth and reduce monetary costs.

It is not entirely clear why the depth of coverage from the 20K samples was less than expected, but we offer a few suggestions. One possibility is that we selected the largest Ranoidea markers for use in the Reduced-Ranoidea set, and because larger markers use more baits there is an increased opportunity to not acquire the full target marker when compared to markers that use fewer baits. Another factor could be off-target capture, where the mean specificity (percent of cleaned reads mapped to target markers) across samples in the 40K was 71 percent and 35 percent in the 20K. However, the large number of unmapped reads in the 20K probe set are not likely a result of off-target capture because the 20K uses a subset of the 40K baits from an already tested genus and there were few paralogs found. This suggests that there was a finite limit of depth that could be achieved from the number of baits; however, it is not clear what explains this possible limit and could have been because of many other technical factors during library preparation or the choice of samples.

3.4.2 Probe design

There are numerous considerations for designing probes from selected markers for high-throughput sequencing; here we compare probe sequences designed from transcriptomes and genomes and discuss probe tiling density. The availability of genomic resources and the type of

resources dictate whether it is possible to design probes directly from a genome, which has the benefit of obtaining more precise exon boundaries, designing markers that include non-coding sequence (more intron, UCEs), and paralog detection. Conversely, using only transcriptomes for probe design could result in a lower capture success if a probe is overlapping across two adjacent exons because introns are not sequenced in RNASeq and it is difficult to adequately screen for paralogs and duplicate genomic matches without a complete genome. Finally, probe tiling density is important in that higher densities have more probes covering a target region which increases the likelihood of obtaining that region while low densities may have lower capture success but enable more regions to be targeted.

We find that the genome-based design (Ranoidea) had a slightly greater capture success than the transcriptome-based (Hyloidea), where many of the uncaptured target markers and paralogs in Hyloidea were transcriptome-based (the shared markers between Ranoidea were largely successful). Both approaches work well on their own and the transcriptome-based approach successfully acquired 70 percent of the target markers, which is consistent with other transcriptome-based studies (e.g. Bi *et al.* 2012; Portik *et al.* 2016). Furthermore, the higher availability of genomic resources when designing the Ranoidea probe set (20 transcriptomes and 1 genome vs. 5 transcriptomes) likely had an impact on the capture sequence between Ranoidea and Hyloidea because the Hyloidea transcriptome markers could not be evaluated as rigorously as the Ranoidea markers and the lack of diverse sampling reduced the generality of the consensus probe sequence. This is evident in the Reduced-Ranoidea probe set that had the highest capture success (sensitivity: ~89 percent; missing marker data: ~5 percent) because the markers were selected from previously captured markers in the target clade.

Probe tiling density is another important variable that differentiates the FrogCap probe set from other frog probe sets. An important tradeoff with tiling density is that higher densities have more probes covering a target region to increase the likelihood of obtaining that region; conversely, lower tiling densities can lead to more target markers within the constraints of limited probes but could have more missing data because of the lower density. Similarly, some studies have included different probes from different species for the same marker to increase the capture success across different taxa (e.g. Portik *et al.* 2016; Hime *et al.* 2019). In our study, we used a lower density 2X tiling scheme (at least 50 percent of each probe overlaps with adjacent probes) that has been recommended as a standard for sequence capture designs (Tewhey *et al.* 2009). In our study, we find a slightly lower capture success (i.e. specificity and missing data) than other studies with more dense designs (this study = 70-75%; Portik *et al.* 2016 = 80%) which leads to a larger amount of missing marker data (this study = 20–25%; Portik *et al.* 2016 = 8–10%) However, the Reduced-Ranoidea design had greater success than these densely tiled studies, indicate that careful selection of markers based on prior successful sequencing can overcome this limitation of using less densely tiled design. In the Hyloidea and Ranoidea sets, even after the removal of poorly sampled markers, the total number of markers and base pairs of data in our dataset are much higher because of the much larger number of target markers at similar levels of missing data to these prior studies (Figure 6). Further, studies assessing missing data in sequence capture studies have found that moderate amounts of missing data (ca. 25–50%) have little impact on phylogenetic analyses (Zheng & Wiens 2015; Streicher *et al.* 2018). Therefore, a lower tiling density is recommended for probe design studies in the future, because this will result in more markers and more homologous data despite the missing data.

3.4.3 Phylogenetic distance

Phylogenetic distance from the design markers is likely one of the most important and predictable factors on the performance of the sequence capture (sensitivity, specificity, missing marker data); higher genetic distances from the targets leads to a decreased likelihood of capturing that marker. The Ranoidea probe set was designed using the *N. parkeri* genome, which is nested within Ranoidea while the Hyloidea probe set was designed using consensus sequences from available transcriptomic data. Probes designed from consensus sequences could be advantageous in minimizing the genetic distance of the samples from the probes and thus increase capture success.

We find that species with a higher genetic distance from the design markers exhibit a predictable decrease in the sequence capture sensitivity and specificity, leading to a higher percent of missing data with increasing genetic distance (Figure 3–4). This is also reflected at different phylogenetic scales, where the percent of missing data is higher at scales that include more divergent taxa (Order and Superfamily; Figure 6D) when compared to shallower phylogenetic scales (Family, Genus, Species; Figure 6D). In particular, the first diverging lineages of Archeobatrachian frog and Salamander lineages had lower capture success than the Hyloidea lineages (Figure 2), and the most divergent (from the target *N. parkeri* genome) Ranoidea family Microhylidae had lower success from the Ranoidea probe set.

We compare the Ranoidea probe set where the *N. parkeri* genome was used as a reference and basis for designing probes and the Hyloidea probe set which was designed from consensus sequences from transcriptomes. Surprisingly, we did not find a substantial difference in capture success (measured by sensitivity and missing marker data; Figure 3–4) by using consensus sequences for the Hyloidea probe set; however, although significant, the relationship

between genetic distance from the Hyloidea design sequences and sensitivity / missing marker data were not strong and were strongly influenced by the outgroup non-target taxa (Figures 3–4). Upon removal of these taxa, the relationships were no longer significant, which suggests that the consensus sequences minimized the negative effects of genetic distance for groups closely related to those used for the transcriptome consensus sequence (possibly improving capture success). Additionally, because genetic distance is not significantly related to capture success in the Hyloidea probe set, other factors could explain missing markers, such as paralogs which are more prevalent in the transcriptome-based sequence capture samples and genetic distance for a subset of the samples not related to the design transcriptomes. Another approach would be to design probes by reconstructing ancestral sequences (Hugall *et al.* 2015) or other clustering and redundancy reducing algorithms for probe design (Mayer *et al.* 2016), which could further optimize probe designs in the future.

3.4.4 Phylogenetic scale

Understanding how different sequence capture designs perform at different phylogenetic scales is important for probe choice and selecting the types of data to include in downstream analyses, and we assess the impact of phylogenetic scale at the order, superfamily, family, genus and species level (Townsend 2007; Taylor & Piel 2004). Generally, at more broad phylogenetic scales (e.g. order, superfamily) the number of alignments decreases because missing data has a greater impact (~25 percent missing data) from marker drop-off in divergent samples (Figure 6D). At shallow phylogenetic scales (e.g. family, genus, species) the amount of missing data is much less (less than 10 percent missing data) and more uniform across samples resulting in more complete alignments (Figure 6D), where the number of marker alignments depends on how

divergent the target group is from the design probes (i.e. Microhylidae genus level comparison would differ from Ceratobatrachidae). To help remedy this, we designed the FrogCap probe sets to be modular, and we demonstrate this with the smaller (20K vs 40K baits) Reduced-Ranoidea probe set. The Reduced-Ranoidea probe set was designed based on successful capture data from one target group of interest (the genus *Occidozyga*), and we find a higher capture success (sensitivity) and much fewer missing data across this group's alignments (~5% vs. ~20%).

3.4.5 Data type comparison

To understand data type differences and data selection for analyses, we evaluate UCE, exon, intron and gene sequence data and compare these data types at different phylogenetic scales. UCEs and exons were included in the marker design, and gene alignments are exons combined from the same gene; however, intronic sequence was indirectly acquired through "by-catch" by sequencing adjacent regions from a captured DNA fragment (e.g. Bi *et al.* 2012; Guo *et al.* 2012; Tewhey *et al.* 2015). Surprisingly, the number of base pairs of data available from non-targeted intronic sequence was 2–3 times higher than explicitly targeted exon sequence (Figure 3), suggesting that intronic sequence is an abundant and potentially important resource. Additionally, intronic sequence could be valuable because of potential neutral evolution when compared to exons which are typically functional and under selection and UCEs which are likely under strong selection to remain ultra-conserved (Katzman *et al.* 2007; Stephen *et al.* 2008).

The most important characteristic to evaluate across different data types is the informativeness or variability of the marker, which could potentially differ based on phylogenetic scale and data type. We show that parsimony informative sites vary markedly between both data type and phylogenetic scale (Figure 7). Among data types, the intron is the

most variable and is similar to UCEs in that the variability increases towards the flanks of the marker alignment; however, UCEs have moderate variability when including the central conserved region. Conversely, exons have a small to moderate amount of variation. Introns show this pattern likely because of neutral evolution or weak selection (Stephen *et al.* 2008), whereas exons remain more conserved because they are under very strong selection (Katzman *et al.* 2007). When considering phylogenetic scale, variability is higher in all data types from shallow up to broad phylogenetic scales. At shallow phylogenetic scales (species or genus) exons and UCEs have little variation while introns remain variable while at broad phylogenetic scales (order, superfamily) the exons and UCEs are more variable while introns are extremely variable. This pattern of variability could have important consequences for downstream analyses because introns at broad phylogenetic scales might be saturated from multiple substitutions at the same site while at shallow scales exons may have no variability and would not be informative for many analyses. A careful evaluation and selection of marker types should be an important step in deciding which datasets to invest resources in sequencing and analyzing.

The number of base pairs within each marker should be considered when including markers for analyses, and the FrogCap probe set includes a mixture of short and long markers (Figure 1B). UCEs have the longest mean length (~500 bp) because they are not separated into two data types (i.e. intron / exon), where the combined exon and intron marker could be analyzed similarly. The mean size of exons was ~250 bp (Table 1) which is similar to the predicted mean exon length across the *N. parkeri* and *Xenopus laevis* genomes (~200 bp); markers 200 bp and less represent the majority of individual markers in the FrogCap probe set. Short exons are advantageous because they indirectly increase the amount of intronic sequence (~500 bp from each marker which are longer than exons; Figure 6) that would be useful for population genetic

and phylogenetics. Additionally, a higher number of short exons allow more SNPs to be incorporated into analyses that require genetically unlinked SNPs (Figure 8). The main disadvantage of short exons is that they may lack sufficient variability for strong support in phylogenetic analyses, which is important for summary species tree methods using individual gene trees. For these types of analyses, FrogCap also includes ~1000 long exons greater than 500bp in length (and 500 exons greater than 1000 bp), which are fewer in number because longer exons require more baits. Long exons would be ideal for analyses where the goal is to have fewer, but stronger statistical support among gene trees. The publicly available FrogCap pipeline separates alignments into these different data types so that researchers will have a great deal of flexibility in analyzing sequence data.

3.4.6 Future directions

We present and test FrogCap, a new modular sequence capture probe set for frogs, that we intend to expand upon in future work. First, although not the focus of this work, a phylogenetic assessment of the different data types and how they perform at different phylogenetic scales across different types of analyses would be important for future FrogCap studies and other phylogenomic studies that include different data types (Hutter *et al. unpublished data*). Second, some smaller amphibian phylogenetic groups are under-represented (Salamanders, Caecilians, and Archeaobatrachian frogs) in FrogCap; work is currently underway on a "universal" module of markers that could be captured reliably across amphibians (but at the cost of fewer informative sites). In addition, specialized probe sets have been designed for specific clades (the genus *Limnonectes*, and families Dendrobatidae, and Microhylidae), which emphasizes the adaptability of FrogCap (*unpublished data*). Third, although sequence capture is

not the best method for acquiring SNP data, we demonstrate that thousands of high-quality SNPs can be discovered; future studies will address the performance of SNP-based analyses resulting from FrogCap. Finally, Version 2.0 of the Ranoidea and Hyloidea probe sets analyzed in this study have been created and exclude markers that did not capture well across our test samples; these were replaced with additional UCEs and longer exons. Both are available, along with Version 1, on the FrogCap GitHub.

3.5 Tables

Table 1. Marker contents targeted for three probe sets designed in this study. The Reduced probe set uses the same markers and probes from the Ranoidea set but was designed with half the number of baits for a specific taxonomic group.

	Hyloidea	**Ranoidea**	**Reduced**
N probes	40,040	40,040	20,020
N base pairs	2,929,956	3,983,022	1,519,233
N markers	10,633	13,621	3,247
N exons	8788	12,934	3,161
N UCEs	2360	651	0
N Legacy	86	36	86
Mean marker length	317.2	255.5	467.8

Table 2. Sequence capture evaluation for each probe set. Our Reduced probe set uses the same markers and probes from the Ranoidea set but was designed with half the number of baits for a specific taxonomic group. "X" depth refers to the number of overlapping bases in a given marker.

	Hyloidea	**Ranoidea**	**Reduced**
N probes	40K	40K	20K
N base pairs	2,929,956	3,983,022	1,519,233
N markers	10,633	13,621	3,247
Mean sensitivity (%)	70.3%	70.6%	89.1%
Mean specificity (%)	47.9%	71.1%	35.7%
Mean marker missing data (%)	21.9%	22.7%	4.5%
Median depth of coverage	19.7X	22.1X	26.6X
Median exon depth	40.4X	43.6X	48.1X
Median intron depth	13.8X	13.2X	15.8X

Table 3. Summary of alignments at each phylogenetic scale.

Scale	Order	Superfamily	Superfamily	Family	Genus	Species	Reduced
Clade	Anura	Hyloidea	Ranoidea	Mantellidae	*Cornufer*	*vertebralis*	*Genus*
N samples	48	24	24	8	24	16	30
N markers	5500	8712	13,099	12106	12701	12009	3156
Total bp after trim	1,806,209	4678657	5421176	8129529	7526490	7061983	2268852
Mean length	328.4	537.0	413.9	671.5	592.6	588.1	718.9
Total IS	944195	1432769	2144350	818032	1032575	243238	243238

3.6 Figures

Figure 1. The modularity of the FrogCap probe set permits the selection of different types of markers. The data category in A) shows the quantity of different marker types (Legacy, UCE, Exon, Gene) used in the design of each probe set (40K bait set used for Ranoidea and Hyloidea; 20K bait set used for Reduced-Ranoidea). The marker size distribution in B) shows the general size classes of markers used for each of the probe sets. The "Combined" probe set refers to the number of unique markers across all probe sets to represent the total available markers for FrogCap. Different configurations can be created based on bait kit size, modules, marker size or phylogenetic group.

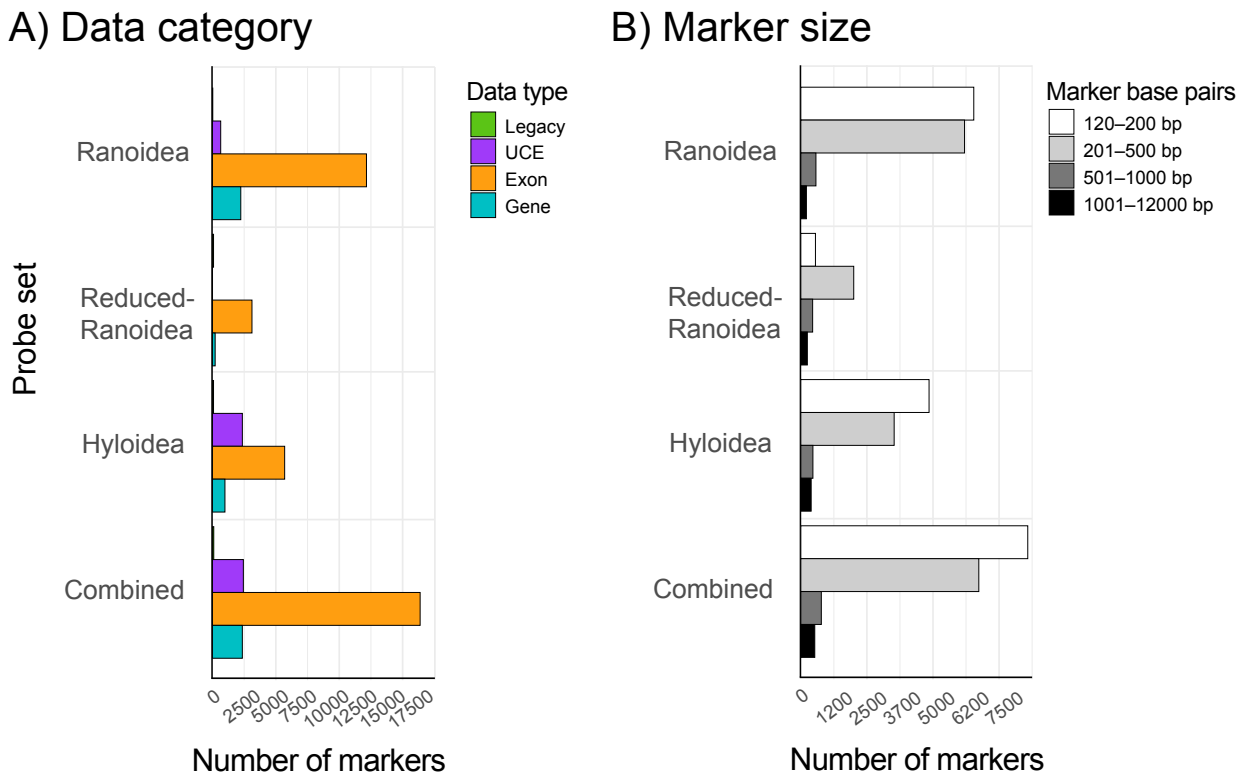

Figure 2. A summary of the data obtained for each sample, shown at each phylogenetic scale. The total number of markers in A) are those obtained after matching to the target loci and removal of paralogs. In B), the proportion is the sample total number of markers divided by the number of target markers. Finally, in C) the total number of megabase pairs are the number of aligned bases before (light green) and after trimming (dark green).

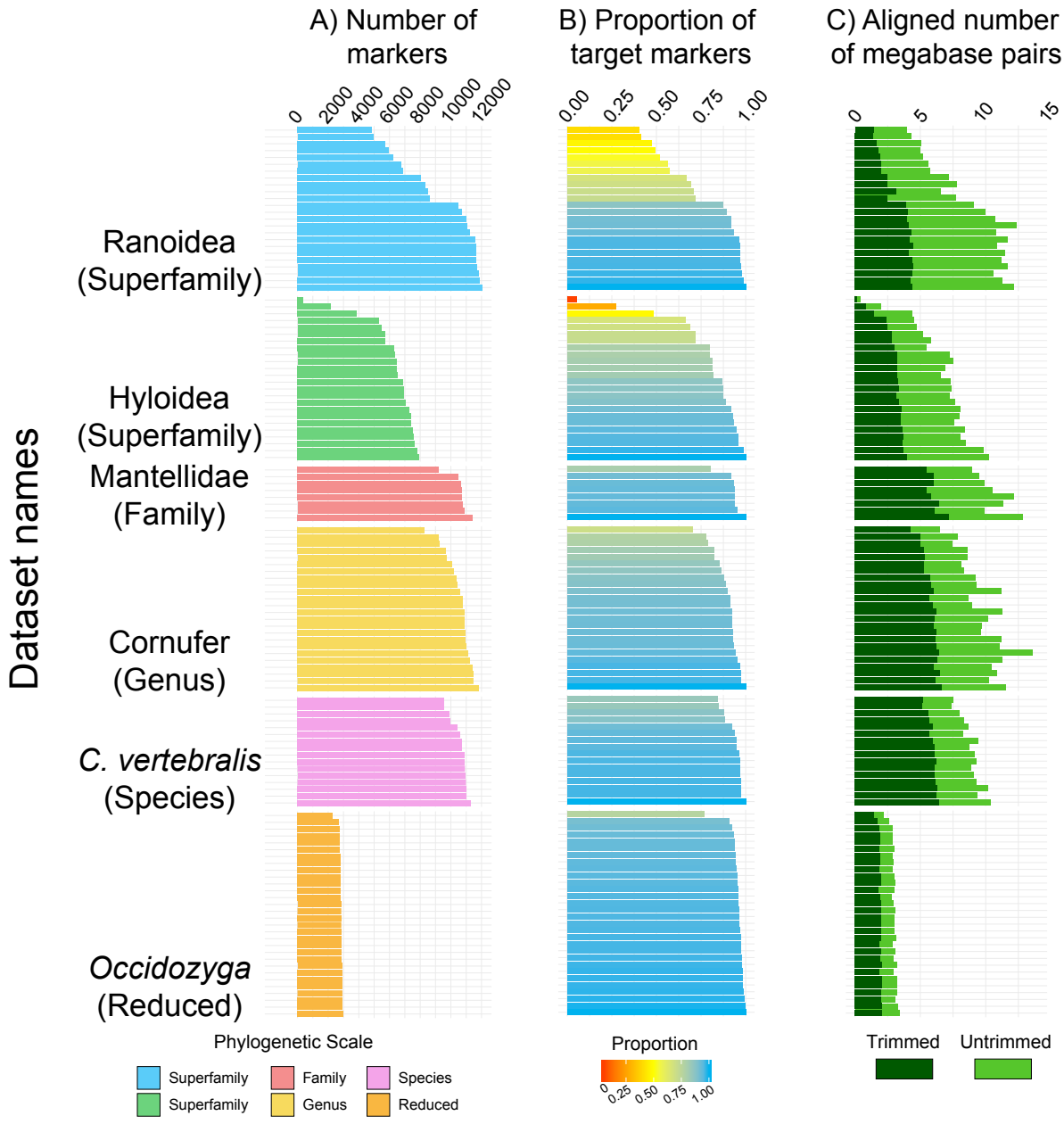

Figure 3. Sample sensitivity and specificity compared among three different probe sets (Hyloidea, Ranoidea, Reduced-Ranoidea). In addition, relationships between genetic distance and sensitivity / specificity, evaluated for Hyloidea and Ranoidea probe sets (Reduced-Ranoidea not included because samples are all from a single genus and have the same genetic distances). The box plots show the distribution of sensitivity (A) and specificity (B) values across the probe sets. Sensitivity (A) has a significant negative relationship with genetic distance in Ranoidea and a weaker but still significant relationship in Hyloidea. Specificity (B) has a significant negative relationship in Ranoidea and a weak and non-significant relationship in Hyloidea. 95 percent confidence intervals of the estimated regression line indicated by green and blue shading.

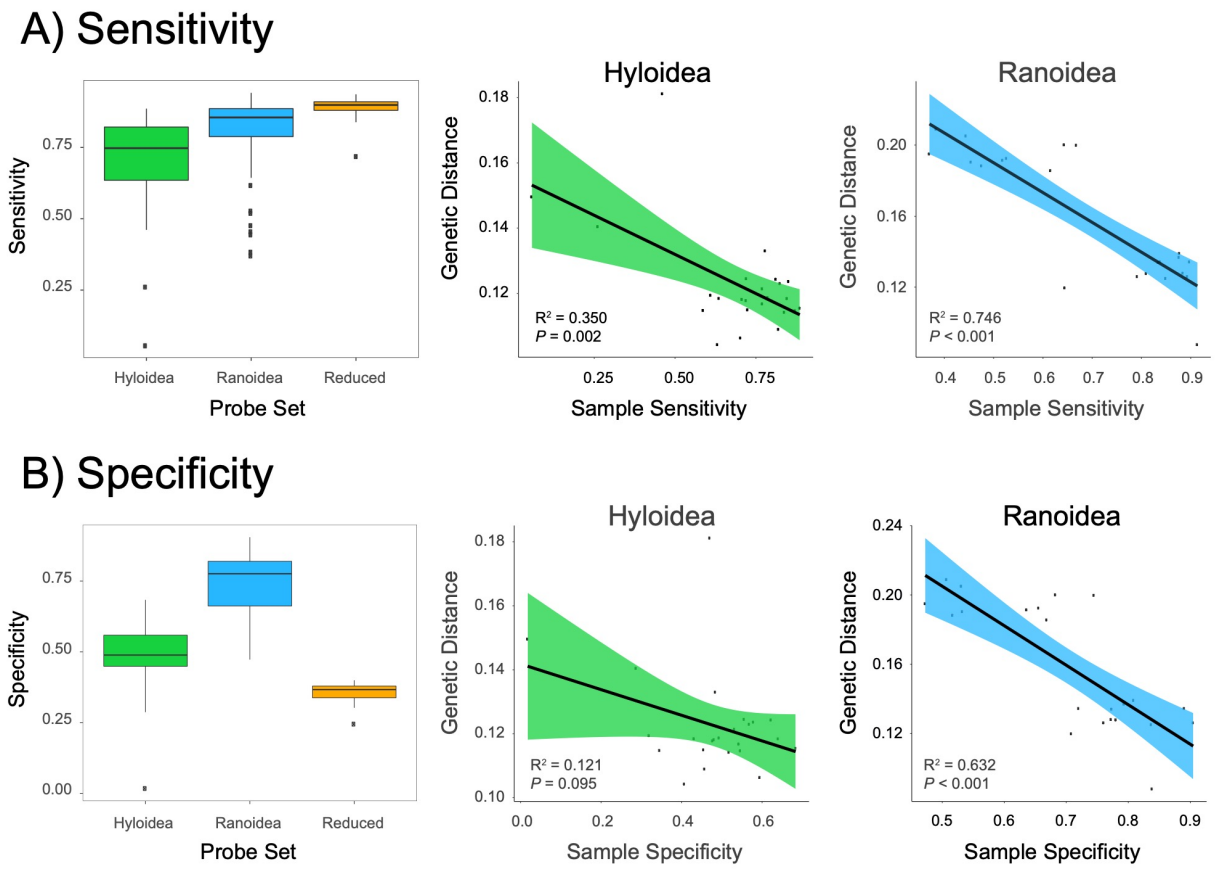

Figure 4. Missing data are compared for three different probe sets (Hyloidea, Ranoidea, Reduced-Ranoidea). Base pair missing data (also the inverse of sensitivity) in A) is the percent of missing data calculated from the number of missing bases pairs across alignments for each sample. Marker missing data in B) is the percent of missing markers across alignments for each sample. The consensus-based marker design missing data from Hyloidea in C) has a weak but significant positive relationship with genetic distance. Conversely, the genome-based missing data from Ranoidea in D) has a strong and significant positive relationship with genetic distance. Reduced-Ranoidea not included because samples are all from a single genus and have the same genetic distances). 95 percent confidence intervals of the estimated regression line indicated with green and blue shading.

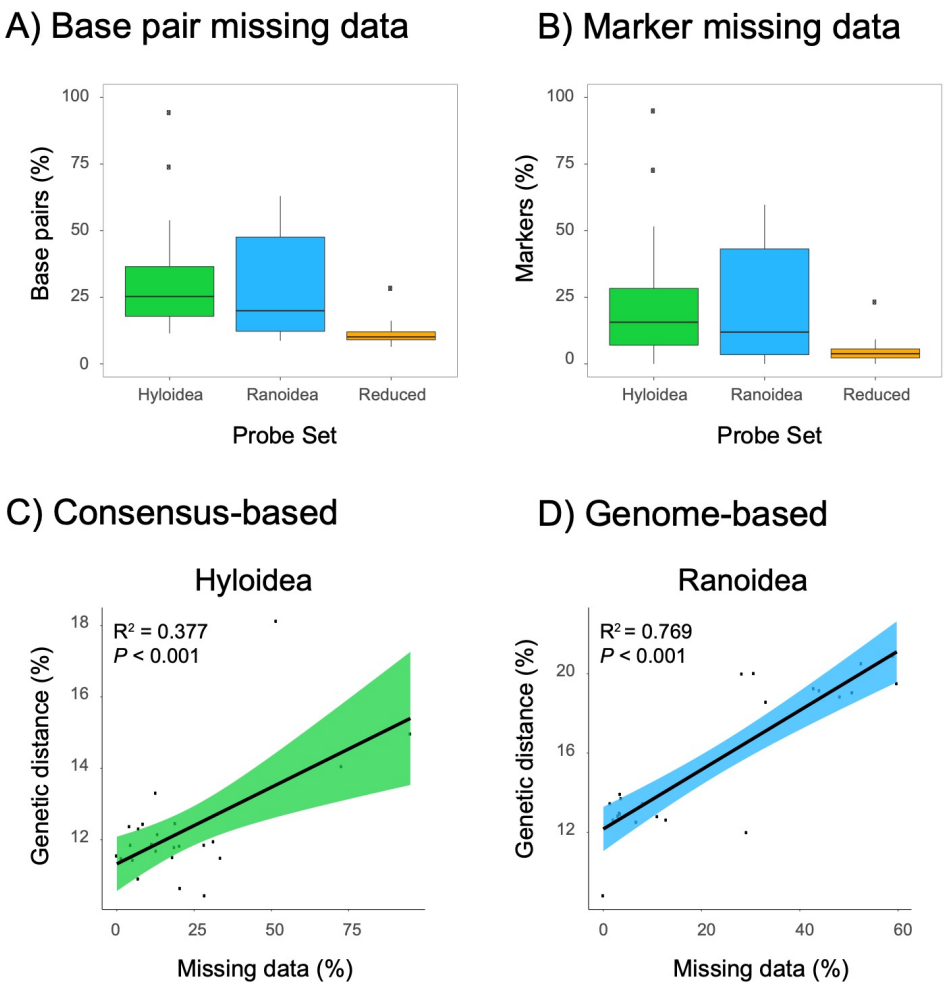

Figure 5. Depth of coverage statistics, calculated for three different probe sets. Depth is summarized for A) median depth of markers within samples; B) median depth calculated between markers; C) median depth of markers was calculated for the exon and intron separately; and (D–F). Depth was calculated across each full-length marker contig by aligning the cleaned reads to the aligned sample contigs and counting the number of bases within each 1 percent bin (100 total bins per marker), and the median for each bin across markers was plotted. The gray coloration represents the standard deviation within each 1 percent bin across markers. The vertical dotted lines in each plot give the mean position where exon-intron boundaries occur, with the standard deviation shown in the red-colored shading.

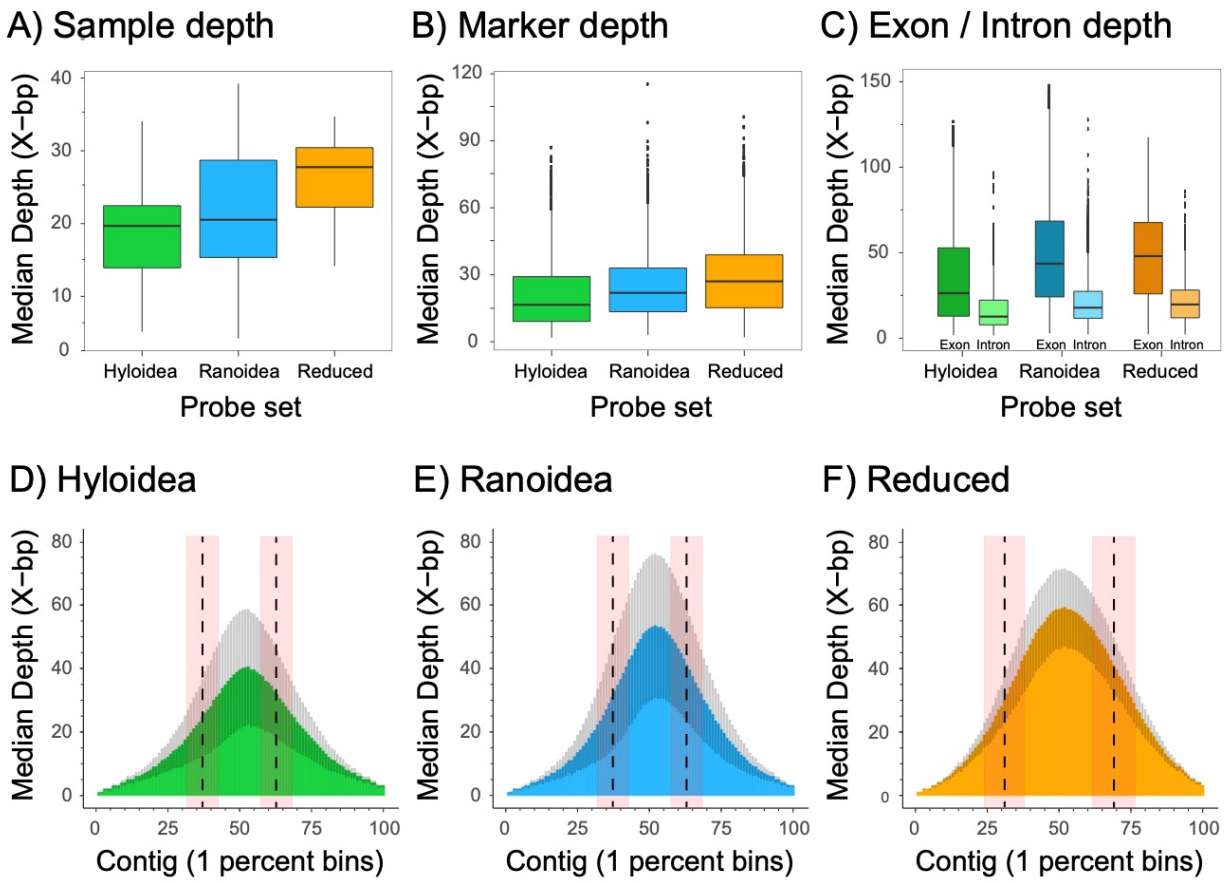

Figure 6. Summary statistics of alignments, comparing quantity of sequence data for different dataset types across different phylogenetic scales after filtration, alignment, trimming and dataset partitioning. Comparisons include: A) number of alignments for each dataset at each phylogenetic scale; B) number of base pairs and parsimony informative sites (shown as the darker shading) plotted for each dataset within each phylogenetic scale; C) mean alignment length (with standard deviation shown as error bars) is compared for different data types and phylogenetic scales; and D) percent of missing marker data (measured across markers with standard deviation shown as error bars) is compared for different datasets.

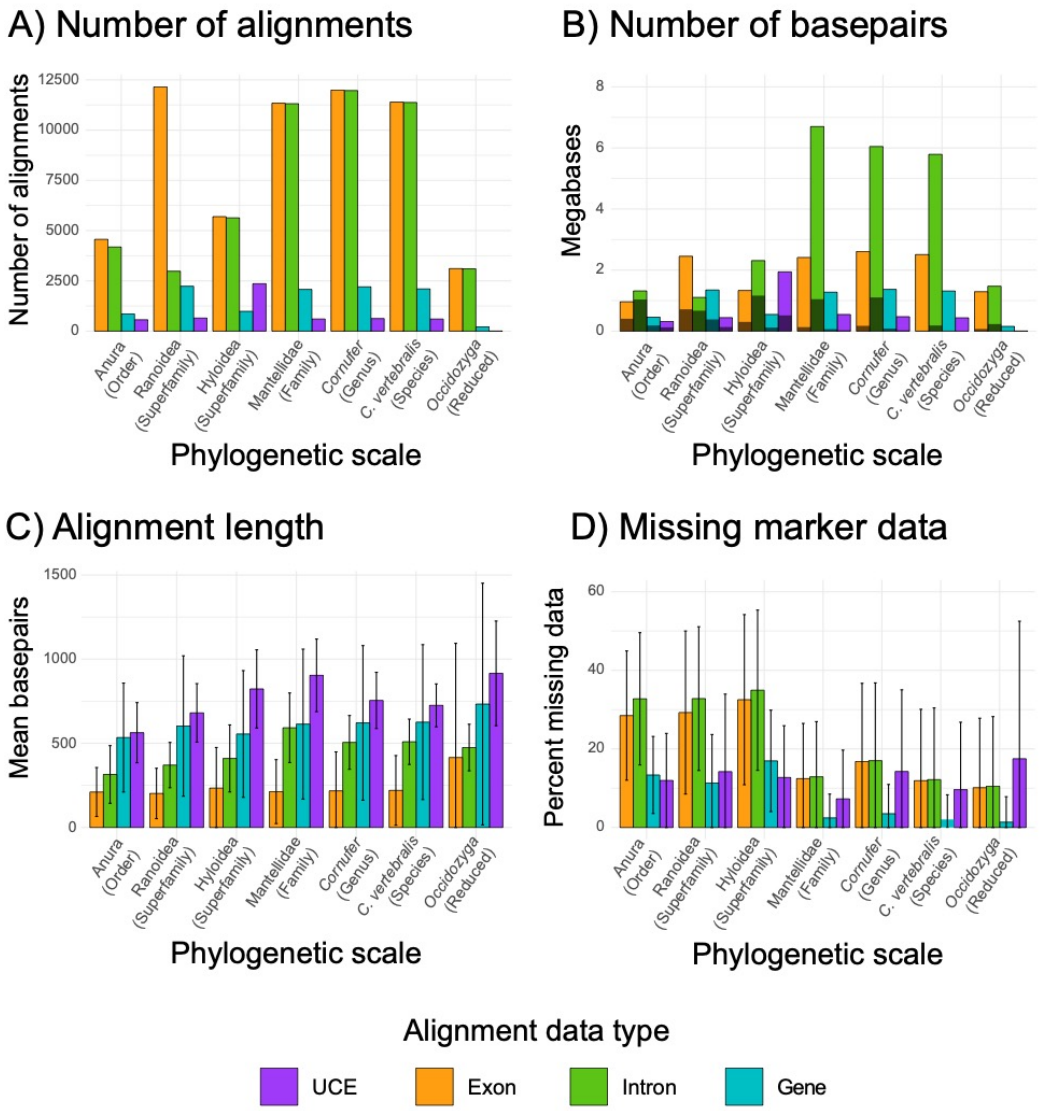

Figure 7. Comparisons of percent of parsimony informative sites, for each data type, at phylogenetic scales. Introns are the most variable data type across phylogenetic scales and display moderate variation even at the species level. Exons and UCEs had moderate amounts of variation, where both data types had little variation at the species level.

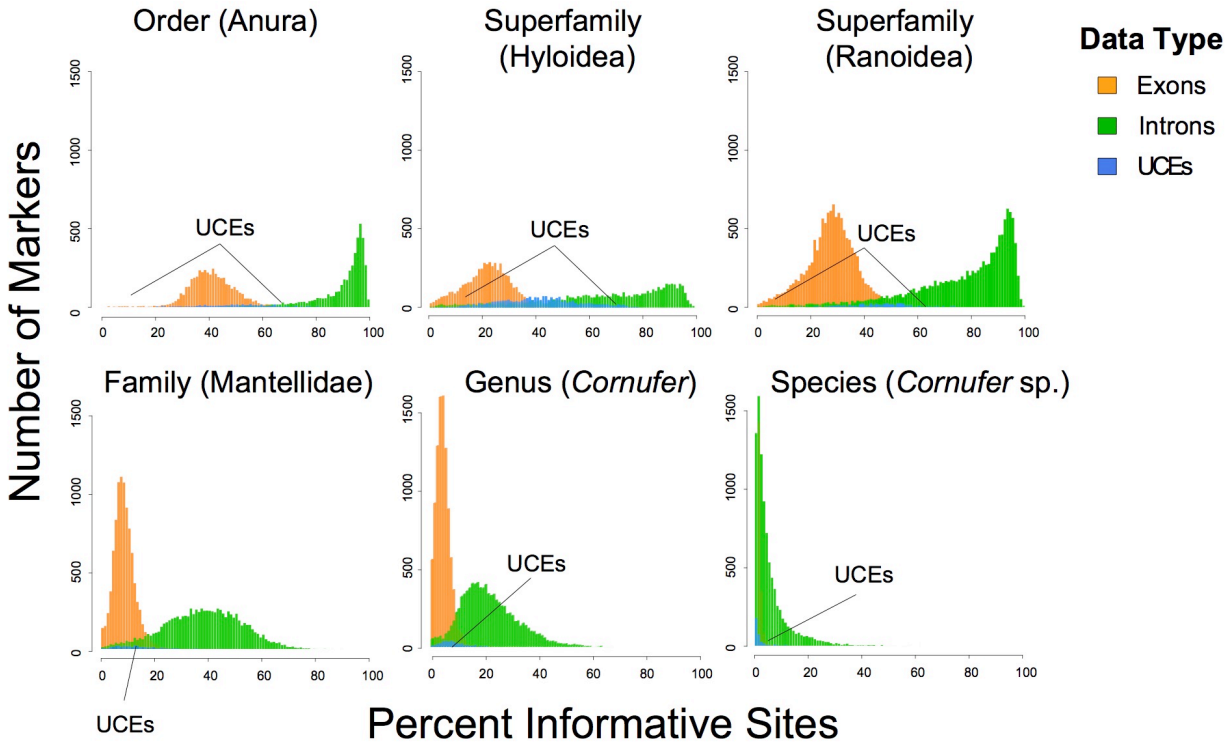

Figure 8. Mean number of variants across samples after different filtration schemes are shown at each phylogenetic scale (Anura not shown). The different variant filtering are: A) All variants: all variants after moderate filtering (quality > 5); B) High quality variants including SNPs, MNPs, and indels (quality > 20); C) SNPs: the number of SNPs after high-quality filtering (quality > 20); and D) Unique markers: the number of unique markers from the probe sets that contain SNPs.

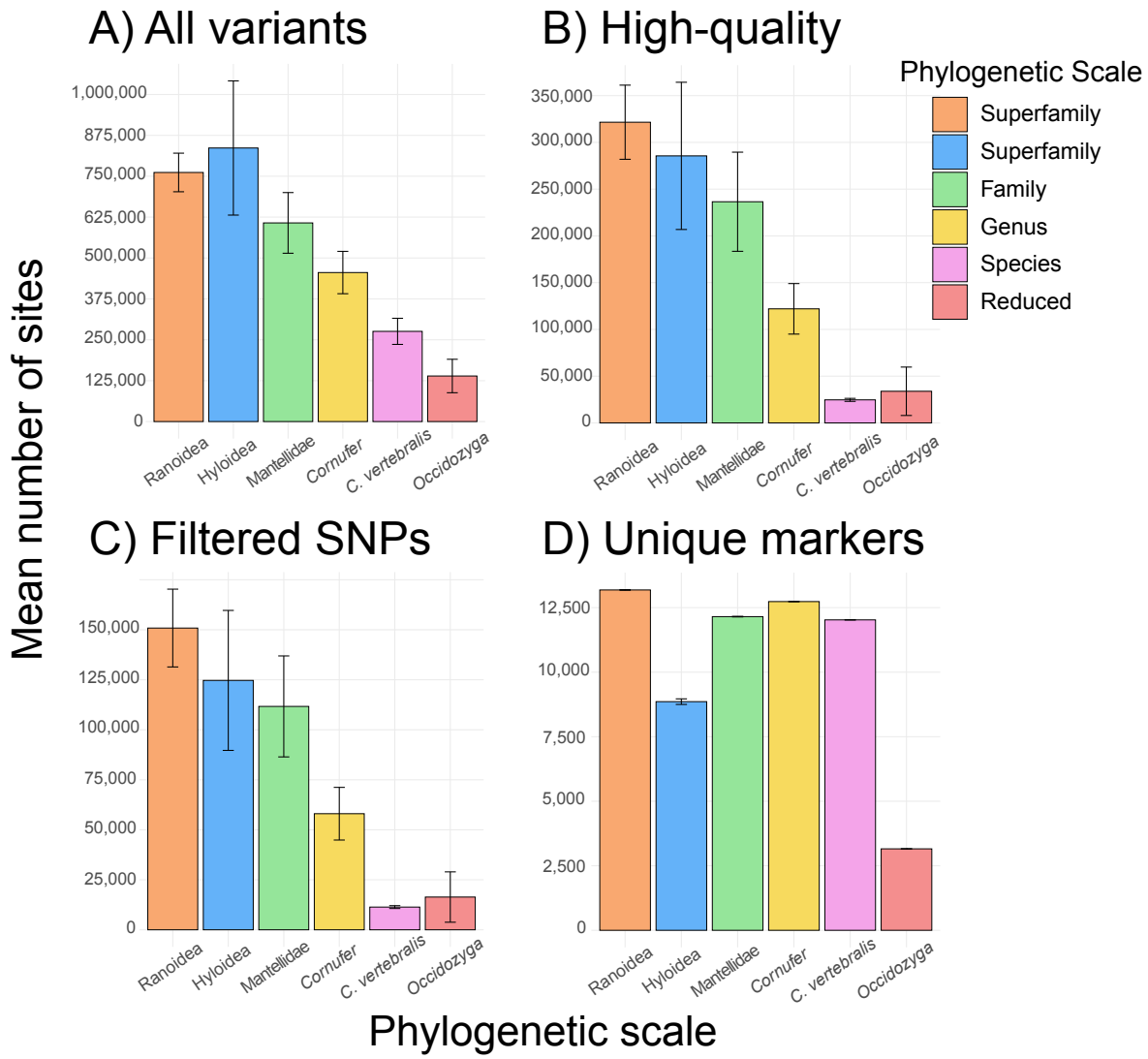

CHAPTER 4

Transcriptomes or sequence capture for phylogenomics? A comparison of their efficacy and gene tree discordance in the frog family Mantellidae from Madagascar

Carl R. Hutter, Iker Irisarri, Loïs Rancilhac, Frank Glaw, Walter Cocca, Angelica Crottini, Sven Künzel, Andolalao Rakotoarison, Mark Scherz, Hervé Philippe, Miguel Vences; unpublished

4.1 Introduction

The ability to sequence large portions of an organism's genome has led to new and exciting challenges for systematic and evolutionary biologists in revisiting challenging phylogenetic questions and pursuing the new analytical questions that arise when provided millions of base pairs of data. While whole genome sequencing for non-model organisms remains costly, high throughput sequencing of targeted genomic regions has enabled numerous approaches in creating reduced genomic representation datasets at a much lower financial cost per nucleotide (Kircher & Kelso 2010; Rohland & Reich 2012). Among the freely-available methods to sequence moderately-divergent orthologous markers of interest for systematics are targeted sequence capture and transcriptome sequencing (Wang *et al.* 2009; Jones & Good 2016).

The objective of sequence capture is to sequence genomic regions typically through hybridization-based capture from a previously designed set of known markers (e.g. Faircloth *et al.* 2012; Hancock-Hanser *et al.* 2013; Jones & Good 2016). Sequence capture benefits from the potential to acquire markers that are useful at all evolutionary time-scales—for example, moderately variable exons across families can be advantageous at the species level when using highly-variable regions flanking the target such as ultra-conserved elements (UCEs) or introns adjacent to target exons (**Chapter 3**). Disadvantages of sequence capture are that target markers need to be known before probe design which requires genomes and/or transcriptomes of a related species. Phylogenomics from sequence capture have helped resolve numerous uncertain relationships at very deep to shallow time scales (Johnson *et al.* 2013; Prum *et al.* 2015; Gentekaki *et al.* 2017).

Similarly, transcriptome sequencing has the potential to sequence the entire expressed exome by targeting RNA molecules to reveal the presence and quantity of RNA in a given tissue (RNASeq; Wang *et al.* 2009). Transcriptome sequencing is promising because it can acquire a large portion of the exome which is advantageous when no genomic resources are available to target specific genomic regions or if more data is desired (Wang *et al.* 2009). A large proportion of phylogenetically informative core orthologous markers can be obtained by low-coverage RNAseq (Irisarri *et al.* 2017), making this a more economical and flexible option when compared to high-coverage RNASeq. Transcriptomes may be disadvantageous for systematics when fresh tissue is difficult to acquire or if the tissue has been degraded (Romero *et al.* 2014; Sudmant *et al.* 2015), which would compose the vast majority of tissues stored in biodiversity museum archives (VertNet 2019). In addition, high-variability intronic regions and other non-coding regions are not sequenced through this method, leading to a loss in potentially valuable informative regions. Phylotranscriptomics have been used to provide strong statistical support for previously poorly supported relationships across broad time scales (e.g. land plants: Wickett *et al.* 2013; jawed vertebrates: Irisarri *et al.* 2017; tuna fish: Ciezarek *et al.* 2018), but also have proven useful to successfully recover shallow relationships (e.g., Rodríguez *et al.* 2017 and references therein).

A common issue that has emerged from the analysis of massive amounts of sequence data sampled from across the genome is when the species tree differs from individual gene trees used to estimate that species tree. This pattern has been shown in numerous organisms using genomic, transcriptomic, sequence capture, and other reduced genomic representation approaches (Cacti: Copetti *et al.* 2017; *Drosophila*: Pollard *et al.* 2006; Frogs: Hime *et al.* 2019; Squamates: Linkem *et al.* 2016; Mammals: Song *et al.* 2015). In addition, several methods have been developed to

address this discordance in a coalescent-based framework (species-tree methods: ASTRAL: Zhang *et al.* 2018; MP-EST: Liu *et al.* 2010; BUCKY: Larget *et al.* 2010). Usually, gene tree discordance is attributed to evolutionary processes such as incomplete lineage sorting, horizontal gene transfer, gene loss or duplication, or hybridization (Knowles 2009; Knowles *et al.* 2018). In addition, discordance could be caused by non-biological properties of the dataset, such as the alignment length, few informative sites, or errors in sequence assembly or alignment (Xi *et al.* 2015; Richards *et al.* 2018). One approach to address the non-biological component is binning together separate exons from the same gene or transcript into a single alignment for the estimation of a single tree (Mirarab *et al.* 2014); however, it is not clear if these exons maintain linkage because of unknown recombination distance, the amount and variation in intron length, and physical distance from other exons in the genome. Past studies addressing individual exon trees provide evidence that they are discordant from the overall combined "gene" tree, and suggest that recombination often occurs at small scales within single genes (Scornavacca & Galtier 2017; Spring & Gatesy 2018), which violates an important assumption in coalescent-based species tree methods. Given that this issue remains little explored, we aim to use both transcriptomic and sequence capture data to shed light on the impact combining exons from the same gene or transcript have on gene tree discordance.

For amphibians, a comparison of these different reduced-representation genomic approaches remains largely unexplored because of the relative lack of publicly available genomic resources until recently. Originating from these resources, a new probe-set, "FrogCap" (**Chapter 3**), has been designed to sequence markers in frogs. FrogCap contains ~12,500 new exons and unifies all previous sequencing work on frogs by including 1000 legacy Sanger and UCE markers previously used in phylogenetic studies (Pyron & Wiens 2011; Feng *et al.* 2017;

Streicher *et al.* 2017). Several past studies have used UCEs (Alexander *et al.* 2016; Streicher *et al.* 2017) and AHE (Lemmon *et al.* 2012; Peloso *et al.* 2015; Heinicke *et al.* 2018), while one additional study created a customized probe set for a clade of several African families (Portik *et al.* 2016). While UCEs have been used in frogs, they are problematic because they were designed for amniotes and only about half the UCE loci are typically captured (~2300 loci; Streicher *et al.* 2017). Additionally, transcriptomes are available for numerous species of frog, but no explicit systematic study has been conducted in frogs using transcriptomes. In this study, we test and compare the FrogCap probe-set and RNASeq to estimate the phylogenetic relationships of an group of frogs from Madagascar challenged by a turbulent systematic history.

The systematics of frogs from the family Mantellidae have had a long and contentious history. Mantellid frogs are endemic to Madagascar and the Comoroan Island of Mayotte, and are extremely diverse with 224 species contained in 12 genera (AmphibiaWeb 2019). Mantellidae was considered a family relatively recently, with some of the first molecular systematic studies concluding that mantellid frogs are a well-supported monophyletic group (Vences *et al.* 2000; Glaw & Vences 2006). Prior to this it was thought the different groups in Madagascar were non-monophyletic and were thought to be from several different families: species from Mantellinae were often included as a subfamily in Ranidae (Blommers-Schlösser 1979); *Boophis* was placed in the family Rhacophoridae Hoffman 1932 (Blommers-Schlösser 1979); *Laliostoma* was considered a member of the genus *Tomopterna* Duméril and Bibron 1841 (Cope 1868; Glaw *et al.* 1998*)*; and *Aglytodactylus* was more turbulent, being included in all these prior mentioned groups (Glaw *et al.* 1998). Additionally, Mantellidae was occasionally used to refer to some of the currently recognized mantellid frogs, although without phylogenetic evidence (Blommers-Schlosser & Blanc 1991).

With the first molecular phylogenetic evidence these seemingly disparate lineages were found to be closely related and were united into the family Mantellidae and initially classified into three subfamilies and five genera: (1) Laliostominae: *Aglytodactylus*, *Laliostoma*; (2) Boophinae: *Boophis*; and (3) Mantellinae: *Mantella* and *Mantidactylus* (Vences & Glaw 2001). Once Mantellidae was established as a single monophyletic radiation, to accommodate the exceptional morphological and reproductive diversity in Mantellinae, the number of genera in the subfamily was increased from five to eleven (Glaw *et al.* 2006). Finally, a new genus *Tsingymantis* was recently discovered (Raselimanana *et al.* 2007), which has not been placed consistently in any subfamily (Raselimanana *et al.* 2007; Kurabayashi *et al.* 2008; Wollenberg *et al.* 2011). Some studies have found *Tsingymantis* to be most closely related to Mantellinae through morphological and molecular evidence and is currently placed in this subfamily based on these prior findings (Glaw & Vences 2007; Raselimanana *et al.* 2007; Wollenberg *et al.* 2011). Since these pioneering molecular systematic studies, the taxonomy of Mantellidae has remained relatively stable; however, the phylogenetic systematic relationships among the three mantellid subfamilies and *Tsingymantis* have remained unclear (Figure 1). Prior studies that have been unable to resolve these relationships have used up to eight Sanger markers (Wollenberg *et al.* 2011), suggesting the limits of phylogenetic inference have been reached with these data.

To address the questions and challenges outlined herein, we collected two phylogenomic datasets from sequence capture with FrogCap and transcriptomes with RNASeq. Our objective is to provide one of the first comparison of sequence capture and transcriptome data for phylogenomic systematics (but see Portik *et al.* 2016 and Teasdale *et al.* 2016, which generated transcriptomes to design probes for sequence capture); this study can serve as an important resource for future researchers planning studies across all organisms. Our second main objective

is to understand how gene discordance could be caused by statistical noise in the datasets by comparing the amount of discordance in gene trees estimated from transcripts and exons separated from the transcripts, and also between sequence capture exons and genes. Finally, we will use the information acquired from these analyses to test longstanding phylogenetic questions on the relationships among subfamilies in the family Mantellidae. Resolution at this phylogenetic scale is frequently a recurring problem that can be clarified through new and expansive phylogenomic datasets, which would be important for future taxonomy and to better understand the evolution of this exceptional rapid radiation.

4.2 Materials and Methods

4.2.1 Data availability

All raw sequencing reads will be deposited and made available in the GenBank SRA upon acceptance of this manuscript in a peer-reviewed journal. All alignments analyzed and materials for replicating analyses will be made available on the Open Science Framework following manuscript acceptance. Finally, the data analysis pipeline and scripts for all analyses here are available on Carl R. Hutter's GitHub (https://github.com/chutter/FrogCap-Sequence-Capture).

4.2.2 Probe design, library preparation and sequencing

We selected one species from each of the 12 genera in Mantellidae (*Aglyptodactylus, Blommersia, Boehmantis, Boophis, Gephyromantis, Guibemantis, Laliostoma, Mantella, Mantidactylus, Spinomantis, Tsingymantis,* and *Wakea*). We supplemented this dataset with

previously sequence outgroups from **Chapter 3** (*Rhacophorus bipunctatus, Kalophrynus pleurostigma, Amolops ricketti,* and *Playmantis corrugatus*). Tissue samples for molecular work were obtained from the museum holdings of The University of Kansas (KU), Zoologische Staatssammlung München, Munich (ZSM), and amphibian collections of the Mention Zoologie et Biodiversité Animale of the Université d'Antnanarivo (UADBA-A). Genomic DNA was extracted from 12 tissue samples through the use of a PROMEGA Maxwell bead extraction robot. The resultant DNA was quantified using a PROMEGA Quantus Fluorometer. Approximately 500 ng total DNA was acquired and set to a volume of 50 ul through dilution with Promega elution buffer or concentration using a vacuum centrifuge of the extraction when necessary.

Probe design follows **Chapter 3** and is summarized here. Probes were synthesized as biotinylated RNA oligos in a MYBAITS kit (Arbor Biosciences, formerly MYcroarray Ann Arbor, MI) by matching publicly available frog transcriptomes to genomes to find orthologous markers. Matching sequences were clustered by their genomic coordinates to detect presence/absence across species and to achieve full locus coverage. To narrow the locus selection to coding regions, each cluster was matched to available coding region annotations from the *Nanorana parkeri* genome (Sun *et al.* 2015). Loci from all matching species were then aligned using MAFFT (Katoh & Standley 2013) and had various statistics calculated to aid in loci selection. Finally, the selected loci were separated into 120 bp-long bait sequences with 2x tiling (50% overlap among baits) using the MyBaits-2 kit (40,040 baits) with 120mer sized baits. These loci also have an additional bait at each end extending into the intronic region to increase the coverage and capture success of these areas. The baits were then filtered, keeping those: without sequence repeats, a GC content of 30%–50%, and baits that did not match to their

reverse complement or multiple genomic regions. Additionally, 500 ultra-conserved elements (UCEs) and 40 commonly used Sanger-based legacy loci in phylogenetic analyses of frogs were included to enable direct comparisons and inclusion of publicly available data from past phylogenetic studies.

The genomic libraries for the samples were prepared by MYcroarray library preparation service. Prior to library preparation, the genomic DNA samples were quantified with fluorescence and up to 4 ug was then taken to sonication with a QSonica Q800R instrument. After sonication and SPRI bead-based size-selection to modal lengths of roughly 300 nt, up to 500 ng of each sheared DNA sample were taken to Illumina Truseq-style sticky-end library preparation. Following adapter ligation and fill-in, each library was amplified for 6 cycles using unique combinations of i7 and i5 indexing primers, and then quantified with fluorescence. For each capture reaction, 125 ng of 8 libraries were pooled, and subsequently enriched for targets using the MYbaits v 3.1 protocol. Following enrichment, library pools were amplified for 10 cycles using universal primers and subsequently pooled in equimolar amounts for sequencing. Samples were sequenced on an Illumina HiSeq 3000 with 150bp paired-end reads.

4.2.3 RNASeq for transcriptome sequencing

For this study, we selected the following 10 transcriptomic samples from *Boophis*, *Tsingymantis*, *Aglyptodactylus*, 2 *Mantella*, 2 *Gephyromantis*, 2 *Mantidactylus*, *Spinomantis*, and 3 outgroups from *Rana*, *Pelophylax*, and *Polypedates*. Samples were collected in the field from specimens sacrificed by MS222 overdose, and immediately preserved in RNAlater. Samples were transported at environmental temperature during variable amounts of time and eventually frozen at -80°C until RNA extraction. We extracted RNA from ca. 100 mg of tissue of each

sample, consisting of combined or separate skin, muscle, or liver tissues, using standard trizol protocols. Sequencing of the majority of samples was carried out on an Illumina NextSeq machine with a High Output 150 cycle kit; the *Gephyromantis* samples were instead sequenced on an Illumina HiSeq instrument.

Illumina reads were quality-trimmed and filtered using Trimmomatic v. 0.32 (Bolger *et al.* 2014) with default settings and later filtered for rRNA sequences with SortMeRNA (Kopylova *et al.* 2012). We used paired and unpaired filtered reads for *de novo* transcriptome assembly using Trinity v. 2.1.0 (Grabherr *et al.* 2011) according to published protocols (Haas *et al.* 2013). We identified and translated candidate coding regions within transcript sequences from the final assembly using Transdecoder 2.1.0 (Haas *et al.* 2013).

We used a previously compiled alignment of 4593 (no paralogs across vertebrates) + 1506 (1 case of deep paralogy across vertebrates) + 1195 (2 cases of deep paralogy) nuclear genes from Irisarri *et al.* (2017) as a reference for ortholog selection, hereafter named reference set. Coding sequences of the new transcriptomes were aligned to the reference set using the software Forty-Two (D. Baurain; https://bitbucket.org/dbaurain/42/). For sequence decontamination and paralog resolution we followed the protocol established in Irisarri *et al.* (2017). In brief, the protocol consists of (1) detecting sequences from invertebrates using BLAST and removing them; (2) for the samples represented at a single gene by several transcripts that could not be assembled, removal of sequences that were either redundant (i.e. > 95% of length overlap) or too divergent; (3) gene tree inference using RAxML (Stamatakis *et al.* 2018) removal of sequences for which the patristic distance with the other sequences at one gene was significantly greater or lower than at the other genes, as these were considered cross-contaminations; (4) again, inference of gene trees, and splitting the alignments by looking for the branch that maximizes the taxonomic

diversity, in order to remove ancient paralogs. We then translated the sequences from amino acids to nucleotides using leel (D. Baurain, unpublished). All downstream analyses were based on nucleotide alignments.

For this study, we extracted the mantellids as well as several outgroups from the complete dataset from this sequencing batch. We removed columns that consisted only of gaps and removed samples that had less than 30 percent of the total alignment length. We also lightly filtered alignments to exclude those with three or fewer samples and had less than 100 base pairs in length of data. These processing steps resulted in 5,433 transcript alignments. We next assessed missing data and found that the *Aglyptodactylus* sample had very low sampling with 241 transcripts (4% of the total transcripts) which could lead to biased results. To try to remedy this we created two alternative datasets: (1) we removed the *Aglyptodactylus* sample from the 5433 transcript alignments; and (2) we included only transcripts that were shared with *Aglyptodactylus* for a dataset of 241 transcripts. Finally, because the dataset was assembled into transcripts, which are essentially a collection of concatenated exons for a given gene, the individual exons might no longer be genetically linked if they occur across large enough genomic regions to allow for recombination. Because we do not have the genome or a genome of a related species to directly address this question, we instead created an alternative dataset composed of separate exon alignments derived from the transcripts. To accomplish this task, we blasted the consensus sequences from each transcript alignment to the *Nanorana* genome and separated each alignment into exon alignments when they matched to the coding regions from the *Nanorana genome* annotations. We next filtered each new alignment as described above which resulted in 35,957 exon alignments.

4.2.4 Data processing pipeline

A bioinformatics pipeline for filtering adapter contamination, assembling loci, and exporting alignments in different formats and types of data is available at (https://github.com/chutter/FrogCap-Sequence-Capture).The pipeline is scripted in R statistical software (R Development Core Team 2018) using the BIOCONDUCTOR suit of packages (Ramos *et al.* 2017). The pipeline also wraps together open source software publicly available and commonly used in bioinformatics, but with no user-friendly set of scripts to easily use across multiple samples. The pipeline first cleans the raw reads of adapter contamination, low complexity sequences, and other sequencing artifacts using the program FASTP (default settings; Chen *et al.* 2018). Adapter-cleaned reads are next matched to a database of publicly available genomes from bacteria, invertebrates, and other organisms to detect cross-contaminated reads (see Hutter *et al.* in prep for genomes used), using the program BBMap from BBTools (https://jgi.doe.gov/data-and-tools/bbtools/), Next, paired-end reads are merged using BBMerge (Bushnell *et al.* 2017), which also fills in missing gaps between non-overlapping paired-end reads by assembling the missing data from the other paired-end reads. Finally, exact duplicates are also removed using "dedupe" from BBTools, removing read-pairs when both pairs were duplicated. Additionally, duplicates from the set of merged paired-end contigs were removed if they were exact duplicates or were contained within another merged set of reads.

The merged singletons and paired-end reads were next *de novo* assembled using the program SPADES v.3.12 (Bankevich *et al.* 2012), which runs BAYESHAMMER (Nikolenko *et al.* 2013) error correction on the reads internally. Data were assembled using several different k-mer values (21, 33, 55, 77, 99, 127), where orthologous contigs resulting from the different k-mer assemblies were merged. We used the DIPSPADES (Sofanova *et al.* 2015) function from

this program to better assemble exons that were polymorphic by generating a consensus sequence from both haplotypes from orthologous regions.

The consensus haplotype contigs were then matched against reference loci sequences from the *N. parkeri* genome used to design the probes with BLAST (dc-megablast), keeping only those contigs that matched uniquely to the reference probe sequences. Contigs were discarded if they did not match to at least 30 percent of the reference locus. Finally, we merged all discrete contigs that matched to the same reference locus, joining them together with Ns based on their match position within the locus.

4.2.5 Alignment and trimming

The final set of matching loci was next aligned using MAFFT local pair alignment (max iterations = 1000; ep = 0.123; op = 3). Each locus was separately aligned with its corresponding reference the probes were designed from. We screened each alignment for samples that were greater than 40 percent divergent from the reference sequence, which are almost always incorrectly assigned contigs. Alignments were kept if they had greater than three taxa and had more than 100 base pairs. We next separated the alignments into datasets: (1) “exons-only”, which trimmed off the intronic region from each locus using the reference loci as a guide for trimming; and (2) “full-contigs”, which included the entire matching contig to the reference locus and UCE markers. Finally, the introns and UCE datasets were internally trimmed using TRIMAL (automatic1 function; Capella-Gutiérrez *et al.* 2009) and alignments were externally trimmed to ensure that at least 50 percent of the samples had sequence data present.

4.2.6 Final sequence alignments

The exons-only and full-contigs sets of alignments were further trimmed into usable datasets for phylogenetic analyses and data type comparisons: (1) exons, each alignment was adjusted to be in an open-reading frame in multiples of three bases and trimmed to the largest reading frame that included >90% of the sequences; (2) introns, the exon previously delimited was trimmed out of the full-contigs dataset, and the two intronic regions were concatenated; (3) UCEs, were separately saved and not modified; (4) legacy, markers from prior studies (excluding UCEs) were saved separately for ease of access and comparison; (5) gene, after separating the exons from their flanking intron sequence, exons were concatenated and grouped together if they were found from the same predicted gene from the *Nanorana parkeri* and *Xenopus tropicalis* genomes because these exons are likely to be strongly linked genetically. We also assessed missing data using two different methods: we assessed the number of missing bases per alignment from samples included in the alignment (i.e. missing basepair data) and the number of samples completely missing from an alignment (i.e. missing marker data).

A persistent and difficult to detect problem in phylogenomic datasets are detecting and removing errors present in the alignments. Typically, researchers have been able to visually inspect some of these alignments and remove any obvious erroneous sequences, but this practice is no feasible because datasets are now containing thousand to tens of thousands of alignments. Some of these problems include misaligned portions of a single sample's sequence within an alignment, sequence alignment errors, and contamination all leading to an inaccurate estimate of the phylogeny that includes that sample. We address these potential problems using several approaches: (1) we created a custom script to assess each sample in each alignment using 100bp windows, and if that window had greater than a 40% divergence from the consensus, that

sequence was replaced with Ns; (2) we used the program TREESHRINK (Mai & Mirarab 2018) on each alignment, which detects sequences with unexpectedly long branch lengths when compared to other gene trees in the dataset and removes these problematic sequences from each alignment; and (3) to address decontamination, we had initially filtered out raw reads that matched to the genomes of other organisms, and TREESHRINK should also provide a second pass at removing this type of error.

4.2.7 Concatenated tree datasets

We concatenated the sets of markers described above into single alignments for maximum likelihood (ML) and Bayesian inference (BI) phylogenetic analyses. We separated alignment matrices into three different amounts of completeness (50, 70, and 90 percent); where individual markers were only retained if the number of samples in each alignment met that completeness threshold. For phylogenetic analyses, we first used the maximum-likelihood method IQ-Tree v.1.6.7 (Nguyen *et al.* 2015) to estimate phylogenetic trees from concatenated data. For these analyses, we employed models of molecular evolution identified via ModelFinder (Kalyaanamoorthy *et al.* 2017) built into IQ-Tree, which identified an optimal partitioning scheme and models of molecular evolution for each partition. We assessed support for the resulting topology using 1000 ultrafast bootstrap replicates (Minh *et al.* 2013). Additionally, we also used ExaBayes (Aberer *et al.* 2014) for BI analyses, which can analyze genome-scale data while being computationally tractable. With ExaBayes, we analyzed a fully partitioned dataset by marker, where we used the GTR+GAMMA model (the only model available) for the nucleotide sequences. Two coupled chains were run twice independently for 200,000 generations

to verify independent convergence. We checked for convergence by ensuring that ESS values were greater than 100 for all parameters.

4.2.8 Concatenated gene jackknifing

We scripted a gene-jackknifing (i.e. resampling without replacement) workflow in R to estimate topological precision across concatenated phylogenetic analyses. This approach also benefits from being able to utilize full model selection and partitioning across data matrices, which are not computationally tractable on full datasets. The jackknifing approach used ML with IQ-Tree and followed the procedure: 1) Genes for the data matrix were randomly selected without replacement, where genes were selected up until a threshold of 200,000 bp had been reached so that each matrix was nearly the same size; 2) alignments were partitioned by codon position for exons and by marker for non-coding regions; 3) ModelFinder was used to select the best model for each partition; 4) the analysis was run across 1000 jackknifed datasets; and 5) the 1000 replicate trees were summarized by generating a maximum clade credibility tree, which collapsed nodes into polytomies that were not supported by at least 50% of the jackknife replicates. The script was coded in R and is available on GITHUB (https://github.com/chutter/FrogCap-Sequence-Capture).

4.2.9 Gene tree discordance

Recent studies have cautioned that concatenation analyses can give the incorrect topology with strong support under certain conditions. Concatenation may be statistically inconsistent in the presence of incomplete lineage sorting or anomaly zones that result in species trees that are different from their gene trees (Degnan & Rosenberg 2009; Roch & Steel 2015). To address this

possibility, we used the software ASTRAL-III (Zhang *et al.* 2017), which conducts a summary-coalescent species tree analysis that is statistically consistent under the multi-species coalescent model. As input for ASTRAL-III, individual trees for each gene and marker were needed, so we performed maximum likelihood (ML) concatenation analyses on each alignment using IQ-Tree. We ran the analyses separately on the exon, intron, and gene datasets; and we also combined the exon and intron datasets together in a final analysis. To improve accuracy, we collapsed branches that were below 10% bootstrap support (Zhang *et al.* 2017). Finally, we used local branch support to assess topological support for the coalescent trees generated by ASTRAL-III because this method out-performs multi-locus bootstrapping (Sayyari & Mirarab 2016).

4.3 Results

4.3.1 Sequence capture evaluation

We sequenced 12 samples for this study using the FrogCap probe-set, which totaled 13,032 mega base pairs (Mbp) of raw sequence data for these samples. Each sample had a mean base pair yield of 1086.0 ± 355.4 (range: 535.2–1905.0) Mbp and a mean 7,191,728 ± 2,353,682 (range: 3,544,544–12,616,048) reads (Figure 2A). Raw reads were then filtered to remove exact duplicates, low complexity and poor-quality bases, adapter and contamination from other non-target organisms, which resulted in a mean 91.2% ± 2.3% of reads (range: 87.8–95.3%) passing the quality filtration steps (mean: 984.8 ± 319.9 Mbp; range: 477.3–1690.7 Mbp). After merging paired-end reads and reducing redundancy (removing duplicate and containment reads), there was a mean 301,416 ± 113,184 (range: 154,093–519,622) merged paired-end reads (and singletons) used as input for assembly. After assembly, the samples yielded a mean 13,000 ±

1051.9 (range: 10,967–14,596) contigs, which had a mean length of 963.3 ± 84.9 (range: 129–23,642) base pairs. See Table S1 for detailed summary statistics from each sample.

4.3.2 Alignment summary

Alignment and quality control of the multiple sequence alignments prior to trimming results in 12,133 total aligned markers, with a mean 13.4 ± 2.7 (range: 3–16) samples per alignment, which remained consistent across datasets (Figure 3). Multiple sequence alignments have a mean 1703.1 ± 748.4 (range: 245–24,139) base pairs per alignment, totaling 18,386,634 base pairs (prior to trimming). After separating the intron and exon sequence from the aligned set of contigs and trimming, the exon dataset had 11,339 exon alignments totaling 2,413,164 base pairs, and the intron dataset containing only non-coding flanking sequence from both ends of the exons had 11,314 joined intron alignments totaling 6,700,598 base pairs of sequence data (Figure 3A–B). Additionally, the exon dataset had an average 227.7 ± 229.3 (range 81–4908) bases per alignment, while the intron dataset has an average 445.6 ± 154.2 (range 81–1349) bases per alignment (Figure 3A–B). Multiple sequence alignments for the UCE dataset had 604 aligned UCEs totaling 545,819 base pairs of data after filtration and trimming. The UCE dataset had an average 903.7 ± 215.8 (range 400–1361) bases per alignment (Figure 3A–B). The final set of alignments for the FrogCap data concatenated individual exons from the same gene, which resulted in 2077 gene alignments totaling 1,275,423 base pairs. The gene dataset had an average 614.1 ± 445.5 (range 183–7403) bases per alignment (Figure 3A–B). Missing basepair data was much higher in the sequence capture dataset when compared to the phylotranscriptomic dataset, where samples present in the alignments had more sequence data for that alignment (Figure 4A). However, this contrasts with the lower missing marker data, which would result in less missing

data overall given that alignments have more samples, and therefore more flexibility is given when selecting alignments with fewer missing samples.

The phylotranscriptomic dataset had 5432 total aligned markers after alignment and quality control of the multiple sequence alignments, totaling 8,864,432 base pairs long. The alignments had a mean 9.2 ± 2.1 (range: 3–13) samples per alignment. Multiple sequence alignments have a mean 1631.9 ± 1109.1 (range: 132–15,258) base pairs per alignment (Figure 3A–B). Missing base pair data was much lower in the phylotranscriptomic dataset (Figure 4B); however, this contrasts with the higher missing marker data, which would result in more missing data overall given the elevated number of missing samples from alignments.

4.3.3 Phylogenetics

The recovered relationships from most FrogCap datasets gave a novel topology where Boophinae is sister to Mantellinae; *Tsingymantis* is sister to Boophinae + Mantellinae; and Laliostominae is the most basal lineage in Mantellidae (Figure 5; Figure 6). All concatenated analyses except one (out of 15 analyses; intron 10% missing data matrix; Figure 5A) gave the same topology with strong support at every node (Figure 5). The jackknife concatenated analyses also strongly supported the same topology, with a relatively small proportion of jackknife replicates weakly supporting or not supporting the phylogenetic relationships of *Tsingymantis* to other lineages (Figure 5B). Finally, the Astral-III species-tree analyses all gave the same topology as the other analyses (Figure 6) except the intron analysis (Figure 6B), which found *Tsingymantis* sister to Laliostominae, but with weak support and a nearly equal number of gene trees. The remaining all-markers, exons, and gene analyses all strongly supported the dominant

relationship, with the UCE analysis (which had the fewest number of input gene trees) only moderately supported this relationship (Figure 6C).

The phylotranscriptomic analyses were hindered by missing data and the relationships were less decisive than the sequence capture dataset (Figure 4); but despite this, the most common topology was the same topology recovered from the sequence capture analyses (Figure 7–8). The concatenated analyses all found the sequence capture topology as the best topology but in every analysis the *Tsingymantis* + (Boophinae + Mantellinae) relationship was not strongly supported (Figure 7). Removing *Aglyptodactylus* (which only sampled 4% of the transcripts) resulted in the *Tsingymantis* + (Boophinae + Mantellinae) relationship and all analyses strongly supported this topology (Figure 7). In addition, in the dataset where only transcripts that included *Aglyptodactylus* were analyzed, the *Tsingymantis* + (Boophinae + Mantellinae) relationship was also strongly supported in the single concatenated analysis and the jackknifing analysis, although only ~60 percent of the jackknife replicates supported this relationship (Figure 7). However, in the ASTRAL-III analysis, the sequence capture topology was only recovered in the exon dataset and the dataset where *Aglyptodactylus* was removed (Figure 8). In datasets that included *Aglyptodactylus*, the analysis found *Tsinymantis* + other mantellids, with ca. a third of the gene trees supporting this and the other relationship (Figure 8A–B). Much of this discordance is related to missing data in *Aglyptodactylus*, because when removed, the majority of gene trees support the sequence capture topology (Figure 8C).

4.4 Discussion

4.4.1 Transcriptomics versus sequence capture

We provide one of the first comparisons between sequence capture using FrogCap (**Chapter 3**) and transcriptomic sequencing with RNASeq to address the same phylogenetic systematic question (Table 1). The phylotranscriptomic dataset had more targeted genomic regions than the sequence capture, but only amounted to ~25 percent more sequence data when considering other data types sequenced with the sequence capture (Figure 3). We find that the two datasets perform similarly and generally recover the same phylogenetic relationships; however, the transcriptomic dataset was hampered by missing data (Figure 2, 4), likely because some samples were too degraded for optimal use in RNASeq, which requires fresh or salt-preserved and frozen tissue samples (Romero *et al.* 2014; Sudmant *et al.* 2015). Despite this, the transcriptomes overall had less gene discordance than the sequence capture datasets, which surprisingly suggests that this discordance results from the dataset being analyzed rather than an evolutionary property of relationships among groups (discussed below).

FrogCap sequence capture also provided several advantages over the transcriptomic data; FrogCap sequences non-protein coding markers from across the genome, such that these other types of markers could be useful by providing sequence data from potentially neutrally evolving genomic regions and also can serve as another line of phylogenetic evidence when compared to other data types (Dool *et al.* 2016; Hosner *et al.* 2016). While the transcriptomic dataset has more base pairs of data targeted for sequencing, the sequence capture dataset almost equalizes the amount of data through this intronic bycatch. Especially useful is that sequence capture acquires regions flanking the area targeted by probes and ~500bp of intronic sequence data is acquired with each exon marker (Figure 3). Intronic sequence data has been shown to be

effective at resolving close phylogenetic relationships comparable to mitochondrial data (Dool *et al.* 2016; Chen *et al.* 2017); however, intronic data might not be useful at increasing phylogenetic scales because base turnover and saturation could introduce bias (**Chapter 3**). In our study, the intronic data recovers the same relationships as the other sequence capture datasets except in the Astral-III analysis, but it is not strongly supported by local posterior scores and an almost equal number of gene trees support the alternative topology (Figure 5,6). It has been suggested that the FrogCap intronic data has variability that would be useful at lower phylogenetic scales, such as the genus and species -level (**Chapter 3**), which we find for all other close relationships in the intronic dataset phylogenetic analyses.

We show that both datasets accomplish the goals of this study; however, while the transcriptomic dataset has more data and less gene-tree species-tree discordance, it was challenged by missing data from poor performing samples resulting in uncertain results. The transcriptomic method has the potential to result in much more protein-coding data, sampling more densely across the genome, and a dataset with long alignments that have minimal discordance in gene trees when compared to the species tree (Figure 8A). However, it is more difficult to acquire a full dataset given the sample requirements, where even slightly degraded samples could result in substantial missing data (Figure 1B, 4). In addition, the per sample cost is around 5 times higher when using low coverage transcriptomic sequencing because more data is being acquired and thus fewer samples can be multiplexed in a single sequencing run. If these two disadvantages are not problematic for the study design and the desire is to acquire more of the exome, then transcriptomics would be the optimal choice. On the other hand, most studies in systematics that use ethanol preserved tissue samples housed at museums would not be feasible here, and therefore sequence capture would be a necessity. Importantly, the sequence capture

results demonstrate that comparable phylogenetic resolution and quantity of data can be acquired when compared to the technically superior transcriptomic sequencing, and at a lower financial cost.

4.4.2 Patterns of gene discordance

Surprisingly, while addressing the same subfamily relationships using different types of sequence data, we find that gene discordance is much less in the phylotranscriptomic than the sequence capture dataset, which is explained primarily by non-biological variation from systematic error in gene tree estimation. Most studies assume that discordance is caused by an evolutionary mechanism such as incomplete lineage sorting or hybridization (Knowles 2009; Knowles *et al.* 2018), and few studies consider the importance of systematic error in driving gene discordance (Richards *et al.* 2018). We find that discordance is caused mostly by the properties of the alignments themselves, where datasets that consist of longer alignments have less discordance, suggesting that systematic error is driving the majority of (Figure 3, 6, 8). The phylotranscriptomic dataset is composed of transcripts, which are adjoined exons sequenced from RNASeq that contain no intronic sequence, and as a result are much longer than all other datatypes in this study (Figure 3C). Because of the longer length, there is more likely to be more informative sites resulting in more strongly supported relationships and therefore less discordance among the genes.

We explored this hypothesis further by separating the exons from the transcripts and analyzed them separately, confirming that discordance is substantially higher in the exon dataset (Figure 8A, B). To directly test whether alignment length is related to the number of informative sites, we used a simple linear regression between these two variables in all datasets and found

that marker length has a significant and positive relationship with the number of informative sites (R^2 = 0.499–0.859; $P < 0.001$). Despite the potential advantage of using full transcripts to achieve a greater amount of information for individual phylogenetic tree analyses, this practice could be problematic if the gene is large enough to undergo recombination and could bias results towards conflicting topologies.

The results presented here suggest that the main driver of gene-tree species-tree discordance are markers that are too short resulting in more statistical noise or conflicting results. This problem remains underappreciated but has been addressed in mitochondrial gene trees (Richards *et al.* 2018), but to our knowledge has not been tested using nuclear genome-wide sampling. This problem could be widespread throughout most organisms because the mean exon length is small at about 150–300bp (Xenopus: 200bp; Chicken = 152bp; Mouse = 170bp; Fish = 170bp; *Drosophila* = 370bp; Zhu *et al.* 2009), so they are more likely to be targeted in sequence capture and transcriptomic studies, and we show that smaller alignments are less informative than larger alignments. To remedy this problem, shorter markers could be filtered out of gene tree analyses and combining linked regions could provide adequate phylogenetic resolution via statistical binning (Mirarab *et al.* 2014) or combining exons from the same gene which we described above. However, this approach could be problematic if exons do not share the same evolutionary history because of recombination and could provide misleading or poorly supported phylogenetic relationships.

4.4.3 Recombination

One important assumption of the coalescent model is that there is no recombination within genes and free recombination between genes, where genes are treated as conditionally

independent as a result. Genes that are physically more distant from each other are more likely to undergo recombination, and therefore would become unlinked and may have different evolutionary histories (Mirarab *et al.* 2014; Springer & Gatesy 2018). Common practice in phylogenomics has been to bin genomic regions with the same tree or use entire transcripts (which are mostly exons from a gene) under this no recombination assumption (Mirarab *et al.* 2014); however, recently several studies have suggested that individual exons do not share the same the evolutionary history as the gene and that recombination may occur on smaller scales than previously assumed (Richards *et al.* 2018; Springer & Gatesy 2018).

To understand how these factors might be related in frogs, we plot the genomic coordinates of the sequence capture and phylotranscriptomic markers on the *Nanorana parkeri* and *Xenopus tropicalis* genomes to understand how physical distance and the markers analyzed in this study are related to each other (Figure 9). We generally find that the genomic representation of both datasets is randomly sampled from throughout the genome across all the chromosomes in *Xenopus* or thousands of scaffolds in *Nanorana*. We find that the *N. parkeri* genome has more sequence data in between exons calculated from the exome (mean distance: 30,024 bp), likely because of its larger genome size and higher number of transposable elements (Sun *et al.* 2015), while in the smaller *X. tropicalis* genome exons are closer together and might be more likely to be linked in these groups (mean distance: 15,222 bp). These results suggest that intronic distance between exons is highly variable across frogs, and therefore recombination is likely a concerning issue in any phylogenomic study. Future studies should assess these markers more thoroughly from different phylogenetic scales to measure the typical intronic distance between exons in frogs and test how individual exon trees are related to the overall tree for that gene.

In practice, these results reveal that it is difficult to make a decision combining exons from the same gene because the intronic distance is not often well-known between the exons, especially in the case of transcriptomes without associated genomes. When we compare the gene trees from transcripts and combined exons from the same gene, we find that the transcript result in less gene discordance and stronger statistical support (Figure 7, 8). In addition, when analyzing the exons separately from the transcripts, we recover the same topology but some have lower support and higher amounts of gene discordance (Figure 7, 8), which is likely the result of statistical noise rather than biological processes. Together these results suggest that phylogenetic inference of genes are not heavily affected by within-gene recombination and generally share the same evolutionary history across exon trees. Despite these unexpected results, past studies in bacterial genomes and a simulation study have suggested that phylogenetic inference is robust to recombination within markers, but demographic analysis is not (Lanier & Knowles 2012; Hedge & Wilson 2014). Although the evidence available suggests recombination does not create enough statistical noise to affect phylogenetic inference, caution is recommended when using binning approaches, especially in analyses that require marker independence.

4.4.4 Mantellidae systematics

We address different phylogenetic hypotheses for the relationships among subfamilies in the Malagasy frog family Mantellidae. Surprisingly, the most frequent and strongly supported topologies we have found support a novel topology not yet recovered in a past phylogenetic or morphological study (Figure 1; Figure 5–8). The new topology differs in that it finds *Tsingymantis* sister to the subfamilies Boophinae + Mantellinae, and Laliostominae is the most basal subfamily in Mantellidae. These relationships are strongly supported in the sequence

capture dataset in all analyses except one intron analysis (Figure 5, 6), and the transcriptomic datasets most often recover this same topology, but with lessened support. In the transcriptomic dataset, the lower support is likely because of the missing data for *Aglyptodactylus*, which is sampled in less than 5% of the alignments (Figure 7). In addition, the Astral-III topology for the transcript phylotranscriptomic dataset differs from the topology found in the sequence capture datasets; however, both datasets are supported by the same proportion of gene trees (Figure 8). We tested including markers where *Aglyptodactylus* was sampled (256 markers) and found stronger support for the sequence capture topology in concatenated and jackknifing analyses and weaker support in Astral-III analyses from the lower number of gene trees (Figure 8). Additionally, when removing *Aglyptodactylus* from all alignments, we recover the topology of *Tsingymantis* + (Boophinae + Mantellinae), which is strongly supported in all analyses.

The results from this study answer the question on whether *Tsingymantis* is an independently evolving lineage that would warrant the description of a new subfamily and also answers some questions on subfamily relationships in Mantellidae. In past studies, *Tsingymantis* has been found closely related to Mantellinae using molecular data (Vieites *et al.* 2009; Wollenburg *et al.* 2011) and morphological data (Raselimanana *et al.* 2007, 2008); therefore, it has been considered as part of Mantellinae based on these prior studies (Amphibian Species of the World 2019). Our results are surprising because *Tsingymantis* is not sister to Mantellinae in any analysis and it can equivocally be recognized as an independently evolving lineage in this family. These results are also reinforced by the unique morphology and ecology of *Tsingymantis* because it is the only Malagasy frog lineage that is restricted to limestone karst habitat, has nuptial pads and lacks femoral glands (Raselimanana *et al.* 2008; Rakotoarison *et al.* 2013).

Furthermore, tadpole morphology shows strong similarity with Laliostominae tadpoles, which would be consistent evolutionary with our main phylogenetic results.

When considering other subfamily relationships, the sequence capture datasets are all in agreement with each other, while the transcriptomic dataset shows some different, but not strongly supported relationships. While the sequence capture dataset strongly supports Laliostominae + all other mantellids (Figure 5, 6), the transcriptome datasets sometimes weakly support *Tsingymantis* + all other mantellids, where Laliostominae and *Tsingymantis* are swapped (Figure 7, 8). Removing *Aglyptodactylus* from the transcriptome dataset still provides strong support for *Tsingymantis* + all other mantellids, suggesting the low support in these datasets results from the missing data in *Aglyptodactylus*. All together, these results strongly support the Laliostominae + (*Tsingymantis* + (Boophinae + Mantellinae)) general topology and warrant the description of a new subfamily for *Tsingymantis*, which has equivocally demonstrated that it is a separately evolving lineage from other frogs in Mantellidae.

4.5 Tables

Table 1. Comparison table between transcriptome and sequence capture which could be used as to provide information for selecting one of these reduced representation approaches.

Consideration	Transcriptomics	Sequence capture
Sample requirements	Fresh, sensitive RNA extractions	Ethanol preserved, anything that would work in PCR
Genomic resources	None required	Genome and transcriptomes needed for probe design
Amount of data	~9 Mbs of alignment data	~7 Mbs of alignment data
Variability	Less variable	Equally variable exons, more variable introns and UCEs
Data types	Only exons, more complete genes/transcripts	Exons, introns, and UCE
Other benefits	Transcripts more resolved, very long	Less missing data, and variability from introns
Financial cost	~5X more than Sequence capture per sample	$100 USD (July 2019)

4.6 Figures

Figure 1. Past topologies recovered in other phylogenetic studies of Mantellidae are show in the illustration below. Subfamilies are colored to show their inferred relationships across many different studies. Also note the instability of *Tsingymantis* across studies. Branch lengths are arbitrary.

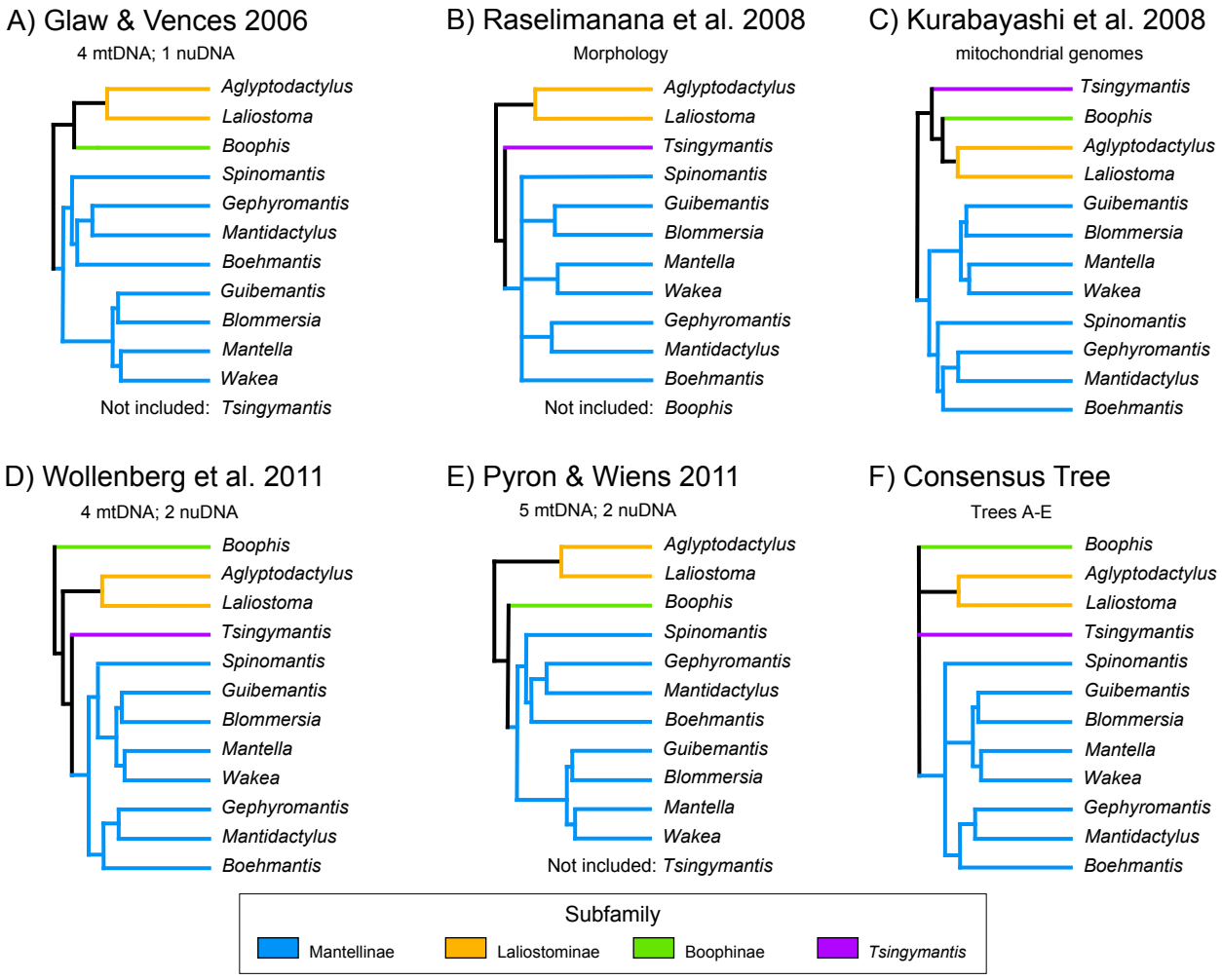

Figure 2. The proportion of markers obtained per sample (i.e. occupancy) is illustrated below. The (A) FrogCap alignments and (B) transcriptome alignments are shown separately.

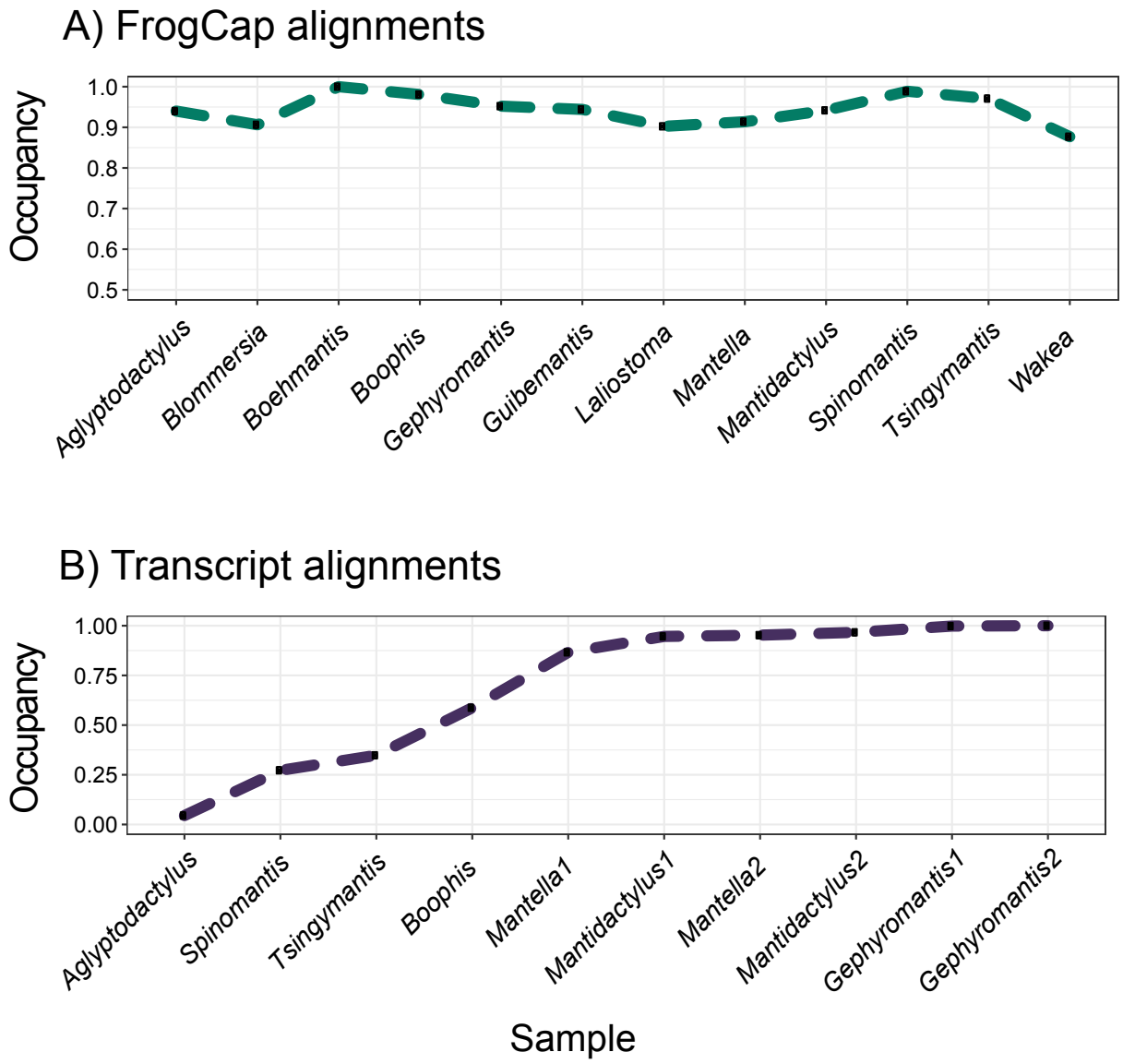

Figure 3. Summary statistics to quantify and compare alignments from the different phylotranscriptomic and sequence capture datasets after filtration, alignment, trimming and dataset partitioning. The different comparisons are: (A) number of alignments for each dataset; (B) number of base pairs plotted for each dataset within each phylogenetic scale; and (C) the mean alignment length (with standard deviation shown as error bars).

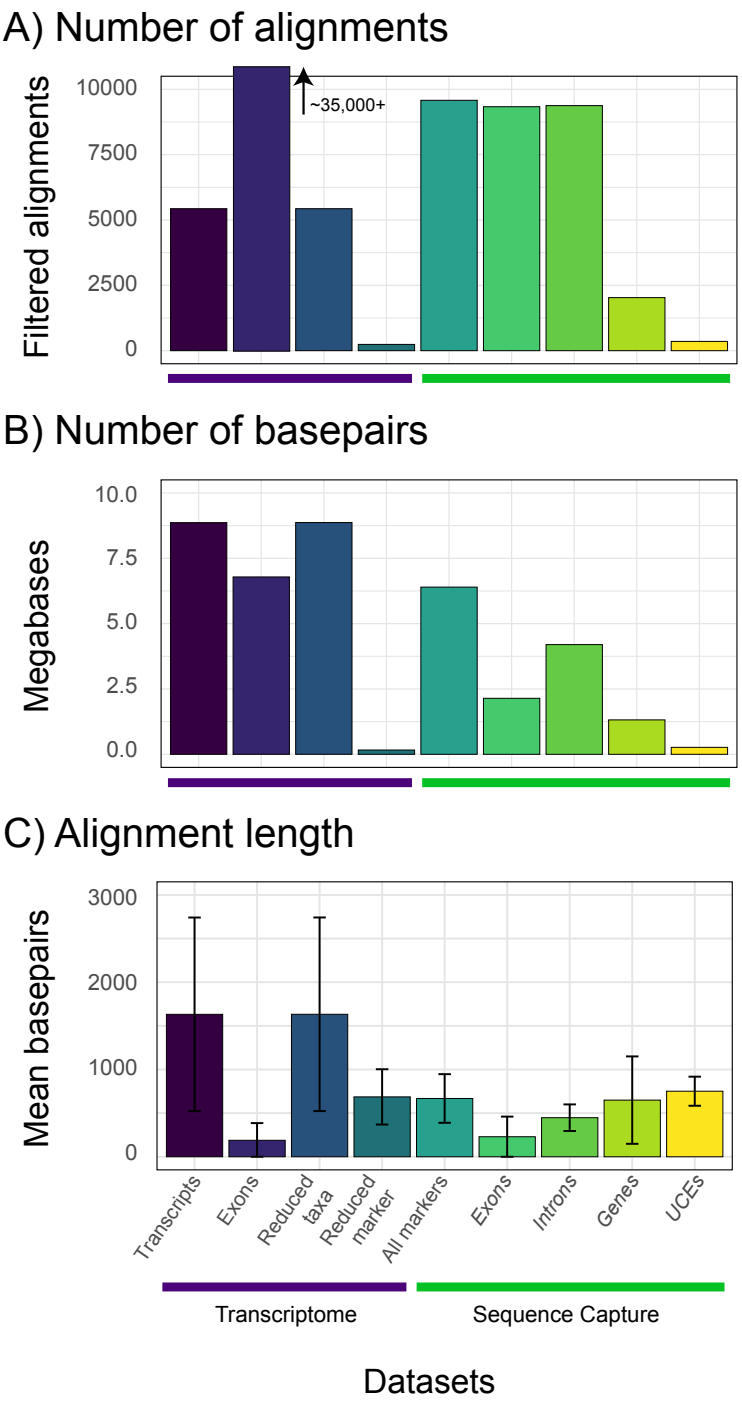

Figure 4. Missing data are compared for (A) sequence capture and (B) phylotranscriptomic datasets. Base pair missing data in the top row is the percent of missing data calculated from the number of missing bases pairs across alignments for each sample when the sample is present in the alignment. Marker missing data in the bottom row is the proportion of missing data calculated from the number of missing samples across each set of alignments.

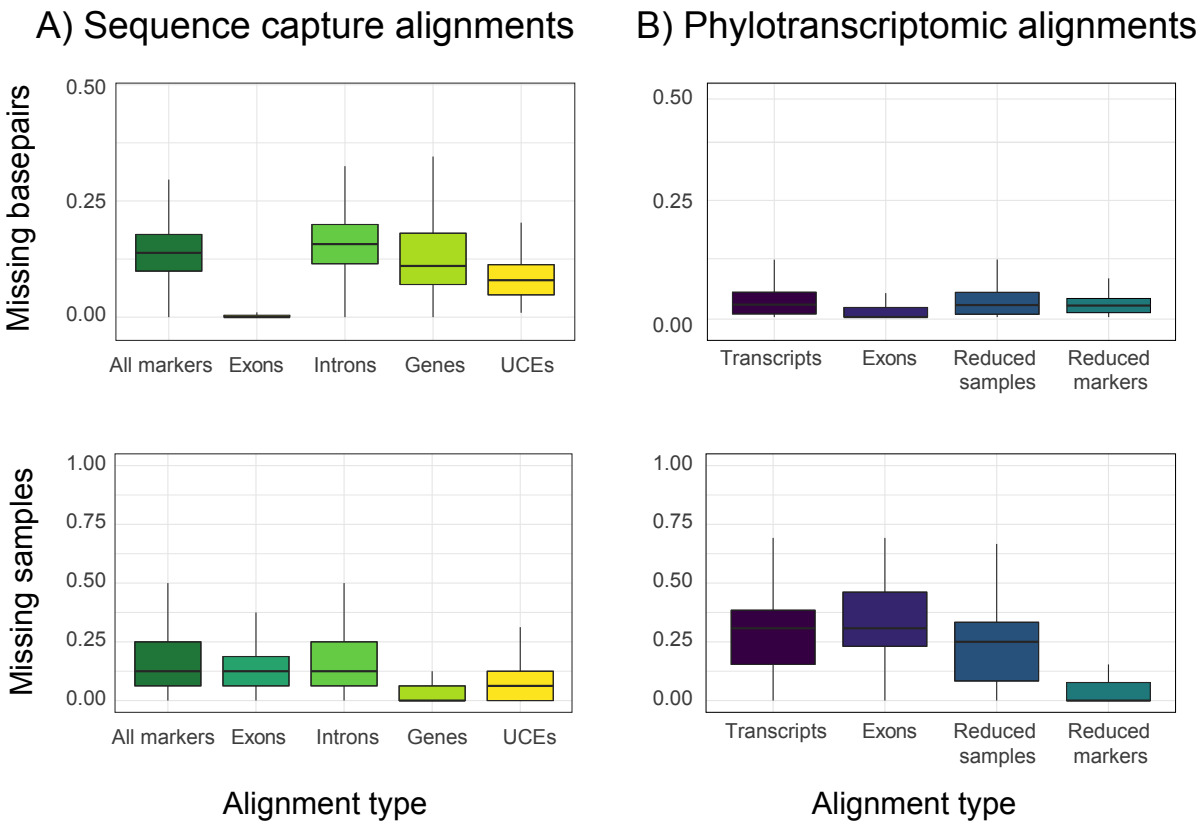

Figure 5. Consensus topologies from the concatenated and jackknifing analyses for the sequence capture datasets. The concatenated tree (A) is taken from the 50 percent missing data alignment branch lengths where all trees shared the same topology. In the 10 percent missing data alignment for introns, the node indicated in red was poorly supported (less than 95 bootstrap in IQTree). In the jackknife analysis (B) branch lengths are the average branch length across jackknife replicates, where all replicates had the same topology. The pies shown at some nodes are those not equivocally supported across jackknife replicates and show the proportion of replicates for each of the three most common topologies.

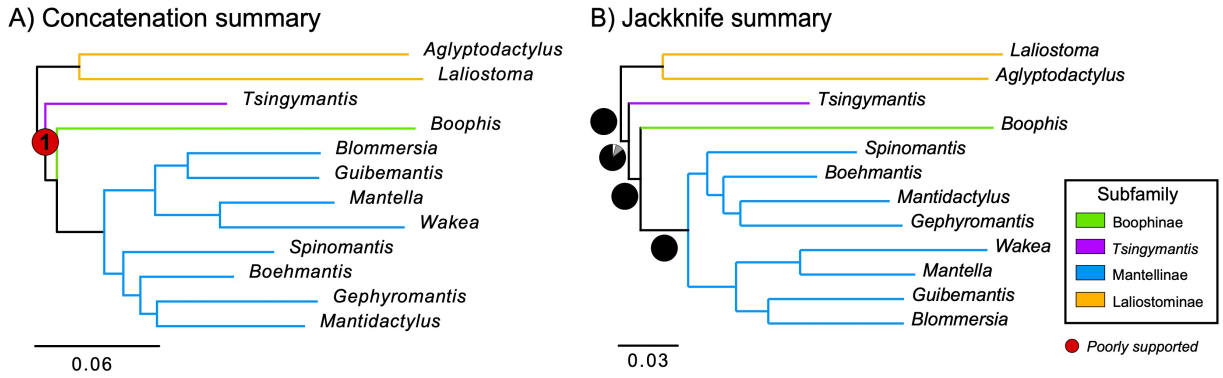

Figure 6. Consensus topologies from ASTRAL-III analyses for the different marker types from the sequence capture datasets. Branch lengths are in coalescent units, where the length of the branch is proportion to the amount of gene/species tree discordance in the dataset (i.e. shorter branch have more discordance). The pies below each branch represents the proportion of gene trees that support that given quadra-partition out of the three possible topologies. The black pie is the most common gene tree, the grey the second most common and white is the least common proportion. A red dot on a node indicates a poorly supported node from the local posterior probably calculated in Astral-III (less than 95 percent probability).

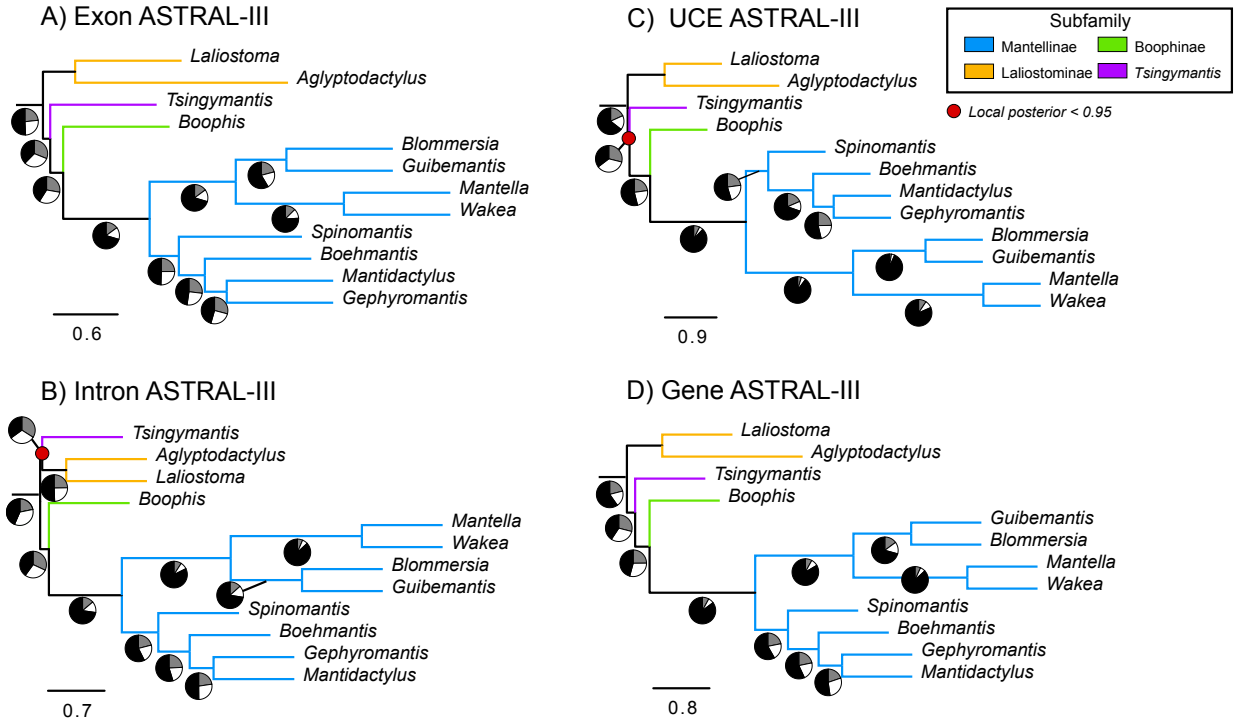

Figure 7. Consensus topologies from the concatenated and jackknifing analyses for the phylotranscriptomic datasets. The concatenated trees (A–D) are taken from the 50 percent missing data alignment branch lengths where all trees shared the same topology. In the 10 percent missing data alignment, the nodes indicated in red were poorly supported (less than 95 bootstrap in IQTree). In the jackknife analysis (E–H) branch lengths are the average branch length across jackknife replicates, where all replicates had the same topology. The pies shown at some nodes are those not equivocally supported across jackknife replicates and show the proportion of replicates for each of the three most common topologies. The black pie is the most common jackknife tree, the grey the second most common and white is the least frequent.

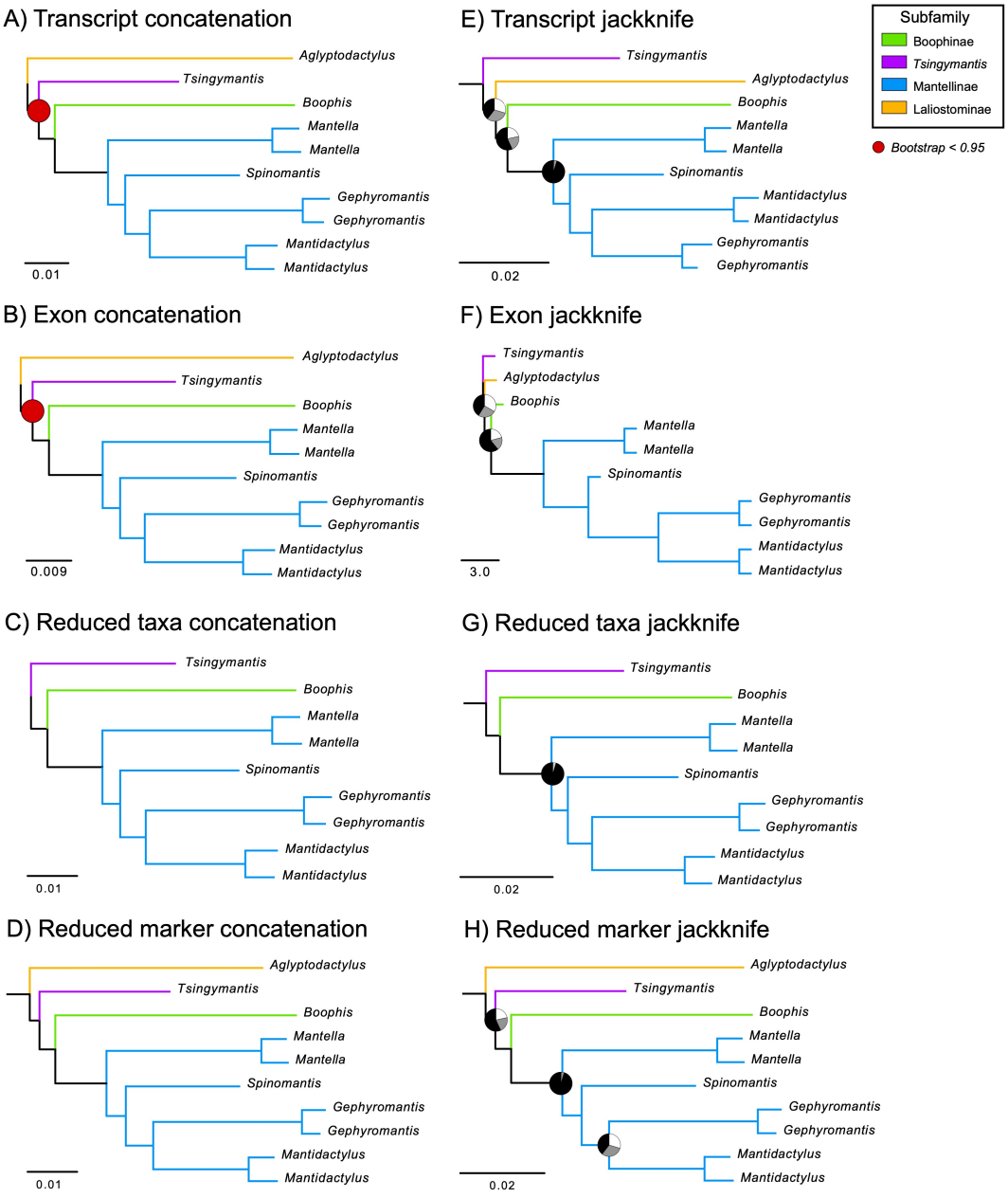

Figure 8. Consensus topologies from ASTRAL-III analyses for the different phylotranscriptomic datasets. Branch lengths are in coalescent units, where the length of the branch is proportion to the amount of gene/species tree discordance in the dataset. The pies below each branch represents the proportion of gene trees that support that given quadra-partition out of the three possible topologies. The black pie is the most common gene tree, the grey the second most common and white is the least common proportion. A red dot on a node indicates a poorly supported node from the local posterior probably calculated in Astral-III.

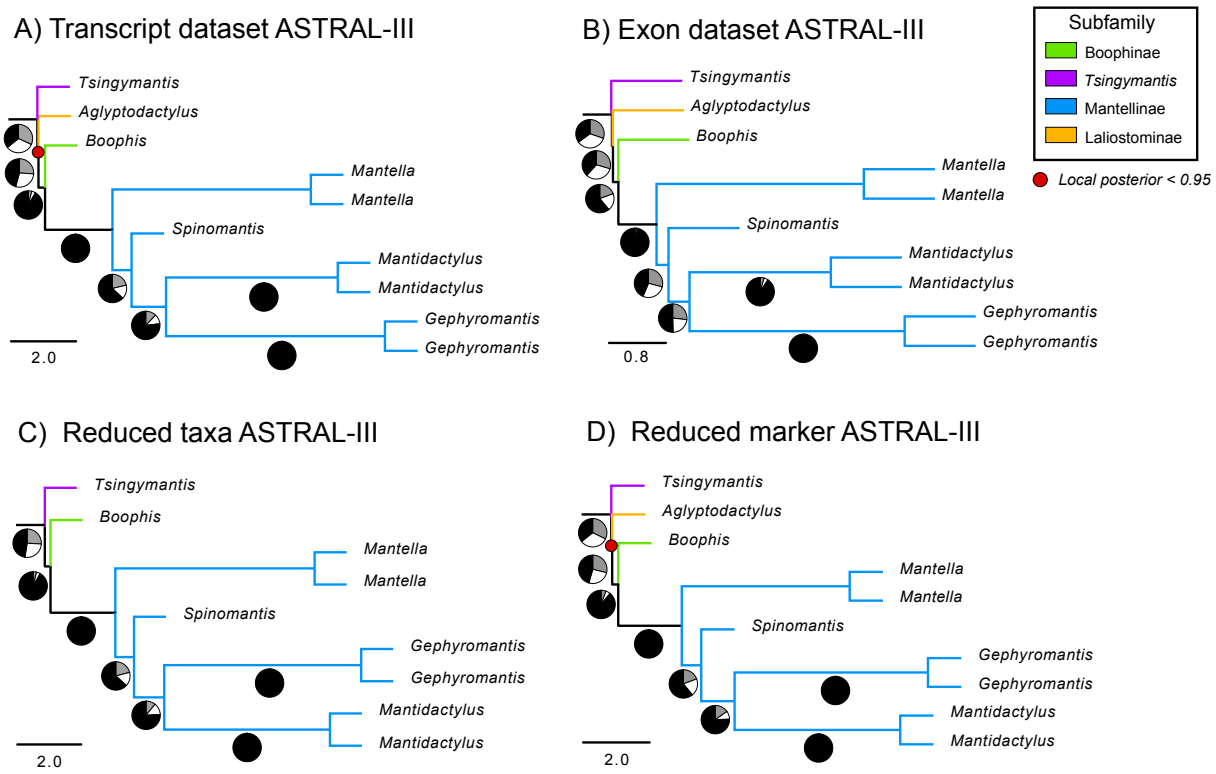

Figure 9. The genomic location of markers from this study are mapped to the (A) *Nanorana parkeri* genome and (B) The *Xenopus tropicalis* genome. The outer ring represents a random sample of ~50 Mbp from each of the genomes (as displaying the entire genome is not feasible given the relatively small lengths of alignments). Each inner ring shows the dataset plotted by colored background with the black lines marking the genomic location of markers from that dataset. The inner-most black ring shows in white the markers shared between the phylotranscriptomic and sequence capture datasets. All datasets are well-represented across both genomes when resampled.

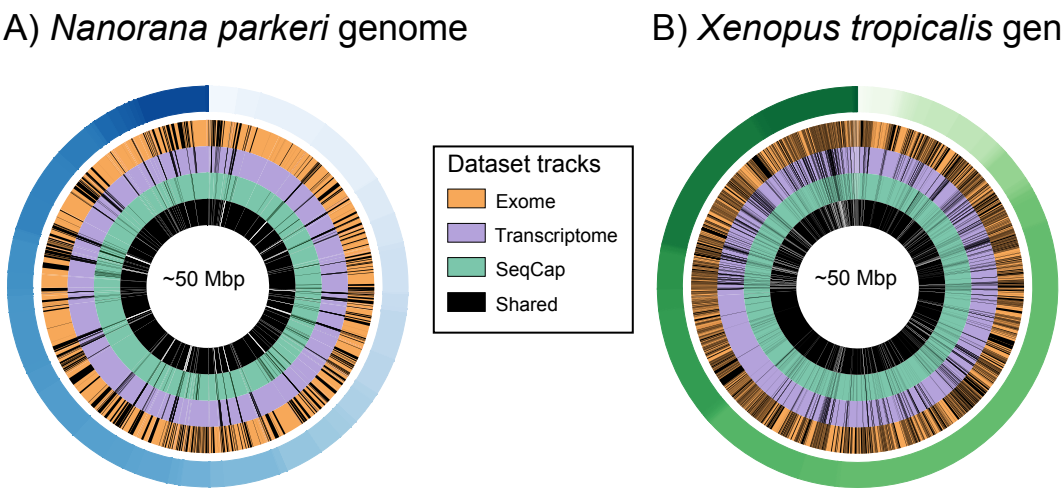

CHAPTER 5

Environmental acoustic interference from loud streams drives the evolution of higher frequency signals in Malagasy tree frogs (Mantellidae: *Boophis*)

Carl R. Hutter, Daniel Paluh, Frank Glaw, Miguel Vences; not yet published

5.1 Introduction

The large diversity of animal communication signals demonstrates the importance of these signals for species interactions in variable and structurally complex environments. Acoustic signals—including insect and bird songs, frog calls, and mammal vocalizations—are expected to be under strong selection from mate choice, species interactions, predation, and environmental factors (Tuttle & Ryan 1981; Vamosi *et al.* 2009; Hoskin & Higgie 2010). Sexual selection is generally considered the primary mechanism driving acoustic signal divergence among closely related organisms and populations, such as crickets, lacewings, frogs, and birds (Gray & Cade 2000; Boul *et al.* 2007; Toews & Irwin 2008; Shaw & Lesnick 2009). Acoustic signals are also expected to be under strong selection from environmental factors because signals are emitted by senders through heterogeneous habitats to be perceived by long-distance receivers (Morton 1975; Marten & Marler 1977; Wiley & Richards 1978; Parker & Smith 1990; Endler 1992).

To explain the coevolution of signals, sensory systems, and microhabitat choice that is required for effective communication, researchers have focused on testing the Acoustic Adaptation Hypothesis (AAH: Morton 1975; Marten & Marler 1977; Wiley & Richards 1978; Ryan & Kime 2003; Ey & Fischer 2009). This hypothesis is a subset of a broader sensory drive framework (Endler 1992) and predicts that natural selection will drive optimization of signal attenuation and perception across different habitats (Morton 1975; Marten & Marler 1977; Ey & Fischer 2009). Under the AAH, physical features of the environment are predicted to play an important role in driving the evolution of acoustic signals in animals (Morton 1975; Endler 1992; Penna & Meier 2011). These environmental factors can include vegetation (density, type, height), aquatic features (stream speed, ambient noise), or substrate type (Zimmerman 1983; Penna & Solis 1998; Kime *et al.* 2000; Ziegler *et al.* 2011). Through experiments, environmental

features have been shown to affect signal transmission, because particular aspects of the signal are amplified or attenuated by the surrounding environment (Morton 1975; Zimmerman 1983; Penna & Solis 1998).

The AAH has been tested in many different organisms globally but has received ambiguous support. Several studies in birds, mammals, and frogs have suggested that their vocal signals are well-adapted to the acoustic conditions of their native habitat (Birds: Gish & Morton 1981, Nemeth *et al.* 2006; Mammals: Brown *et al.* 1995, Mason & Narins 2001; Frogs: Ryan *et al.* 1990, Gingras *et al.* 2013). Despite the increasing support for the AHH in the literature, many other studies did not find evidence to suggest acoustic adaptation (Birds: Date & Lemmon 1993, Saunders & Slotow 2004; Mammals: Daniel & Blumstein 1998; Frogs: Erdtmann & Lima 2013; Vargas-Salinas & Amézquita 2014). As a result, the conflicting support questions the importance of the AHH and whether ecological factors play an important role in generating acoustic diversity.

We aim to address the AAH in frogs because they rely primarily on highly stereotyped, species-specific acoustic signals for mate and conspecific recognition and are found in a variety of discrete habitats (Wells 2007). To explain the diversity of acoustic signals in frogs, the importance of female mate choice on signal divergence has been well tested (Kirkpatrick 1982; Ryan & Cummings 2013); however, whether ecological factors play an important role in generating acoustic diversity is poorly understood in frogs (review in Erdtmann & Lima 2013). Despite the potential significance of the AAH to frogs, it has proven challenging to test because of potentially confounded variables, such as call plasticity due to temperature and body size, and sampling deficiencies (e.g. Gerhardt 1978; Gayou 1984; Narins *et al.* 2006; Gingras *et al.* 2013; Rohr *et al.* 2016). Generally in frogs and other organisms, there is an expected linear negative

relationship between body size and acoustic signal frequency (i.e. pitch of the signal) from allometric scaling of the larynx, and failing to remove the impact of body size from analyses could conflate whether selection is acting on the body size in response to another ecological factor (McClelland *et al.* 1996; McClelland *et al.* 1998; Narins *et al.* 2006; Wells 2007; Guerra *et al.* 2014). Adding to this challenge is that acquiring call data from a diverse range of frogs that takes these confounding variables into account is typically not available, so studies have focused on single species or very small groups when addressing acoustic signal optimization (Ryan & Rand 1993; Cocroft & Ryan 1995; Cannatella *et al.* 1998; Robillard *et al.* 2006; Goicoechea *et al.* 2010). The importance of broad-scale phylogenetic analyses is not often considered, but shared ancestry could be an alternative explanation to signal optimization for some patterns of signal diversity.

One prediction of the acoustic adaptation hypothesis is that environmental ambient noise, which is the background level of sound in the environment, will drive signal evolution if the noise is sufficiently similar and lessens the receiver's perception of the signal (Figure 1; Boonman & Kurniati 2011; Cardoso & Atwell 2011; Both & Grant 2012; Goodwin & Podos 2013). One important potential source of acoustic interference for frogs is the sound of rushing water generated from stream habitats, where the frequency of this interference is low at or below 2500–3000 Hz, and could mask the advertisement calls of male frogs in this habitat if they had overlapping frequencies (Feng *et al.* 2006; Hödl & Amézquita 2001; unpublished data). If the characteristics of the signal evolved *in-situ* in loud stream habitats, the acoustic interference would then cause strong selection on the sensory systems shaping the advertisement call. Furthermore, an alternative hypothesis is that frogs evolved their advertisement call frequencies *ex-situ* from their present habitat and then dispersed into local communities from a regional

species pool, and only persisted in habitats where their call could best be heard (i.e. species sorting; Leibold *et al.* 2004). As a result, support for ambient noise driving signal evolution remains contentious and challenging to test (Hoskin *et al.* 2009; Hoskin *et al.* 2009; Röhr *et al.* 2015); in frogs tests of this hypothesis are often limited to a single species (Feng *et al.* 2006; Boeckle *et al.* 2009), do not correct frequencies for body size (Röhr *et al.* 2015; Goutte *et al.* 2016), or have not considered phylogenic history (e.g. Kime *et al.* 2000; Hoskin *et al.* 2009).

To test the hypothesis that ambient background noise drives acoustic signal evolution, I will use *Boophis* (Mantellidae) frogs, which are an endemic radiation within Madagascar and the nearby Comoros Islands. *Boophis* are nocturnal tree frogs that communicate acoustically during a rainy and short breeding season and aggregate around water bodies in high abundance (Glaw & Vences 2007), making it a model system to address these questions. Madagascar presents an ideal geographic location to answer these questions, as relative to land area, Madagascar has the highest species richness and endemism across all vertebrates in the world (Glaw & Vences 2007). *Boophis* tree frogs have experienced an increase in recognized diversity recently because of the integration of DNA barcoding and bioacoustic analyses have revealed a large amount of cryptic diversity (e.g. Penny *et al.* 2014; Glaw *et al.* 2018; **Chapter 1**). Additionally, *Boophis* systematics has begun to receive attention; Wollenberg *et al.* (2011) obtained a multi-locus phylogeny for Mantellidae which had low marker and species sampling for *Boophis*. More recently, Hutter *et al.* (2018) [**Chapter 2**] expanded the genomic sampling for *Boophis* and published a multi-locus phylogeny of six nuclear and four mitochondrial markers that included complete taxon sampling for the genus. Despite the increased sampling of markers and taxa, much of the backbone of the tree remained poorly supported statistically, which harms the

confidence in the results from phylogenetic comparative methods because of error propagation (Donoghue & Ackerly 1996; Davies *et al.* 2012).

In order to overcome poor statistical support for phylogenetic relationships and test the AAH in *Boophis* tree frogs, we generate a new phylogenetic hypothesis for *Boophis* using a newly developed sequence capture probe set for frogs called FrogCap (**Chapter 3**). FrogCap is a sequence capture probe set that obtains high-throughput sequence data from across an organism's genome; FrogCap can be used to sequence up to 13,000 markers, which includes exons, introns, and UCEs for data analysis. We targeted samples from all the major clades of *Boophis* to help resolve uncertain relationships among species groups by sequencing 40 samples (37 *Boophis*; 3 outgroups), which represents ~50 percent of the nominal species in *Boophis*. Additionally, because FrogCap was designed to contain previous Sanger legacy markers, we incorporated all the data from **Chapter 2** into a single data matrix for a fully taxon sample dataset and estimated a new time-calibrated phylogeny for *Boophis* with complete species sampling.

Using this new time-calibrated tree and phylogenetic comparative methods, we test the hypothesis that ambient background noise from the sound of rapids in fast-flowing streams interferes with male acoustic signals and drive signals to evolve frequencies that are non-overlapping with the frequency of the interference. We assemble an unprecedent dataset that integrates data from: (1) a massive dataset of 300+ acoustic recordings from nearly every species in the genus; (2) a new *Boophis* time-calibrated phylogeny using a backbone of ~15,000 genomic markers acquired from sequence capture combined with GenBank data for full species sampling; and (3) used soft tissue computed tomography (CT scanning) on 28 species to acquire detailed morphological information from the larynges of males with associated acoustic recordings using

Diffusible Iodine-based Contrast-enhanced Computed Tomography (DiceCT). We first will test the prediction that frogs that call from loud streams have significantly higher frequencies than frogs that call from quiet streams. The second prediction we will test is whether loud stream frogs evolve higher frequency signals greater than the expected constraint on frequencies due to body size, testing for a significantly higher frequencies in loud stream habitat frogs after correcting the frequencies for body size. Third, we will use internal morphological larynx measurements from DiceCT scans to test whether the evolution of the larynx has become decoupled from an expected linear relationship with body size in loud stream frogs.

5.2 Materials and Methods

5.2.1 Acoustic data collection

To obtain a nearly complete collection (95% of named species; 4 species missing) of acoustic recordings for frogs from the genus *Boophis*, we collected data from multiple sources. We first collected new acoustic recordings in the field across several field seasons from Madagascar from three different geographic areas in the north, central, and southern part of the eastern rainforest belt (Marojejy, Andasibe, Ranomafana) to obtain nonoverlapping communities of *Boophis* species. Calling males were located in streams and recorded in the field at less than 2 m distance from the calling individual. As species of *Boophis* call frequently and simultaneously, we ensured that the male being recorded was the same captured through visual inspection of vocal sac movement under a red light. We used a combination of the following recording equipment: Shotgun microphones: Sennheiser K6+ME66 or Sennheiser MKH 8060; handheld recording devices: Olympus L-10, Marantz PMD661-MKII, or Tascam DR-100mkIII. The calls were recorded in WAV format with a sampling rate of 44.1 kHz/s with 16 bits/sample. To record

temperature, we used an infrared digital thermometer (Fluke 62 MAX Plus) to obtain the calling frogs' surface body temperature after recording; however, we did not find substantial variation in temperature (17–20ºC) because we sampled at similar elevations and habitats at night. We collected voucher specimens for most of the recorded males, and toe clips from a small number. We collected acoustic recording data from 201 individual frogs from 44 species with a mean of 4 individuals per species (range: 1–14); frogs with vouchered specimens was a smaller dataset at 143 individuals with a mean of 3 individuals per species with a voucher. Finally, we supplemented this dataset with previously published data and gathered 103 acoustic recordings (Vences *et al.* 2006; Penny *et al.* 2014; **Chapter 1**) which included 67 species with 1–3 individuals recorded per species. The total number of recordings was 304 audio files representing 96 species (including candidate species) of *Boophis*. When counting the number of calls recorded across all individuals and recordings, the number of calls totals 5,530 calls with a mean of 18.25 calls per individual. See Table S1 for a summary of collected acoustic data.

Because of the large amount of call data to analyze, we created a custom call analysis pipeline in R (R Development Core Team 2019), using the package SEEWAVE to extract acoustic information and analyze hundreds of calls rapidly (Sueur *et al.* 2008). The scripts were initially developed in **Chapter 1** the custom analysis scripts were tested and compared to the manual measurement of advertisement calls and found to be generally similar. The pipeline used here is based off of that previously published (**Chapter 1**; Hutter *et al.* 2016), where we collected a reduced set of statistics only on frequency characteristics: fundamental frequency, dominant frequency, and frequency bandwidth (Figure S1); with the ultimate goal of acquiring the highest frequencies values for each species (excluding harmonic frequencies). We collected this data from all acoustic recordings assigned to a given species, regardless of

metadata quality, because the objective was to associate the highest frequencies with the maximum male body size reported in the literature.

5.2.2 Morphological data collection

We want to understand whether there is a relationship between male frog body size and advertisement call dominant frequency, so we measured the snout-vent length (SVL). Morphological measurements taken were simply the snout-vent length from the largest individual male *Boophis* collected, using a Mituyo digital caliper (precision 0.01 mm) rounded to the nearest 0.1 mm. We surveyed the literature for the maximum SVL from a male for each species to associate with the maximum frequency traits (explained above).

To understand how morphological evolution ties into acoustic trait evolution, we obtained detailed morphological information from the larynges of males through soft tissue computed tomography (CT scanning) of specimens using Diffusible Iodine-based Contrast-enhanced Computed Tomography (DiceCT). DiceCT is a relatively new technique that allows for the 3D visualization and reconstruction of soft tissue morphology (e.g. organs, vasculature, glands; frog tongues: Kleinteich & Gorb 2015) in preserved specimens. DiceCT involves soaking specimens in an iodine solution and scanning with a micro-CT scanner (Metscher 2009; Gignac *et al.* 2016). For this analysis, we carefully selected 28 *Boophis* specimens that had verifiable acoustic recordings and temperature data, were formaline preserved to ensure the structures are comparable and not biased by preservation type and have been DNA barcoded to verify their species identity (Table S2). One sample was not formaline preserved and 2 other samples lacked acoustic data for those specimens, which we acquired from similar-sized specimens from the same species. See Table S2 for a detailed summary of measurements.

We visualized and collected measurements from the larynges of specimens (e.g. length, width, height, posterior opening width, anterior opening width; Figure S2 shows the measurements). After measuring the morphological data, we natural log-transformed these values and used a principal component analysis (PCA) on the set of measurements to reduce the dimensionality of the data, selecting the first principal component for hypothesis testing.

5.2.3 Genetic data collection

For sequence capture using FrogCap (see next section), we selected 38 samples from *Boophis* (~50% of named species in the genus), 10 samples from other genera in Mantellidae, and 3 samples from other families in Ranoidea as outgroups (Table S3). Genomic DNA was extracted from these eight tissue samples using a PROMEGA Maxwell bead extraction robot. The resultant DNA was quantified using a Quantus DNA Broad-range assay (PROMEGA). Approximately 1000 ng DNA was acquired and set to a volume of 50 ul through dilution (with H20) or concentration (using a vacuum centrifuge) of the extraction when necessary.

We integrated new and previously published Sanger data from GenBank into the FrogCap dataset to expand the number of samples in the tree and also to confirm the identification of FrogCap samples (all samples matched correctly existing species' genetic data). We included 10 genetic markers previously sequenced for *Boophis* from all 77 nominal *Boophis* species and 5 candidate species (missing base pair data from the matrix is around 40% missing data) and also included 16S from additional candidate species with call data for a total of 102 total terminals. All markers had 75% species sampling or greater for recognized species (except rhodopsin) and when including candidate species, the marker sampling dropped to 58%. We aligned these Sanger data with the corresponding FrogCap markers using MAFFT (Katoh &

Standley 2013), which included all the mitochondrial markers from *de novo* mitochondrial assembly from the FrogCap sample raw reads (described below).

The sequence capture probe set used for this study is the FrogCap Ranoidea v1 and v2 probe sets (https://github.com/chutter/FrogCap-Sequence-Capture;; Hutter *et al.* **Chapter 3**). Probe design follows Hutter *et al.* (in prep) and is summarized here. Probes were synthesized as biotinylated RNA oligos in a myBaits kit (Arbor Biosciences, formerly MYcroarray Ann Arbor, MI) by matching 25 publicly available transcriptomes to the *Nanorana parkeri* and *Xenopus tropicalis* genomes using the program BLAT (Kent 2002). Matching sequences were clustered by their genomic coordinates to detect presence/absence across species and to achieve full locus coverage. To narrow the marker selection to coding regions, each cluster was matched to available coding region annotations from the *Nanorana* genome using the program (Sun *et al.* 2015). Markers from all matching species were then aligned using MAFFT (Katoh & Standley 2013) and subsequently separated into 120 bp-long bait sequences with 2x tiling (50% overlap among baits) using the myBaits-2 kit (40,040 baits) with 120mer sized baits. These loci have an additional bait at each end extending into the intronic region to increase the coverage and capture success of these areas. Baits were then filtered, retaining those without sequence repeats, a GC content of 30%–50%, and baits that did not match to multiple places in the genome. Additionally, 2300 ultra-conserved elements (UCEs) and 95 commonly used Sanger-based legacy loci from phylogenetic analyses of frogs (i.e. *RAG1*, *POMC*, *TYR;* Feng *et al.* 2017) were included to enable direct comparisons and inclusion of publicly available data from past phylogenetic studies.

The genomic libraries for the samples were prepared by Arbor Biosciences library preparation service. Prior to library preparation, the genomic DNA samples were quantified with fluorescence and up to 4 ug was then taken to sonication with a QSonica Q800R instrument. After sonication and SPRI bead-based size-selection to modal lengths of roughly 300 nt, up to 500 ng of each sheared DNA sample were taken to Illumina Truseq-style sticky-end library preparation. Following adapter ligation and fill-in, each library was amplified for 6 cycles using unique combinations of i7 and i5 indexing primers, and then quantified with fluorescence. For each capture reaction, 125 ng of 8 libraries were pooled, and subsequently enriched for targets using the MYbaits v 3.1 protocol. Following enrichment, library pools were amplified for 10 cycles using universal primers and subsequently pooled in equimolar amounts for sequencing. Samples were sequenced on an Illumina HiSeq 3000 with 150bp paired-end reads.

5.2.4 Data processing and alignment

A bioinformatics pipeline for filtering adapter contamination, assembling markers, and exporting alignments is available at (https://github.com/chutter/FrogCap-Sequence-Capture).The pipeline is scripted in R statistical software (R Development Core Team 2018) using the BIOCONDUCTOR suit of packages (Ramos *et al.* 2017) in addition to open source software publicly available and commonly used in bioinformatics. First, the raw reads were cleaned of adapter contamination, low complexity sequences, and other sequencing artifacts using the program FASTP (default settings; Chen *et al.* 2018). Adapter-cleaned reads were then matched to the UNIVEC bacterial genome database to ensure that no contamination was in the final dataset. We decontaminated the adapter-cleaned reads with the program BBMap (https://jgi.doe.gov/data-and-tools/bbtools/), where we matched the cleaned reads to each

contamination genome at >95 percent similarity. Next, we merged paired-end reads using BBMerge (Bushnell *et al.* 2017) and removed duplicates using "dedupe". The merged singletons and paired-end reads were next *de novo* assembled using the program SPADES v.3.12 (Bankevich *et al.* 2012), which runs BAYESHAMMER (Nikolenko *et al.* 2013) error correction on the reads internally. Data were assembled using several different k-mer values (21, 33, 55, 77, 99, 127), where orthologous contigs resulting from the different k-mer assemblies were merged.

The consensus haplotype contigs were then matched against reference loci sequences from the *N. parkeri* genome used to design the probes with BLAST (*dc-megablast*), keeping only those contigs that matched uniquely to the reference probe sequences. Contigs were discarded if they did not match to at least 30 percent of the reference marker. Finally, we merged all discrete contigs that matched to the same reference marker, joining them together with Ns based on their match position. The final set of matching contigs were named with the name of the marker followed by the sample name in a single file to be parsed out separately for multiple sequence alignment.

The final set of matching contigs were next aligned separately for each marker using MAFFT local pair alignment (max iterations = 1000; ep = 0.123; op = 3). We screened each alignment for samples that were greater than 40 percent divergent from the consensus sequence, which are almost always incorrectly assigned contigs. Alignments were kept if they had greater than 3 taxa, had more than 100 base pairs, and a mean breadth of coverage of greater than 50 percent across the alignment. We applied internal trimming using TRIMAL (automatic1 function; Capella-Gutiérrez *et al.* 2009). All alignments were externally trimmed to ensure that at least 50 percent of the samples had sequence data present.

The raw alignments were further processed and trimmed into usable datasets for phylogenetic analyses and data type comparisons: (1) all-markers, each alignment treated at a single partitioned unit that includes exons and introns together and only trimmed generally; (2) exons, each alignment was adjusted to be in an open-reading frame in multiples of three bases and trimmed to the largest reading frame that included >90% of the sequences; (3) introns, the exon previously delimited was trimmed out of the full-contigs dataset, and the two intronic regions were concatenated; (4) UCEs, were separately saved and not modified; (5) legacy, markers from prior studies (excluding UCEs) were saved separately for ease of access and comparison; and (6) gene, after separating the exons from their flanking intron sequence, exons were concatenated and grouped together if they were found from the same predicted gene from the *Nanorana parkeri* and *Xenopus tropicalis* genomes because these exons are likely to be strongly linked genetically. We addressed potential contamination and used the program TREESHRINK (Mai & Mirarab 2018) on each alignment, which detects sequences with unexpectedly long branch lengths when compared to other gene trees in the dataset and removes these problematic sequences from each alignment. We also assessed missing data using two different methods: we assessed the number of missing bases per alignment from samples included in the alignment (i.e. missing basepair data) and the number of samples completely missing from an alignment (i.e. missing marker data).

5.2.5 Concatenated tree datasets

We first estimated concatenated phylogenetic trees by creating separate datasets with variable amounts of missing sequence data for the different FrogCap dataset types. We separated alignment matrices into three different amounts of missing data (10, 30, and 50 percent); where

individual markers were only retained if the number of samples in each alignment met that completeness threshold. First, we used the maximum-likelihood method IQ-Tree v.1.6.7 (Nguyen *et al.* 2015) to estimate phylogenetic trees from concatenated data. For these analyses, we employed models of molecular evolution identified via ModelFinder (Kalyaanamoorthy *et al.* 2017) built into IQ-Tree, which identified an optimal partitioning scheme and models of molecular evolution for each partition. We assessed support for the resulting topology using 1000 ultrafast bootstrap replicates (Minh *et al.* 2013).

5.2.6 Gene jackknifing

We scripted a gene-jackknifing workflow to estimate concatenated trees utilizing full model selection and partitioning across data matrices, which were often not computationally tractable on full datasets. In addition, this approach allowed us to verify that the topology was consistent across the jackknife replicates. The jackknifing approach used ML with IQ-Tree and followed the procedure: (1) Genes for the data matrix were randomly selected without replacement, where genes were selected up until a threshold of 50,000 bp had been reached so that each matrix was nearly the same size; (2) We partitioned by codon position for exons and by marker for non-coding regions; (3) We used ModelFinder to select the best model for each partition; (4) we ran the analysis 1000 times to generate 1000 jackknife tree replicates; and (5) the 1000 replicate trees were summarized by generating a maximum clade credibility tree, which collapsed nodes into polytomies that were not supported by at least 50% of the jackknife replicates.

5.2.7 Species tree methods

It is possible that concatenation analyses can be statistically inconsistent in the presence of incomplete lineage sorting or anomaly zones that result in gene trees that are discordant when compared to the species tree (Degnan & Rosenberg 2009; Roch & Steel 2015). To address this possibility, we used the software ASTRAL-III (Zhang *et al.* 2017), which conducts a summary-coalescent species tree analysis that is statistically consistent under the multi-species coalescent model. As input for ASTRAL-III, individual trees for each gene and marker were needed, so we performed maximum likelihood (ML) concatenation analyses on each alignment using IQ-Tree. We ran the analyses separately on the all-marker, exon, intron, and gene datasets; and we also combined the exon and intron datasets together in a final analysis. To improve accuracy, we collapsed branches that were below 10% bootstrap support (Zhang *et al.* 2017). Finally, we used local branch support to assess topological support for the coalescent trees generated by ASTRAL III because this method out-performs multi-locus bootstrapping (Sayyari & Mirarab 2016).

5.2.8 Time calibrated phylogeny

We generated time calibrated phylogenetic trees from the topologies generated via ASTRAL-III using the MCMCTREE program in the PAML package (Yang 1997; Yang 2007). In addition to the ASTRAL-III datasets, we also time-calibrated the concatenated sequence capture dataset that combines the legacy dataset with the all-markers dataset. For these analyses, we follow this program's requirement by setting all branch lengths in the input phylogeny to the same length. We then used PAML's BASEML function to generate branch lengths for the input topology via Maximum Likelihood as a single partition with the GTR + Gamma model (dividing the alignment into multiple partitions would be computationally intractable).

For the calibration ages, we calibrated the phylogeny using divergence dates estimated from Feng *et al.* (2017) for shared nodes, which estimated a time-calibrated phylogeny across all anurans using 8 fossil calibration points and 95 loci. Past studies have used the *Indorana prasadi* fossil (applied to the stem of Rhacophoridae), but this fossil might be problematic because it has not been included in a cladistic analysis to verify its phylogenetic placement and the original description of the fossil expressed some uncertainty in its taxonomic placement ("Rhacophoridae?"; Folie *et al.* 2012). Additionally, past studies assessing the fossil calibration suggested that nodes are much older when compared to other calibrations (**Chapter 2**). Because of these concerns, we applied the 95% confidence intervals of the age estimated from Feng *et al.* (2017) as a normal distribution with a mean of 42.5 Myr (35.9–48.9 Myr). This study included the largest molecular dataset of 95 markers for frogs and also a robust selection of eight fossils verified through cladistics and expert analyses. We selected four calibration points using the highest posterior density 95% confidence intervals (HPD 95% CI), which were: (1) crown age of Mantellidae (mean = 42.7; range = 35.9–48.9 Mya); (2) crown age of Rhacophoridae (mean = 42.5; range = 37.3–48.1 Mya); (3) stem age of Mantellidae and Rhacophoridae (mean = 53.7; range = 48.6–59.0 Mya); and (4) stem age of Ranidae (MRCA Ranidae + [Rhacophoridae + Mantellidae]).

For MCMCTREE analyses of the input phylogeny with branch lengths generated via BASEML, we set priors as follows: (a) overall substitution rate: rgene gamma = (1, 20, 1), (b) rate drift parameter: sigma2 gamma = (1, 10, 1); (c) alpha for gamma rates at sites = 1. We next applied a normal probability distribution between the age ranges above with soft bounds and 2.5 percent tail probabilities. We set rate priors for internal nodes using the independent rates model.

We ran MCMCTREE for 50,000 generations, sampling every 1000 generations, with a burn-in of 25 percent and ran each analysis twice to assess convergence.

5.2.9 Hypothesis testing

To understand how body size is related to advertisement call frequencies, we tested for a relationship between these two variables. We used phylogenetic generalized least-squares regression (PGLS; Martins & Hansen 1997), which takes into account the phylogenetic correlation structure of the data, to test for a significant negative relationship between natural log-transformed SVL and the square root of frequencies. Prior to PGLS regression, we compared four models of continuous trait evolution for the frequency measures: (1) white noise: traits evolve independently of phylogeny; (2) Brownian motion: trait evolution follows a random walk and is perfectly correlated with the phylogeny; (3) lambda: trait evolution is explained by phylogeny under a random walk model using a maximum likelihood estimate of Pagel's (1994) lambda (where a lambda of 1 is equivalent to the Brownian motion model and 0 is equivalent to white noise); and (4) Ornstein-Uhlenbeck (OU): constrained random walk where traits tend to deviate from a single optimal value and also return to this optimum at an estimated rate. We then calculated the sample-size corrected Akaike Information Criterion (AICc) to compare the log-likelihood values of these models (while accounting for the different numbers of parameters) and selected the model with the lowest AICc that has a change of at least 4 AICc from the next lowest model (following recommendations from Burnham & Anderson 1998). Significant support for a negative relationship between SVL and frequencies would support the hypothesis that body size plays an important role in shaping the frequency of advertisement calls, and downstream analyses can correct for this potentially confounding factor. To correct for body

size the residuals from the linear regression equation were used and analyzed using the same methodology applied to the uncorrected values. These analyses were all performed in R using the packages APE (v3.0; Paradis *et al.* 2004), GEIGER (Harmon *et al.* 2008), and PHYTOOLS (Revell *et al.* 2012).

To explore if there is an association between advertisement call frequency and noisy and loud stream habitats, we categorized each frog species based on its stream type into three categories: ”quiet” or “loud” based on their observed habitat. Stream type is determined from an assessment of several different factors: (1) direct field observations of the male calling in a noisy environment and presence of white rapids generating noise from the rushing water; (2) measuring the background noise in the recordings to determine if the environment is noisy with a quantitative threshold of 5% noise or greater (i.e. stream background noise will be present on the recordings of frogs from loud streams); and (3) comparing these stream speed categorizations to those reported in the literature and also with the tadpole morphology, where tadpoles that have suctorial mouthparts occur in fast streams, being collected while adhering to rocky substrate (Andreone *et al.* 2002; Linsenmair & Glos 2005; Raharivololoniaina *et al.* 2006; Randrianiaina *et al.* 2012), with these tadpoles only being found in fast flowing streams (StrauB *et al.* 2013). We acknowledge that a direct measurement of stream speed would have been ideal, but these tools were not available, and the categorization is simplified with only two states that we hope is general enough to explain call variation.

After collecting acoustic data and applying the species categorizations, we used phylogenetic logistic regression (Ives & Garland 2010) to test whether there is a difference in signal frequency between quiet and loud stream frogs, correcting for phylogenetic relatedness. A significant relationship between noisy streams and higher frequencies would support the

hypothesis that noisy streams have frogs with higher frequencies. However, to explain whether this pattern has evolved *in-situ* in response to acoustic interference, we assessed whether frequency values might be related to body size (described above) and we will use the residuals from the PGLS regression between SVL and frequencies as described above if a relationship is found. Therefore, when correcting for body size, a significant relationship between stream habitat type and frequency would support the hypothesis that frequencies are evolving separately from body size in noisy streams environments. If this relationship is not significant, it would support *ex-situ* signal evolution and species-sorting as the dominant mechanism in explaining why loud streams have frogs with higher frequency calls.

We used the DiceCT scan measurements (described above) to test the hypothesis that frogs that reproduce in loud streams have evolved higher frequencies because the allometric scaling of larynx structural measurements has become decoupled from body size, such that the larynx is evolving greater variation in structure than would be predicted by body size. We tested this hypothesis using PGLS regression (methods described above), using the natural log-transformed larynx size measurements and SVL measurements taken from the associated specimen. The PGLS regression was performed separately on the quiet and loud stream habitat species, where a significant positive relationship between laryngeal measures and body size would suggest that the expected allometric scaling relationship remains intact while a negative or insignificant relationship would support the presumption that the allometric scaling and evolution of laryngeal dimensions and body size has become decoupled.

However, it is also possible that the scaling relationship has evolved in a different direction separate from the expected body size scaling. To test this alternative hypothesis, we used a phylogenetic analysis of co-variance (ANCOVA), testing whether the PGLS regression

slopes between body size and larynx size are significantly different between the loud and quiet stream categorizations. A significantly different slope, with a larger slope for loud stream frogs, would support the hypothesis that loud stream frogs are evolving higher frequencies in response to ambient noise than predicted by body size. Our hypothesis that loud stream frogs are evolving larynges and thus frequencies separately from the predicted allometric scaling of larynges would be supported if there was a significant PGLS relationship between body size and larynx size in slow stream frogs and no significant relationship in loud stream frogs. If both relationships are strongly supported, a significantly different slope between loud and quiet stream frogs from the phylogenetic ANCOVA would also support our hypothesis.

5.3 Results

5.3.1 Sequence capture evaluation

We sequenced 51 samples for this study using the FrogCap probe-set, which totaled 62,005 mega base pairs (Mbp) of raw sequence data for these samples (Figure 2). Each sample had a mean base pair yield of 1265.4 ± 324.8 (range: 535.2–1953.4) Mbp and a mean 8,547,246 ± 2,388,256 (range: 3,544,544–15,626,930) reads. Raw reads were then filtered to remove exact duplicates, low complexity and poor-quality bases, adapter and contamination from other non-target organisms, which resulted in a mean 92.5% ± 2.4% of reads (range: 84.6–95.9%) passing the quality filtration steps. After merging paired-end reads and reducing redundancy (removing duplicate and containment reads), there was a mean 514,893 ± 305,471 (range: 154,093–1,344,496) merged paired-end reads (and singletons) used as input for assembly. After assembly, the samples yielded a mean 13,869 ± 1666.8 (range: 10,891–18,752) contigs, which had a mean length of 896.6 ± 89.8 (range: 100–28,479) base pairs. Finally, after matching the contigs to the

target markers, samples contigs matched to a mean 10,967.6 ± 536.2 (range: 9988–12,122) markers (Figure 3). See Table S3 for a detailed summary for each sample.

5.3.2 Alignment summary

Alignment and quality control of the multiple sequence alignments prior to trimming results in 14,738 total aligned markers, with a mean 39.1 ± 13.8 (range: 3–51) samples per alignment, which remained consistent across datasets (Figure 4A). Multiple sequence alignments have a mean 1703.1 ± 748.4 (range: 245–24,139) bp per alignment, totaling 18,386,634 bp (prior to trimming). After trimming, we considered this dataset the all-markers dataset, which does not have any trimming related to the type of data. The all-markers dataset had 14,728 alignments with a mean 39.1 ± 13.8 (range: 4–51) samples per alignment; these alignments totaled to 7,120,049 bp of sequence data where alignments had a mean 483.1 ± 275.6 (range: 100–9040) bases (Figure 4).

The following datasets begin with the untrimmed all-markers dataset and applies different types of trimming and filtration to achieve separate datasets composed of different types of genomic data. After separating the intron and exon sequence from the aligned set of contigs and trimming, the exon dataset had 10,827 exon alignments totaling 2,644,878 base pairs and had a mean 244.3 ± 272.1 (range 78–7437) bases per alignment. The intron dataset containing only non-coding flanking sequence from both ends of the exons had 10,784 joined intron alignments totaling 4,428,802 base pairs of sequence data (Figure 4A–B), while the intron alignments had 410.7 ± 153.4 (range 81–2568) bases per alignment (Figure 4A–B). Multiple sequence alignments for the UCE dataset had 2258 aligned UCEs totaling 1,541,348 base pairs of data with a mean 682.6 ± 167.4 (range 98–2367) bases per alignment (Figure 4A–B). Finally,

we concatenated individual exons from the same gene, which resulted in 2397 gene alignments totaling 1,480,722 base pairs and a mean 617.7 ± 533.5 (range 81–7614) bases per alignment (Figure 4A–B).

Missing data varied throughout the dataset, but was minimal overall (Figure 4D–E); however, UCEs and some legacy markers had about 50 percent missing data because version 2 of the FrogCap Ranoidea probe set removed markers that were unsuccessful from version 1 and replaced them with additional UCEs and legacy data. In addition, the combined exon gene datasets had fewer missing marker data and slightly higher missing base pair data. When assessing the number and proportion of parsimony informative sites of the markers, the introns are the most informative while the UCEs have the least number of informative sites (Figure 4F).

5.3.3 Phylogenetic systematics

Analyses with concatenated alignments (Figure 5A), gene jackknifing (Figure 5B), and species-tree methods (Figure 6) all gave strong support for the same topology, except the relationships among the three taxa *Boophis nauticus, B. doulioti,* and *B. tephyraeomystax* varied among analyses, usually with weak statistical support. About half the jackknife replicates and several of the different marker types supported alternative relationships among these taxa (Figure 5A). Using species-tree methods, we recover the same topology as the gene jackknifing analyses (Figure 5B), with about the same proportion of gene trees supporting each of the two major alternative topologies (Figure 6). Node support for relationships among other species groups and taxa in the tree were all strongly supported in every other analysis.

5.3.4 Time-calibrated phylogeny

We used secondary calibration points to calibrate nodes shared between the Feng *et al.* (2017) and our sequence capture dataset, using MCMCTree to calibrate the phylogeny. We ran each analysis twice and verified that they were consistent and conducted a prior only run to ensure the results without data were not dramatically different than those with sequence data. We find a mixture of two different sets of ages for clades, which is related to the type of sequence data used as input for the analysis. Using the highly variable, and potentially more neutrally evolving nuclear markers (introns, UCEs) we surprisingly recover much younger clade ages, finding a crown age of ~15 Mya for *Boophis*, and younger ages for the contained species groups; while in mitochondrial DNA, we found the oldest ages estimating ~47 Mya for the crown of *Boophis* (Figure 7). In contrast, using the markers potentially undergoing selection (exons, genes, legacy) leads to older ages of ~25–35 Mya for the crown age of *Boophis*. In addition, the all-markers dataset, which includes both exons and introns, is intermediate in age between these two sets of ages at ~25 Mya for the *Boophis* crown age. In addition, for our analyses we are not interested in the absolute ages on the phylogeny but rather our goal was to obtain relative ages for comparative methods. All analyses in the main text will use the all-markers MCMCTree results because the ages are intermediate between the two extremes reported previously, and it incorporates all the different data types (Figure 7).

5.3.5 Hypothesis testing

We find that larger-bodied frogs are more likely to occur in quiet streams and smaller frogs in loud streams (Figure 8A), which shows the expected inverse pattern in frequency measures (Figure 8B-C) and when plotted as continuous characters on the phylogeny reveal a

potential relationship (Figure 9). We predict a negative relationship between body size (SVL) and frequencies, which would show that body size is an important variable in determining frequency. We used PGLS regression and found a significant negative relationship between SVL and all frequency measures tested (Figure 10). For all following analyses comparing frequencies, frequency values were replaced with the residuals from the respective PGLS regression, unless otherwise noted.

If male frogs that reproduce in loud streams have advertisement calls with higher frequencies than quiet streams, we would expect to find a significant relationship between stream habitat (loud and quiet streams) and uncorrected frequency measures using phylogenetic logistic regression. We find significant relationships using logistic regression across frequency measures ($P < 0.001$; Figure 11A), which strongly suggests that loud, noisy streams are occupied by male frogs with higher frequency calls. Next, to test the second hypothesis that these higher frequencies evolved *in-situ*, we used phylogenetic logistic regression to test for a significant relationship between stream habitat type (loud and quiet streams) and the frequency variables corrected for the effect of body size measured with SVL. We find significant relationships with the higher frequency and dominant frequency variables ($P < 0.032$; Figure 11B); however, the lower frequency variables and bandwidth were not significant. These results strongly support our hypothesis that higher frequency advertisement calls evolved in response to these loud and noisy stream environments, and also suggests that frequencies have become decoupled and are evolving independently from body size because we find a significant relationship despite correcting for body size.

We CT scanned 28 *Boophis* specimens and collected measurement data from the length, width, height, volume, anterior and posterior openings of larynges for these males. From

precisely measured traits for these specimens, we find strong partitioning in body size (Figure 12A) and the first PC axis of laryngeal measures (Figure 12B), and precisely measured acoustic frequencies (Figure 12C–D). After conducting a PCA analysis on the measurements, we used the first PC axis to represent the larynx size and with natural log-transformed SVL to test for a relationship between these variables using PGLS regression. We found a significant relationship in the quiet stream habitat frogs ($R^2 = 0.797$; $P < 0.001$; Figure 13B), suggesting that body size is strongly linked to the size of the larynx. However, we did not find a significant relationship in the loud stream habitat frogs ($R^2 = 0.114$; $P = 0.199$; Figure13A), where along with the substantial variation in larynx size strongly suggests that the evolution of body size and larynx size have become decoupled.

5.4 Discussion

The large variety of animal communication signals in nature and their evolutionary histories have long captivated the interest of scientists and have been crucial to understanding the drivers of natural and sexual selection. Here, we shed light on the co-evolution of acoustic signals, sensory systems, and microhabitat, which are potentially driven by background noise generated from the sound of rushing water in the montane stream habitats where these frogs reproduce. We tested the acoustic adaptation hypothesis (AAH) in *Boophis* tree frogs from Madagascar, which are the ideal model system for addressing the evolution of male advertisement calls.

We first showed that male frogs that reproduce and call in loud stream habitats have significant higher frequencies than frogs calling in quiet streams (Figure 11A), providing strong support for our initial assumption of this association. We next found that male frogs calling in loud stream habitats have significantly higher frequencies after correcting for body size, which

suggests that natural selection is driving the evolution of frequencies that have become decoupled from the expected body size / frequency relationship (Figure 11B). This is further evidenced by the surprising lack of a relationship between loud stream frog larynx morphological measurements and frog body size, where in contrast we find a strong relationship between quiet stream frog body size and larynx measurements (Figure 13). Together our results suggest that noisy acoustic environments are an important influence intertwined in the coevolution of frog acoustic signals, the morphology driving acoustic signal difference, and microhabitat, which can lead to the evolutionary decoupling of body size and structural morphology critical to acoustic communication.

Our results demonstrate the importance of body size for explaining a substantial amount of variation in advertisement call frequencies. We show that body size has a significant negative relationship with frequencies (Figure 10), which is most often shown in studies of individual species (Narins *et al.* 2006; Wells 2007), but has not often been shown across a large phylogenetic scale (Gingras *et al.* 2014; Rohr *et al.* 2016). Furthermore, this pattern in body size influencing these signals has also been observed in many other organisms that communicate acoustically (Birds: Derryberry *et al.* 2018; Primates: Fitch 1998; Insects: Benelli *et al.* 2015; Carnivores: Bowling *et al.* 2017). In frogs, the allometric scaling (natural-log scaling) of the larynx with body size is expected to be the causative factor of this relationship as past studies have shown that these frequency and other call parameters are biomechanically related to laryngeal size in frogs, which in turn is predicted by body size (McClelland *et al.* 1996; McClelland *et al.* 1998; Guerra *et al.* 2014). Importantly, our results suggest that understanding the relationship between body size and call characteristics is critical to testing the AAH and other

hypotheses regarding natural or sexual selection on communication because selection could be acting on body size rather than the acoustic signal.

Prior to correcting for body size, we find that loud stream frogs have significantly higher frequencies than frogs that reproduce in quiet streams (Figure 11A), providing strong evidence and confirmation that loud noisy streams have males with calls that can be heard by females. However, this test does not yet provide evidence for the AAH because it does not test whether the calls have evolved in response to the environment versus the alternative of species sorting (Leibold *et al.* 2004), where the calls evolved first regionally and dispersed from the regional pool into the local communities that species are best adapted (Leibold *et al.* 2004; Belmaker & Jetz 2012). In the literature, there are many studies that support results similar to those here, where many organisms have been shown to avoid habitats with acoustic interference that could mask their own acoustic signals (e.g. Birds: Brenowitz 1982, Brumm 2004; Insects: Lampe *et al.* 2014; Frogs: Goutte *et al.* 2018; Monkeys: Brumm *et al.* 2004; Whales: Parks *et al.* 2010), but these studies do not directly test whether natural selection is driving the evolution of divergent acoustic signals.

We directly addressed whether the frequencies (and the physiology and morphology underlying them) are evolving in response to environment noise by correcting the frequencies for body size such that frequency differences are being compared and found that frogs that reproduce in loud stream habitats have significantly higher dominant frequencies than frogs in quiet habitats (Figure 11A). When removing the effect of body size on frequencies, the relationship remains significant which supports the AAH and suggests that frogs that reproduce in loud environments are evolving frequencies that are decoupled from the expected body size and frequency relationships we show in this group (Figure 11B). We provide evidence that

selection is acting on the sensory systems and morphology that directly generate the acoustic frequencies because of the strong selection pressures to communicate from the acoustic interference in loud stream habitats, which has to our knowledge never before been shown.

Through CT Scans of the larynx, our results illuminate how strong selection from acoustic interference leads to morphological adaptions of sensory systems that results in higher frequency signals that can avoid being masked. The allometric natural-log based scaling of laryngeal measurements with body size is expected to be the causative factor for frequency variation frog calls (McClelland *et al.* 1998; Guerra *et al.* 2014), and we provided strong support for this expected relationship in frogs from quiet stream habitats where selection from interreference is weak. Surprisingly, we did not find any support for a relationship between laryngeal measurements and body size in frogs from loud stream habitats because we predicted a shift in the body size allometric relationships rather than a decoupling. Our results support the hypothesis that selection from acoustic interference has driven the evolution of novel solutions to generating acoustic signal differences rather than modifying body size, and these solutions have unexpectedly caused a decoupling in expected allometric scaling relationships.

This idea is further supported by the near equal variation in laryngeal measurements from loud stream habitat frog to quiet environment frogs, despite the SVL range of loud stream frogs being several times smaller than quiet stream frogs (Figure 12). The evolution of this new variation in laryngeal morphology occurs in the smallest body sized species (Figure 12–13; Figure S4), which are at lower extremes for tree frog body size where more energy is expended calling (McClelland *et al.* 1997) and thus it might be evolutionary more costly to reduce body size beyond this limit. We speculate that once a lower limit in body size

has been reached, then it becomes maladaptive to evolve smaller body sizes and instead evolve different laryngeal morphology in response to environmental noise.

Remarkably, our results also demonstrate how natural selection can disrupt the tight correlated evolution of body size, laryngeal morphology, and acoustic signal frequencies. These novel traits and variation in laryngeal morphology have arisen through the decoupling of larynx evolution from body size constraints, which has never been shown before for morphology critical to sensory systems to our knowledge. Morphological decoupling in larynx and body size have been observed in mammals, but the morphological factors contributing to a more complex vocal repertoire and different mechanisms of sound production lend to this more frequent decoupling (Hauser 1993; Fitch 1998; Charlton *et al.* 2011; Garcia *et al.* 2017). In most frogs the vocal morphology is highly reduced, and biomechanics are much simpler: the frog contracts their trunk muscles to push air out the lungs through the larynx which vibrates the vocal cords and larynx (Martin & Gans 1972; Dudley & Rand 1991), such that modifying the larynx size has a large impact on call frequencies. Furthermore, simple modifications to the larynx can lead to dramatic differences where past studies have demonstrated that the presence of a fibrous mass on the larynx of male tüngura frogs affected the frequencies and attractiveness of the call when surgically removed (Gridi-Papp *et al.* 2006; Baugh *et al.* 2017).

Another potential explanation for the rapid divergence in larynges measures and call frequencies in loud stream habitat frogs is that there might be intense competition for "signal space" or acoustic niche space in these habitats. Past studies show that the montane rainforests of Madagascar contain the majority of the species that reproduce in loud streams (Brown *et al.* 2016; **Chapter 2**); competition of acoustic niche space should be much more intense in these habitats when compared to the less species-rich lowlands. There has been some support for

acoustic interference from co-occurring species in other organisms; prior research suggests that bird co-occurrences are structured temporally and spatially such that song overlap in signal space is minimized while research on frog assemblages found little evidence for signal competition (Duellman & Pyle 1983; Chek *et al.* 2003; Luther 2009; Vamosi *et al.* 2009; Tobias *et al.* 2010; Hoskin & Higgie 2010). Supporting the general idea of competitive signal space, some signal variables can only occupy a limited range of values, such as frequencies (Duellman & Trueb 1994). A possible explanation for the larger variation in loud stream frog larynges is increased selection pressures from co-occurring species leading to novel modifications of the larynx, which should be addressed by future research when a larger dataset of DiceCT scans can be collected.

This study confirms the phylogenetic results of **Chapter 2** which despite the majority of the nodes in the tree not being strongly supported, had the same general relationships we find here (Figure 5–7). We again recover *B. lilianae* not monophyletic with *B. baetkei* + *B. ulftunni*, but found these two taxa as monophyletic and no longer nested with the *B. majori* group (**Chapter 2**). Therefore the *B. ulftunni* group could justifiably be resurrected and applied to these two taxa; however, more taxon sampling in this clade would be necessary to confirm that they are not nested with the *B. majori* group. Furthermore, we also combined GenBank legacy data with the sequence capture data, and demonstrate that this approach to including genetic samples is successful in dramatically reducing the number of weakly supported relationships when compared to the GenBank Sanger data alone (Figure 7; **Chapter 2**).

One uncertain set of relationships in the sequence capture analyses (*B. tephraeomystax, B. nauticus, B. douloti*) does not appear that it could be resolved as alternative topologies are equally strongly supported by equal numbers of gene trees. In some analyses more gene trees support the alternative topology than the species tree, making this a candidate system to test for

an anomaly zone with an empirical example (Kubatko & Dengnan 2007; Linkem *et al.* 2016). Furthermore, *B. nauticus* is a species that has recently arrived on the island of Mayotte through overwater dispersal (Glaw *et al.* 2018), which could indicate that the conflict at these nodes is a result of incomplete lineage sorting, rather than discordance generated by statistical noise (**Chapter 4**), whereby most nodes in the tree are strongly supported by a majority of gene trees (Figure 7).

5.5 Figures

Figure 1. The illustration provides an example of a situation where stream frequencies (the dotted blue line; 2-2.5 kHz) would not be overlapping with call frequencies (the black lines). This pattern could be the result of interference from the sound of the stream selecting for call frequencies to be non-overlapping with this interference

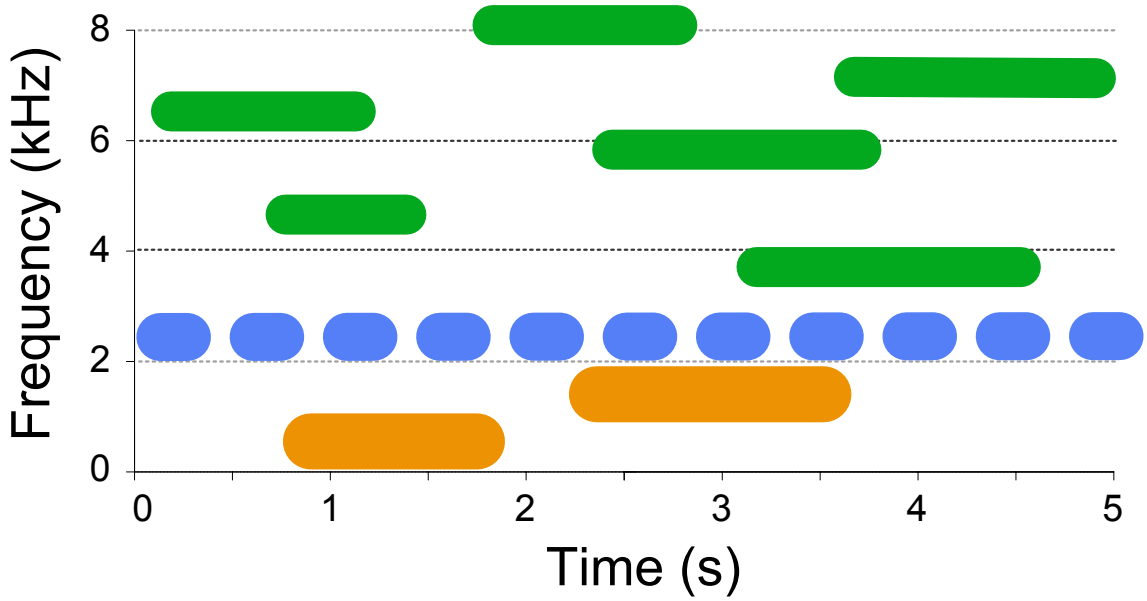

Figure 2. Example DiceCT scan from which internal auditory morphology was measured.

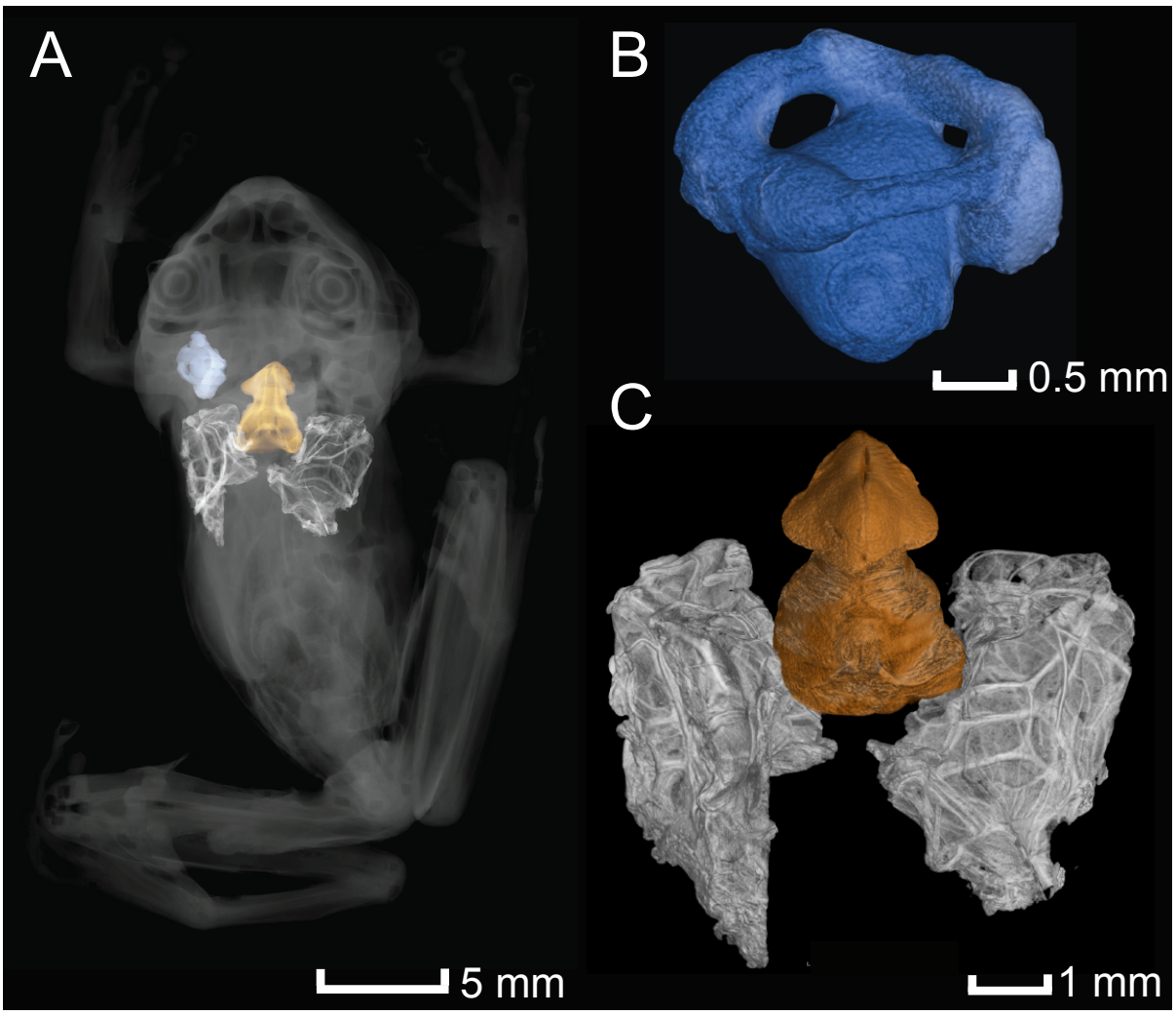

Figure 3. The proportion of markers obtained per sample (i.e. occupancy) is illustrated below. The FrogCap alignments for the ingroup Boophis samples are shown in green on the left and the outgroups from Mantellidae and other lineages are shown in orange on the right

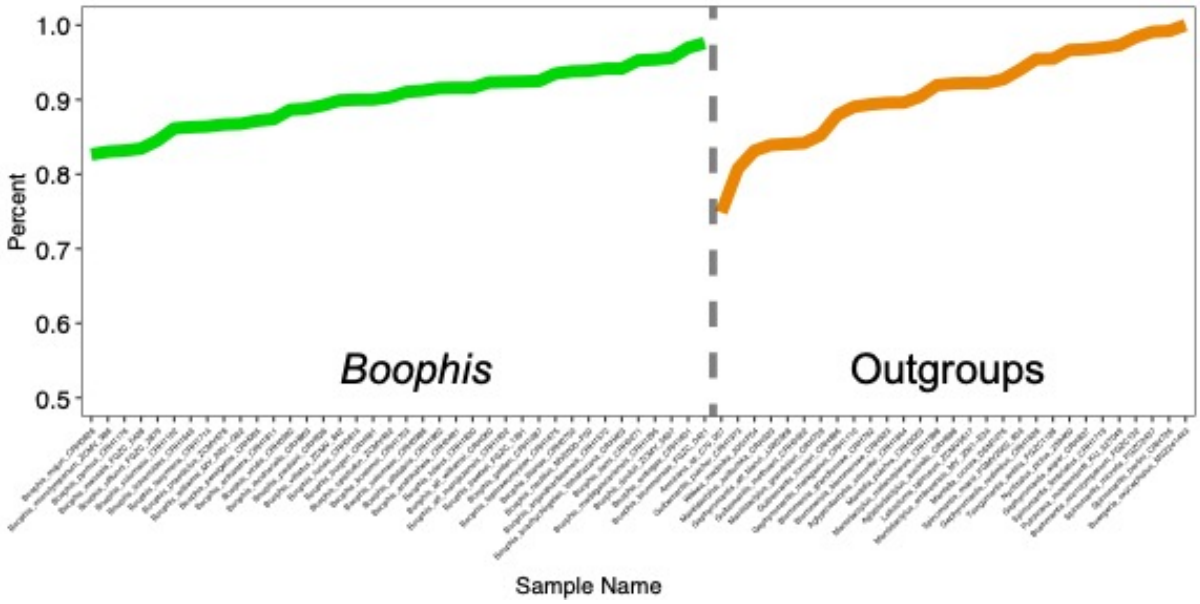

Figure 4. Summary statistics to quantify and compare alignments from the different sequence capture datasets after filtration, alignment, trimming and dataset partitioning. The different comparisons are: (A) number of alignments for each dataset; (B) number of base pairs plotted for each dataset within each phylogenetic scale; and (C) the mean alignment length (with standard deviation shown as error bars); (D) Base pair missing data in the top row is the percent of missing data calculated from the number of missing bases pairs across alignments for each sample when the sample is present in the alignment; (E) Marker missing data in the bottom row is the proportion of missing data calculated from the number of missing samples across each set of alignments; and (F) Parsimony informative sites, plotted as a histogram for each of the datasets.

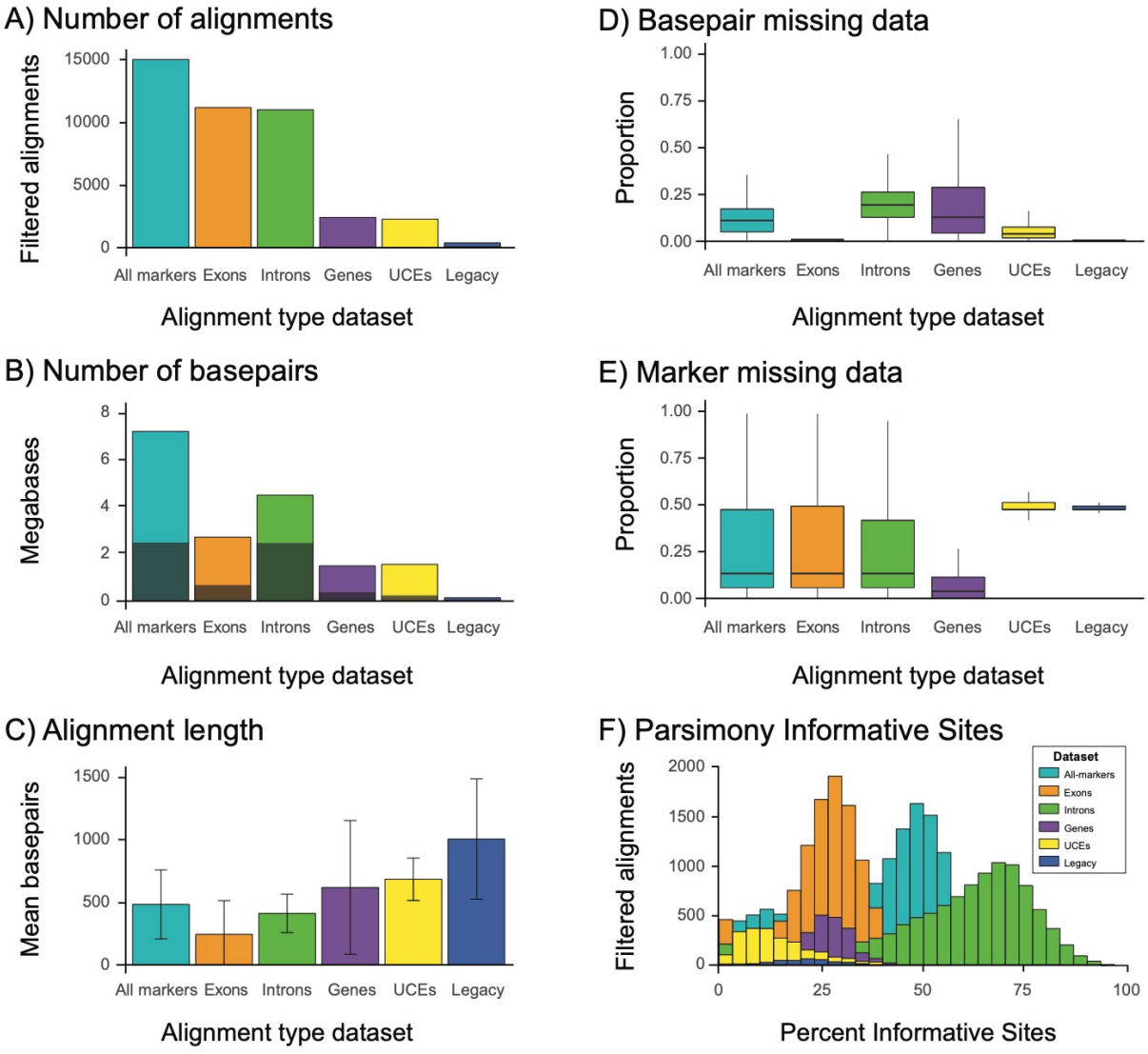

Figure 5. Consensus topologies from the (A) gene jackknifing and (B) concatenated analyses for the FrogCap *Boophis* dataset. In the jackknife analysis (A) branch lengths are the average branch length across jackknife replicates, where all replicates had the same topology. The pies shown at some nodes are those not equivocally supported across jackknife replicates and show the proportion of replicates for each of the three most common topologies. The black pie is the most common jackknife tree, the grey the second most common and white is the least frequent. The concatenated trees (B) are taken from the 50 percent missing marker data all-marker alignment branch lengths. In the 10 percent missing data alignments for exons and genes, the node indicated in blue/red was poorly supported (less than 95 bootstrap in IQTree) in both analyses. In addition, the purple node is a poorly supported node in the all-markers 30 percent missing marker data concatenated alignment. Nodes without annotations are strongly supported in every analysis.

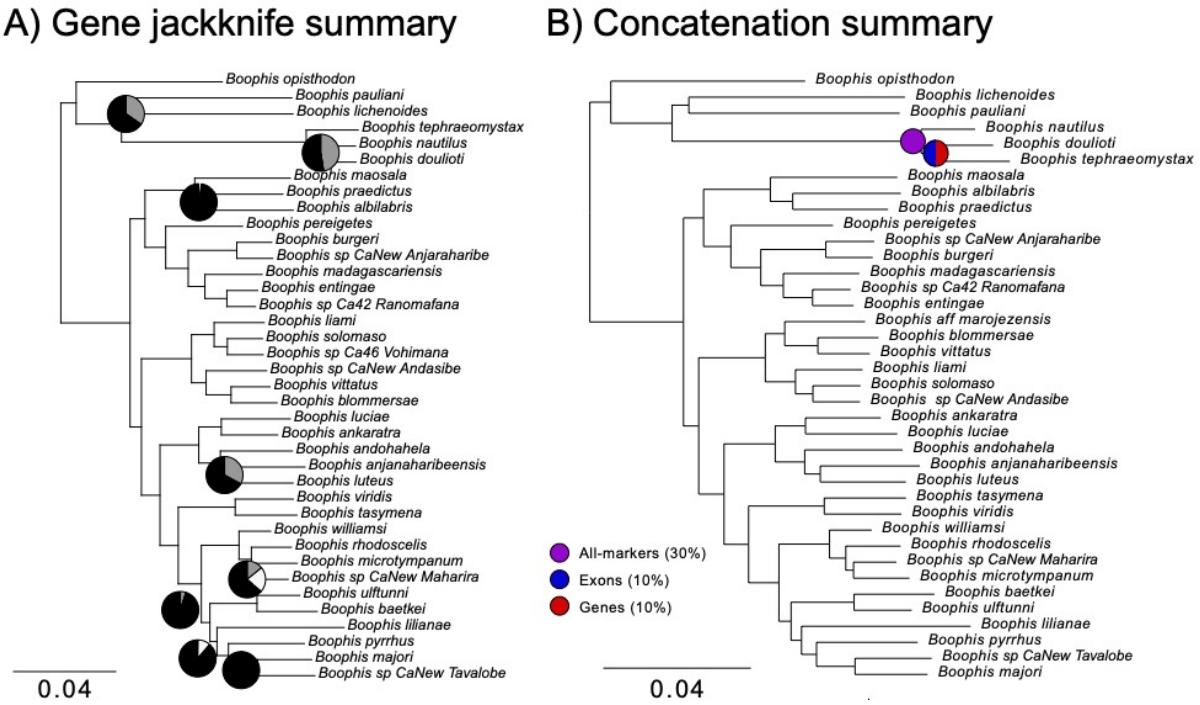

Figure 6. Consensus topology from ASTRAL-III analyses that combines all the different marker types from the *Boophis* FrogCap dataset. Branch lengths are in coalescent units, where the length of the branch is proportion to the amount of gene/species tree discordance in the dataset (i.e. shorter branch have more discordance). The pies below each branch represents the proportion of gene trees that support that given quadra-partition out of the three possible topologies. The green pie is the most common gene tree, the blue the second most common and purple is the least common proportion. All nodes were strongly supported with local posterior values (=1.0).

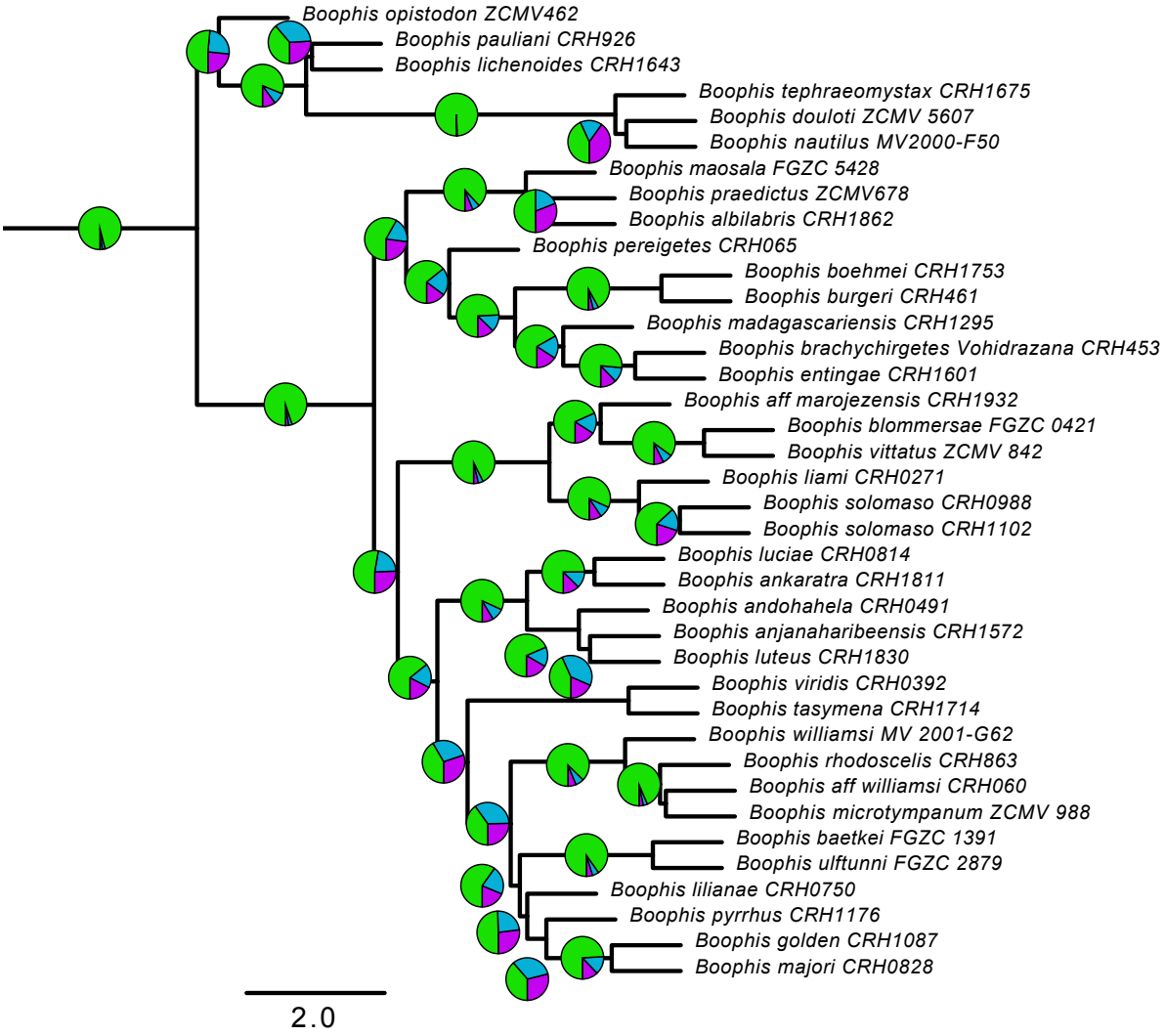

Figure 7. Ultrametric phylogeny of the genus *Boophis* that combined sequence capture data with GenBank mitochondrial and nuclear genetic markers that includes all known species of *Boophis*. The age estimates are obtained from Bayesian Inference (BI) with MCMCTree and are combined with support values from the Maximum Likelihood (ML) analysis from IQTree. Red circles at nodes represent poorly supported nodes from IQTree (less than 95 bootstrap). Colored branches represent species groups as labelled at nodes, which corresponds to the inset phylogeny and node support from **Chapter 2**.

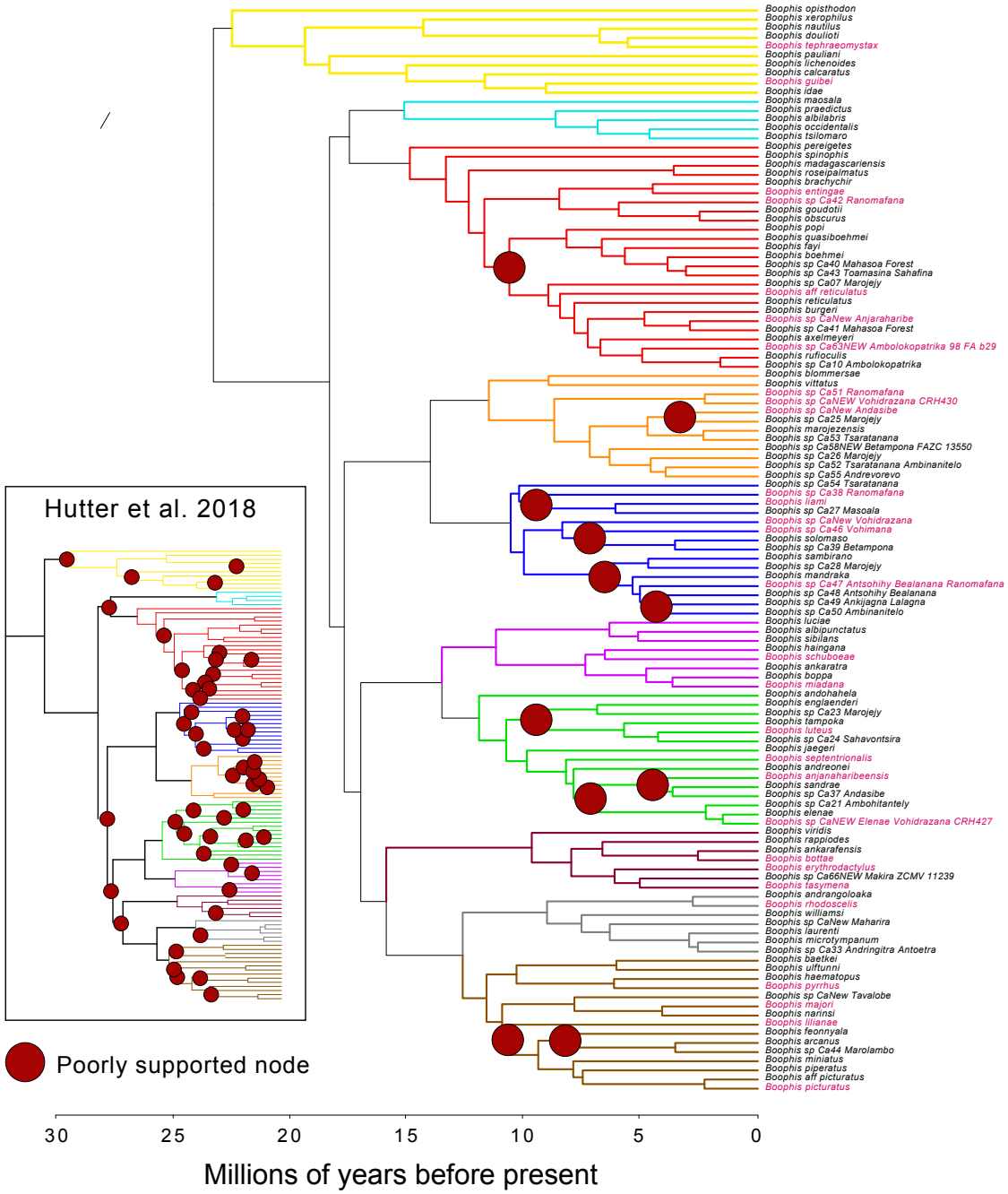

Figure 8. The ultrametric phylogeny with the snout-vent length (SVL) and higher dominant frequency traits mapped onto the phylogeny after performing ancestral reconstructions in PHYTOOLS. A general pattern of small bodied frogs in blue corresponding to higher frequency frogs in red can be observed.

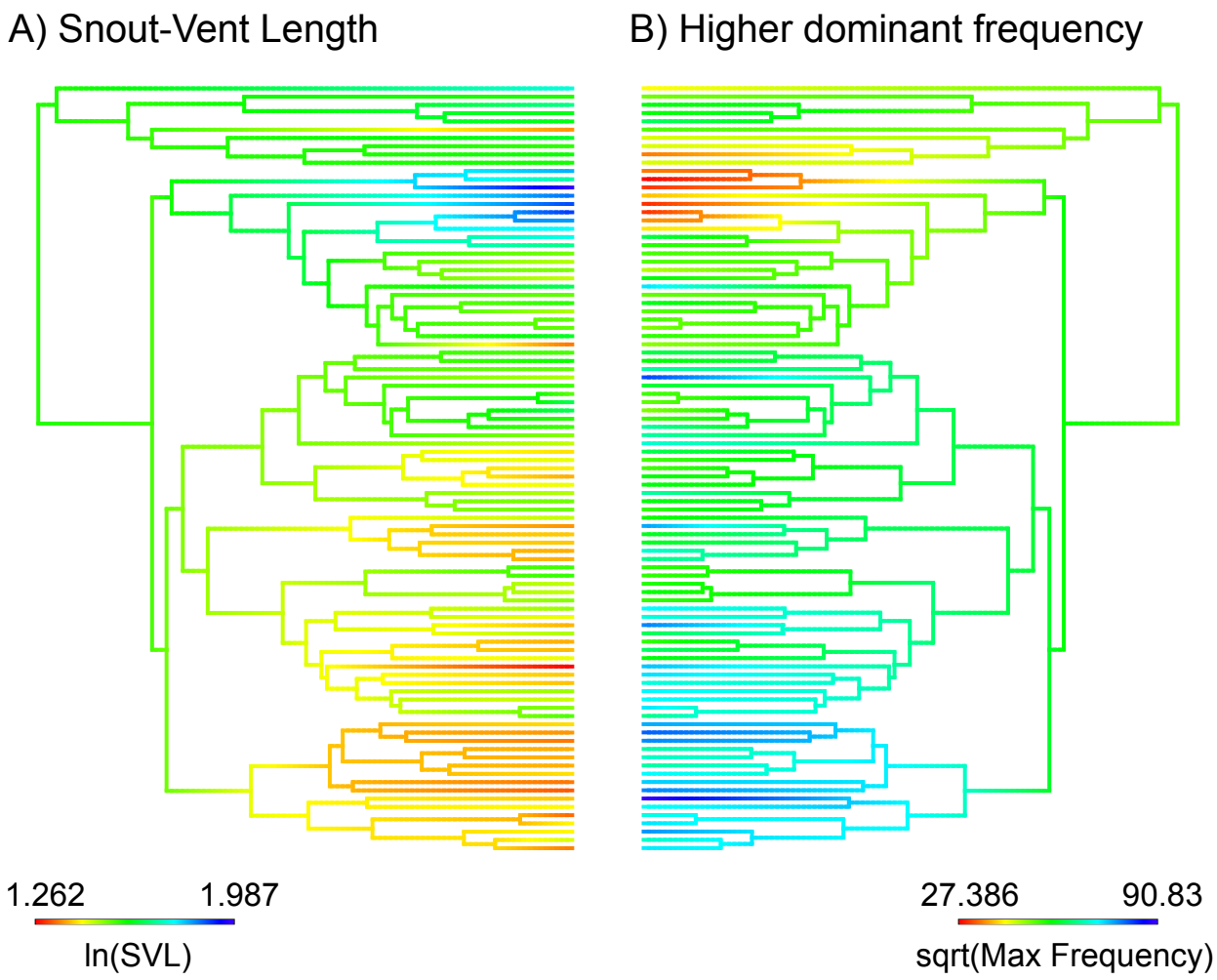

Figure 9. A summary of the *Boophis* body size and frequency datasets (**Dataset 1**), which have been plotted according to the species' stream habitat type. The measurements are summarized as: (A) Maximum SVL recorded for a species; (B) the maximum higher dominant frequency limit; and (C) the maximum dominant frequency. Note that loud stream habitat frequencies are distributed above the frequency of background noise from loud streams (3000 Hz).

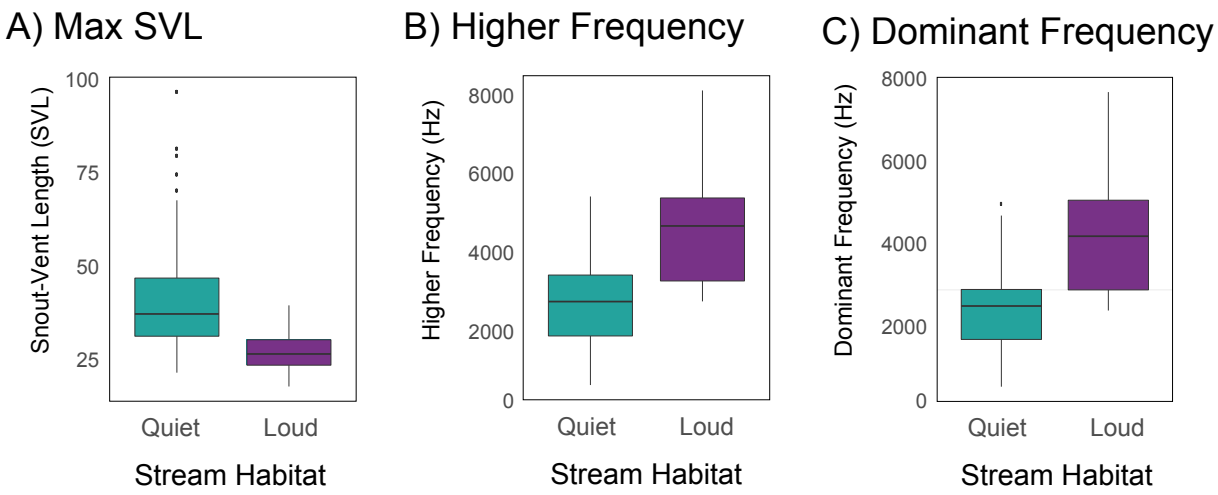

Figure 10. The results of the PGLS regression analysis of body size and frequency, supporting the hypothesis that frequencies are related to body size. The frequencies shown are: (A) the maximum higher limit of the dominant frequency; (B) the maximum dominant frequency; (C) the minimum lower limit of the dominant frequency; and (D) the frequency bandwidth (higher minus lower frequency), which did not have a significant relationship with body size.

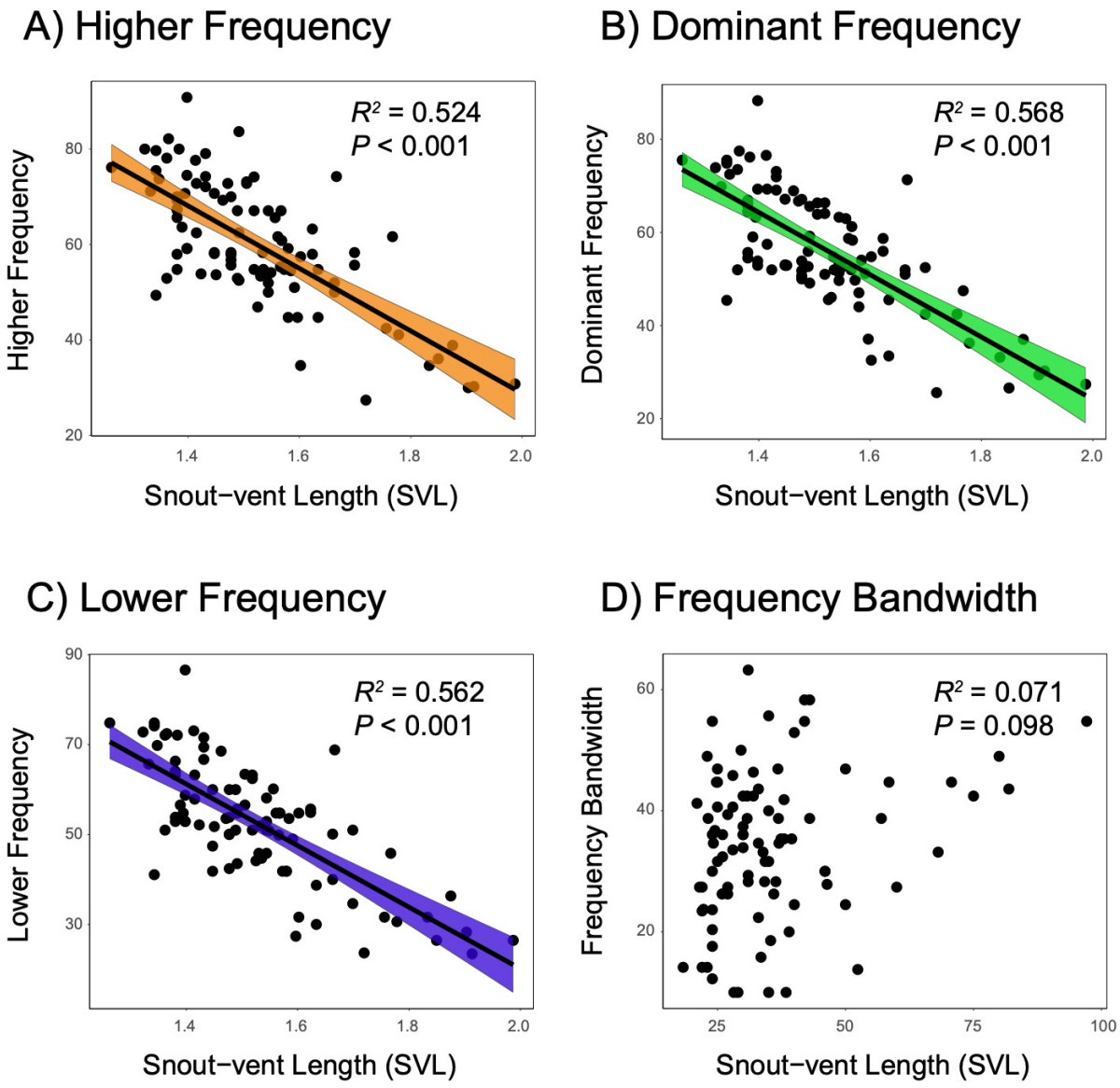

Figure 11. Phylogenetic logistic regression results that (A) strongly support the hypothesis that frogs that live in loud streams have higher frequencies (without correcting for body size). In (B) the second hypothesis is also strongly supported, which suggests that higher frequency calls are evolving in loud streams when corrected for body size.

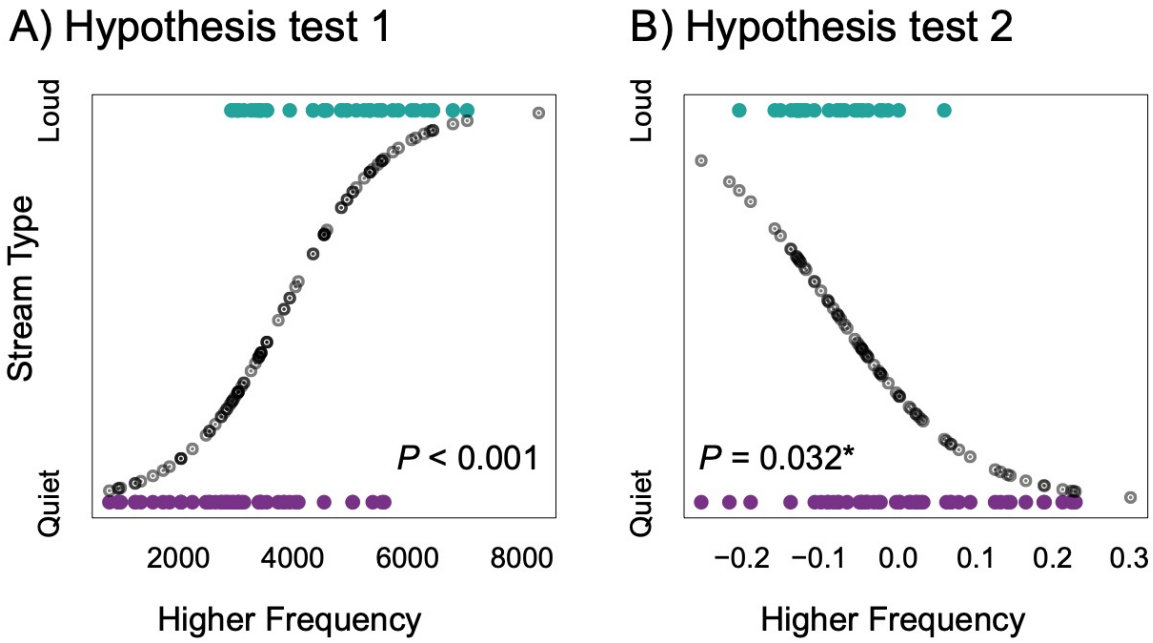

Figure 12. A summary of the CT Scanned *Boophis* measurements, which have been plotted according to the species' stream habitat type. The measurements are summarized as: (A) the SVL recorded for each scanned species; (B) PC1 of a principal component analysis of laryngeal measurements; (C) the mean higher dominant frequency limit from each specimen; and (D) the mean dominant frequency from all calls recorded for a specimen. Note that loud stream habitat frequencies are distributed above the frequency of the background noise (less than 3000 Hz).

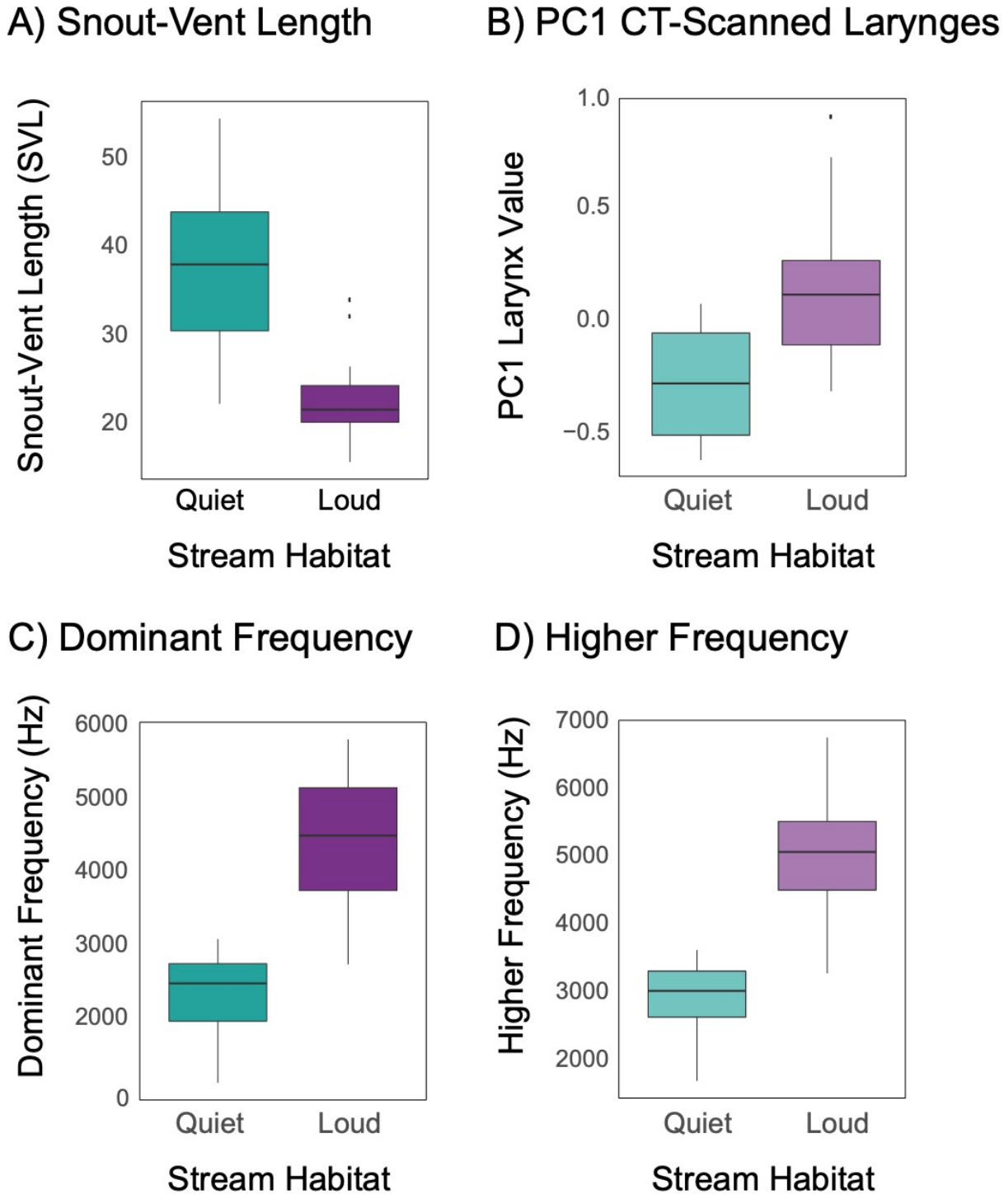

Figure 13. The results of the PGLS regression analysis of larynx measurements and body size, supporting the hypothesis that loud stream frogs (A) have larynges decoupled from their expected relationship to body size as shown in quiet stream frogs (B). In addition, we do not find a significant relationship between frequency and larynx measures in loud stream frogs or quiet stream frogs; however, the relationship was barely non-significant in quiet stream frogs possible from lower sample sizes.

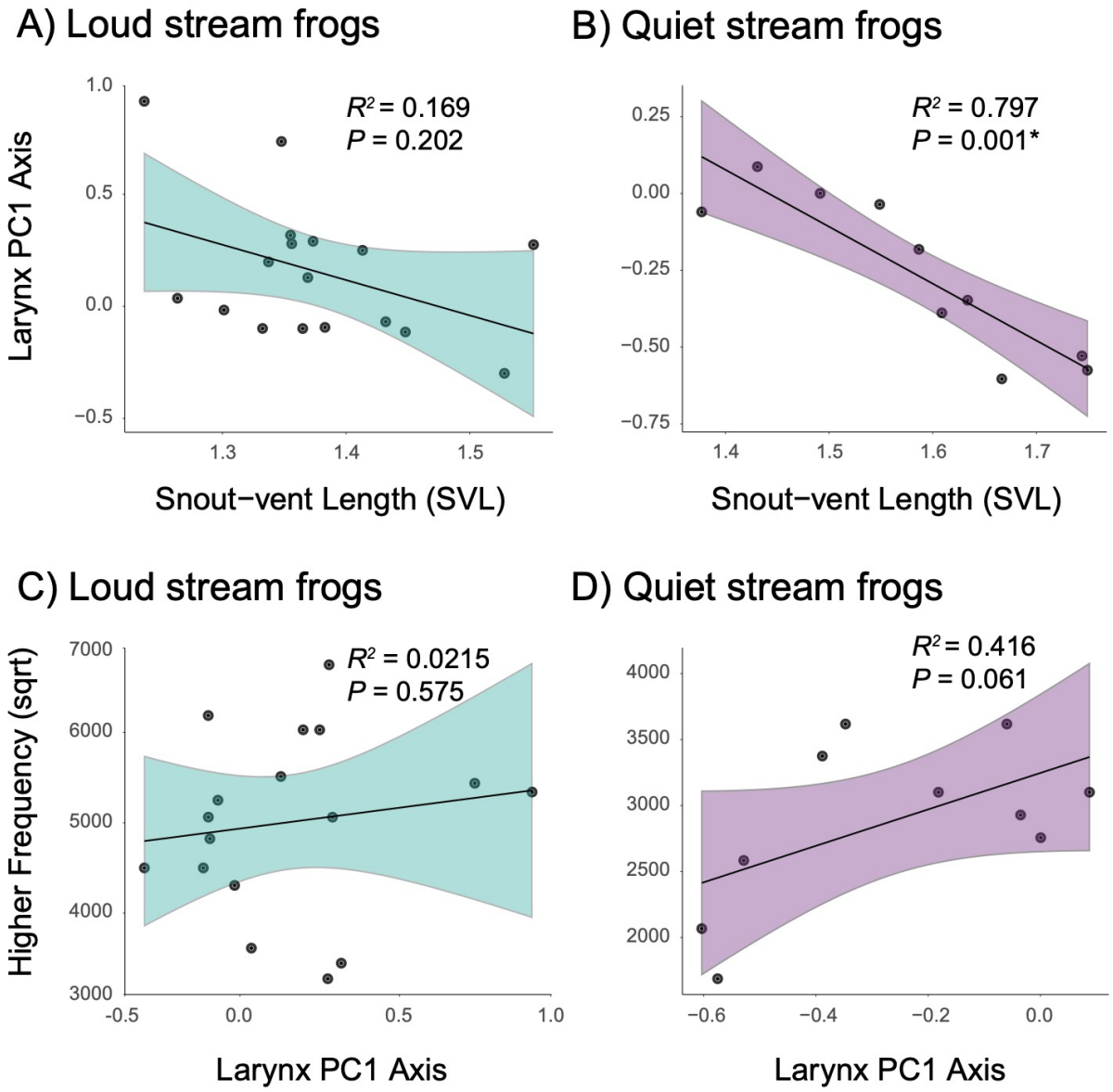

REFERENCES

Alexander, A. M., Su, Y. C., Oliveros, C. H., Olson, K. V., Travers, S. L., & Brown, R. M. (2016). Genomic data reveals potential for hybridization, introgression, and incomplete lineage sorting to confound phylogenetic relationships in an adaptive radiation of narrow-mouth frogs. *Evolution*, *71*(2), 475–488. http://doi.org/10.1111/evo.13133

Alexander, R. P., Fang, G., Rozowsky, J., Snyder, M., & Gerstein, M. B. (2010). Annotating non-coding regions of the genome. *Nature Reviews Genetics*, *11*(8), 559–571. http://doi.org/10.1038/nrg2814

Ali, J. R. (2018). Geological data indicate that the interpretation for the age-calibrated phylogeny for the *Kurixalus*-genus frogs of South, South-East and East Asia (Lv et al., 2018) needs to be rethought. *Molecular Phylogenetics and Evolution*, in press, available online: https://doi.org/10.1016/j.ympev.2018.02.011.

Altig, R. & McDiarmid, R. W. (2006). Descriptions and biological notes on three unusual mantellid tadpoles (Amphibia: Anura: Mantellidae) from southeastern Madagascar. *Proceedings of the Biological Society Washington 119*, 418–425. http://dx.doi.org/10.2988/0006-324X(2006)119%5B418:DABNOT%5D2.0.CO;2

AmphibiaWeb. (2019). Information on amphibian biology and conservation. Retrieved August 8, 2019, from http://www.amphibiaweb.org

Andreone, F. (1993). Two new treefrogs of the genus *Boophis* (Anura: Rhacophoridae) from central-eastern Madagascar. *Bollettino del Museo Regionale di Scienze Naturali di Torino*, *11*, 289–313. No DOI.

Andreone, F. (1994). The amphibians of Ranomafana rain forest, Madagascar - preliminary community analysis and conservation considerations. *Oryx*, *28*, 207–214. http://dx.doi.org/10.1017/S003060530002857X

Andreone, F. (1996). Another new green treefrog, *Boophis anjanaharibeensis* n. sp. (Ranidae: Rhacophorinae), from northeastern Madagascar. *Aqua*, *2*, 25–32. No DOI.

Andreone, F., Cadle, J. E., Cox, N., Glaw, F., Nussbaum, R. A., Raxworthy, C .J., Stuart, S. N., Vallan, D. & Vences, M. (2005). Species review of amphibian extinction risks in Madagascar: conclusions from the Global Amphibian Assessment. *Conservation Biology*, *19*, 1790–1802. http://dx.doi.org/10.1111/j.1523-1739.2005.00249.x

Andreone, F., Vences, M., Guarino, F. M., Glaw, F., & Randrianirina, J. E. (2002). Natural history and larval morphology of *Boophis occidentalis* (Anura: Mantellidae: Boophinae) provide new insights into the phylogeny and adaptive radiation of endemic Malagasy frogs. *Journal of Zoology*, *257*(4), 425–438. http://doi.org/10.1017/S0952836902001036

Andreone, F., Vences, M., Vieites, D. R., Glaw, F. & Meyer, A. (2005). Recurrent ecological adaptations revealed through a molecular analysis of the secretive cophyline frogs of Madagascar. *Molecular Phylogenetics and Evolution, 34*, 315–322. http://dx.doi.org/10.1016/j.ympev.2004.10.013

Aprea, G., Andreone, F., Capriglione, T., Odierna, G. & Vences, M. (2004). Evidence for a remarkable stasis of chromosome evolution in Malagasy treefrogs (*Boophis*: Mantellidae). *Italian Journal of Zoology, Suppl. 2*, 237–243. http://dx.doi.org/10.1080/11250000409356641

Audru, J. C., Bitri, A., Desprats, J. F., Dominique, P., Eucher, G., Hachim, S., Jossot, O., Mathon, C., Nédellec, J. L., Sabourault, P. & Sedan, O. (2010). Major natural hazards in a tropical volcanic island: a review for Mayotte Island, Comoros archipelago, Indian Ocean. *Engineering Geology 114*, 364–381. http://dx.doi.org/10.1016/j.enggeo.2010.05.014

Avise, J. C. (2000). *Phylogeography: the history and formation of species.* Harvard University Press, Cambridge, Massachusetts, U.S.A., 447 pp.

Balakrishnan, C. N., Mukai, M., Gonser, R. A., Wingfield, J. C., London, S. E., Tuttle, E. M., & Clayton, D. F. (2014). Brain transcriptome sequencing and assembly of three songbird model systems for the study of social behavior. *PeerJ*, *2*(34), e396. http://doi.org/10.7717/peerj.396

Bandelt, H., Forster, P. & Röhl, A. (1999). Median-joining networks for inferring intraspecific phylogenies. *Molecular Biology and Evolution, 16*, 37–48. http://dx.doi.org/10.1093/oxfordjournals.molbev.a026036

Bankevich, A., Nurk, S., Antipov, D., Gurevich, A. A., Dvorkin, M., Kulikov, A. S., et al. (2012). SPAdes: A New Genome Assembly Algorithm and Its Applications to Single-Cell Sequencing. *Journal of Computational Biology*, *19*(5), 455–477. http://doi.org/10.1089/cmb.2012.0021

Baugh, A. T., Gridi-Papp, M., & Ryan, M. J. (2017). A laryngeal fibrous mass impacts the acoustics and attractiveness of a multicomponent call in túngara frogs (Physalaemus pustulosus). *Bioacoustics*, 1–13. http://doi.org/10.1080/09524622.2017.1317288

Bejerano, G., Pheasant, M., Makunin, I., Stephen, S., Kent, W. J., Mattick, J. S., & Haussler, D. (2004). Ultraconserved Elements in the Human Genome. *Science*, *304*(5675), 1321–1325. http://doi.org/10.1126/science.1098119

Belmaker, J. & Jetz, W. (2012). Regional Pools and Environmental Controls of Vertebrate Richness. *The American Naturalist*, *179*(4), 512–523. http://doi.org/10.1086/664610

Benelli, G., Donati, E., Romano, D., Ragni, G., Bonsignori, G., Stefanini, C., & Canale, A. (2016). Is bigger better? Male body size affects wing-borne courtship signals and mating success in the olive fruit fly, *Bactrocera oleae* (Diptera: Tephritidae). *Insect Science*, *23*(6), 869–880. http://doi.org/10.1111/1744-7917.12253

Bi, K., Vanderpool, D., Singhal, S., Linderoth, T., Moritz, C., & Good, J. M. (2012). Transcriptome-based exon capture enables highly cost-effective comparative genomic data collection at moderate evolutionary scales. *BMC Genomics*, *13*(1), 403. http://doi.org/10.1186/1471-2164-13-403

Blair, M. E., Sterling, E. J., Dusch, M., Raxworthy, C. J., & Pearson, R. G. (2013). Ecological divergence and speciation between lemur (*Eulemur*) sister species in Madagascar. *Journal of Evolutionary Biology*, *26*(8), 1790–1801. http://doi.org/10.1111/jeb.12179

Bletz, M. C., Rosa, G. M., Andreone, F., Courtois, E. A., Schmeller, D. S., Rabibisoa, N. H. C., Rabemananjara, F. C. E., Raharivololoniaina, L., Vences, M., Weldon, C., Edmonds, D., Raxworthy, C. J., Harris, R. N., Fisher, M. C. & Crottini, A. (2015). Widespread presence of the pathogenic fungus *Batrachochytrium dendrobatidis* in wild amphibian communities in Madagascar. *Scientific Reports*, 5, 8633. http://dx.doi.org/10.1038/srep08633

Blommers-Schlösser, R. (1979). Biosystematics of the Malagasy frogs II. The Genus *Boophis* (Rhacophoridae). *Bijdragen Tot De Dierkunde*, (49), 261–312. No DOI.

Blommers-Schlösser, R. M. A. & Blanc, C. P. (1991). Amphibiens (première partie). Paris. No DOI.

Boeckle, M., Preininger, D., & Hödl, W. (2009). Communication in noisy environments I: acoustic signals of *Staurois latopalmatus* Boulenger 1887. *Herpetologica*, *65*(2), 154–165. http://doi.org/10.1655/07-071R1.1

Bouckaert, R., Heled, J., Kühnert, D., Vaughan, T., Wu, C. H., Xie, D., Suchard, M. A., Rambaut, A., & Drummond, A. J. (2014). BEAST 2: A Software Platform for Bayesian Evolutionary Analysis. *PLoS Computational Biology 10*, e1003537. http://dx.doi.org/10.1371/journal.pcbi.1003537

Boul, K. E., Funk, W. C., Darst, C. R., Cannatella, D. C., & Ryan, M. J. (2007). Sexual selection drives speciation in an Amazonian frog. *Proceedings of the Royal Society B*, *274*(1608), 399–406. http://doi.org/10.1098/rspb.2006.3736

Boumans, L., Vieites, D. R., Glaw, F., & Vences, M. (2007). Geographical patterns of deep mitochondrial differentiation in widespread Malagasy reptiles. *Molecular Phylogenetics and Evolution*, *45*(3), 822–839. http://doi.org/10.1016/j.ympev.2007.05.028

Bowling, D. L., Garcia, M., Dunn, J. C., Ruprecht, R., Stewart, A., Frommolt, K. H., & Fitch, W. T. (2017). Body size and vocalization in primates and carnivores. *Scientific Reports*, *7*(1), 41070. http://doi.org/10.1038/srep41070

Bragg, J. G., Potter, S., Bi, K., & Moritz, C. (2016). Exon capture phylogenomics: efficacy across scales of divergence. *Molecular Ecology Resources*, *16*(5), 1059–1068. http://doi.org/10.1111/1755-0998.12449

Brandley, M. C., Bragg, J. G., Singhal, S., Chapple, D. G., Jennings, C. K., Lemmon, A. R., et al. (2015). Evaluating the performance of anchored hybrid enrichment at the tips of the tree of life: a phylogenetic analysis of Australian *Eugongylus* group scincid lizards. *BMC Evolutionary Biology*, *15(62),* 1–14. http://doi.org/10.1186/s12862-015-0318-0

Brenowitz, E. A. (1982). Long-range communication of species identity by song in the Red-winged Blackbird. *Behavioral Ecology and Sociobiology*, *10*(1), 29–38. http://dx.doi.org/10.1007/BF00296393

Broad Institute. (2019). Picard Tools. Broad Institute, GitHub repository. Accessed on February 20, 2019 from http://broadinstitute.github.io/picard/

Brown, J. L., Cameron, A., Yoder, A. D., & Vences, M. (2014). A necessarily complex model to explain the biogeography of the amphibians and reptiles of Madagascar. *Nature Communications*, *5*(1), 5046. http://doi.org/10.1038/ncomms6046

Brown, J. L., Sillero, N., Glaw, F., Bora, P., Vieites, D. R., & Vences, M. (2016). Spatial biodiversity patterns of Madagascar's amphibians and reptiles. *PLoS ONE*, *11*(1), e0144076. http://doi.org/10.1371/journal.pone.0144076

Brown, W. L. & Wilson, E. O. (1956). Character displacement. *Systematic Zoology*, *5*(2), 49-64. http://dx.doi.org/10.2307/2411924

Brumm, H. (2004). The impact of environmental noise on song amplitude in a territorial bird. *Journal of Animal Ecology*, *73*(3), 434–440. http://doi.org/10.1111/j.0021-8790.2004.00814.x

Brumm, H., Voss, K., Köllmer, I., & Todt, D. (2004). Acoustic communication in noise: regulation of call characteristics in a New World monkey. *Journal of Experimental Biology*, *207*(3), 443–448. http://doi.org/10.1242/jeb.00768

Burnham, K. P. & Anderson, D. R. (1998). Model selection and multimodel inference: a practical information-theoretic approach. New York: Springer.

Bushnell, B., Rood, J., & Singer, E. (2017). BBMerge – Accurate paired shotgun read merging via overlap. *PLoS ONE*, *12*(10), e0185056–15. http://doi.org/10.1371/journal.pone.0185056

Butlin, R. (1987). Speciation by reinforcement. *Trends in Ecology & Evolution*, *2*, 8–13. http://dx.doi.org/10.1016/0169-5347(87)90193-5

Cadle, J. E. (2003). *Boophis*. *In:* Goodman, S.M. & Benstead, J.P. (Eds.), *The Natural History of Madagascar*. University of Chicago Press, Chicago, Illinois, U.S.A., pp. 916–919.

Candolin, U. (2003). The use of multiple cues in mate choice. *Biological Reviews*, *78*(4), 575–595. http://doi.org/10.1017/S1464793103006158

Cannatella, D. C., Hillis, D. M., Chippindale, P. T., Weigt, L., Rand, A. S., & Ryan, M. J. (1998). Phylogeny of frogs of the *Physalaemus pustulosus* species group, with an examination of data incongruence. *Systematic Biology*, *47*(2), 311–335. http://doi.org/10.1080/106351598260932

Capella-Gutierrez, S., Silla-Martinez, J. M., & Gabaldon, T. (2009). trimAl: a tool for automated alignment trimming in large-scale phylogenetic analyses. *Bioinformatics*, *25*(15), 1972–1973. http://doi.org/10.1093/bioinformatics/btp348

Cardoso, G. C. & Atwell, J. W. (2011). On the relation between loudness and the increased song frequency of urban birds. *Animal Behaviour*, *82*(4), 831–836. http://doi.org/10.1016/j.anbehav.2011.07.018

Cariou, M., Duret, L., & Charlat, S. (2013). Is RAD-seq suitable for phylogenetic inference? An in silico assessment and optimization. *Ecology and Evolution*, *3*(4), 846–852. http://doi.org/10.1002/ece3.512

Charif, D. & Lobry, J. R. (2007). SeqinR 1.0-2: A Contributed Package to the R Project for Statistical Computing Devoted to Biological Sequences Retrieval and Analysis. In *Structural Approaches to Sequence Evolution* (Vol. 3, pp. 207–232). Berlin, Heidelberg: Springer, Berlin, Heidelberg. http://doi.org/10.1007/978-3-540-35306-5_10

Charlton, B. D., Ellis, W. A. H., McKinnon, A. J., Cowin, G. J., Brumm, J., Nilsson, K., & Fitch, W. T. (2011). Cues to body size in the formant spacing of male koala (Phascolarctos cinereus) bellows: honesty in an exaggerated trait. *Journal of Experimental Biology*, *214*(20), 3414–3422. http://doi.org/10.1242/jeb.061358

Chek, A. A., Bogart, J. P., & Lougheed, S. C. (2003). Mating signal partitioning in multi-species assemblages: a null model test using frogs. *Ecology Letters*, *6*(3), 235–247. http://doi.org/10.1046/j.1461-0248.2003.00420.x

Chen, M. Y., Liang, D., & Zhang, P. (2017a). Phylogenomic Resolution of the Phylogeny of Laurasiatherian Mammals: Exploring Phylogenetic Signals within Coding and Noncoding Sequences. *Genome Biology and Evolution*, *9*(8), 1998–2012. http://doi.org/10.1093/gbe/evx147

Chen, S., Huang, T., Zhou, Y., Han, Y., Xu, M., & Gu, J. (2017b). AfterQC: automatic filtering, trimming, error removing and quality control for fastq data. *BMC Bioinformatics*, (18:80), 92–175. http://doi.org/10.1186/s12859-017-1469-3

Chen, S., Zhou, Y., Chen, Y., & Gu, J. (2018). fastp: an ultra-fast all-in-one FASTQ preprocessor. *bioRxiv*, 1–12. http://doi.org/10.1101/274100

Ciezarek, A. G., Osborne, O. G., Shipley, O. N., Brooks, E. J., Tracey, S. R., McAllister, J. D., et al. (2019). Phylotranscriptomic Insights into the Diversification of Endothermic *Thunnus* Tunas. *Molecular Biology and Evolution*, *36*(1), 84–96. http://doi.org/10.1093/molbev/msy198

Cocroft, R. B. & Ryan, M. J. (1995). Patterns of advertisement call evolution in toads and chorus frogs. *Animal Behaviour*, *49*(2), 283–303. http://doi.org/10.1006/anbe.1995.0043
Colwell, R. K. & Lees, D. C. (2000). The mid-domain effect: geometric constraints on the geography of species richness. *Trends in Ecology and Evolution, 15*, 70–76. http://dx.doi.org/10.1016/S0169-5347(99)01767-X
Cope, E. D. (1868). An Examination of the Reptilia and Batrachia Obtained by the Orton Expedition to Equador and the Upper Amazon, with Notes on Other Species. *Proceedings of the Academy of Natural Sciences of Philadelphia*, *20*, 96–140. http://doi.org/10.2307/4059850
Copetti, D., Búrquez, A., Bustamante, E., Charboneau, J. L. M., Childs, K. L., Eguiarte, L. E., et al. (2017). Extensive gene tree discordance and hemiplasy shaped the genomes of North American columnar cacti. *Proceedings of the National Academy of Sciences*, *114*(45), 12003–12008. http://doi.org/10.1073/pnas.1706367114
Coyne, J. A. & Orr, H. A. (2004). *Speciation.* Sinaeur Associates, Inc., Sunderland, Massachusetts, U.S.A., 545 pp.
Crawford, N. G., Faircloth, B. C., McCormack, J. E., Brumfield, R. T., Winker, K., & Glenn, T. C. (2012). More than 1000 ultraconserved elements provide evidence that turtles are the sister group of archosaurs. *Biology Letters*, *8*(5), 783–786. http://doi.org/10.1098/rsbl.2012.0331
Crottini, A., Madsen, O., Poux, C., Strauß, A., Vieites, D. R. & Vences, M. (2012). Vertebrate time-tree elucidates the biogeographic pattern of a major biotic change around the K–T boundary in Madagascar. *Proceedings of the National Academy of Sciences*, *109*, 5358–5363. http://dx.doi.org/10.1073/pnas.1112487109
Daniel, J. C. & Blumstein, D. T. (1998). A test of the acoustic adaptation hypothesis in four species of marmots. *Animal Behaviour*, *56*(6), 1517–1528. http://doi.org/10.1006/anbe.1998.0929
Dayrat, B. (2005). Towards integrative taxonomy. *Biological Journal of the Linnaean Society*, *85*, 407–415. http://dx.doi.org/10.1111/j.1095-8312.2005.00503.x
Davies, T. J., Kraft, N. J. B., Salamin, N., & Wolkovich, E. M. (2012). Incompletely resolved phylogenetic trees inflate estimates of phylogenetic conservatism. *Ecology*, *93*(2), 242–247. http://doi.org/10.1890/11-1360.1
Davies, W. I. L., Turton, M., Peirson, S. N., Follett, B. K., Halford, S., Garcia-Fernandez, J. M., et al. (2011). Vertebrate ancient opsin photopigment spectra and the avian photoperiodic response. *Biology Letters*, *8*(2), rsbl20110864–294. http://doi.org/10.1098/rsbl.2011.0864
D'Cruze, N. C., Henson, D., Olsson, A. & Emmett, D. A. (2009). The importance of herpetological survey work in conserving Malagasy biodiversity: Are we doing enough? *Herpetological Review*, *40*, 19–25. No DOI.
de Queiroz, K. (1998). The general lineage concept of species, species criteria, and the process of speciation: A conceptual unification and terminological recommendations. *In:* Howard, D. J. & Berlocher, S. H. (Eds.), *Endless Forms: Species and Speciation*. Oxford University Press, Oxford, U.K., pp. 57–75.
de Queiroz, K. (2005). Ernst Mayr and the modern concept of species. *Proceedings of the National Academy of Sciences*, *102*, 6600–6607. http://dx.doi.org/10.1073/pnas.0502030102
de Queiroz, K. (2007). Species concepts and species delimitation. *Systematic Biology, 56*, 879–886. http://dx.doi.org/10.1080/10635150701701083

Degnan, J. H., & Rosenberg, N. A. (2009). Gene tree discordance, phylogenetic inference and the multispecies coalescent. *Trends in Ecology & Evolution*, *24*(6), 332–340. http://doi.org/10.1016/j.tree.2009.01.009

Dehling, J.M. (2012). An African glass frog: a new *Hyperolius* species (Anura: Hyperoliidae) from Nyungwe National Park, southern Rwanda. *Zootaxa 3391*, 52–64. No DOI.

Derryberry, E. P., Seddon, N., Derryberry, G. E., Claramunt, S., Seeholzer, G. F., Brumfield, R. T., & Tobias, J. A. (2018). Ecological drivers of song evolution in birds: Disentangling the effects of habitat and morphology. *Ecology and Evolution*, *8*(3), 1890–1905. http://doi.org/10.1002/ece3.3760

Donoghue, P. C. J. & Ackerly, D. D. (1996). Phylogenetic uncertainties and sensitivity analyses in comparative biology. *Philosophical Transactions Biological Sciences*, *351*(1345), 1241–1249. No DOI.

Dool, S. E., Puechmaille, S. J., Foley, N. M., Allegrini, B., Bastian, A., Mutumi, G. L., et al. (2016). Nuclear introns outperform mitochondrial DNA in inter-specific phylogenetic reconstruction: Lessons from horseshoe bats (Rhinolophidae: Chiroptera). *Molecular Phylogenetics and Evolution*, *97*, 196–212. http://doi.org/10.1016/j.ympev.2016.01.003

Drummond, A. J., Suchard, M. A., Xie, D., & Rambaut, A. (2012). Bayesian phylogenetics with BEAUti and the BEAST 1.7. *Molecular Biology and Evolution 29*, 1969–1973. http://dx.doi.org/10.1093/molbev/mss075

Dudley, R. & Rand, A. S. (1991). Sound Production and Vocal Sac Inflation in the Tungara Frog, *Physalaemus pustulosus* (Leptodactylidae). *Copeia*, *1991*(2), 460. http://doi.org/10.2307/1446594

Duellman, W. E. & Pyles, R. A. (1983). Acoustic resource partitioning in anuran communities. *Copeia*, *1983*(3), 639. http://doi.org/10.2307/1444328

Duellman, W. E. & Trueb, L. (1994). *Biology of Amphibians.* Johns Hopkins University Press, London, U.K., 670 pp.

Endler, J. A. (1992). Signals, signal conditions, and the direction of evolution. *The American Naturalist*, *139*, S125–S153. http://doi.org/10.1086/285308

Erdtmann, L. K. & Lima, A. P. (2013). Environmental effects on anuran call design: what we know and what we need to know. *Ethology Ecology & Evolution*, *25*(1), 1–11. http://doi.org/10.1080/03949370.2012.744356

Esselstyn, J. A., Garcia, H. J., Saulog, M. G., & Heaney, L. R. (2008). A new species of *Desmalopex* (Pteropodidae) from the Philippines, with a phylogenetic analysis of the Pteropodini. *Journal of Mammalogy*, *89*, 815–825. http://dx.doi.org/10.1644/07-MAMM-A-285.1

Everson, K. M., Soarimalala, V., Goodman, S. M., & Olson, L. E. (2016). Multiple Loci and Complete Taxonomic Sampling Resolve the Phylogeny and Biogeographic History of Tenrecs (Mammalia: Tenrecidae) and Reveal Higher Speciation Rates in Madagascar's Humid Forests. *Systematic Biology*, *65*(5), 890–909. http://doi.org/10.1093/sysbio/syw034

Ey, E. & Fischer, J. (2009). The “acoustic adaptation hypothesis"—a review of the evidence from birds, anurans and mammals. *Bioacoustics*, *19*(1-2), 21–48. http://doi.org/10.1080/09524622.2009.9753613

Faircloth, B. C., Branstetter, M. G., White, N. D., & Brady, S. G. (2014). Target enrichment of ultraconserved elements from arthropods provides a genomic perspective on relationships among Hymenoptera. *Molecular Ecology Resources*, *15*(3), 489–501. http://doi.org/10.1111/1755-0998.12328

Faircloth, B. C., McCormack, J. E., Crawford, N. G., Harvey, M. G., Brumfield, R. T. & Glenn, T. C. (2012). Ultraconserved elements anchor thousands of genetic markers spanning multiple evolutionary timescales. *Systematic Biology*, *61*(5), 717–726. http://doi.org/10.1093/sysbio/sys004

Feng, A. S., Narins, P. M., Xu, C. H., Lin, W. Y., Yu, Z. L., Qiu, Q., et al. (2006). Ultrasonic communication in frogs. *Nature*, *440*(7082), 333–336. http://doi.org/10.1038/nature04416

Feng, Y. J., Blackburn, D. C., Liang, D., Hillis, D. M., Wake, D. B., Cannatella, D. C., & Zhang, P. (2017). Phylogenomics reveals rapid, simultaneous diversification of three major clades of Gondwanan frogs at the Cretaceous–Paleogene boundary. *Proceedings of the National Academy of Sciences*, *114*(29), E5864–E5870. http://doi.org/10.1073/pnas.1704632114

Fitch, W. T. (1998). Vocal tract length and formant frequency dispersion correlate with body size in rhesus macaques. *The Journal of the Acoustical Society of America*, *102*(2), 1213–1222. http://doi.org/10.1121/1.421048

FitzJohn, R.G. (2012). Diversitree: comparative phylogenetic analyses of diversification in R. *Methods in Ecology and Evolution 3*, 1084–1092. http://dx.doi.org/10.1111/j.2041-210X.2012.00234.x

Folie, A. (2012). Early Eocene frogs from Vastan Lignite Mine, Gujarat, India. *Acta Palaeontologica Polonica*. http://doi.org/10.4202/app.2011.0063

Folie, A., Rana, R. S., Rose, K. D., Sahni, A., Kumar, K., Singh, L. & Smith, T., (2013). Early Eocene frogs from Vastan Lignite Mine, Gujarat, India. *Acta Palaeontologica Polonica 58*, 511–524. http://dx.doi.org/10.4202/app.2011.0063

Frost, D. R., Grant, T., Faivovich, J., Baina, R. H., Haas, A., Haddad, C. F. B., de Sá, R. O., Channing, A., Wilkinson, M., Donnellan, S. C., Raxworthy, C. J., Campbell, J. A., Blotto, B. L., Moler, P., Drewes, R. C., Nussbaum, R. A., Lynch, J. D., Green, D. M. & Wheeler, W. C., (2006). The amphibian tree of life. *Bulletin of the American Museum of Natural History 297*, 1–291. http://dx.doi.org/10.1206/0003-0090(2006)297%5B0001:TATOL%5D2.0.CO;2

Garcia, M., Herbst, C. T., Bowling, D. L., Dunn, J. C., & Fitch, W. T. (2017). Acoustic allometry revisited: morphological determinants of fundamental frequency in primate vocal production. *Scientific Reports*, *7*(1), 10450. http://doi.org/10.1038/s41598-017-11000-x

Gavryushkina, A., Welch, D., Stadler, T., & Drummond, A. J. (2014). Bayesian inference of sampled ancestor trees for epidemiology and fossil calibration. *PLOS Computational Biology*, *10*(12), e1003919. http://doi.org/10.1371/journal.pcbi.1003919

Gayou, D. C. (1984). Effects of temperature on the mating call of *Hyla versicolor*. *Copeia*, *1984*(3), 733. http://doi.org/10.2307/1445157

Geneious R8. (2015). created by Biomatters. Available from http://www.geneious.com/

Gentekaki, E., Kolisko, M., Gong, Y., & Lynn, D. (2017). Phylogenomics solves a long-standing evolutionary puzzle in the ciliate world: The subclass Peritrichia is monophyletic. *Molecular Phylogenetics and Evolution*, *106*, 1–5. http://doi.org/10.1016/j.ympev.2016.09.016

Gerhardt, H. C., Tanner, S. D., Corrigan, C. M. & Walton, H. C. (2000). Female preference functions based on call duration in the gray tree frog (*Hyla versicolor*). *Behavioral Ecology*, *11*, 663–669. http://dx.doi.org/10.1093/beheco/11.6.663

Gignac, P. M., Kley, N. J., Clarke, J. A., Colbert, M. W., Morhardt, A. C., Cerio, D., et al. (2016). Diffusible iodine-based contrast-enhanced computed tomography (diceCT): an emerging tool for rapid, high-resolution, 3-D imaging of metazoan soft tissues. *Journal of Anatomy*, *228*(6), 889–909. http://doi.org/10.1111/joa.12449

Gingras, B., Boeckle, M., Herbst, C. T., & Fitch, W. T. (2012). Call acoustics reflect body size across four clades of anurans. *Journal of Zoology*, *289*(2), 143–150. http://doi.org/10.1111/j.1469-7998.2012.00973.x

Glaw, F., Hawlitschek, O., Glaw, K., & Vences, M. (2019). Integrative evidence confirms new endemic island frogs and transmarine dispersal of amphibians between Madagascar and Mayotte (Comoros archipelago), *Science of Nature, 108*, 1–14. http://doi.org/10.1007/s00114-019-1618-9

Glaw, F., Hoegg, S., & Vences, M. (2006). Discovery of a new basal relict lineage of Madagascan frogs and its implications for mantellid evolution. *Zootaxa 1334*, 27–43. No DOI.

Glaw, F., Koehler, J., De la Riva, I., Vieites, D. R., & Vences, M. (2010). Integrative taxonomy of Malagasy treefrogs: combination of molecular genetics, bioacoustics and comparative morphology reveals twelve additional species of *Boophis*. *Zootaxa*, *2383*, 1–82. No DOI.

Glaw, F. & Thiesmeier, B. (1993) Bioakustische Differenzierung in der *Boophis luteus*-Gruppe (Anura: Rhacophoridae), mit Beschreibung einer neuen Art und einer neuen Unterart. *Salamandra*, *28*, 258–269. No DOI.

Glaw, F. & Vences, M. (1997). Anuran eye colouration: definitions, variation, taxonomic implications and possible functions. *In:* Böhme, W., Bischoff, W. & Ziegler, T. (Eds.), *Herpetologia Bonnensis*. SEH Proceedings, Bonn, Germany, pp. 125–138.

Glaw, F. & Vences, M. (2002). A new cryptic treefrog species of the *Boophis luteus* group from Madagascar: bioacoustic and genetic evidence (Amphibia, Anura, Mantellidae). *Spixiana*, *25*, 173–181. No DOI.

Glaw, F., Vences, M., Andreone, F. & Vallan, D. (2001). Revision of the *Boophis majori* group (Amphibia: Mantellidae) from Madagascar, with descriptions of five new species. *Zoological Journal of the Linnean Society*, *133*, 495–529. http://dx.doi.org/10.1111/j.1096-3642.2001.tb00637.x

Glaw, F. & Vences, M. (2006). Phylogeny and genus-level classification of mantellid frogs (Amphibia, Anura). *Organisms Diversity & Evolution*, *6*(3), 236–253. http://doi.org/10.1016/j.ode.2005.12.001

Glaw, F. & Vences, M. (2007). *A Field Guide to the Amphibians and Reptiles of Madagascar, Third Edition.* Self-published, Köln, Germany, 496 pp.

Glaw, F., Vences, M., & Andreone, F. (2001). Revision of the *Boophis majori* group (Amphibia: Mantellidae) from Madagascar, with descriptions of five new species. *Zoological Journal of the Linnean Society*, *133*, 495–529. http://doi.org/10.1006/zjls.2001.0301

Glaw, F., Vences, M., & Böhme, W. (1998). Systematic revision of the genus *Aglyptodactylus* Boulenger, 1919 (Amphibia: Ranidae), and analysis of its phylogenetic relationships to other Madagascan ranid genera (*Tomopterna*, *Boophis, Mantidactylus*, and *Mantella*). *Journal of Zoological Systematics and Evolutionary Research*, *36*, 17–37. http://doi.org/10.1111/j.1439-0469.1998.tb00775.x

Gnirke, A., Melnikov, A., Maguire, J., Rogov, P., LeProust, E. M., Brockman, W., et al. (2009). Solution hybrid selection with ultra-long oligonucleotides for massively parallel targeted sequencing. *Nature Biotechnology*, *27*(2), 182–189. http://doi.org/10.1038/nbt.1523

Goicoechea, N., De La Riva, I., & Padial, J. M. (2010). Recovering phylogenetic signal from frog mating calls. *Zoologica Scripta*, *39*(2), 141–154. http://doi.org/10.1111/j.1463-6409.2009.00413.x

Goldberg, E. E., Lancaster, L. T., & Ree, R. H. (2011). Phylogenetic inference of reciprocal effects between geographic range evolution and diversification. *Systematic Biology 60*, 451–465. http://dx.doi.org/10.1093/sysbio/syr046

Goodman, S. M. & Benstead, J. P. (2003). *Natural history of Madagascar*. University of Chicago Press, Chicago, Illinois, U.S.A., 1709 pp.

Goodwin, S. E. & Podos, J. (2013). Shift of song frequencies in response to masking tones. *Animal Behaviour*, *85*(2), 435–440. http://doi.org/10.1016/j.anbehav.2012.12.003

Goutte, S., Dubois, A., Howard, S. D., Marquez, R., Rowley, J. J. L., Dehling, J. M., et al. (2016). Environmental constraints and call evolution in torrent-dwelling frogs. *Evolution*, *70*(4), 811–826. http://doi.org/10.1111/evo.12903

Goutte, S., Dubois, A., Howard, S. D., Márquez, R., Rowley, J. J. L., Dehling, J. M., et al. (2018). How the environment shapes animal signals: a test of the acoustic adaptation hypothesis in frogs. *Journal of Evolutionary Biology*, *31*(1), 148–158. http://doi.org/10.1111/jeb.13210

Gray, D. A., & Cade, W. H. (2000). Sexual selection and speciation in field crickets. *Proceedings of the National Academy of Sciences*, *97*(26), 14449–14454. http://doi.org/10.1073/pnas.97.26.14449

Gridi-Papp, M., Rand, A. S., & Ryan, M. J. (2006). Complex call production in the túngara frog. *Nature*, *441*(7089), 38–38. http://doi.org/10.1038/441038a

Grosjean, S., Randrianiaina, R. D., Strauß, A. & Vences, M., (2011). Sand-eating tadpoles in Madagascar: morphology and ecology of the unique larvae of the treefrog *Boophis picturatus*. *Salamandra 47*, 63–76. No DOI.

Guayasamin, J. M., Castroviejo-Fisher, S., Trueb, L., Ayarzagüena, J., Rada, M. & Vilà, C., (2009). Phylogenetic systematics of glassfrogs (Amphibia: Centrolenidae) and their sister taxon *Allophryne ruthveni*. *Zootaxa 2100*, 1–97. No DOI.

Guerra, M. A., Ryan, M. J., & Cannatella, D. C. (2014). Ontogeny of Sexual Dimorphism in the Larynx of the Túngara Frog, *Physalaemus pustulosus*. *Copeia*, *2014*(1), 123–129. http://doi.org/10.1643/CG-13-051

Guibé, J. (1978). Les batraciens de Madagascar. *Bonn Zoological Monographs, 11*, 1–140.

Guo, Y., Long, J., He, J., Li, C. I., Cai, Q., Shu, X. O., et al. (2012). Exome sequencing generates high quality data in non-target regions. *BMC Genomics*, *13*(194), 1–10. http://doi.org/10.1186/1471-2164-13-194

Hahn, C., Bachmann, L., & Chevreux, B. (2013). Reconstructing mitochondrial genomes directly from genomic next-generation sequencing reads--a baiting and iterative mapping approach. *Nucleic Acids Research*, *41*(13), 1–9. http://doi.org/10.1093/nar/gkt371

Hancock-Hanser, B. L., Frey, A., Leslie, M. S., Dutton, P. H., Archer, F. I., & Morin, P. A. (2013). Targeted multiplex next-generation sequencing: advances in techniques of mitochondrial and nuclear DNA sequencing for population genomics. *Molecular Ecology Resources*, *13*(2), 254–268. http://doi.org/10.1111/1755-0998.12059

Harmon, L. J., Weir, J. T., Brock, C. D., Glor, R. E., & Challenger, W. (2008). GEIGER: investigating evolutionary radiations. *Bioinformatics*, *24*(1), 129–131. http://doi.org/10.1093/bioinformatics/btm538

Hauser, M. D. (1993). The Evolution of Nonhuman Primate Vocalizations: Effects of Phylogeny, Body Weight, and Social Context. *The American Naturalist*, *142*(3), 528–542. http://doi.org/10.1086/285553

Hawlitschek, O., Toussaint, E. F., Gehring, P. S., Ratsoavina, F. M., Cole, N., Crottini, A., Nopper, J., Lam, A. W., Vences, M. & Glaw, F. (2017). Gecko phylogeography in the Western Indian Ocean region: the oldest clade of *Ebenavia inunguis* lives on the youngest island. *Journal of Biogeography, 44*, 409–420. http://dx.doi.org/10.1111/jbi.12912

Heath, T. A., Huelsenbeck, J. P., & Stadler, T. (2014). The fossilized birth-death process for coherent calibration of divergence-time estimates. *Proceedings of the National Academy of Sciences*, *111*(29), E2957–E2966. http://doi.org/10.1073/pnas.1319091111

Hedge, J. & Wilson, D. J. (2014). Bacterial phylogenetic reconstruction from whole genomes is robust to recombination but demographic inference is not. *mBio*, *5*(6), e02158. http://doi.org/10.1128/mBio.02158-14

Hedtke, S. M., Morgan, M. J., Cannatella, D. C., & Hillis, D. M. (2013). Targeted enrichment: maximizing orthologous gene comparisons across deep evolutionary time. *PLoS ONE*, *8*(7), e67908. http://doi.org/10.1371/journal.pone.0067908

Heinicke, M. P., Lemmon, A. R., Lemmon, E. M., McGrath, K., & Hedges, S. B. (2018). Phylogenomic support for evolutionary relationships of New World direct-developing frogs (Anura: Terraranae). *Molecular Phylogenetics and Evolution*, *118*, 145–155. http://doi.org/10.1016/j.ympev.2017.09.021

Hijmans, R. J. & van Etten, J. (2012). raster: Geographic data analysis and modeling. *R package version, 2*, p. 15.

Ho, S. Y. & Phillips, M. J. (2009). Accounting for calibration uncertainty in phylogenetic estimation of evolutionary divergence times. *Systematic Biology, 58*, 367–380. http://dx.doi.org/10.1093/sysbio/syp035

Hochkirch, A. & Lemke, I. (2011). Asymmetric mate choice, hybridization, and hybrid fitness in two sympatric grasshopper species. *Behavioral Ecology and Sociobiology*, *65*(8), 1637–1645. http://doi.org/10.1007/s00265-011-1174-6

Hoskin, C. J. & Higgie, M. (2010). Speciation via species interactions: the divergence of mating traits within species. *Ecology Letters*, *13*(4), 409–420. http://doi.org/10.1111/j.1461-0248.2010.01448.x

Hosner, P. A., Braun, E. L., & Kimball, R. T. (2016). Rapid and recent diversification of curassows, guans, and chachalacas (Galliformes: Cracidae) out of Mesoamerica: Phylogeny inferred from mitochondrial, intron, and ultraconserved element sequences. *Molecular Phylogenetics and Evolution*, *102*, 320–330. http://doi.org/10.1016/j.ympev.2016.06.006

Howard, D. J. (1993). Reinforcement: origin, dynamics, and fate of an evolutionary hypothesis. *In:* Harrison, R.G. (Eds.), *Hybrid Zones and the Evolutionary Process.* Oxford University Press, New York, New York, U.S.A., pp. 46–69.

Hödl, W. & Amézquita, A. (2001). Visual signaling in anuran amphibians. In M. J. Ryan (Ed.), *Anuran communication* (pp. 121–141). Washington: Smithsonian Inst. press.

Huang, X. & Madan, A. (1999). CAP3: A DNA sequence assembly program. *Genome Research*, (9), 868–877. http://dx.doi.org/10.1101/gr.9.9.868

Hugall, A. F., O'Hara, T. D., Hunjan, S., Nilsen, R., & Moussalli, A. (2016). An Exon-Capture System for the Entire Class Ophiuroidea. *Molecular Biology and Evolution*, *33*(1), 281–294. http://doi.org/10.1093/molbev/msv216

Hutter, C. R. & Guayasamin, J. M. (2012). A new cryptic species of glassfrog (Centrolenidae: *Nymphargus*) from Reserva Las Gralarias, Ecuador. *Zootaxa,* 3257, 1–21. No DOI.

Hutter, C. R., Guayasamin, J. M., & Wiens, J. J. (2013). Explaining Andean megadiversity: the evolutionary and ecological causes of glassfrog elevational richness patterns. *Ecology Letters*, *16*(9), 1135–1144. http://doi.org/10.1111/ele.12148

Hutter C. R. & Guayasamin J. M. (2015). Cryptic diversity concealed in the Andean cloud forests: two new species of rainfrogs (*Pristimantis*) uncovered by molecular and bioacoustic data. *Neotropical Biodiversity, 1*, 36–59. https://doi.org/10.1080/23766808.2015.1100376

Hutter, C. R., Lambert, S. M., Andriampenomanana, Z. F., Glaw, F., & Vences, M. (2018). Molecular phylogeny and diversification of Malagasy bright-eyed tree frogs (Mantellidae: *Boophis*). *Molecular Phylogenetics and Evolution*. http://doi.org/10.1016/j.ympev.2018.05.027

Hutter, C. R., Lambert, S. M. & Wiens, J. J. (2017). Rapid diversification and time explain amphibian richness at different scales in the Tropical Andes, Earth's most biodiverse hotspot. *American Naturalist, 190*, 828–843. https://doi.org/10.1086/694319

Hutter, C. R., Lambert, S. M., Cobb, K. A., Andriampenomanana, Z. F., & Vences, M. (2015). A new species of bright-eyed treefrog (Mantellidae) from Madagascar, with comments on call evolution and patterns of syntopy in the *Boophis ankaratra* complex. *Zootaxa*, *4034*(3), 531–555. http://doi.org/10.11646/zootaxa.4034.3.6

Hutter, C. R., Escobar-Lasso, S., Rojas-Morales, J. A., Gutiérrez-Cárdenas, P. D. A, Imba, H. & Guayasamin, J. M. (2013). The territoriality, vocalizations and aggressive interactions of the red–spotted glassfrog, *Nymphargus grandisonae*, Cochran and Goin, 1970 (Anura: Centrolenidae). *Journal of Natural History,* 47, 3011–3032. http://dx.doi.org/10.1080/00222933.2013.792961

Irisarri, I., Baurain, D., Brinkmann, H., Delsuc, F., Sire, J. Y., Kupfer, A., et al. (2017). Phylotranscriptomic consolidation of the jawed vertebrate timetree. *Nature Publishing Group*, *22*, 225–9. http://doi.org/10.1038/s41559-017-0240-5

IUCN. (2001). *IUCN Red List Categories and Criteria: Version 3.1.* IUCN, Switzerland and Cambridge, U.K.

Ives, A. R. & Garland, T. J. (2010). Phylogenetic logistic regression for binary dependent variables. *Systematic Biology*, *59*(1), 9–26. http://doi.org/10.1093/sysbio/syp074

Jang, Y. & Gerhardt, H. C. (2006). Divergence in female calling song discrimination between sympatric and allopatric populations of the southern wood cricket *Gryllus fultoni* (Orthoptera: Gryllidae). *Behavioral Ecology and Sociobiology*, *60*(2), 150–158. http://doi.org/10.1007/s00265-005-0151-3

Johnson, B. R., Borowiec, M. L., Chiu, J. C., Lee, E. K., Atallah, J., & Ward, P. S. (2013). Phylogenomics Resolves Evolutionary Relationships among Ants, Bees, and Wasps. *Current Biology*, *23*(20), 2058–2062. http://doi.org/10.1016/j.cub.2013.08.050

Jones, M. R. & Good, J. M. (2016). Targeted capture in evolutionary and ecological genomics. *Molecular Ecology*, *25*(1), 185–202. http://doi.org/10.1111/mec.13304

Kaffenberger, N., Wollenberg, K. C., Köhler, J., Glaw, F., Vieites, D. R., & Vences, M. (2012). Molecular phylogeny and biogeography of Malagasy frogs of the genus *Gephyromantis*. *Molecular Phylogenetics and Evolution*, *62*(1), 555–560. http://doi.org/10.1016/j.ympev.2011.09.023

Kalyaanamoorthy, S., Minh, B. Q., Wong, T. K. F., Haeseler, von, A., & Jermiin, L. S. (2017). ModelFinder: fast model selection for accurate phylogenetic estimates. *Nature Methods*, *14*(6), 587–589. http://doi.org/10.1038/nmeth.4285

Karin, B. R., Gamble, T., & Jackman, T. R. (2019). Optimizing Phylogenomics with Rapidly Evolving Long Exons: Comparison with Anchored Hybrid Enrichment and Ultraconserved Elements. *bioRxiv*, *9*, 672238. http://doi.org/10.1101/672238

Katoh, K. & Standley, D. M. (2013). MAFFT multiple sequence alignment software version 7: improvements in performance and usability. *Molecular Biology and Evolution*, *30*(4), 772–780. http://doi.org/10.1093/molbev/mst010

Katzman, S., Kern, A. D., Bejerano, G., Fewell, G., Fulton, L., Wilson, R. K., et al. (2007). Human Genome Ultraconserved Elements Are Ultraselected. *Science*, *317*(5840), 915–915. http://doi.org/10.1126/science.1142430

Kent, W. J. (2002). BLAT—the BLAST-like alignment tool. *Genome Research*, *12*(4), 656–664. http://doi.org/10.1101/gr.229202

Kime, N. M., Turner, W. R., & Ryan, M. J. (2000). The transmission of advertisement calls in Central American frogs. *Behavioral Ecology*, *11*(1), 71–83. http://doi.org/10.1093/beheco/11.1.71

Kircher, M., & Kelso, J. (2010). High-throughput DNA sequencing – concepts and limitations. *BioEssays*, *32*(6), 524–536. http://doi.org/10.1002/bies.200900181

Kirkpatrick, M. (1996). Good genes and direct selection in the evolution of mating preferences. *Evolution*, *50*(6), 2125. http://doi.org/10.2307/2410684

Kirkpatrick, M. & Barton, N. H. (1997). The strength of indirect selection on female mating preferences. *Proceedings of the National Academy of Sciences*, *94*(4), 1282–1286. http://doi.org/10.1073/pnas.94.4.1282

Kirkpatrick, M. & Ravigné, V. (2002). Speciation by natural and sexual selection: models and experiments. *The American Naturalist*, *159*(S3), S22–S35. http://doi.org/10.1086/338370

Kleinteich, T., & Gorb, S. N. (2015). Frog tongue acts as muscle-powered adhesive tape. *Royal Society Open Science*, *2*(9), 150333. http://doi.org/10.1098/rsos.150333

Knowles, L. L. (2009). Estimating species trees: methods of phylogenetic analysis when there is incongruence across genes. *Systematic Biology*, *58*(5), 463–467. http://doi.org/10.1093/sysbio/syp061

Knowles, L. L. & Carstens, B. (2007). Delimiting Species without Monophyletic Gene Trees. *Systematic Biology*, *56*(6), 887–895. http://doi.org/10.1080/10635150701701091

Knowles, L. L., Huang, H., Sukumaran, J., & Smith, S. A. (2018). A matter of phylogenetic scale: Distinguishing incomplete lineage sorting from lateral gene transfer as the cause of gene tree discord in recent versus deep diversification histories. *American Journal of Botany*, *105*(3), 376–384. http://doi.org/10.1002/ajb2.1064@10.1002

Köhler, J., Glaw, F. & Vences, M. (2007). A new green treefrog, genus *Boophis* Tschudi 1838 (Anura Mantellidae), from arid western Madagascar: phylogenetic relationships and biogeographic implications. *Tropical Zoology*, *20*, 215–227. No DOI.

Köhler, J., Glaw, F. & Vences, M. (2008). Two additional treefrogs of the *Boophis ulftunni* species group (Anura: Mantellidae) discovered in rainforests of northern and south-eastern Madagascar. *Zootaxa*, *1814*, 37–48. No DOI.

Köhler, J., Vieites, D. R., Bonett, R. M., Hita García, F., Glaw, F., Steinke, D. & Vences, M. (2005). Boost in species discoveries in a highly endangered vertebrate group: new amphibians and global conservation. *BioScience*, *55*, 693–696. http://dx.doi.org/10.1641/0006-3568(2005)055

Kozak, K. H. & Wiens, J.J. (2010). Niche conservatism drives elevational diversity patterns in Appalachian salamanders. *American Naturalist, 176*, 40–54. https://doi.org/10.1086/653031

Kremen, C., Cameron, A., Moilanen, A., Phillips, S. J., Thomas, C. D., Beentje, H., Dransfield, J., Fisher, B. L., Glaw, F., Good, T. C., Harper, G. J., Hijmans, R. J., Lees, D. C., Louis Jr., E., Nussbaum, R. A., Raxworthy, C. J., Razafimpahanana, A., Schatz, G. E., Vences, M., Vieites, D. R. & Zjhra, M. L. (2008) Aligning conservation priorities across taxa in Madagascar with high-resolution planning tools. *Science*, 320, 222–226. http://dx.doi.org/10.1126/science.1155193

Kubatko, L. S. & Degnan, J. H. (2007). Inconsistency of phylogenetic estimates from concatenated data under coalescence. *Systematic Biology*, *56*(1), 17–24. http://doi.org/10.1080/10635150601146041

Kurabayashi, A., Sumida, M., Yonekawa, H., Glaw, F., Vences, M., & Hasegawa, M. (2008). Phylogeny, Recombination, and Mechanisms of Stepwise Mitochondrial Genome Reorganization in Mantellid Frogs from Madagascar. *Molecular Biology and Evolution*, *25*(5), 874–891. http://doi.org/10.1093/molbev/msn031

Lagman, D., Ocampo Daza, D., Widmark, J., Abalo, X. M., Sundström, G., & Larhammar, D. (2013). The vertebrate ancestral repertoire of visual opsins, transducin alpha subunits and oxytocin/vasopressin receptors was established by duplication of their shared genomic region in the two rounds of early vertebrate genome duplications. *BMC Evolutionary Biology*, *13*(1), 238. http://doi.org/10.1186/1471-2148-13-238

Laloy, F., Rage, J. C., Evans, S. E., Boistel, R., Lenoir, N., & Laurin, M. (2013). A re-interpretation of the eocene anuran thaumastosaurus based on MicroCT examination of a "mummified" specimen. *PLoS ONE*, *8*(9), e74874. http://doi.org/10.1371/journal.pone.0074874

Lambert, S. M., Geneva, A. J., Mahler, D. L. & Glor, R. E. (2013). Using genomic data to revisit an early example of reproductive character displacement in Haitian *Anolis* lizards. *Molecular Ecology*, *22*, 3981–3995. http://dx.doi.org/10.1111/mec.12292

Lampe, U., Reinhold, K., & Schmoll, T. (2014). How grasshoppers respond to road noise: developmental plasticity and population differentiation in acoustic signalling. *Functional Ecology*, *28*(3), 660–668. http://doi.org/10.1111/1365-2435.12215

Landis, M. J., Matzke, N. J., Moore, B. R., & Huelsenbeck, J. P. (2013). Bayesian analysis of biogeography when the number of areas is large. *Systematic Biology, 62*, 789–804. https://doi.org/10.1093/sysbio/syt040

Lanfear, R., Frandsen, P. B., Wright, A. M., Senfeld, T. & Calcott, B. (2017). PartitionFinder 2: New methods for selecting partitioned models of evolution for molecular and morphological phylogenetic analyses. *Molecular Biology and Evolution, 34*, 772–773. https://doi.org/10.1093/molbev/msw260

Lanier, H. C. & Knowles, L. L. (2012). Is Recombination a Problem for Species-Tree Analyses? *Systematic Biology*, *61*(4), 691–701. http://doi.org/10.1093/sysbio/syr128

Larget, B. R., Kotha, S. K., Dewey, C. N., & Ané, C. (2010). BUCKy: Gene tree/species tree reconciliation with Bayesian concordance analysis. *Bioinformatics*, *26*(22), 2910–2911. http://doi.org/10.1093/bioinformatics/btq539

Lawrence, M., Huber, W., Pagès, H., Aboyoun, P., Carlson, M., Gentleman, R., et al. (2013). Software for Computing and Annotating Genomic Ranges. *PLOS Computational Biology*, *9*(8), e1003118. http://doi.org/10.1371/journal.pcbi.1003118

Leibold, M. A., Holyoak, M., Mouquet, N., Amarasekare, P., Chase, J. M., Hoopes, M. F., et al. (2004). The metacommunity concept: a framework for multi-scale community ecology. *Ecology Letters*, *7*(7), 601–613. http://doi.org/10.1111/j.1461-0248.2004.00608.x

Lemmon, A. R., Emme, S. A., & Lemmon, E. M. (2012). Anchored Hybrid Enrichment for Massively High-Throughput Phylogenomics. *Systematic Biology*, *61*(5), 727–744. http://doi.org/10.1093/sysbio/sys049

Li, H. & Durbin, R. (2010). Fast and accurate long-read alignment with Burrows–Wheeler transform. *Bioinformatics*, *26*(5), 589–595. http://doi.org/10.1093/bioinformatics/btp698

Li, H., Handsaker, B., Wysoker, A., Fennell, T., Ruan, J., Homer, N., et al. (2009). The Sequence Alignment/Map format and SAMtools. *Bioinformatics*, *25*(16), 2078–2079. http://doi.org/10.1093/bioinformatics/btp352

Li, J. T., Li, Y., Klaus, S., Rao, D. Q., Hillis, D. M., & Zhang, Y. P. (2013). Diversification of rhacophorid frogs provides evidence for accelerated faunal exchange between India and Eurasia during the Oligocene. *Proceedings of the National Academy of Sciences U.S.A., 110*, 3441–3446. https://doi.org/10.1073/pnas.1300881110

Li, J., He, Q., Hua, X., Zhou, J., Xu, H., Chen, J. & Fu, C. (2009). Climate and history explain the species richness peak at mid-elevation for *Schizothorax* fishes (Cypriniformes: Cyprinidae) distributed in the Tibetan Plateau and its adjacent regions. *Global Ecology and Biogeography, 18*, 264–272. https://doi.org/10.1111/j.1466-8238.2008.00430.x

Li, W. & Godzik, A. (2006). Cd-hit: a fast program for clustering and comparing large sets of protein or nucleotide sequences. *Bioinformatics*, *22*(13), 1658–1659. http://doi.org/10.1093/bioinformatics/btl158

Linkem, C. W., Minin, V. N., & Leaché, A. D. (2016). Detecting the Anomaly Zone in Species Trees and Evidence for a Misleading Signal in Higher-Level Skink Phylogeny (Squamata: Scincidae). *Systematic Biology*, *65*(3), 465–477. http://doi.org/10.1093/sysbio/syw001

Linsenmair, K. E. & Glos, J. (2005). Description of the tadpoles of *Boophis doulioti* and *B. xerophilus* from Western Madagascar with notes on larval life history and breeding ecology. *Amphibia-Reptilia*, *26*(4), 459–466. http://doi.org/10.1163/156853805774806287

Liu, L., Yu, L., & Edwards, S. V. (2010). A maximum pseudo-likelihood approach for estimating species trees under the coalescent model. *BMC Evolutionary Biology*, *10*(1), 302. http://doi.org/10.1186/1471-2148-10-302

Losos, J. B. (1985). An experimental demonstration of the species-recognition role of *Anolis* dewlap color. *Copeia*, *1985*(4), 905. http://doi.org/10.2307/1445240

Losos, J. B. (2000). Ecological character displacement and the study of adaptation. *Proceedings of the National Academy of Sciences*, *97*(11), 5693–5695. http://doi.org/10.1073/pnas.97.11.5693

Luther, D. (2009). The influence of the acoustic community on songs of birds in a neotropical rain forest. *Behavioral Ecology*, *20*(4), 864–871. http://doi.org/10.1093/beheco/arp074

Lv, Y. Y., He, K., Klaus, S., Brown, R. M., & Li, J. T. (2018). A comprehensive phylogeny of the genus *Kurixalus* (Rhacophoridae, Anura) sheds light on the geographical range evolution of frilled swamp treefrogs. *Molecular Phylogenetics and Evolution, 121*, 224–232. https://doi.org/10.1016/j.ympev.2017.09.019

Maan, M. E., Hofker, K. D., van Alphen, J. J. M., & Seehausen, O. (2006). Sensory drive in cichlid speciation. *The American Naturalist*, *167*(6), 947–954. http://doi.org/10.1086/503532

Mai, U., & Mirarab, S. (2018). TreeShrink: fast and accurate detection of outlier long branches in collections of phylogenetic trees. *BMC Genomics*, *19*(5), 272. http://doi.org/10.1186/s12864-018-4620-2

Manthey, J. D., Campillo, L. C., Burns, K. J., & Moyle, R. G. (2016). Comparison of Target-Capture and Restriction-Site Associated DNA Sequencing for Phylogenomics: A Test in Cardinalid Tanagers (Aves, Genus: *Piranga*). *Systematic Biology*, *65*(4), 640–650. http://doi.org/10.1093/sysbio/syw005

Marten, K., & Marler, P. (1977). Sound transmission and its significance for animal vocalization. *Behavioral Ecology and Sociobiology*, *2*(3), 271–290. http://doi.org/10.1007/BF00299740

Martin, W. F. & Gans, C. (1972). Muscular control of the vocal tract during release signaling in the toad *Bufo valliceps*. *Journal of Morphology*, *137*(1), 1–27. http://doi.org/10.1002/jmor.1051370102

Martins, E. P. & Hansen, T. F. (1997). Phylogenies and the comparative method: a general approach to incorporating phylogenetic information into the analysis of interspecific data. *The American Naturalist*, *149*(4), 646–667. http://doi.org/10.2307/2463542

Matzke, N. J. (2014). Model Selection in Historical Biogeography Reveals that Founder-Event Speciation Is a Crucial Process in Island Clades. *Systematic Biology*, *63*(6), 951–970. http://doi.org/10.1093/sysbio/syu056

Mayer, C., Sann, M., Donath, A., Meixner, M., Podsiadlowski, L., Peters, R. S., et al. (2016). BaitFisher: A Software Package for Multispecies Target DNA Enrichment Probe Design. *Molecular Biology and Evolution*, *33*(7), 1875–1886. http://doi.org/10.1093/molbev/msw056

McClelland, B. E., Wilczynski, W., & Ryan, M. J. (1996). Correlations between call characteristics and morphology in male cricket frogs (*Acris crepitans*). *Journal of Experimental Biology*, *199*(Pt. 9), 1907–1919.

McClelland, B. E., Wilczynski, W., & Ryan, M. J. (1998). Intraspecific variation in laryngeal and ear morphology in male cricket frogs (*Acris crepitans*). *Biological Journal of the Linnean Society*, *63*, 51–67. http://doi.org/10.1111/j.1095-8312.1998.tb01638.x

McCormack, J. E., Faircloth, B. C., Crawford, N. G., Gowaty, P. A., Brumfield, R. T., & Glenn, T. C. (2012). Ultraconserved elements are novel phylogenomic markers that resolve placental mammal phylogeny when combined with species-tree analysis. *Genome Research*, *22*(4), 746–754. http://doi.org/10.1101/gr.125864.111

McKenna, A., Hanna, M., Banks, E., Sivachenko, A., Cibulskis, K., Kernytsky, A., et al. (2010). The Genome Analysis Toolkit: a MapReduce framework for analyzing next-generation DNA sequencing data. *Genome Research*, *20*(9), 1297–1303. http://doi.org/10.1101/gr.107524.110

Metscher, B. D. (2009). MicroCT for developmental biology: A versatile tool for high-contrast 3D imaging at histological resolutions. *Developmental Dynamics*, *238*(3), 632–640. http://doi.org/10.1002/dvdy.21857

Miller, M. R., Dunham, J. P., Amores, A., Cresko, W. A., & Johnson, E. A. (2007). Rapid and cost-effective polymorphism identification and genotyping using restriction site associated DNA (RAD) markers. *Genome Research*, *17*(2), 240–248. http://doi.org/10.1101/gr.5681207

Miller, M. A., Pfeiffer, W. & Schwartz, T. (2010). Creating the CIPRES Science Gateway for inference of large phylogenetic trees. In: *Proceedings of the Gateway Computing Environments Workshop* (GCE), IEEE, 2010, 1–8.

Minh, B. Q., Nguyen, M. A. T., & Haeseler, Von, A. (2013). Ultrafast Approximation for Phylogenetic Bootstrap. *Molecular Biology and Evolution*, *30*(5), 1188–1195. http://doi.org/10.1093/molbev/mst024

Mirarab, S., Bayzid, M. S., Boussau, B., & Warnow, T. (2014). Statistical binning enables an accurate coalescent-based estimation of the avian tree. *Science*, *346*(6215), 1250463–1250463. http://doi.org/10.1126/science.1250463

Moen, D. S., Irschick, D. J., & Wiens, J. J. (2013). Evolutionary conservatism and convergence both lead to striking similarity in ecology, morphology and performance across continents in frogs. *Proceedings of the Royal Society B*, *280*(1773), 20132156–20132156. http://doi.org/10.1098/rspb.2013.2156

Moen, D. S., Morlon, H., & Wiens, J. J. (2015). Testing convergence versus history: convergence dominates phenotypic evolution for over 150 million years in frogs. *Systematic Biology*, *65*(1), 146–160. http://doi.org/10.1093/sysbio/syv073

Moen, D. S., Smith, S. A., & Wiens, J. J. (2009). Community assembly through evolutionary diversification and dispersal in middle American treefrogs. *Evolution*, *63*(12), 3228–3247. http://doi.org/10.1111/j.1558-5646.2009.00810.x

Molloy, E. K., & Warnow, T. (2018). Statistically consistent divide-and-conquer pipelines for phylogeny estimation using NJMerge, 1–30. http://doi.org/10.1101/469130

Moore, W. & Robertson, J. A. (2014). Explosive Adaptive Radiation and Extreme Phenotypic Diversity within Ant-Nest Beetles. *Current Biology*, *24*(20), 2435–2439. http://doi.org/10.1016/j.cub.2014.09.022

Morgan, M., Pagés, H., Obenchain, V., & Hayden, N. (2019). *Rsamtools: Binary alignment (BAM), FASTA, variant call (BCF), and tabix file import.* Retrieved from http://bioconductor.org/packages/release/bioc/html/Rsamtools.html

Myers, N., Mittermeier, R. A., Mittermeier, C. G., da Fonseca, G. A. B., & Kent, J. (2000). Biodiversity hotspots for conservation priorities. *Nature*, *403*(6772), 853–858. http://doi.org/10.1038/35002501

Narins, P. M., Feng, A. S., Fay, R. R., & Popper, A. N. (Eds.). (2006). Hearing and sound communication in amphibians (Vol. 28). Springer New York. http://doi.org/10.1007/978-0-387-47796-1

Nemeth, E., Dabelsteen, T., Pedersen, S. B., & Winkler, H. (2006). Rainforests as concert halls for birds: Are reverberations improving sound transmission of long song elements? *The Journal of the Acoustical Society of America*, *119*(1), 620–626. http://doi.org/10.1121/1.2139072

Nguyen, L. T., Schmidt, H. A., Haeseler, von, A., & Minh, B. Q. (2014). IQ-TREE: A Fast and Effective Stochastic Algorithm for Estimating Maximum-Likelihood Phylogenies. *Molecular Biology and Evolution*, *32*(1), 268–274. http://doi.org/10.1093/molbev/msu300

Nikolenko, S. I., Korobeynikov, A. I., & Alekseyev, M. A. (2013). BayesHammer: Bayesian clustering for error correction in single-cell sequencing. *BMC Genomics*, *14*(1), S7. http://doi.org/10.1186/1471-2164-14-S1-S7

Padial, J. M., Miralles, A., De la Riva, I. & Vences, M. (2010). The integrative future of taxonomy. *Frontiers in Zoology*, *7*, 1–14. http://dx.doi.org/10.1186/1742-9994-7-16

Pagel, M. (1994). Detecting correlated evolution on phylogenies: a general method for the comparative analysis of discrete characters. *Proceedings of the Royal Society B*, *255*(1342), 37–45. http://doi.org/10.1098/rspb.1994.0006

Pagel, M. (1999). The maximum likelihood approach to reconstructing ancestral character states of discrete characters on phylogenies. *Systematic Biology, 48*, 612–622. No DOI.

Paradis, E. & Schliep, K. (2019). ape 5.0: an environment for modern phylogenetics and evolutionary analyses in R. *Bioinformatics*, *35*(3), 526–528. http://doi.org/10.1093/bioinformatics/bty633

Paradis, E., Claude, J., & Strimmer, K. (2004). APE: analyses of phylogenetics and evolution in R language. *Bioinformatics*, *20*(2), 289–290. http://doi.org/10.1093/bioinformatics/btg412

Parker, G. A. & Smith, J. M. (1990). Optimality theory in evolutionary biology. *Nature*, *348*(6296), 27–33. http://doi.org/10.1038/348027a0

Parks, S. E., Johnson, M., Nowacek, D. & Tyack, P. L. (2011). Individual right whales call louder in increased environmental noise. *Biology Letters*, *7*(1), 33–35. http://doi.org/10.1098/rsbl.2010.0451

Parham, J. F., Donoghue, P. C., Bell, C. J., Calway, T. D., Head, J. J., Holroyd, P. A., Inoue, J. G., Irmis, R. B., Joyce, W. G., Ksepka, D. T., & Patané, J. S. (2011). Best practices for justifying fossil calibrations. *Systematic Biology, 61*, 346–359. https://doi.org/10.1093/sysbio/syr107

Pearson, R. G., & Raxworthy, C. J. (2009). The evolution of local endemism in Madagascar: watershed versus climatic gradient hypotheses evaluated by null biogeographic models. *Evolution*, *63*(4), 959–967. http://doi.org/10.1111/j.1558-5646.2008.00596.x

Peloso, P. L. V., Frost, D. R., Richards, S. J., Rodrigues, M. T., Donnellan, S., Matsui, M., et al. (2016). The impact of anchored phylogenomics and taxon sampling on phylogenetic inference in narrow-mouthed frogs (Anura, Microhylidae). *Cladistics*, *32*(2), 113–140. http://doi.org/10.1111/cla.12118

Peloso, P. L. V., Frost, D. R., Richards, S. J., Rodrigues, M. T., Donnellan, S., Matsui, M., Raxworthy, C. J., Biju, S. D., Lemmon, E. M., Lemmon, A. R., & Wheeler, W. C. (2015). The impact of anchored phylogenomics and taxon sampling on phylogenetic inference in narrow-mouthed frogs (Anura, Microhylidae). *Cladistics*, *32*(2), 113–140. http://doi.org/10.1111/cla.12118

Penna, M. & Meier, A. (2011). Vocal strategies in confronting interfering sounds by a frog from the southern temperate forest, *Batrachyla antartandica*. *Ethology*, *117*(12), 1147–1157. http://doi.org/10.1111/j.1439-0310.2011.01973.x

Penna, M. & Solís, R. (1998). Frog call intensities and sound propagation in the South American temperate forest region. *Behavioral Ecology and Sociobiology*, *42*(6), 371–381. http://doi.org/10.1007/s002650050452

Penny, S., Andreone, F., Crottini, A., Holderied, M., Rakotozafy, L., Schwitzer, C., & Rosa, G. (2014). A new species of the *Boophis rappiodes* group (Anura, Mantellidae) from the Sahamalaza Peninsula, northwest Madagascar, with acoustic monitoring of its nocturnal calling activity. *ZooKeys*, *435*, 111–132. http://doi.org/10.3897/zookeys.435.7383

Perl, R. B., Nagy, Z. T., Sonet, G., Glaw, F., Wollenberg, K. C. & Vences, M. (2014). DNA barcoding Madagascar's amphibian fauna. *Amphibia-Reptilia*, *35*, 197–206. http://dx.doi.org/10.1163/15685381-00002942

Pfennig, K. S. & Pfennig, D. W. (2009). Character displacement: ecological and reproductive responses to a common evolutionary problem. *The Quarterly Review of Biology*, *84*(3), 253–276. http://doi.org/10.1086/605079

Picardi, E. & Pesole, G. (2012). Mitochondrial genomes gleaned from human whole-exome sequencing. *Nature Methods*, *9*(6), 523–524. http://doi.org/10.1038/nmeth.2029

Pollard, D. A., Iyer, V. N., Moses, A. M., & Eisen, M. B. (2006). Widespread Discordance of Gene Trees with Species Tree in Drosophila: Evidence for Incomplete Lineage Sorting. *PLoS Genetics*, *2*(10), e173. http://doi.org/10.1371/journal.pgen.0020173

Pontarp, M., Canbäck, B., Tunlid, A., & Lundberg, P. (2012). Phylogenetic analysis suggests that habitat filtering is structuring marine bacterial communities across the globe. *Microbial Ecology*, *64*(1), 8–17. http://doi.org/10.1007/s00248-011-0005-7

Portik, D. M., Smith, L. L., & Bi, K. (2016). An evaluation of transcriptome-based exon capture for frog phylogenomics across multiple scales of divergence (Class: Amphibia, Order: Anura). *Molecular Ecology Resources*, *16*(5), 1069–1083. http://doi.org/10.1111/1755-0998.12541

Posada, D. (2008). jModelTest: phylogenetic model averaging. *Molecular Biology and Evolution, 25*, 1253–1256. http://dx.doi.org/10.1093/molbev/msn083

Powers, T. R., Virk, S. M., Trujillo-Provencio, C., & Serrano, E. E. (2012). Probing the *Xenopus laevis* inner ear transcriptome for biological function. *BMC Genomics*, *13*(1), 225. http://doi.org/10.1186/1471-2164-13-225

Prell, W.L. & Kutzbach, J.E. (1992). Sensitivity of the Indian monsoon to forcing parameters and implications for its evolution. *Nature 360*, 647–652. No DOI.

Prum, R. O., Berv, J. S., Dornburg, A., Field, D. J., Townsend, J. P., Lemmon, E. M., & Lemmon, A. R. (2015). A comprehensive phylogeny of birds (Aves) using targeted next-generation DNA sequencing. *Nature*, *526*(7574), 569–573. http://doi.org/10.1038/nature15697

Puechmaille, S. J., Gouilh, M. A., Piyapan, P., Yokubol, M., Mie, K. M., Bates, P. J., et al. (2011). The evolution of sensory divergence in the context of limited gene flow in the bumblebee bat. *Nature Communications*, *2*, 573. http://doi.org/10.1038/ncomms1582

Pyron, R. A. (2014). Biogeographic analysis reveals ancient continental vicariance and recent oceanic dispersal in amphibians. *Systematic Biology*, *63*(5), 779–797. http://doi.org/10.1093/sysbio/syu042

Pyron, R. A. & Wiens, J. J. (2011). A large-scale phylogeny of Amphibia including over 2800 species, and a revised classification of extant frogs, salamanders, and caecilians. *Molecular Phylogenetics and Evolution*, *61*(2), 543–583. http://doi.org/10.1016/j.ympev.2011.06.012

R Development Core Team. (2015–2019). R: A language and environment for statistical computing. R Foundation for Statistical Computing, Vienna, Austria. Available from http://www.R-project.org.

Raharivololoniaina, L., Grosjean, S., Raminosoa, N. R., Glaw, F., & Vences, M. (2006). Molecular identification, description, and phylogenetic implications of the tadpoles of 11 species of Malagasy treefrogs, genus *Boophis*. *Journal of Natural History*, *40*(23-24), 1449–1480. http://doi.org/10.1080/00222930600902399

Rakotoarinivo, M., Blach-Overgaard, A., Baker, W. J., Dransfield, J., Moat, J., & Svenning, J. C. (2013). Palaeo-precipitation is a major determinant of palm species richness patterns across Madagascar: a tropical biodiversity hotspot. *Proceedings of the Royal Society B*, *280*(1757), 20123048–20123048. http://doi.org/10.1098/rspb.2012.3048

Rakotoarison, A., Koehler, J., Glaw, F., & Vences, M. (2013). The advertisement call of the relict frog *Tsingymantis antitra* from Madagascar (Anura, Mantellidae). *Spixiana*, *36*(1), 143–148. No DOI.

Rakotoarison, A., Scherz, M. D., Glaw, F., Köhler, J., Andreone, F., Franzen, M., et al. (2017). Describing the smaller majority: integrative taxonomy reveals twenty-six new species of tiny microhylid frogs (genus *Stumpffia*) from Madagascar. *Vertebrate Zoology*, *67*(3), 271–398.

Ramos, M., Schiffer, L., Re, A., Azhar, R., Basunia, A., Rodriguez, C., et al. (2017). Software for the Integration of Multiomics Experiments in Bioconductor. *Cancer Research*, *77*(21), e39–e42. http://doi.org/10.1158/0008-5472.CAN-17-0344

Randrianiaina, R. D., Raharivololoniaina, L., Preuss, C., Strauß, A., Glaw, F., Teschke, M., Glos, J., Raminosoa, N. & Vences, M. (2009). Descriptions of the tadpoles of seven species of Malagasy treefrogs, genus *Boophis*. *Zootaxa, 2021*, 23–41. No DOI.

Randrianiaina, R. D., Straub, A., Glos, J., & Vences, M. (2012). Diversity of the strongly rheophilous tadpoles of Malagasy tree frogs, genus *Boophis* (Anura, Mantellidae), and identification of new candidate species via larval DNA sequence and morphology. *ZooKeys*, *178*(2), 59–124. http://doi.org/10.3897/zookeys.178.1410

Raselimanana, A. P., Glaw, F., & Vences, M. (2007). Lack of secondary sexual characters in a male of *Tsingymantis antitra* confirms its position as most basal mantelline frog lineage. *Zootaxa*, *1557*(1), 67. http://doi.org/10.11646/zootaxa.1557.1.5

Raxworthy, C. J., Pearson, R. G., Zimkus, B. M., Reddy, S., Deo, A. J., Nussbaum, R. A., & Ingram, C. M. (2008). Continental speciation in the tropics: contrasting biogeographic patterns of divergence in the *Uroplatus* leaf-tailed gecko radiation of Madagascar. *Journal of Zoology*, *275*(4), 423–440. http://doi.org/10.1111/j.1469-7998.2008.00460.x

Reddy, S., Driskell, A., Rabosky, D. L., Hackett, S. J., & Schulenberg, T. S. (2012). Diversification and the adaptive radiation of the vangas of Madagascar. *Proceedings of the Royal Society B*, *279*(1735), 2062–2071. http://doi.org/10.1098/rspb.2011.2380

Ree, R. H. & Smith, S. A. (2008). Maximum likelihood inference of geographic range evolution by dispersal, local extinction, and cladogenesis. *Systematic Biology, 57*, 4–14. https://doi.org/10.1080/10635150701883881

Revell, L. J. (2012). PHYTOOLS: an R package for phylogenetic comparative biology (and other things). *Methods in Ecology and Evolution*, *3*(2), 217–223. http://doi.org/10.1111/j.2041-210X.2011.00169.x

Rice, A. M. & Pfennig, D. W. (2010). Does character displacement initiate speciation? Evidence of reduced gene flow between populations experiencing divergent selection. *Journal of Evolutionary Biology*, *23*(4), 854–865. http://doi.org/10.1111/j.1420-9101.2010.01955.x

Richards, C. M., Nussbaum, R. A., & Raxworthy, C. J., (2000). Phylogenetic relationships within the Madagascan boophids and mantellids as elucidated by mitochondrial ribosomal genes. *African Journal of Herpetology, 49*, 23–32. https://doi.org/10.1080/21564574.2000.9650013

Richards, E. J., Brown, J. M., Barley, A. J., Chong, R., & Thomson, R. C. (2018). Variation across mitochondrial gene trees provides evidence for systematic error: How much gene tree variation is biological? *Systematic Biology*, *67*(5), 847–860. https://doi.org/10.1093/sysbio/syy013

Ricklefs, R. E. (1987). Community diversity: relative roles of local and regional processes. *Science*, *235*(4785), 167–171. http://doi.org/10.1126/science.235.4785.167

Robillard, T., Höbel, G., & Gerhardt, C. H. (2006). Evolution of advertisement signals in North American hylid frogs: vocalizations as end-products of calling behavior. *Cladistics*, *22*(6), 533–545. http://doi.org/10.1111/j.1096-0031.2006.00118.x

Roch, S. & Steel, M. (2015). Likelihood-based tree reconstruction on a concatenation of aligned sequence data sets can be statistically inconsistent. *Theoretical Population Biology*, *100*, 56–62. http://doi.org/10.1016/j.tpb.2014.12.005

Rognes, T., Flouri, T., Nichols, B., Quince, C., & Mahé, F. (2016). VSEARCH: a versatile open source tool for metagenomics. *PeerJ*, *4*(17), e2584–22. http://doi.org/10.7717/peerj.2584

Rohland, N. & Reich, D. (2012). Cost-effective, high-throughput DNA sequencing libraries for multiplexed target capture. *Genome Research*, *22*(5), 939–946. http://doi.org/10.1101/gr.128124.111

Romero, I. G., Pai, A. A., Tung, J., & Gilad, Y. (2014). RNA-seq: impact of RNA degradation on transcript quantification. *BMC Biology*, *12*(1), 42. http://doi.org/10.1186/1741-7007-12-42

Ronquist, F. (1997). Dispersal-vicariance analysis: a new approach to the quantification of historical biogeography. *Systematic Biology, 46*, 195–203. https://doi.org/10.1093/sysbio/46.1.195

Ronquist, F., Teslenko, M., van der Mark, P., Ayres, D. L., Darling, A., Höhna, S., Larget, B., Liu, L., Suchard, M. A., & Huelsenbeck, J. P. (2012). MrBayes 3.2: efficient Bayesian phylogenetic inference and model choice across a large model space. *Systematic Biology, 61*, 539–542. http://dx.doi.org/10.1093/sysbio/sys029

Röhr, D. L., Paterno, G. B., Camurugi, F., Juncá, F. A., & Garda, A. A. (2015). Background noise as a selective pressure: stream-breeding anurans call at higher frequencies. *Organisms Diversity & Evolution*, *16*(1), 269–273. http://doi.org/10.1007/s13127-015-0256-0

Ruane, S., Raxworthy, C. J., Lemmon, A. R., Lemmon, E. M., & Burbrink, F. T. (2015). Comparing species tree estimation with large anchored phylogenomic and small Sanger-sequenced molecular datasets: an empirical study on Malagasy pseudoxyrhophiine snakes. *BMC Evolutionary Biology*, 1–14. http://doi.org/10.1186/s12862-015-0503-1

Rubin, B. E. R., Ree, R. H., & Moreau, C. S. (2012). Inferring Phylogenies from RAD Sequence Data. *PLoS ONE*, *7*(4), e33394. http://doi.org/10.1371/journal.pone.0033394

Rundle, H. D. & Schluter, D. (1998). Reinforcement of stickleback mate preferences: sympatry breeds contempt. *Evolution*, *52*(1), 200. http://doi.org/10.2307/2410935

Ryan, M. J. & Rand, A. S. (1990). The sensory basis of sexual selection for complex calls in the túngara frog, *Physalaemus pustulosus* (sexual selection for sensory exploitation). *Evolution*, *44*, 305–314. http://dx.doi.org/10.2307/2409409

Ryan, M. J. & Rand, A. S. (1993). Species recognition and sexual selection as a unitary problem in animal communication. *Evolution*, *47*(2), 647. http://doi.org/10.2307/2410076

Ryan, M. J., Cocroft, R. B., & Wilczynski, W. (1990). The role of environmental selection in intraspecific divergence of mate recognition signals in the cricket frog, *Acris crepitans*. *Evolution*, *44*(7), 1869. http://doi.org/10.2307/2409514

Safonova, Y., Bankevich, A., & Pevzner, P. A. (2015). dipSPAdes: Assembler for Highly Polymorphic Diploid Genomes. *Journal of Computational Biology*, *22*(6), 528–545. http://doi.org/10.1089/cmb.2014.0153

Sanderson, N., Szymura, J. M., & Barton, N. H. (1992). Variation in mating call across the hybrid zone between the fire-bellied toads *Bombina bombina* and *B. variegata*. *Evolution*, *46*(3), 595. http://doi.org/10.2307/2409630

Sayyari, E., & Mirarab, S. (2016). Fast Coalescent-Based Computation of Local Branch Support from Quartet Frequencies. *Molecular Biology and Evolution*, *33*(7), 1654–1668. http://doi.org/10.1093/molbev/msw079

Schwarz, G. (1978). Estimating the dimension of a model. *The Annals of Statistics*, *6*, 461–464. http://dx.doi.org/10.1214/aos/1176344136
Schoener, T. W. (1965). The evolution of bill size differences among sympatric congeneric species of birds. *Evolution*, *19*(2), 189. http://doi.org/10.2307/2406374
Scornavacca, C., & Galtier, N. (2016). Incomplete Lineage Sorting in Mammalian Phylogenomics. *Systematic Biology*, *5*, syw082–9. http://doi.org/10.1093/sysbio/syw082
Shah, N., Nute, M. G., Warnow, T., & Pop, M. (2019). Misunderstood parameter of NCBI BLAST impacts the correctness of bioinformatics workflows. *Bioinformatics*, *35*(9), 1613–1614. http://doi.org/10.1093/bioinformatics/bty833
Shaw, K. L., & Lesnick, S. C. (2009). Genomic linkage of male song and female acoustic preference QTL underlying a rapid species radiation. *Proceedings of the National Academy of Sciences*, *106*(24), 9737–9742. http://doi.org/10.1073/pnas.0900229106
Shen, X. X., Liang, D., Feng, Y. J., Chen, M. Y., & Zhang, P. (2013). A versatile and highly efficient toolkit including 102 nuclear markers for vertebrate phylogenomics, tested by resolving the higher level relationships of the Caudata. *Molecular Biology and Evolution*, *30*(10), 2235–2248. http://doi.org/10.1093/molbev/mst122
Shendure, J. & Ji, H. (2008). Next-generation DNA sequencing. *Nature Biotechnology*, *26*(10), 1135–1145. http://doi.org/10.1038/nbt1486
Shokralla, S., Gibson, J. F., Nikbakht, H., Janzen, D. H., Hallwachs, W., & Hajibabaei, M. (2014). Next-generation DNA barcoding: using next-generation sequencing to enhance and accelerate DNA barcode capture from single specimens. *Molecular Ecology Resources*, *14*(5), 892–901. http://doi.org/10.1111/1755-0998.12236
Simpson, G.G. (1961). *Principles of animal taxonomy*. Columbia University Press, New York, New York, U.S.A., 247 pp.
Singhal, S., Grundler, M., Colli, G., & Rabosky, D. L. (2017). Squamate Conserved Loci (SqCL): A unified set of conserved loci for phylogenomics and population genetics of squamate reptiles. *Molecular Ecology Resources*, *17*(6), e12–e24. http://doi.org/10.1111/1755-0998.12681
Smith, B. T., Harvey, M. G., Faircloth, B. C., Glenn, T. C., & Brumfield, R. T. (2013). Target capture and massively parallel sequencing of Ultraconserved Elements for comparative studies at shallow evolutionary time scales. *Systematic Biology*, *63*(1), 83–95. http://doi.org/10.1093/sysbio/syt061
Song, Sen, Liu, L., Edwards, S. V., & Wu, S. (2012). Resolving conflict in eutherian mammal phylogeny using phylogenomics and the multispecies coalescent model. *Proceedings of the National Academy of Sciences*, *109*(37), 14942–14947. http://doi.org/10.1073/pnas.1211733109
Springer, M. S., & Gatesy, J. (2018). Delimiting Coalescence Genes (C-Genes) in Phylogenomic Data Sets. *Genes*, *9*(3), 123. http://doi.org/10.3390/genes9030123
Stamatakis, A. (2014). RAxML version 8: a tool for phylogenetic analysis and post-analysis of large phylogenies. *Bioinformatics*, *30*, 1312–1313. http://dx.doi.org/10.1093/bioinformatics/btu033
Stebbins, G. L. (1974). Flowering plants: evolution above the species level. London: Arnold xviii.
Stephen, S., Pheasant, M., Makunin, I. V., & Mattick, J. S. (2008). Large-Scale Appearance of Ultraconserved Elements in Tetrapod Genomes and Slowdown of the Molecular Clock. *Molecular Biology and Evolution*, *25*(2), 402–408. http://doi.org/10.1093/molbev/msm268

Stephens, M., Smith, N.J., & Donnelly, P. (2001). A new statistical method for haplotype reconstruction from population data. *American Journal of Human Genetics*, *68*, 978–989. http://dx.doi.org/10.1086/319501

Stephens, M. & Donnelly, P. (2003). A comparison of Bayesian methods for haplotype reconstruction. *American Journal of Human Genetics*, *73*, 1162–1169. http://dx.doi.org/10.1086/379378

Stephens, P. R., & Wiens, J. J. (2003). Explaining species richness from continents to communities: the time-for-speciation effect in emydid turtles. *The American Naturalist*, *161*(1), 112–128. http://doi.org/10.1086/345091

Strauß, A., Randrianiaina, R. D., Vences, M., & Glos, J. (2012). Species distribution and assembly patterns of frog larvae in rainforest streams of Madagascar. *Hydrobiologia*, *702*(1), 27–43. http://doi.org/10.1007/s10750-012-1301-z

Streicher, J. W., Miller, E. C., Guerrero, P. C., Correa, C., Ortiz, J. C., Crawford, A. J., et al. (2018). Evaluating methods for phylogenomic analyses, and a new phylogeny for a major frog clade (Hyloidea) based on 2214 loci. *Molecular Phylogenetics and Evolution*, *119*, 128–143. http://doi.org/10.1016/j.ympev.2017.10.013

Stuart, Y. E., & Losos, J. B. (2013). Ecological character displacement: glass half full or half empty? *Trends in Ecology & Evolution*, *28*(7), 402–408. http://doi.org/10.1016/j.tree.2013.02.014

Sudmant, P. H., Alexis, M. S., & Burge, C. B. (2015). Meta-analysis of RNA-seq expression data across species, tissues and studies. *Genome Biology*, *16*(1), 287. http://doi.org/10.1186/s13059-015-0853-4

Sueur, J., Aubin, T., & Simonis, C. (2008). SEEWAVE, a free modular tool for sound analysis and synthesis. *Bioacoustics*, *18*(2), 213–226. http://doi.org/10.1080/09524622.2008.9753600

Sullivan, J., Swofford, D. L., & Naylor, G. J. (1999). The effect of taxon sampling on estimating rate heterogeneity parameters of maximum-likelihood models. *Molecular Biology and Evolution, 16,* 1347–1347. https://doi.org/10.1093/oxfordjournals.molbev.a026045

Sulonen, A. M., Ellonen, P., Almusa, H., Lepistö, M., Eldfors, S., Hannula, S., et al. (2011). Comparison of solution-based exome capture methods for next generation sequencing. *Genome Biology*, *12*(9), R94. http://doi.org/10.1186/gb-2011-12-9-r94

Sun, Y. B., Xiong, Z. J., Xiang, X. Y., Liu, S. P., Zhou, W. W., Tu, X. L., et al. (2015). Whole-genome sequence of the Tibetan frog *Nanorana parkeri* and the comparative evolution of tetrapod genomes. *Proceedings of the National Academy of Sciences*, *112*(11), E1257–E1262. http://doi.org/10.1073/pnas.1501764112

Talavera, G. & Castresana, J. (2007). Improvement of phylogenies after removing divergent and ambiguously aligned blocks from protein sequence alignments. *Systematic Biology, 56*, 564–577. https://doi.org/10.1080/10635150701472164

Taylor, D. J. (2004). An Assessment of Accuracy, Error, and Conflict with Support Values from Genome-Scale Phylogenetic Data. *Molecular Biology and Evolution*, *21*(8), 1534–1537. http://doi.org/10.1093/molbev/msh156

Teasdale, L. C., Köhler, F., Murray, K. D., O'Hara, T., & Moussalli, A. (2016). Identification and qualification of 500 nuclear, single-copy, orthologous genes for the Eupulmonata (Gastropoda) using transcriptome sequencing and exon capture. *Molecular Ecology Resources*, *16*(5), 1107–1123. http://doi.org/10.1111/1755-0998.12552

Tewhey, R., Nakano, M., Wang, X., Pabón-Peña, C., Novak, B., Giuffre, A., et al. (2009). Enrichment of sequencing targets from the human genome by solution hybridization. *Genome Biology*, *10*(10), R116. http://doi.org/10.1186/gb-2009-10-10-r116

Tobias, J. A., Aben, J., Brumfield, R. T., Derryberry, E. P., Halfwerk, W., Slabbekoorn, H., & Seddon, N. (2010). Song divergence by sensory drive in amazonian birds. *Evolution*, *64*(10), 2820–2839. http://doi.org/10.1111/j.1558-5646.2010.01067.x

Tobias, J. A., Cornwallis, C. K., Derryberry, E. P., Claramunt, S., Brumfield, R. T., & Seddon, N. (2013). Species coexistence and the dynamics of phenotypic evolution in adaptive radiation. *Nature*, *506*(7488), 359–363. http://doi.org/10.1038/nature12874

Toews, D. P., & Irwin, D. E. (2008). Cryptic speciation in a Holarctic passerine revealed by genetic and bioacoustic analyses. *Molecular Ecology*, *17*(11), 2691–2705. http://doi.org/10.1111/j.1365-294X.2008.03769.x

Townsend, J. (2007). Profiling phylogenetic informativeness. *Systematic Biology*, *46*(2), 222–231. https://doi.org/10.1080/10635150701311362

Townsend, T. M., Vieites, D. R., Glaw, F., & Vences, M. (2009). Testing species-level diversification hypotheses in Madagascar: the case of microendemic *Brookesia* leaf chameleons. *Systematic Biology, 58*, 641–656. https://doi.org/10.1093/sysbio/syp073

Tschudi, J.J.v. (1838). Classification der Batrachier mit Berücksichtigung der fossilen Thiere dieser Abtheilung der Reptilien. Neuchâtel: Petitpierre. http://dx.doi.org/10.5962/bhl.title.59545

Tuttle, M. D. & Ryan, M. J. (1981). Bat predation and the evolution of frog vocalizations in the neotropics. *Science*, *214*(4521), 677–678. http://doi.org/10.1126/science.214.4521.677

Uy, J. A. C. & Borgia, G. (2007). Sexual selection drives rapid divergence in bowerbird display traits. *Evolution*, *54*(1), 273–278. http://doi.org/10.1111/j.0014-3820.2000.tb00027.x

Vallin, N., Rice, A. M., Bailey, R. I., Husby, A., & Qvarnström, A. (2011). Positive feedback between ecological and reproductive character displacement in a young avian hybrid zone. *Evolution*, *66*(4), 1167–1179. http://doi.org/10.1111/j.1558-5646.2011.01518.x

Vamosi, S. M., Heard, S. B., Vamosi, J. C., & Webb, C. O. (2009). Emerging patterns in the comparative analysis of phylogenetic community structure. *Molecular Ecology*, *18*(4), 572–592. http://doi.org/10.1111/j.1365-294X.2008.04001.x

Van der Auwera, G. A., Carneiro, M. O., Hartl, C., Poplin, R., del Angel, G., Moonshine, A. L., et al. (2013). From FastQ Data to High-Confidence Variant Calls: The Genome Analysis Toolkit Best Practices Pipeline. *Current Protocols in Bioinformatics*, *11*(1100), 11.10.1–11.10.33. http://doi.org/10.1002/0471250953.bi1110s43

Vargas-Salinas, F. & Amézquita, A. (2013). Abiotic noise, call frequency and stream-breeding anuran assemblages. *Evolutionary Ecology*, *28*(2), 341–359. http://doi.org/10.1007/s10682-013-9675-6

Vences, M., Andreone, F., Glaw, F., Kosuch, J., Meyer, A., Schaefer, H. C., & Veith, M. (2002). Exploring the potential of life-history key innovation: brook breeding in the radiation of the Malagasy treefrog genus *Boophis*. *Molecular Ecology*, *11*(8), 1453–1463. http://doi.org/10.1046/j.1365-294X.2002.01543.x

Vences, M., Andreone, F., Glos, J. & Glaw, F. (2010). Molecular and bioacoustic differentiation of *Boophis occidentalis* with description of a new treefrog from north-western Madagascar. *Zootaxa, 2544*, 54–68. No DOI.

Vences, M., Chiari, Y., Teschke, M., Randrianiaina, R. D., Raharivololoniaina, L., Bora, P., Vieites, D. R. & Glaw, F. (2008). Which frogs are out there? A preliminary evaluation of survey techniques and identification reliability of Malagasy amphibians. *In:* Andreone, F. (Eds.), *A Conservation Strategy for the Amphibians of Madagascar.* Monografie del Museo Regionale di Scienze Naturali di Torino 45, Turin, Italy, pp. 233–253.

Vences, M., Gehara, M., Kohler, J., & Glaw, F. (2012). Description of a new Malagasy treefrog (*Boophis*) occurring syntopically with its sister species, and a plea for studies on non-allopatric speciation in tropical amphibians. *Amphibia-Reptilia*, *33*, 503–520. https://doi.org/10.1163/15685381-00002856

Vences, M. & Glaw, F. (2001). When molecules claim for taxonomic changes: new proposals on the classification of Old World treefrogs (Amphibia, Anura, Ranoidea). *Spixiana 24*, 85–92. No DOI.

Vences, M. & Glaw, F. (2002). Two new treefrogs of the *Boophis rappiodes* group from eastern Madagascar. *Tropical Zoology*, *15*, 141–163. http://dx.doi.org/10.1080/03946975.2002.10531171

Vences, M., Glaw, F., Kosuch, J., Das, I., & Veith, M. (2000). Polyphyly of *Tomopterna* (Amphibia: Ranidae) based on sequences of the mitochondrial 16S and 12S rRNA genes, and ecological biogeography of Malgasy relict amphibian groups. In W. R. Lourenco & S. M. Goodman (Eds.), *Mémoires de la Société de Biogéographie* (pp. 229–242). Paris: mvences.de.

Vences, M., Glaw, F., & Marquez, R. (2006). The calls of the frogs of Madagascar. Barcelona: Fonoteca Zoológica & Alosa.

Vences, M., Guayasamin, J. M., Miralles, A. & De La Riva, I. (2013). To name or not to name: Criteria to promote economy of change in Linnaean classification schemes. *Zootaxa*, *3636*, 201–244. http://dx.doi.org/10.11646/zootaxa.3636.2.1

Vences, M., Wahl-Boos, G., Hoegg, S., Glaw, F., Spinelli Oliveira, E., Meyer, A., & Perry, S. (2007). Molecular systematics of mantelline frogs from Madagascar and the evolution of their femoral glands. *Biological Journal of the Linnean Society*, *92*(3), 529–539. http://doi.org/10.1111/j.1095-8312.2007.00859.x

Vences, M. & Wake, D. B. (2007). Speciation, species boundaries and phylogeography of amphibians. *In:* Heatwole, H.H. & Tyler, M. (Eds.), *Amphibian Biology, Vol. 6, Systematics*. Surrey Beatty & Sons, Chipping Norton, Australia, pp. 2613–2669.

Vences, M., Wollenberg, K. C., Sonet, G., Glaw, F., Nagy, Z. T., & Perl, R. G. B. (2014). DNA barcoding Madagascar's amphibian fauna. *Amphibia-Reptilia*, *35*(2), 197–206. http://doi.org/10.1163/15685381-00002942

Vences, M., Wollenberg, K. C., Vieites, D. R., & Lees, D. C. (2009). Madagascar as a model region of species diversification. *Trends in Ecology & Evolution*, *24*(8), 456–465. http://doi.org/10.1016/j.tree.2009.03.011

Vieites, D. R., Wollenberg, K. C., Andreone, F., Kohler, J., Glaw, F., & Vences, M. (2009). Vast underestimation of Madagascar's biodiversity evidenced by an integrative amphibian inventory. *Proceedings of the National Academy of Sciences*, *106*(20), 8267–8272. http://doi.org/10.1073/pnas.0810821106

Walker, T. J. (1974). Character displacement and acoustic insects. *American Zoologist*, *14*(4), 1137–1150. http://doi.org/10.1093/icb/14.4.1137

Wang, Z., Gerstein, M., & Snyder, M. (2009). RNA-Seq: a revolutionary tool for transcriptomics. *Nature Reviews Genetics*, *10*(1), 57–63. http://doi.org/10.1038/nrg2484

Wasserman, M. & Koepfer, H. R. (1977). Character displacement for sexual isolation between *Drosophila mojavensis* and *Drosophila arizonensis*. *Evolution*, *31*(4), 812. http://doi.org/10.2307/2407442

Wells, K. D. (2007). *The ecology and behavior of amphibians*. The University of Chicago Press, Chicago, Illinois, U.S.A., 1400 pp. http://dx.doi.org/10.7208/chicago/9780226893334.001.0001

Wickett, N. J., Mirarab, S., Nguyen, N., Warnow, T., Carpenter, E., Matasci, N., et al. (2014). Phylotranscriptomic analysis of the origin and early diversification of land plants. *Proceedings of the National Academy of Sciences*, *111*(45), E4859–E4868. http://doi.org/10.1073/pnas.1323926111

Wiens, J. J., Sukumaran, J., Pyron, R. A., & Brown, R. M. (2009). Evolutionary and biogeographic origins of high tropical diversity in old world frogs (Ranidae). *Evolution*, *63*(5), 1217–1231. http://doi.org/10.1111/j.1558-5646.2009.00610.x

Wiley, E.O. (1978). The evolutionary species concept reconsidered. *Systematic Zoology*, *27*, 17–26. http://dx.doi.org/10.2307/2412809

Wiley, R. H. & Richards, D. G. (1978). Physical constraints on acoustic communication in the atmosphere: Implications for the evolution of animal vocalizations. *Behavioral Ecology and Sociobiology*, *3*(1), 69–94. http://doi.org/10.1007/BF00300047

Wilmé, L., Goodman, S. M., & Ganzhorn, J. U. (2006). Biogeographic Evolution of Madagascar's Microendemic Biota. *Science*, *312*(5776), 1063–1065. http://doi.org/10.1126/science.1122806

Wollenberg, K. C., Andreone, F., Glaw, F. & Vences, M. (2008). Pretty in pink: a new treefrog species of the genus *Boophis* from north-eastern Madagascar. *Zootaxa*, *1684*, 58–68. No DOI.

Wollenberg, K. C., Vieites, D. R., Glaw, F., & Vences, M. (2011). Speciation in little: the role of range and body size in the diversification of Malagasy mantellid frogs. *BMC Evolutionary Biology*, *11*(1), 217. http://doi.org/10.1186/1471-2148-11-217

Wollenberg, K. C., Vieites, D. R., van der Meijden, A., Glaw, F., Cannatella, D. C., & Vences, M. (2008). Patterns of endemism and species richness in Malagasy cophline frogs support a key role of mountainous areas for speciation. *Evolution*, *62*(8), 1890–1907. http://doi.org/10.1111/j.1558-5646.2008.00420.x

Wollenberg Valero, K. C, Garcia-Porta, J., Rodríguez, A., Arias, M., Shah, A., Randrianiaina, R. D., Brown, J. L., Glaw, F., Amat, F., Künzel, S., Metzler, D. (2017). Transcriptomic and macroevolutionary evidence for phenotypic uncoupling between frog life history phases. *Nature Communications, 8*, 15213. https://doi.org/10.1038/ncomms15213

Wollerman, L. (1999). Acoustic interference limits call detection in a Neotropical frog *Hyla ebraccata*. *Animal Behaviour*, *57*(3), 529–536. http://doi.org/10.1006/anbe.1998.1013

Wong, K. H., Jin, Y., & Moqtaderi, Z. (2001). Multiplex illumina sequencing using dna barcoding. Hoboken, NJ, USA: John Wiley & Sons, Inc. http://doi.org/10.1002/0471142727.mb0711s101

Wong, S., Parada, H., & Narins, P. M. (2009). Heterospecific acoustic interference: effects on calling in the frog *oophaga pumilioin* Nicaragua. *Biotropica*, *41*(1), 74–80. http://doi.org/10.1111/j.1744-7429.2008.00452.x

Xi, Z., Liu, L., & Davis, C. C. (2015). Genes with minimal phylogenetic information are problematic for coalescent analyses when gene tree estimation is biased. *Molecular Phylogenetics and Evolution*, *92*(C), 63–71. http://doi.org/10.1016/j.ympev.2015.06.009

Yang, Z. (1997). PAML: a program package for phylogenetic analysis by maximum likelihood. *Computer Applications in the Biosciences: CABIOS*, *13*(5), 555–556.
Yang, Z. (2006) *Computational molecular evolution.* Oxford University Press, New York, New York, U.S.A., 376 pp. http://dx.doi.org/10.1093/acprof:oso/9780198567028.001.0001
Yang, Z. (2007). PAML 4: phylogenetic analysis by maximum likelihood. *Molecular Biology and Evolution*, *24*(8), 1586–1591. http://doi.org/10.1093/molbev/msm088
Yoder, A. D. & Nowak, M. D. (2006). Has Vicariance or Dispersal Been the Predominant Biogeographic Force in Madagascar? Only Time Will Tell. *Annual Review of Ecology, Evolution, and Systematics*, *37*(1), 405–431. http://doi.org/10.1146/annurev.ecolsys.37.091305.110239
Zhang, C., Rabiee, M., Sayyari, E., & Mirarab, S. (2018). ASTRAL-III: polynomial time species tree reconstruction from partially resolved gene trees. *BMC Bioinformatics*, *19*(6), 15–30. http://doi.org/10.1186/s12859-018-2129-y
Zhang, P., Liang, D., Mao, R. L., Hillis, D. M., Wake, D. B. & Cannatella, D. C. (2013). Efficient sequencing of anuran mtDNAs and a mitogenomic exploration of the phylogeny and evolution of frogs. *Molecular Biology and Evolution*, *30*, 1899–1915. http://dx.doi.org/10.1093/molbev/mst091
Zhou, M., Chen, T., Walker, B., & Shaw, C. (2005). Novel frenatins from the skin of the Australasian giant white-lipped tree frog, Litoria infrafrenata: Cloning of precursor cDNAs and identification in defensive skin secretion. *Peptides*, *26*(12), 2445–2451. http://doi.org/10.1016/j.peptides.2005.05.019
Zhu, L., Zhang, Y., Zhang, W., Yang, S., Chen, J. Q., & Tian, D. (2009). Patterns of exon-intron architecture variation of genes in eukaryotic genomes. *BMC Genomics*, *10*(1), 47. http://doi.org/10.1186/1471-2164-10-47
Ziegler, L., Arim, M., & Narins, P. M. (2011). Linking amphibian call structure to the environment: the interplay between phenotypic flexibility and individual attributes. *Behavioral Ecology*, *22*(3), 520–526. http://doi.org/10.1093/beheco/arr011
Zimmerman, B. L. (1983). A Comparison of Structural Features of Calls of Open and Forest Habitat Frog Species in the Central Amazon. *Herpetologica*, *39*(3), 235–246. http://doi.org/10.2307/3892567

Appendix I.

From:

CHAPTER 1

A new species of bright-eyed treefrog (Mantellidae) from Madagascar, with comments on call evolution and patterns of syntopy in the *Boophis ankaratra* complex

Hutter C.R., Lambert S.M., Cobb K.A., Andriampenomanana Z.F., and Vences M. (2015). A new species of bright-eyed treefrog (Mantellidae) from Madagascar, with comments on call evolution and patterns of syntopy in the *Boophis ankaratra* complex. *Zootaxa* 4034(3): 531–555. http://dx.doi.org/10.11646/zootaxa.4034.3.6

Specimens examined. The specimens examined for comparisons in this study and their corresponding museum or collection numbers.

Boophis ankaratra

Madagascar: *Fianarantsoa province*: Ranomafana National Park, Maharira (21°20'06.3"S, 47°24'28.31"E; 1233 m, a.s.l.), KU 336830 and UADBA-Uncatalogued (CRH-177).

Boophis boppa

Madagascar: *Fianarantsoa province*: Ranomafana National Park, Maharira (21°20'06.3"S, 47°24'28.31"E; 1233 m, a.s.l.), KU 336824 (holotype), KU 336825–336829, UADBA-Uncatalogued (CRH 080), UADBA-Uncatalogued (CRH 168), and UADBA-Uncatalogued (CRH 178). Ranomafana National Park, Andemaka (21°07'43.4"S, 47°30'19.4"E, 1237 m, a.s.l.), Uncatalogued (CRH 775).

Boophis luciae

Madagascar: *Fianarantsoa province*: Ranomafana National Park, Maharira (21°20'06.3"S, 47°24'28.31"E; 1233 m, a.s.l.), KU 336854. Ranomafana National Park, Valohoaka (21°17'51.3"S, 47°26'20.1"E; 1064 m, a.s.l.), KU 336855 and UADBA-Uncatalogued (CRH 002).

Boophis schuboeae

Madagascar: *Fianarantsoa province*: Ranomafana National Park, Ambatolahy (21°14'38"S, 47°25'34.3"E; 919 m, a.s.l.), UADBA-Uncatalogued (CRH 818) and UADBA-Uncatalogued (CRH 846).

Table S1. Newly generated GenBank accession numbers for taxa used in this study. All localities are within Madagascar.

			GenBank Accession ID	
Museum or collection ID	**Species**	**Locality**	**16S**	**DNAH-3**
KU 336830	*Boophis ankaratra*	Fianarantsoa, Ranomafana National Park, Maharira	KT588032	KT588046
ZCMV 09739	*Boophis ankaratra*	Fianarantsoa, Ranomafana National Park, Imaloka		KT588047
KU 336825	*Boophis boppa*	Fianarantsoa, Ranomafana National Park, Maharira	KT588033	KT588049
KU 336828	*Boophis boppa*	Fianarantsoa, Ranomafana National Park, Maharira	KT588034	KT588050
KU 336883	*Boophis boppa*	Fianarantsoa, Ranomafana National Park, Maharira	KT588035	
UADBA-CRH168	*Boophis boppa*	Fianarantsoa, Ranomafana National Park, Maharira	KT588036	
KU 336829	*Boophis boppa*	Fianarantsoa, Ranomafana National Park, Maharira	KT588037	KT588051
KU 336827	*Boophis boppa*	Fianarantsoa, Ranomafana National Park, Maharira	KT588038	
UADBA-CRH080	*Boophis boppa*	Fianarantsoa, Ranomafana National Park, Maharira	KT588039	
KU 336824	*Boophis boppa*	Fianarantsoa, Ranomafana National Park, Maharira	KT588040	KT588048
UADBA-CRH178	*Boophis boppa*	Fianarantsoa, Ranomafana National Park, Maharira	KT588041	
FGZC 2390	*Boophis haingana*	Andohahela		KT588042
ZSM 674/2001	*Boophis liami*	Andasibe, Vohidrazana		KT588043
ZCMV 0687	*Boophis luciae*	Fianarantsoa, Ranomafana National Park		KT588044
FGZC 2389	*Boophis miadana*	Andohahela		KT588045
KU 336858	*Boophis periegetes*	Fianarantsoa, Ranomafana National Park, Maharira	KT588031	
ZSM 39 2002	*Boophis sibilans*	Andasibe		KT588052

Table S2. Previously available GenBank accession numbers used in this study for the mitochondrial marker 16S. GenBank Accession ID's with an asterisk are those used in the phylogenetic analyses while all sequences listed were used for genetic distances.

Museum or Collection ID	Species	Genbank Accession ID
ZCMV 4946	*Boophis albipunctatus*	GU974374
ZCMV 4942	*Boophis albipunctatus*	GU974373
MRSN A6371	*Boophis albipunctatus*	HM364574
MRSN A6219	*Boophis albipunctatus*	HM364573
MRSN A6197	*Boophis albipunctatus*	HM364572
FGZC 291	*Boophis albipunctatus*	AY848446*
ZCMV 10348	*Boophis ankaratra*	KF609605*
ZCMV 5989	*Boophis ankaratra*	GU974475*
ZCMV 4917	*Boophis ankaratra*	GU974476*
FGMV 2001/480	*Boophis ankaratra*	AF411612
FGMV 2002/1699	*Boophis ankaratra*	DQ068398
FGMV 2002/1697	*Boophis ankaratra*	DQ068396*
FAZC 13998	*Boophis ankaratra*	JF903873
ZCMV 09739	*Boophis boppa*	KF609604*
ZSM 1164/2007	*Boophis boppa*	GU974477*
FAZC 11480	*Boophis boppa*	AY848438*
FAZC 11462	*Boophis boppa*	AY848437*
FAZC 11454	*Boophis boppa*	AY848436*
FGZC 239	*Boophis haingana*	AY848463*
FGZC 232	*Boophis haingana*	AY848462*
FGZC 220	*Boophis haingana*	AY848461*
FGZC 219	*Boophis haingana*	AY848460*
FGZC 218	*Boophis haingana*	AY848459*
FGZC 2390	*Boophis haingana*	FJ559142*
ZCMV 687	*Boophis luciae*	AY848443
ZCMV 10501	*Boophis luciae*	KF609714
ZCMV 10100	*Boophis luciae*	KF609745
ZCMV 09106	*Boophis luciae*	KF609730*
ZCMV 4564	*Boophis luciae*	GU975078
ZCMV 4202	*Boophis luciae*	GU975079
ZCMV 09744	*Boophis luciae*	KF610983
ZCMV 09740	*Boophis luciae*	KF610982
ZCMV 09731	*Boophis luciae*	KF610981
ZCMV 09192	*Boophis luciae*	KF610980*
ZCMV 09513	*Boophis luciae*	KF610971
ZCMV 09628	*Boophis luciae*	KF610968
ZCMV 09626	*Boophis luciae*	KF610967
FGZC 2389	*Boophis miadana*	FJ559141*
ZCMV 09349	*Boophis schuboeae*	KF610486*

ZCMV 5090	*Boophis schuboeae*	GU974829*
ZCMV 5080	*Boophis schuboeae*	GU974830*
FGMV 2002/1804	*Boophis schuboeae*	DQ068395*
FGMV 2002/1800	*Boophis schuboeae*	DQ068394*
FGMV 2002/1790	*Boophis schuboeae*	DQ068393*

Appendix II.

From:

CHAPTER 2

Molecular phylogeny and diversification of Malagasy bright-eyed tree frogs (Mantellidae: *Boophis*)

Hutter C.R., Lambert S.M., Andriampenomanana Z.F., Glaw F., and Vences M. (2018). Molecular systematics and diversification of Malagasy bright-eyed tree frogs (Mantellidae: *Boophis*). *Molecular Phylogenetics and Evolution* 127: 568–578. https://doi.org/10.1016/j.ympev.2018.05.027

Figure S1. Biogeographic analysis from BIOGEOBEARS using 10 regions.

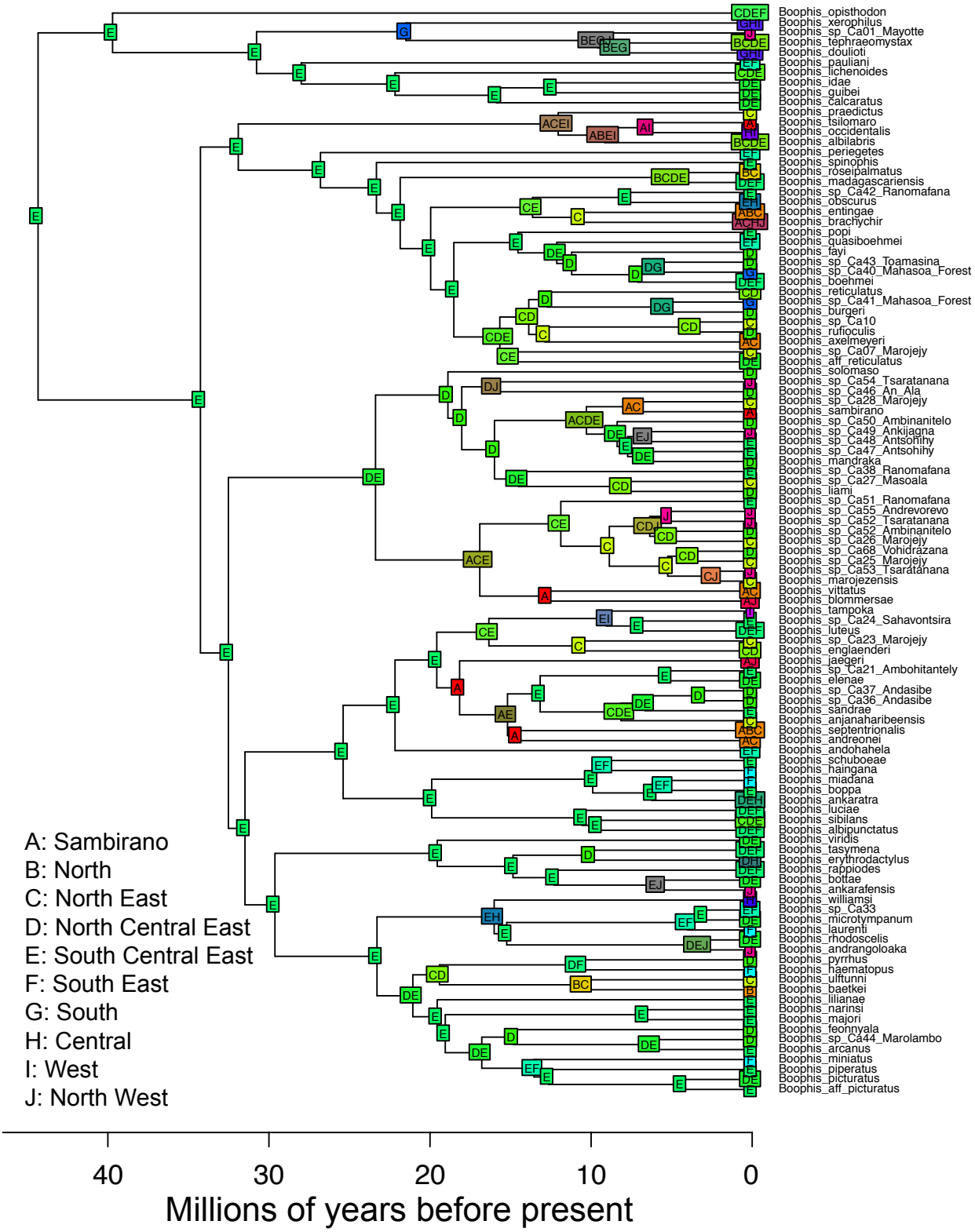

Figure S2. Biogeographic analysis from BIOGEOBEARS using 4 regions, displayed as pie charts proportional to their marginal probability.

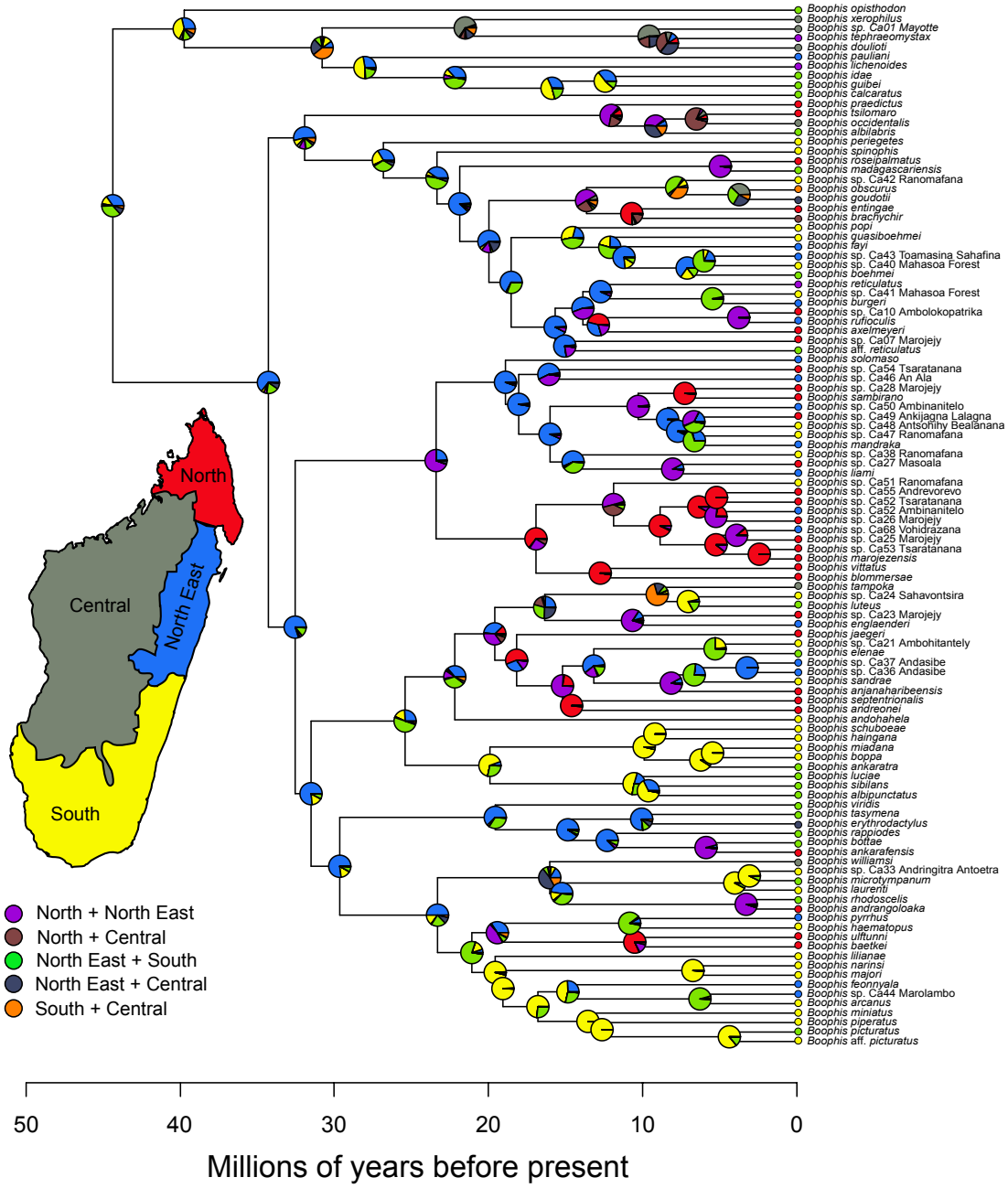

Table S1 part 1. Mitochondrial GenBank markers used for Chapter 2 and Chapter 5.

Species	Voucher	Locality	12S	16S p1	16S p2
B. aff marojezensis	ZSM 189/2002	Vohidrazana	AY341617	AY341674	FJ559128
B. aff marojezensis	ZSM 326/2000	Vohidrazana			
B. aff marojezensis	ZSM 330/2000	Vohidrazana			
B. aff picturatus	CRH 669	Ranomafana, Maharira			
B. aff picturatus	ZCMV 09867	Ranomafana		KF611065	
B. aff picturatus	ZCMV 210	Ranomafana, Maharira			AY848644
B. aff picturatus	ZCMV 5862	Ranomafana			
B. aff reticulatus	ZCMV 211	Ranomafana	MH422619	AY848613	AY848613
B. albilabris	FGMV 2002.807 (UADBA)	Manongarivo			
B. albilabris	RAX 2714	Tsaratanana	DQ283033	DQ283033	DQ283033
B. albilabris	ZCMV 2808	Ambatolahy			
B. albipunctatus	ZSM 157/2004 (FGZC 291)	Manantantely	MH422582	MH422634	AY848446
B. andohahela	FGZC 2372	Andohahela	MH422583		FJ559121
B. andohahela	ZCMV 09900	Vatoharanana		KF610898	
B. andrangoloaka	FGZC 2139	Ambohitantely	MH422584	MH422635	GU205779
B. andreonei	FGMV 2002.806	Manongarivo	MH422585	MH422636	AY848450
B. anjanaharibeensis	FGZC 2762	Marojejy	MH422586	MH422637	FJ559122
B. ankarafensis	MRSN A6975	Sahamalaza			KJ438141
B. ankaratra	KU 336830	Ranomafana, Maharira		MH422638	
B. ankaratra	ZSM 367/2000 (FGMV 2000.68)	Manjakatompo	MH422587		AJ315911
B. arcanus	ZCMV 392 (UADBA 24299)	Mahakajy	MH422588	MH422639	AY848632
B. axelmeyeri	FGMV 2002.809	Manongarivo	MH422589	MH422640	DQ118668
B. baetkei	FGZC 1391	Foret d'Ambre			EU314954
B. blommersae	FGMV 2002.925	Antakarana	MH422590	MH422641	
B. blommersae	ZSM 906/2003	Montagne d'Ambre			AY848451
B. boehmei	FGMV 201.1205 (UADBA)	Andasibe	AY341612	AY341669	AY341717
B. boehmei	ZCMV 1490	Andasibe			
B. boppa	KU 336825	Ranomafana, Maharira			KT588037
B. bottae	ZSM 344/2000 (ZCMV 65)	Andasibe	MH422591	MH422642	JX570154
B. brachychir	FGMV 2002.702	Manongarivo	MH422592	MH422643	AY848538
B. burgeri	FGMV 2001.1246	Andasibe		MH422644	AY848566
B. burgeri	KU 340719	Vohidrazana			

B. calcaratus	NMBE 862/95	Ambavaniasy	MH422593	MH422645	FJ559134
B. doulioti	FGZC 726	Tsingy de Bemaraha		MH422646	
B. doulioti	FGZC 92	Tolagnaro			
B. doulioti	ZSM 29/2006	Tsingy de Bemaraha	AY341608		FJ559123
B. elenae	UADBA 24141	Ranomafana, Maharira			AY848470
B. elenae	ZCMV 192	Ranomafana, Maharira	MH422594	MH422647	
B. englaenderi	ZSM 418/2005 (ZCMV 856)	Marojejy	MH422595	MH422648	FJ559124
B. entingae	FGMV 2002.911	Montagne d'Ambre		MH422649	MH422691
B. entingae	ZSM 899/2003	Montagne d'Ambre			
B. erythrodactylus	CRH 422 (UADBA)	Vohidrazana	MH422596	MH422650	
B. erythrodactylus	ZSM 342/2000	Mandraka			AJ314814
B. fayi	MRSN A6596	Betampona			HM364595
B. feonnyala	ZSM 313/2000	Andasibe			AJ315922
B. goudotii	FMGV 2002.45	Antoetra	MH422597	MH422651	AY848570
B. goudotii	ZMA 19544	Antoetra			
B. guibei	KU 340594	Andasibe	MH422598	MH422652	
B. guibei	ZSM 348/2000 (FGMV 2000-50, A9)	Andasibe			JX570182
B. haematopus	ZSM 120/2004 (FGZC 215)	Andohahela	MH422599	MH422653	AY848633
B. haingana	ZSM 5109/2005 (FGZC 2390)	Andohahela	MH422600	MH422654	FJ559142
B. idae	ZSM 45/2002	Andasibe	AY341609	AY341666	AY848481
B. jaegeri	ZSM 587/2001 (2002.F24)	Nosy Be	MH422601	MH422655	FJ559125
B. laurenti	ZSM 727/2001 (MV 2001 535, C34)	Andringitra	MH422602	MH422656	AY848575
B. liami	ZSM 310/2000 (MV 2001 A4)	Vohidrazana	MH422603	MH422657	AJ315919
B. lichenoides	FAZC 5679	Sahavontsira	MH422604	MH422658	FJ664184
B. lilianae	ZSM 201/2006 (ZCMV 2864)	Ifanadiana	MH422605	MH422659	EU314953
B. luciae	KU 340828	Ranomafana, Miranony			
B. luciae	ZCMV 0687	Ranomafana, Ambatolahy	MH422606	MH422660	
B. luciae	ZMA 20306	Ranomafana, Ambatolahy			AY848443
B. luteus	FGMV 2000.063 (UADBA)	Andasibe	AY341614	AY341671	
B. luteus	FGMV 2001.A24	Mandraka			

B. luteus	FGMV 2002.1612	Andasibe			JX570039
B. madagascariensis	CRH 415 (UADBA) mtGenome	Vohidrazana			
B. madagascariensis	(Kurabayashi)	Unknown			
B. madagascariensis	ZCMV 344	Ranomafana	AF458120	AB239572	AY848585
B. majori	ZCMV 196	Ranomafana, Maharira	MH422607	MH422661	
B. majori	ZMA 20068	Ranomafana, Maharira			AY848586
B. mandraka	ZCMV 5332	Ranomafana, Ambatolahy		MH422662	FJ559126
B. marojezensis	ZSM 108/2005 (FGZC 2857)	Marojejy	MH422608	MH422663	FJ559127
B. miadana	ZSM 5108/2005 (FGZC 2389)	Andohahela	MH422609	MH422664	FJ559141
B. microtympanum	ZSM 112/2005 (FGZC 2200)	Ambohitantely	AY341613	AY341670	FJ559129
B. miniatus	ZSM 142/2004 (FGZC 269)	Manantantely	MH422610	MH422665	AY848639
B. narinsi	ZCMV 09242	Ranomafana		KF611049	
B. narinsi	ZCMV 2976	Ranomafana			FJ559151
B. narinsi	ZSM 296/2006	Ranomafana	MH422611		
B. obscurus	ZCMV 347	Ranomafana, Ranomafanakely		MH422666	AY848606
B. obscurus	ZMA 20219	Ranomafana, Ranomafanakely			
B. occidentalis	ZCMV 5551	Isalo			
B. occidentalis	ZSM 44/2002	Near Antoetra	AY341620	AY341677	AY341720
B. opisthodon	ZCMV 462	Monombo	MH422612	MH422667	
B. opisthodon	ZFMK 70480	Cap Est			AF215331
B. pauliani	ZCMV 8044	Andasibe			
B. pauliani	ZSM 345/2000	Andasibe	EF100476	EF100469	AJ315924
B. periegetes	FGZC 2430	Andohahela	MH422613	MH422668	FJ559130
B. picturatus	ZSM 272/2006 (ZCMV 1457)	An'Ala, Vohimana	MH422614	MH422669	EU252140
B. piperatus	ZCMV 341	Ranomafana	MH422615	MH422670	
B. piperatus	ZSM 377/2004 (ZCMV 320)	Ranomafana			AY848627
B. popi	ZCMV 235	Ranomafana, Maharira	MH422616	MH422671	AY848535
B. popi	ZMA 20193	Ranomafana, Maharira			
B. praedictus	ZCMV 678	Vevembe	MH422617	MH422672	
B. praedictus	ZMA 20131				AY848528
B. pyrrhus	UADBA 24315	Ifanadiana			AY848645
B. pyrrhus	ZCMV 381	Ifanadiana	MH422618	MH422673	
B. quasiboehmei	ZCMV 2951	Ranomafana			

B. quasiboehmei	ZMB 79257	Ranomafana	KF991250		KF991270
B. quasiboehmei	ZSM 227/2006 (ZCMV 3045)	Ranomafana		MH422674	
B. rappiodes	FGMV 2002.540	Andasibe			
B. rappiodes	UADBA 2000.59	Andasibe			AJ314816
B. rappiodes	ZSM 347/2000	Andasibe	AY341618	AY341675	
B. reticulatus	FGMV 2002.3045	Vohidrazana			AY848612
B. reticulatus	KU 340673	Vohidrazana			
B. rhodoscelis	ZCMV 316	Ranomafana	MH422620	MH422675	AY848620
B. roseipalmatus	FGMV 2002/910	Montagne d'Ambre	MH422621		
B. roseipalmatus	ZSM 898/2003	Montagne d'Ambre			AF261266
B. rufioculis	2002 GA272	An'Ala			AY848623
B. sambirano	ZSM 810/2003 (FGMV 2002.707)	Manongarivo	MH422622	MH422676	AY848544
B. sandrae	ZCMV 352	Ranomafana	MH422623	MH422677	AY848442
B. sandrae	ZMA 20133	Ranomafana			
B. schuboeae	ZFMK 62907	Ranomafana			GU974830
B. septentrionalis	ZSM 900/2003 (FGMV 2002.912)	Montagne d'Ambre	MH422624	MH422678	AY848505
B. sibilans	ZSM 39/2002 (FGMV 2001.1273)	Andasibe	AY341615	AY341672	AY341718
B. solomaso	KU 340660	Vohidrazana			MH422692
B. solomaso	NMBE 1046008	Ambavaniasy			
B. sp Ca01	ZCMV 2000/F49	Mayotte, Comoros Islands		MH422679	
B. sp Ca01	ZSM 685/2000	Mayotte, Comoros Islands	AY341610		AY341716
B. sp Ca07	FGZC 2280	Marojejy			FJ559136
B. sp Ca10	FAZC 7331	Ambolokopatrika			AY848547
B. sp Ca21	FGZC 2201	Ambohitantely			FJ559143
B. sp Ca23	FGZC 2257	Marojejy			JQ518193
B. sp Ca24	MVTIS AC460 5591	Sahavontsira			FJ559145
B. sp Ca25	FGZC 2929	Marojejy			FJ559146
B. sp Ca26	FGZC 2953	Marojejy			FJ559147
B. sp Ca27	FAZC 7805	Masoala			FJ559148
B. sp Ca28	ZCMV 2062	Marojejy	MH422625	MH422680	FJ559149
B. sp Ca33	FGMV 2002.540	Antoetra	MH422626	MH422681	
B. sp Ca33	ZSM 731/2001	Andringitra			AY848601
B. sp Ca36	MVTIS LR294	Andasibe			DQ792467
B. sp Ca37	LR243	Andasibe			DQ792466
B. sp Ca38	KU 336890	Ranomafana			MH422693

B. sp Ca40	DRV 5635	Mahasoa Forest			FJ559155
B. sp Ca41	DRV 5665	Mahasoa Forest			FJ559156
B. sp Ca42	KU 340716	Ranomafana		MH422682	MH422694
B. sp Ca43	PSG 313	Toamasina			HM631885
B. sp Ca44	PSG 1518	Marolambo			HM631882
B. sp Ca46	ZCMV 3479	An Ala			JQ518195
B. sp Ca47	ZCMV 13105	Antsohihy-Bealanana			JQ518203
B. sp Ca48	ZCMV 13107	Antsohihy-Bealanana			JQ518206
B. sp Ca49	ZCMV 13155	Ankijagna Lalagna			JQ518208
B. sp Ca50	ZCMV 13173	Ambinanitelo			JQ518213
B. sp Ca51	KU 340730	Ranomafana		MH422683	MH422695
B. sp Ca52	2001 65	Tsaratanana			AY848595
B. sp Ca52	ZCMV 13168	Ambinanitelo			
B. sp Ca53	ZCMV 13203	Tsaratanana			
B. sp Ca54	DRV 6209	Tsaratanana			MH422696
B. sp Ca55	DRV 6293	Andrevorevo			
B. spinophis	ZCMV 691	Ranomafana (Ambatolahy)	MH422627	MH422684	AY848539
B. tampoka	ZSM 96/2006 (FGZC 869)	Tsingy de Bemaraha	MH422628	MH422685	EF682216
B. tasymena	ZCMV 207	Ranomafana, Maharira	MH422629	MH422686	
B. tasymena	ZMA 20241	Ranomafana, Maharira			AY848670
B. tephraeomystax	AMNH A168144	Ramena Valley			
B. tephraeomystax	KU 340936	Ranomafana	MH422630	MH422687	
B. tephraeomystax	UADBA 24183	Montagne d'Ambre			AY848508
B. tsilomaro	MRSN A2000	Berara	MH422631	MH422688	AJ314820
B. ulftunni	ZSM 80/2005 (FGZC 2879)	Illampy, Masoala	MH422632	MH422689	EU252142
B. viridis	FGMV 2001.A9 (UADBA 24363)	Manombo			AY848679
B. viridis	ZCMV 432	Manombo	MH422633	MH422690	
B. viridis	ZSM 338/2000	Andasibe			
B. vittatus	FGMV 2000.82 (UADBA)	Tsaratanana			
B. vittatus	ZSM 423/2005 (ZCMV 842)	Marojejy	AY341616	AY341673	AY341719
B. williamsi	ZSM 734/2001	Ankaratra	JN132838	JN132841	AY848624
B. xerophilus	KCW 134	Kirindy			MH422697
B. xerophilus	ZFMK 66705	Kirindy	AF249008	DQ346999	

Table S1 part 2. Mitochondrial GenBank markers used for Chapter 2 and Chapter 5.

Species	Voucher	Locality	CO1	Cyt-b	ND1
B. aff marojezensis	ZSM 189/2002	Vohidrazana			
B. aff marojezensis	ZSM 326/2000	Vohidrazana			
B. aff marojezensis	ZSM 330/2000	Vohidrazana		DQ235437	
B. aff picturatus	CRH 669	Ranomafana, Maharira			
B. aff picturatus	ZCMV 09867	Ranomafana			
B. aff picturatus	ZCMV 210	Ranomafana, Maharira	KF611422		
B. aff picturatus	ZCMV 5862	Ranomafana			
B. aff reticulatus	ZCMV 211	Ranomafana	JN133116	JN132908	MH422746
B. albilabris	FGMV 2002.807 (UADBA)	Manongarivo	JN133064	JN132855	
B. albilabris	RAX 2714	Tsaratanana			
B. albilabris	ZCMV 2808	Ambatolahy			MH422702
B. albipunctatus	ZSM 157/2004 (FGZC 291)	Manantantely	JN133066	JN132857	MH422703
B. andohahela	FGZC 2372	Andohahela	JN133067	JN132858	MH422704
B. andohahela	ZCMV 09900	Vatoharanana			
B. andrangoloaka	FGZC 2139	Ambohitantely	JN133118	JN132910	MH422705
B. andreonei	FGMV 2002.806	Manongarivo	JN133068	JN132859	MH422706
B. anjanaharibeensis	FGZC 2762	Marojejy	JN133069	JN132860	MH422707
B. ankarafensis	MRSN A6975	Sahamalaza			
B. ankaratra	KU 336830	Ranomafana, Maharira			
B. ankaratra	ZSM 367/2000 (FGMV 2000.68)	Manjakatompo	JN133070	JN132861	MH422708
B. arcanus	ZCMV 392 (UADBA 24299)	Mahakajy	JN133105	JN132896	MH422709
B. axelmeyeri	FGMV 2002.809	Manongarivo	JN133073	JN132864	MH422710
B. baetkei	FGZC 1391	Foret d'Ambre			
B. blommersae	FGMV 2002.925	Antakarana			MH422711
B. blommersae	ZSM 906/2003	Montagne d'Ambre	AY883982	JN132865	
B. boehmei	FGMV 201.1205 (UADBA)	Andasibe	JN133075	DQ235433	
B. boehmei	ZCMV 1490	Andasibe			MH422712
B. boppa	KU 336825	Ranomafana, Maharira			
B. bottae	ZSM 344/2000 (ZCMV 65)	Andasibe	JN133077	JN132867	MH422713
B. brachychir	FGMV 2002.702	Manongarivo	JN133078		
B. burgeri	FGMV 2001.1246	Andasibe	JN133080	JN132869	MH422714
B. burgeri	KU 340719	Vohidrazana			

B. calcaratus	NMBE 862/95	Ambavaniasy	JN133126	MH422700	
B. doulioti	FGZC 726	Tsingy de Bemaraha			MH422715
B. doulioti	FGZC 92	Tolagnaro	DQ116464		
B. doulioti	ZSM 29/2006	Tsingy de Bemaraha		JN132870	
B. elenae	UADBA 24141	Ranomafana, Maharira	JN133082	JN132871	
B. elenae	ZCMV 192	Ranomafana, Maharira			MH422716
B. englaenderi	ZSM 418/2005 (ZCMV 856)	Marojejy	JN133084	JN132873	MH422717
B. entingae	FGMV 2002.911	Montagne d'Ambre			
B. entingae	ZSM 899/2003	Montagne d'Ambre	JN133079	JN132868	
B. erythrodactylus	CRH 422 (UADBA)	Vohidrazana			
B. erythrodactylus	ZSM 342/2000	Mandraka	JN133085	JN132874	
B. fayi	MRSN A6596	Betampona			
B. feonnyala	ZSM 313/2000	Andasibe	JN133086	JN132875	
B. goudotii	FMGV 2002.45	Antoetra	AY883989		MH422718
B. goudotii	ZMA 19544	Antoetra		JN132876	
B. guibei	KU 340594	Andasibe			
B. guibei	ZSM 348/2000 (FGMV 2000-50, A9)	Andasibe	DQ116467		MH422719
B. haematopus	ZSM 120/2004 (FGZC 215)	Andohahela	JN133087	JN132878	MH422720
B. haingana	ZSM 5109/2005 (FGZC 2390)	Andohahela	JN133071	JN132862	MH422721
B. idae	ZSM 45/2002	Andasibe	JN133088	JN132879	MH422722
B. jaegeri	ZSM 587/2001 (2002.F24)	Nosy Be	JN133089	JN132880	MH422723
B. laurenti	ZSM 727/2001 (MV 2001 535, C34)	Andringitra	JN133090	JN132881	MH422724
B. liami	ZSM 310/2000 (MV 2001 A4)	Vohidrazana	JN133091	JN132882	MH422725
B. lichenoides	FAZC 5679	Sahavontsira	JN133092		
B. lilianae	ZSM 201/2006 (ZCMV 2864)	Ifanadiana	JN133115	JN132907	MH422726
B. luciae	KU 340828	Ranomafana, Miranony			
B. luciae	ZCMV 0687	Ranomafana, Ambatolahy			MH422727
B. luciae	ZMA 20306	Ranomafana, Ambatolahy	JN133125	JN132917	
B. luteus	FGMV 2000.063 (UADBA)	Andasibe		DQ235434	MH422728
B. luteus	FGMV 2001.A24	Mandraka	DQ116468		
B. luteus	FGMV 2002.1612	Andasibe			

B. madagascariensis	CRH 415 (UADBA)	Vohidrazana			
B. madagascariensis	mtGenome (Kurabayashi)	Unknown		AB239571	AB239572
B. madagascariensis	ZCMV 344	Ranomafana	JN133095		
B. majori	ZCMV 196	Ranomafana, Maharira			MH422729
B. majori	ZMA 20068	Ranomafana, Maharira	JN133097	JN132887	
B. mandraka	ZCMV 5332	Ranomafana, Ambatolahy	JN133099	JN132889	MH422730
B. marojezensis	ZSM 108/2005 (FGZC 2857)	Marojejy	JN133102	JN132892	MH422731
B. miadana	ZSM 5108/2005 (FGZC 2389)	Andohahela	JN133072	JN132863	MH422732
B. microtympanum	ZSM 112/2005 (FGZC 2200)	Ambohitantely	JN133103	JN132893	
B. miniatus	ZSM 142/2004 (FGZC 269)	Manantantely	KF611419	JN132895	MH422733
B. narinsi	ZCMV 09242	Ranomafana			
B. narinsi	ZCMV 2976	Ranomafana	JN133098	JN132888	
B. narinsi	ZSM 296/2006	Ranomafana			MH422734
B. obscurus	ZCMV 347	Ranomafana, Ranomafanakely			MH422735
B. obscurus	ZMA 20219	Ranomafana, Ranomafanakely	DQ116471	JN132902	
B. occidentalis	ZCMV 5551	Isalo			MH422736
B. occidentalis	ZSM 44/2002	Near Antoetra	JN133106	EF100457	
B. opisthodon	ZCMV 462	Monombo			MH422737
B. opisthodon	ZFMK 70480	Cap Est	JN133108	JN132899	
B. pauliani	ZCMV 8044	Andasibe			MH422738
B. pauliani	ZSM 345/2000	Andasibe	JN133109	EF100458	
B. periegetes	FGZC 2430	Andohahela	JN133110	JN132901	MH422739
B. picturatus	ZSM 272/2006 (ZCMV 1457)	An'Ala, Vohimana	JN133111	JN132903	MH422740
B. piperatus	ZCMV 341	Ranomafana			MH422741
B. piperatus	ZSM 377/2004 (ZCMV 320)	Ranomafana	JN133119	JN132911	
B. popi	ZCMV 235	Ranomafana, Maharira			
B. popi	ZMA 20193	Ranomafana, Maharira	JN133121	JN132913	
B. praedictus	ZCMV 678	Vevembe			MH422742
B. praedictus	ZMA 20131		JN133065	JN132856	
B. pyrrhus	UADBA 24315	Ifanadiana	JN133112	JN132904	
B. pyrrhus	ZCMV 381	Ifanadiana			MH422743
B. quasiboehmei	ZCMV 2951	Ranomafana			

B. quasiboehmei	ZMB 79257	Ranomafana			
B. quasiboehmei	ZSM 227/2006 (ZCMV 3045)	Ranomafana	JN133076	MH422701	MH422744
B. rappiodes	FGMV 2002.540	Andasibe	KF611423		
B. rappiodes	UADBA 2000.59	Andasibe			MH422745
B. rappiodes	ZSM 347/2000	Andasibe		DQ235438	
B. reticulatus	FGMV 2002.3045	Vohidrazana	KF611424		
B. reticulatus	KU 340673	Vohidrazana			
B. rhodoscelis	ZCMV 316	Ranomafana	JN133117	JN132909	MH422747
B. roseipalmatus	FGMV 2002/910	Montagne d'Ambre			MH422748
B. roseipalmatus	ZSM 898/2003	Montagne d'Ambre	JN133096	JN132886	
B. rufioculis	2002 GA272	An'Ala	JN133120	JN132912	
B. sambirano	ZSM 810/2003 (FGMV 2002.707)	Manongarivo	JN133122	JN132914	
B. sandrae	ZCMV 352	Ranomafana			
B. sandrae	ZMA 20133	Ranomafana	JN133083	JN132872	
B. schuboeae	ZFMK 62907	Ranomafana	JN133123	JN132915	
B. septentrionalis	ZSM 900/2003 (FGMV 2002.912)	Montagne d'Ambre	JN133124	JN132916	MH422749
B. sibilans	ZSM 39/2002 (FGMV 2001.1273)	Andasibe	DQ116475	DQ235435	
B. solomaso	KU 340660	Vohidrazana			
B. solomaso	NMBE 1046008	Ambavaniasy	JN133127	JN132919	
B. sp Ca01	ZCMV 2000/F49	Mayotte, Comoros Islands	MH422698		MH422750
B. sp Ca01	ZSM 685/2000	Mayotte, Comoros Islands		AY341733	
B. sp Ca07	FGZC 2280	Marojejy			
B. sp Ca10	FAZC 7331	Ambolokopatri ka			
B. sp Ca21	FGZC 2201	Ambohitantely			
B. sp Ca23	FGZC 2257	Marojejy			
B. sp Ca24	MVTIS AC460 5591	Sahavontsira			
B. sp Ca25	FGZC 2929	Marojejy			
B. sp Ca26	FGZC 2953	Marojejy			
B. sp Ca27	FAZC 7805	Masoala	JN133101	JN132891	
B. sp Ca28	ZCMV 2062	Marojejy	JN133100	JN132890	
B. sp Ca33	FGMV 2002.540	Antoetra			MH422751
B. sp Ca33	ZSM 731/2001	Andringitra	AY883991	JN132894	
B. sp Ca36	MVTIS LR294	Andasibe			
B. sp Ca37	LR243	Andasibe			
B. sp Ca38	KU 336890	Ranomafana			

B. sp Ca40	DRV 5635	Mahasoa Forest	KF611432		
B. sp Ca41	DRV 5665	Mahasoa Forest	KF611431		
B. sp Ca42	KU 340716	Ranomafana			
B. sp Ca43	PSG 313	Toamasina			
B. sp Ca44	PSG 1518	Marolambo			
B. sp Ca46	ZCMV 3479	An Ala			
B. sp Ca47	ZCMV 13105	Antsohihy-Bealanana	KF611426		
B. sp Ca48	ZCMV 13107	Antsohihy-Bealanana			
B. sp Ca49	ZCMV 13155	Ankijagna Lalagna	KF611427		
B. sp Ca50	ZCMV 13173	Ambinanitelo	KF611428		
B. sp Ca51	KU 340730	Ranomafana			
B. sp Ca52	2001 65	Tsaratanana			
B. sp Ca52	ZCMV 13168	Ambinanitelo	KF611429		
B. sp Ca53	ZCMV 13203	Tsaratanana	KF611430		
B. sp Ca54	DRV 6209	Tsaratanana	KF611433		
B. sp Ca55	DRV 6293	Andrevorevo	KF611413		
B. spinophis	ZCMV 691	Ranomafana (Ambatolahy)	MH422699	JN132883	MH422752
B. tampoka	ZSM 96/2006 (FGZC 869)	Tsingy de Bemaraha	JN133128	JN132920	MH422753
B. tasymena	ZCMV 207	Ranomafana, Maharira			MH422754
B. tasymena	ZMA 20241	Ranomafana, Maharira	DQ116476	JN132921	
B. tephraeomystax	AMNH A168144	Ramena Valley			
B. tephraeomystax	KU 340936	Ranomafana			MH422755
B. tephraeomystax	UADBA 24183	Montagne d'Ambre	JN133129	JN132922	
B. tsilomaro	MRSN A2000	Berara	JN133107	JN132898	MH422756
B. ulftunni	ZSM 80/2005 (FGZC 2879)	Illampy, Masoala	JN133114	JN132906	MH422757
B. viridis	FGMV 2001.A9 (UADBA 24363)	Manombo	JN133130		
B. viridis	ZCMV 432	Manombo			MH422758
B. viridis	ZSM 338/2000	Andasibe		DQ235439	
B. vittatus	FGMV 2000.82 (UADBA)	Tsaratanana		DQ235436	
B. vittatus	ZSM 423/2005 (ZCMV 842)	Marojejy	JN133131		MH422759
B. williamsi	ZSM 734/2001	Ankaratra	JN133132	JN132925	MH422760
B. xerophilus	KCW 134	Kirindy			MH422761
B. xerophilus	ZFMK 66705	Kirindy		AF249069	

Table S2 part 1. Nuclear GenBank markers used for Chapter 2 and Chapter 5.

Species	Voucher	rag2	rhod
B. aff marojezensis	ZSM 189/2002		AY341803
B. aff marojezensis	ZSM 326/2000		
B. aff marojezensis	ZSM 330/2000		
B. aff picturatus	CRH 669	MH422935	
B. aff picturatus	ZCMV 09867		
B. aff picturatus	ZCMV 210		
B. aff picturatus	ZCMV 5862		
B. aff reticulatus	ZCMV 211	MH422941	
B. albilabris	FGMV 2002.807 (UADBA)		
B. albilabris	RAX 2714		DQ283762
B. albilabris	ZCMV 2808	MH422902	
B. albipunctatus	ZSM 157/2004 (FGZC 291)	MH422903	
B. andohahela	FGZC 2372		
B. andohahela	ZCMV 09900		
B. andrangoloaka	FGZC 2139	MH422904	
B. andreonei	FGMV 2002.806	MH422905	
B. anjanaharibeensis	FGZC 2762	MH422906	
B. ankarafensis	MRSN A6975		
B. ankaratra	KU 336830		
B. ankaratra	ZSM 367/2000 (FGMV 2000.68)	MH422907	
B. arcanus	ZCMV 392 (UADBA 24299)	MH422908	
B. axelmeyeri	FGMV 2002.809	MH422909	
B. baetkei	FGZC 1391	MH422910	
B. blommersae	FGMV 2002.925	MH422911	
B. blommersae	ZSM 906/2003		
B. boehmei	FGMV 201.1205 (UADBA)	EF100488	AY341798
B. boehmei	ZCMV 1490		
B. boppa	KU 336825		
B. bottae	ZSM 344/2000 (ZCMV 65)	MH422912	
B. brachychir	FGMV 2002.702		
B. burgeri	FGMV 2001.1246	MH422913	
B. burgeri	KU 340719		
B. calcaratus	NMBE 862/95		
B. doulioti	FGZC 726		
B. doulioti	FGZC 92		

B. doulioti	ZSM 29/2006	DQ019519	AY341792
B. elenae	UADBA 24141		
B. elenae	ZCMV 192		
B. englaenderi	ZSM 418/2005 (ZCMV 856)	MH422914	
B. entingae	FGMV 2002.911		
B. entingae	ZSM 899/2003		
B. erythrodactylus	CRH 422 (UADBA)		
B. erythrodactylus	ZSM 342/2000		
B. fayi	MRSN A6596		
B. feonnyala	ZSM 313/2000		
B. goudotii	FMGV 2002.45	MH422915	
B. goudotii	ZMA 19544		AY341797
B. guibei	KU 340594	MH422916	
B. guibei	ZSM 348/2000 (FGMV 2000-50, A9)		
B. haematopus	ZSM 120/2004 (FGZC 215)	MH422917	
B. haingana	ZSM 5109/2005 (FGZC 2390)	MH422918	
B. idae	ZSM 45/2002	EF100489	AY341795
B. jaegeri	ZSM 587/2001 (2002.F24)	MH422919	
B. laurenti	ZSM 727/2001 (MV 2001 535, C34)	MH422920	
B. liami	ZSM 310/2000 (MV 2001 A4)	MH422921	
B. lichenoides	FAZC 5679	MH422922	
B. lilianae	ZSM 201/2006 (ZCMV 2864)	MH422923	
B. luciae	KU 340828		
B. luciae	ZCMV 0687	MH422924	
B. luciae	ZMA 20306		
B. luteus	FGMV 2000.063 (UADBA)	EF100490	AY341800
B. luteus	FGMV 2001.A24		
B. luteus	FGMV 2002.1612		
B. madagascariensis	CRH 415 (UADBA)		
B. madagascariensis	mtGenome (Kurabayashi)		
B. madagascariensis	ZCMV 344		
B. majori	ZCMV 196	MH422925	
B. majori	ZMA 20068		
B. mandraka	ZCMV 5332	MH422926	
B. marojezensis	ZSM 108/2005 (FGZC 2857)	MH422927	
B. miadana	ZSM 5108/2005 (FGZC 2389)	MH422928	
B. microtympanum	ZSM 112/2005 (FGZC 2200)	EF100491	AY341799

B. miniatus	ZSM 142/2004 (FGZC 269)	MH422929	
B. narinsi	ZCMV 09242		
B. narinsi	ZCMV 2976		
B. narinsi	ZSM 296/2006	MH422930	
B. obscurus	ZCMV 347	MH422931	
B. obscurus	ZMA 20219		
B. occidentalis	ZCMV 5551		
B. occidentalis	ZSM 44/2002	EF100492	AY341806
B. opisthodon	ZCMV 462	MH422932	
B. opisthodon	ZFMK 70480		
B. pauliani	ZCMV 8044		
B. pauliani	ZSM 345/2000	EF100493	EF100482
B. periegetes	FGZC 2430	MH422933	
B. picturatus	ZSM 272/2006 (ZCMV 1457)	MH422934	
B. piperatus	ZCMV 341	MH422936	
B. piperatus	ZSM 377/2004 (ZCMV 320)		
B. popi	ZCMV 235		
B. popi	ZMA 20193		
B. praedictus	ZCMV 678	MH422937	
B. praedictus	ZMA 20131		
B. pyrrhus	UADBA 24315		
B. pyrrhus	ZCMV 381	MH422938	
B. quasiboehmei	ZCMV 2951		
B. quasiboehmei	ZMB 79257		
B. quasiboehmei	ZSM 227/2006 (ZCMV 3045)	MH422939	
B. rappiodes	FGMV 2002.540		
B. rappiodes	UADBA 2000.59	MH422940	
B. rappiodes	ZSM 347/2000		AY341804
B. reticulatus	FGMV 2002.3045		
B. reticulatus	KU 340673		
B. rhodoscelis	ZCMV 316	MH422942	
B. roseipalmatus	FGMV 2002/910	MH422943	
B. roseipalmatus	ZSM 898/2003		
B. rufioculis	2002 GA272		
B. sambirano	ZSM 810/2003 (FGMV 2002.707)	MH422944	
B. sandrae	ZCMV 352	MH422945	
B. sandrae	ZMA 20133		
B. schuboeae	ZFMK 62907		
B. septentrionalis	ZSM 900/2003 (FGMV 2002.912)	MH422946	
B. sibilans	ZSM 39/2002 (FGMV 2001.1273)	MH422947	AY341801

B. solomaso	KU 340660		
B. solomaso	NMBE 1046008		
B. sp Ca01	ZCMV 2000/F49		
B. sp Ca01	ZSM 685/2000		AY341796
B. sp Ca07	FGZC 2280		
B. sp Ca10	FAZC 7331		
B. sp Ca21	FGZC 2201		
B. sp Ca23	FGZC 2257		
B. sp Ca24	MVTIS AC460 5591		
B. sp Ca25	FGZC 2929		
B. sp Ca26	FGZC 2953		
B. sp Ca27	FAZC 7805		
B. sp Ca28	ZCMV 2062	MH422948	
B. sp Ca33	FGMV 2002.540	MH422949	
B. sp Ca33	ZSM 731/2001		
B. sp Ca36	MVTIS LR294		
B. sp Ca37	LR243		
B. sp Ca38	KU 336890		
B. sp Ca40	DRV 5635		
B. sp Ca41	DRV 5665		
B. sp Ca42	KU 340716	MH422950	
B. sp Ca43	PSG 313		
B. sp Ca44	PSG 1518		
B. sp Ca46	ZCMV 3479		
B. sp Ca47	ZCMV 13105		
B. sp Ca48	ZCMV 13107		
B. sp Ca49	ZCMV 13155		
B. sp Ca50	ZCMV 13173		
B. sp Ca51	KU 340730		
B. sp Ca52	2001 65		
B. sp Ca52	ZCMV 13168		
B. sp Ca53	ZCMV 13203		
B. sp Ca54	DRV 6209		
B. sp Ca55	DRV 6293		
B. spinophis	ZCMV 691	MH422951	
B. tampoka	ZSM 96/2006 (FGZC 869)		
B. tasymena	ZCMV 207	MH422952	
B. tasymena	ZMA 20241		
B. tephraeomystax	AMNH A168144		DQ283761
B. tephraeomystax	KU 340936		

B. tephraeomystax	UADBA 24183		
B. tsilomaro	MRSN A2000	MH422953	
B. ulftunni	ZSM 80/2005 (FGZC 2879)	MH422954	
B. viridis	FGMV 2001.A9 (UADBA 24363)	EF100494	AY341805
B. viridis	ZCMV 432		
B. viridis	ZSM 338/2000		
B. vittatus	FGMV 2000.82 (UADBA)		
B. vittatus	ZSM 423/2005 (ZCMV 842)	JN132827	AY341802
B. williamsi	ZSM 734/2001	JN132828	JN132834
B. xerophilus	KCW 134	MH422955	
B. xerophilus	ZFMK 66705		AY341794

Table S2 part 2. Nuclear GenBank markers used for Chapter 2 and Chapter 5.

Species	Voucher	DNAH3	POMC	RAG1
B. aff marojezensis	ZSM 189/2002			
B. aff marojezensis	ZSM 326/2000			
B. aff marojezensis	ZSM 330/2000			
B. aff picturatus	CRH 669			MH422880
B. aff picturatus	ZCMV 09867		JX863655	
B. aff picturatus	ZCMV 210			
B. aff picturatus	ZCMV 5862			
B. aff reticulatus	ZCMV 211		MH422819	MH422884
B. albilabris	FGMV 2002.807 (UADBA)			
B. albilabris	RAX 2714			
B. albilabris	ZCMV 2808			MH422847
B. albipunctatus	ZSM 157/2004 (FGZC 291)		MH422796	MH422848
B. andohahela	FGZC 2372	MH422762		MH422849
B. andohahela	ZCMV 09900			
B. andrangoloaka	FGZC 2139	MH422763	MH422797	MH422850
B. andreonei	FGMV 2002.806			MH422851
B. anjanaharibeensis	FGZC 2762	MH422764		MH422852
B. ankarafensis	MRSN A6975			
B. ankaratra	KU 336830	KT588046	MH422798	MH422853
B. ankaratra	ZSM 367/2000 (FGMV 2000.68)			
B. arcanus	ZCMV 392 (UADBA 24299)	MH422765	MH422799	MH422854
B. axelmeyeri	FGMV 2002.809			
B. baetkei	FGZC 1391	MH422766		
B. blommersae	FGMV 2002.925		MH422800	MH422855
B. blommersae	ZSM 906/2003			
B. boehmei	FGMV 201.1205 (UADBA)			
B. boehmei	ZCMV 1490		HQ380152	HQ380163
B. boppa	KU 336825	KT588049		
B. bottae	ZSM 344/2000 (ZCMV 65)	MH422767		
B. brachychir	FGMV 2002.702			
B. burgeri	FGMV 2001.1246			
B. burgeri	KU 340719		MH422801	
B. calcaratus	NMBE 862/95			MH422856
B. doulioti	FGZC 726		MH422802	MH422857
B. doulioti	FGZC 92			

B. doulioti	ZSM 29/2006			
B. elenae	UADBA 24141			
B. elenae	ZCMV 192	MH422768	MH422803	MH422858
B. englaenderi	ZSM 418/2005 (ZCMV 856)	MH422769	MH422804	MH422859
B. entingae	FGMV 2002.911			
B. entingae	ZSM 899/2003			
B. erythrodactylus	CRH 422 (UADBA)	MH422770	MH422805	
B. erythrodactylus	ZSM 342/2000			
B. fayi	MRSN A6596			
B. feonnyala	ZSM 313/2000			
B. goudotii	FMGV 2002.45			MH422860
B. goudotii	ZMA 19544			
B. guibei	KU 340594	MH422771	MH422806	MH422861
B. guibei	ZSM 348/2000 (FGMV 2000-50, A9)			
B. haematopus	ZSM 120/2004 (FGZC 215)	MH422772		MH422862
B. haingana	ZSM 5109/2005 (FGZC 2390)	KT588042	MH422807	MH422863
B. idae	ZSM 45/2002		MH422808	MH422864
B. jaegeri	ZSM 587/2001 (2002.F24)	MH422773	MH422809	MH422865
B. laurenti	ZSM 727/2001 (MV 2001 535, C34)			MH422866
B. liami	ZSM 310/2000 (MV 2001 A4)	KT588043	MH422810	MH422867
B. lichenoides	FAZC 5679	MH422774	MH422811	MH422868
B. lilianae	ZSM 201/2006 (ZCMV 2864)			
B. luciae	KU 340828		MH422812	
B. luciae	ZCMV 0687	KT588044		MH422869
B. luciae	ZMA 20306			
B. luteus	FGMV 2000.063 (UADBA)	MH422775	MH422813	MH422870
B. luteus	FGMV 2001.A24			
B. luteus	FGMV 2002.1612			
B. madagascariensis	CRH 415 (UADBA)		MH422814	
B. madagascariensis	mtGenome (Kurabayashi)			
B. madagascariensis	ZCMV 344			
B. majori	ZCMV 196	MH422776	MH422815	JX863576
B. majori	ZMA 20068			
B. mandraka	ZCMV 5332			MH422871
B. marojezensis	ZSM 108/2005 (FGZC 2857)			MH422872
B. miadana	ZSM 5108/2005 (FGZC 2389)	KT588045		MH422873
B. microtympanum	ZSM 112/2005 (FGZC 2200)			

B. miniatus	ZSM 142/2004 (FGZC 269)	MH422777		MH422874
B. narinsi	ZCMV 09242			
B. narinsi	ZCMV 2976			
B. narinsi	ZSM 296/2006		JX863652	JX863595
B. obscurus	ZCMV 347	MH422778	MH422816	MH422875
B. obscurus	ZMA 20219			
B. occidentalis	ZCMV 5551			MH422876
B. occidentalis	ZSM 44/2002			
B. opisthodon	ZCMV 462	MH422779		MH422877
B. opisthodon	ZFMK 70480			
B. pauliani	ZCMV 8044			MH422878
B. pauliani	ZSM 345/2000			
B. periegetes	FGZC 2430			MH422879
B. picturatus	ZSM 272/2006 (ZCMV 1457)	MH422780		
B. piperatus	ZCMV 341	MH422781		MH422881
B. piperatus	ZSM 377/2004 (ZCMV 320)			
B. popi	ZCMV 235	MH422782	MH422817	
B. popi	ZMA 20193			
B. praedictus	ZCMV 678			MH422882
B. praedictus	ZMA 20131			
B. pyrrhus	UADBA 24315			
B. pyrrhus	ZCMV 381			MH422883
B. quasiboehmei	ZCMV 2951		HQ380153	HQ380164
B. quasiboehmei	ZMB 79257			
B. quasiboehmei	ZSM 227/2006 (ZCMV 3045)			
B. rappiodes	FGMV 2002.540			
B. rappiodes	UADBA 2000.59			
B. rappiodes	ZSM 347/2000			
B. reticulatus	FGMV 2002.3045			
B. reticulatus	KU 340673	MH422783	MH422818	
B. rhodoscelis	ZCMV 316		MH422820	MH422885
B. roseipalmatus	FGMV 2002/910	MH422784	MH422821	MH422886
B. roseipalmatus	ZSM 898/2003			
B. rufioculis	2002 GA272			
B. sambirano	ZSM 810/2003 (FGMV 2002.707)	MH422785	MH422822	MH422887
B. sandrae	ZCMV 352		MH422823	MH422888
B. sandrae	ZMA 20133			
B. schuboeae	ZFMK 62907			
B. septentrionalis	ZSM 900/2003 (FGMV 2002.912)			MH422889
B. sibilans	ZSM 39/2002 (FGMV 2001.1273)	KT588052	MH422824	MH422890

B. solomaso	KU 340660	MH422786	MH422825	
B. solomaso	NMBE 1046008			
B. sp Ca01	ZCMV 2000/F49	MH422787	MH422826	
B. sp Ca01	ZSM 685/2000			JQ073260
B. sp Ca07	FGZC 2280			
B. sp Ca10	FAZC 7331			
B. sp Ca21	FGZC 2201			
B. sp Ca23	FGZC 2257			
B. sp Ca24	MVTIS AC460 5591			
B. sp Ca25	FGZC 2929			
B. sp Ca26	FGZC 2953			
B. sp Ca27	FAZC 7805			
B. sp Ca28	ZCMV 2062	MH422788		MH422891
B. sp Ca33	FGMV 2002.540			MH422892
B. sp Ca33	ZSM 731/2001			
B. sp Ca36	MVTIS LR294			
B. sp Ca37	LR243			
B. sp Ca38	KU 336890			
B. sp Ca40	DRV 5635			
B. sp Ca41	DRV 5665			
B. sp Ca42	KU 340716		MH422827	
B. sp Ca43	PSG 313			
B. sp Ca44	PSG 1518			
B. sp Ca46	ZCMV 3479			
B. sp Ca47	ZCMV 13105			
B. sp Ca48	ZCMV 13107			
B. sp Ca49	ZCMV 13155			
B. sp Ca50	ZCMV 13173			
B. sp Ca51	KU 340730		MH422828	MH422893
B. sp Ca52	2001 65			
B. sp Ca52	ZCMV 13168			
B. sp Ca53	ZCMV 13203			
B. sp Ca54	DRV 6209			
B. sp Ca55	DRV 6293			
B. spinophis	ZCMV 691	MH422789	MH422829	MH422894
B. tampoka	ZSM 96/2006 (FGZC 869)	MH422790	MH422830	MH422895
B. tasymena	ZCMV 207	MH422791		MH422896
B. tasymena	ZMA 20241			
B. tephraeomystax	AMNH A168144			
B. tephraeomystax	KU 340936		MH422831	MH422897

B. tephraeomystax	UADBA 24183			
B. tsilomaro	MRSN A2000		MH422832	MH422898
B. ulftunni	ZSM 80/2005 (FGZC 2879)		MH422833	MH422899
B. viridis	FGMV 2001.A9 (UADBA 24363)			
B. viridis	ZCMV 432	MH422792	MH422834	
B. viridis	ZSM 338/2000			
B. vittatus	FGMV 2000.82 (UADBA)			
B. vittatus	ZSM 423/2005 (ZCMV 842)	MH422793		MH422900
B. williamsi	ZSM 734/2001	MH422794	MH422835	MH422901
B. xerophilus	KCW 134	MH422795	MH422836	
B. xerophilus	ZFMK 66705			AY364209

Table S3. Summary of primers and their reference used for this study. Thermal profiles used can be found in the original reference for each marker. If more than one forward and reverse primer is given, different combinations were used for amplification.

Marker	Reference	Primer
12S	Glaw and Vences, 2006	12SAL: 5'-AAACTGGGATTAGATACCCCACTAT-3' 12SBH: 5'-GAGGGTGACGGGCGGTGTGT-3'
16S (part 1)	Glaw and Vences, 2006	16SAL : 5'-CGCCTGTTTATCAAAAACAT-3' 16SBH : 5'-CCGGTCTGAACTCAGATCACGT-3'
16S (part 2)	Vences et al., 2012; Palumbi et al., 1991	16Sar: 5'-CGC CTG TTT ATC AAA AAC AT-3' 16Sab: 5'-CCG GTY TGA ACT CAG ATC AYG T-3'
CO1	Meyer et al., 2005; Perl et al., 2014	dgLCO1490: 5'-GGTCAACAAATCATAAAGAYATYGG-3' dgHCO2198: 5'-TAAACTTCAGGGTGACCAAARAAYCA-3'
Cyt-b	-	Only GenBank sequences used
ND1	Wiens et al., 2005	16S-frog: 5'-TTACCCTRGGGATAACAGCGCAA -3' tMet-frog: 5'-TTGGGGTATGGGCCCAAAAGCT -3'
DNAH3 (PCR 1)	Zheng et al., 2013	DNAH3: 5'-AATGTKTCNTCNGCNTGYGARGG-3' DNAH3: 5'-GTTKGCCARRTCNGADATRCARAA-3'
DNAH3 (PCR 2)	-	DNAH3: 5'-AGGGTTTTCCCAGTCACGACAAGTGGGTGMGNGCNATGGARGT-3' DNAH3: 5'-AGATAACAATTTCACACAGGTTYTCYTCYARYTCNGGYTTYTC-3'
POMC	Vieites et al., 2007	DRV F1: 5'- ATATGTCATGASCCAYTTYCGCTGGAA-3' DRV R1: 5'- GGCRTTYTTGAAWAGAGTCATTAGWGG-3'
RAG1	Chiari et al., 2004	RAG1 F1: 5'-ACNGGNMGICARATCTTYCARCC-3' RAG1 R1: 5'-GGTGYTTYAACACATCTTCCATYTCRTA-3'
RAG2 (PCR 1)	Wollenburg et al., 2011	31FN.Venk : 5'-TTYGGICARAARGGITGGCC-3' Rag2Lung.460R : 5'-GCATYGRGCATGGACCCARTGICC-3'
RAG2 (PCR 2)	-	Rag2A.F35 : 5'- TGG CCI AAA MGI TCY TGY CCM ACWGG-3' Rag2.Lung.35F: 5'-GGCCAAAGAGRTCYTGTCCIACTGG-3'
rhodopsin (exon 1)	-	Only GenBank sequences used

Table S4. PartionFinder2 partitions and best fitting models for each analysis. Protein-coding genes were partitioned by codon position. The underscore followed by a 1–3 indicates codon partition of that marker.

BEAST (all data, concatenated)

model	partitions
GTR+G	16S p1, 16S p2, 12S
GTR+G	CO1 1
HKY+I	CO1 2
TRN+G	CO1 3
SYM+G	nd1 1, cytb 1
GTR+G	cytb 2, rhod 3
HKY+G	cytb 3
TRN+G	rag1 2, rag2 2, dnah3 1, rag1 1, rag2 1, pomc 1, pomc 2
TRN+I	rhod 1, rhod 2, dnah3 2
HKY+G	dnah3 3
GTR+G	nd1 2
TRN+G	nd1 3
HKY+G	pomc 3, rag2 3, rag1 3

RAxML (all data, concatenated)

GTR+G	All partitions

Table S5 part 1. The different phenotypic trait codings used in Chapter 2 are shown. Coding definitions: Ventral Transparency: 0 = absence; 1 = presence (either partial or fully). Dorsal Color: 0 = brown / other; 1 = green. Elevational analyses: Lower, Upper, Midpoint: elevational distributions in meters.

Species	Ventral Transparency	Dorsal Color
Boophis albilabris	0	1
Boophis occidentalis	0	1
Boophis praedictus	0	1
Boophis tsilomaro	0	1
Boophis albipunctatus	1	1
Boophis ankaratra	1	1
Boophis boppa	1	1
Boophis haingana	1	1
Boophis luciae	1	1
Boophis miadana	1	1
Boophis schuboeae	1	1
Boophis sibilans	1	1
Boophis axelmeyeri	0	0
Boophis boehmei	0	0
Boophis brachychir	0	0
Boophis burgeri	0	0
Boophis entingae	0	0
Boophis fayi	0	0
Boophis goudotii	0	0
Boophis madagascariensis	0	0
Boophis obscurus	0	0
Boophis periegetes	0	0
Boophis popi	0	0
Boophis quasiboehmei	0	0
Boophis reticulatus	0	0
Boophis rufioculis	0	0
Boophis sp Ca07 Marojejy	-	-
Boophis sp Ca10 Ambolokopatrika	-	-
Boophis sp Ca40 Mahasoa Forest	-	-
Boophis sp Ca41 Mahasoa Forest	-	-
Boophis sp Ca42 Ranomafana	0	0
Boophis sp Ca43 Toamasina Sahafina	-	-
Boophis aff reticulatus	0	0
Boophis spinophis	0	0
Boophis roseipalmatus	0	0

Boophis andohahela	0	1
Boophis andreonei	0	1
Boophis anjanaharibeensis	0	1
Boophis elenae	0	1
Boophis englaenderi	0	1
Boophis jaegeri	0	1
Boophis luteus	0	1
Boophis sandrae	0	1
Boophis septentrionalis	0	1
Boophis sp Ca21 Ambohitantely	-	-
Boophis sp Ca23 Marojejy	-	-
Boophis sp Ca24 Sahavontsira	-	-
Boophis sp Ca36 Andasibe	0	1
Boophis sp Ca37 Andasibe	-	-
Boophis tampoka	0	1
Boophis arcanus	0	0
Boophis baetkei	0	1
Boophis feonnyala	0	0
Boophis haematopus	0	0
Boophis lilianae	0	1
Boophis majori	0	0
Boophis miniatus	0	0
Boophis narinsi	0	0
Boophis picturatus	0	0
Boophis piperatus	0	0
Boophis pyrrhus	0	0
Boophis sp Ca44 Marolambo	-	-
Boophis aff picturatus	0	0
Boophis ulftunni	0	1
Boophis liami	1	1
Boophis mandraka	1	1
Boophis sambirano	1	1
Boophis solomaso	1	1
Boophis sp Ca27 Masoala	-	-
Boophis sp Ca28 Marojejy	1	1
Boophis sp Ca38 Ranomafana	1	1
Boophis sp Ca46 An Ala	1	1
Boophis sp Ca47 Antsohihy Bealanana Ranomafana	-	-
Boophis sp Ca48 Antsohihy Bealanana	-	-
Boophis sp Ca49 Ankijagna Lalagna	-	-

Boophis sp Ca50 Ambinanitelo	-	-
Boophis sp Ca54 Tsaratanana	-	-
Boophis blommersae	0	0
Boophis marojezensis	0	0
Boophis sp Ca25 Marojejy	0	0
Boophis sp Ca26 Marojejy	-	-
Boophis sp Ca51 Ranomafana	0	0
Boophis sp Ca52 Tsaratanana	-	-
Boophis sp Ca52 Ambinanitelo	-	-
Boophis sp Ca53 Tsaratanana	-	-
Boophis sp Ca55 Andrevorevo	-	-
Boophis sp Ca68 Vohidrazana	0	0
Boophis vittatus	0	0
Boophis andrangoloaka	0	0
Boophis laurenti	0	0
Boophis microtympanum	0	0
Boophis rhodoscelis	0	0
Boophis sp Ca33 Andringitra Antoetra	0	0
Boophis williamsi	0	0
Boophis ankarafensis	1	1
Boophis bottae	1	1
Boophis erythrodactylus	1	1
Boophis rappiodes	1	1
Boophis tasymena	1	1
Boophis viridis	1	1
Boophis calcaratus	0	0
Boophis doulioti	0	0
Boophis guibei	0	0
Boophis idae	0	0
Boophis lichenoides	0	0
Boophis opisthodon	0	0
Boophis pauliani	1	1
Boophis sp Ca01 Mayotte	0	0
Boophis tephraeomystax	0	0
Boophis xerophilus	0	0

Table S5 part 2. The different phenotypic trait codings used in Chapter 2 are shown. Coding definitions: Ventral Transparency: 0 = absence; 1 = presence (either partial or fully). Dorsal Color: 0 = brown / other; 1 = green. Elevational analyses: Lower, Upper, Midpoint: elevational distributions in meters.

Species	**Lower**	**Upper**	**Midpoint**
Boophis albilabris	100	1000	550
Boophis occidentalis	0	800	400
Boophis praedictus	981	1034	1007.5
Boophis tsilomaro	170	170	170
Boophis albipunctatus	400	900	650
Boophis ankaratra	1200	1800	1500
Boophis boppa	900	1200	1050
Boophis haingana	600	1550	1075
Boophis luciae	247	915	581
Boophis miadana	1550	1550	1550
Boophis schuboeae	900	1000	950
Boophis sibilans	900	900	900
Boophis axelmeyeri	688	1000	844
Boophis boehmei	400	1000	700
Boophis brachychir	470	1600	1035
Boophis burgeri	815	900	857.5
Boophis entingae	730	750	740
Boophis fayi	300	400	350
Boophis goudotii	900	2200	1550
Boophis madagascariensis	0	1700	850
Boophis obscurus	1138	2114	1626
Boophis periegetes	800	1100	950
Boophis popi	1100	1500	1300
Boophis quasiboehmei	600	1020	810
Boophis reticulatus	800	1650	1225
Boophis rufioculis	900	1200	1050
Boophis sp Ca07 Marojejy	800	1200	1000
Boophis sp Ca10 Ambolokopatrika	800	1000	900
Boophis sp Ca40 Mahasoa Forest	900	1000	950
Boophis sp Ca41 Mahasoa Forest	900	1000	950
Boophis sp Ca42 Ranomafana	900	1200	1050
Boophis sp Ca43 Toamasina Sahafina	100	200	150
Boophis aff reticulatus	800	1200	1000
Boophis spinophis	915	915	915
Boophis roseipalmatus	1000	1100	1050

Boophis andohahela	400	1000	700
Boophis andreonei	200	700	450
Boophis anjanaharibeensis	800	1000	900
Boophis elenae	900	1000	950
Boophis englaenderi	300	400	350
Boophis jaegeri	0	200	100
Boophis luteus	300	1100	700
Boophis sandrae	900	1000	950
Boophis septentrionalis	650	1150	900
Boophis sp Ca21 Ambohitantely	1500	1600	1550
Boophis sp Ca23 Marojejy	1300	1400	1350
Boophis sp Ca24 Sahavontsira	400	500	450
Boophis sp Ca36 Andasibe	400	700	550
Boophis sp Ca37 Andasibe	400	700	550
Boophis tampoka	140	1188	664
Boophis arcanus	550	600	575
Boophis baetkei	470	470	470
Boophis feonnyala	900	900	900
Boophis haematopus	200	400	300
Boophis lilianae	468	1000	734
Boophis majori	900	1500	1200
Boophis miniatus	300	800	550
Boophis narinsi	915	1138	1026.5
Boophis picturatus	850	1000	925
Boophis piperatus	1138	1138	1138
Boophis pyrrhus	450	915	682.5
Boophis sp Ca44 Marolambo	400	500	450
Boophis aff picturatus	900	1200	1050
Boophis ulftunni	600	1326	963
Boophis liami	850	900	875
Boophis mandraka	1200	1200	1200
Boophis sambirano	280	1300	790
Boophis solomaso	850	1000	925
Boophis sp Ca27 Masoala	400	600	500
Boophis sp Ca28 Marojejy	500	750	625
Boophis sp Ca38 Ranomafana	900	1100	1000
Boophis sp Ca46 An Ala	900	1200	1050
Boophis sp Ca47 Antsohihy Bealanana Ranomafana	900	1000	950
Boophis sp Ca48 Antsohihy Bealanana	900	1000	950
Boophis sp Ca49 Ankijagna Lalagna	1100	1200	1150

Boophis sp Ca50 Ambinanitelo	100	300	200
Boophis sp Ca54 Tsaratanana	1100	1200	1150
Boophis blommersae	800	1200	1000
Boophis marojezensis	300	1000	650
Boophis sp Ca25 Marojejy	1300	1400	1350
Boophis sp Ca26 Marojejy	1300	1400	1350
Boophis sp Ca51 Ranomafana	800	1200	1000
Boophis sp Ca52 Tsaratanana	1100	1200	1150
Boophis sp Ca52 Ambinanitelo	1100	1200	1150
Boophis sp Ca53 Tsaratanana	1100	1200	1150
Boophis sp Ca55 Andrevorevo	100	1200	650
Boophis sp Ca68 Vohidrazana	1000	1200	1100
Boophis vittatus	500	1100	800
Boophis andrangoloaka	1100	1200	1150
Boophis laurenti	1500	2650	2075
Boophis microtympanum	1400	2400	1900
Boophis rhodoscelis	900	1500	1200
Boophis sp Ca33 Andringitra Antoetra	1300	1700	1500
Boophis williamsi	2100	2100	2100
Boophis ankarafensis	300	350	325
Boophis bottae	800	1000	900
Boophis erythrodactylus	1000	1100	1050
Boophis rappiodes	300	900	600
Boophis tasymena	300	900	600
Boophis viridis	350	1110	730
Boophis calcaratus	0	600	300
Boophis doulioti	0	800	400
Boophis guibei	900	1100	1000
Boophis idae	900	1100	1000
Boophis lichenoides	50	900	475
Boophis opisthodon	0	550	275
Boophis pauliani	0	1100	550
Boophis sp Ca01 Mayotte	100	400	250
Boophis tephraeomystax	0	900	450
Boophis xerophilus	0	100	50

Table S6 part 1. The 10 biogeographic zones for the analyses presented in Figure S1 are coded here for each species in the phylogeny. Refer to Figure S1 in Appendix I for the delimited regions

Species	Sambirano	North	North East	North Central East	South Central East
Boophis albilabris	0	1	1	1	1
Boophis albipunctatus	0	0	0	1	1
Boophis andohahela	0	0	0	0	1
Boophis andrangoloaka	0	0	0	0	0
Boophis andreonei	1	0	1	0	0
Boophis anjanaharibeensis	0	0	1	0	0
Boophis ankarafensis	0	0	0	0	0
Boophis ankaratra	0	0	0	1	1
Boophis arcanus	0	0	0	0	1
Boophis axelmeyeri	1	0	1	0	0
Boophis baetkei	0	1	0	0	0
Boophis blommersae	1	0	0	0	0
Boophis boehmei	0	0	0	1	1
Boophis boppa	0	0	0	0	1
Boophis bottae	0	0	0	1	1
Boophis brachychir	1	0	1	0	0
Boophis burgeri	0	0	0	1	0
Boophis calcaratus	0	0	0	1	1
Boophis doulioti	0	0	0	0	0
Boophis elenae	0	0	0	1	1
Boophis englaenderi	0	0	1	1	0
Boophis entingae	1	1	1	0	0
Boophis erythrodactylus	0	0	0	1	0
Boophis fayi	0	0	0	1	0
Boophis feonnyala	0	0	0	1	0
Boophis goudotii	0	0	0	1	0
Boophis guibei	0	0	0	1	1
Boophis haematopus	0	0	0	0	0
Boophis haingana	0	0	0	0	0
Boophis idae	0	0	0	1	1
Boophis jaegeri	1	0	0	0	0
Boophis laurenti	0	0	0	0	0
Boophis liami	0	0	0	1	0
Boophis lichenoides	0	0	1	1	1
Boophis lilianae	0	0	0	0	1

Boophis luciae	0	0	0	1	1
Boophis luteus	0	0	0	1	1
Boophis madagascariensis	0	0	0	1	1
Boophis majori	0	0	0	0	1
Boophis mandraka	0	0	0	1	0
Boophis marojezensis	0	0	1	0	0
Boophis miadana	0	0	0	0	0
Boophis microtympanum	0	0	0	1	1
Boophis miniatus	0	0	0	0	0
Boophis narinsi	0	0	0	0	1
Boophis obscurus	0	0	0	0	1
Boophis occidentalis	0	0	0	0	0
Boophis opisthodon	0	0	1	1	1
Boophis pauliani	0	0	0	0	1
Boophis periegetes	0	0	0	0	1
Boophis picturatus	0	0	0	1	1
Boophis piperatus	0	0	0	0	1
Boophis popi	0	0	0	0	1
Boophis praedictus	0	0	1	0	0
Boophis pyrrhus	0	0	0	1	0
Boophis quasiboehmei	0	0	0	0	1
Boophis rappiodes	0	0	0	1	1
Boophis reticulatus	0	0	1	1	0
Boophis rhodoscelis	0	0	0	1	1
Boophis roseipalmatus	0	1	1	0	0
Boophis rufioculis	0	0	0	1	0
Boophis sambirano	1	0	0	0	0
Boophis sandrae	0	0	0	0	1
Boophis schuboeae	0	0	0	0	1
Boophis septentrionalis	1	1	1	0	0
Boophis sibilans	0	0	1	1	1
Boophis solomaso	0	0	0	1	0
Boophis spinophis	0	0	0	0	1
Boophis tampoka	0	0	0	0	0
Boophis tasymena	0	0	0	1	1
Boophis tephraeomystax	0	1	1	1	1
Boophis tsilomaro	1	0	0	0	0
Boophis ulftunni	0	0	1	0	0
Boophis viridis	0	0	0	1	1
Boophis vittatus	1	0	1	0	0

Boophis williamsi	0	0	0	0	0
Boophis xerophilus	0	0	0	0	0
Boophis sp Ca01 Mayotte	0	0	0	0	0
Boophis sp Ca07 Marojejy	0	0	1	0	0
Boophis sp Ca10 Ambolokopatrika	0	0	1	0	0
Boophis sp Ca21 Ambohitantely	0	0	0	0	1
Boophis sp Ca23 Marojejy	0	0	1	0	0
Boophis sp Ca24 Sahavontsira	0	0	0	0	1
Boophis sp Ca25 Marojejy	0	0	1	0	0
Boophis sp Ca26 Marojejy	0	0	1	0	0
Boophis sp Ca27 Masoala	0	0	1	0	0
Boophis sp Ca28 Marojejy	0	0	1	0	0
Boophis sp Ca33 Andringitra Antoetra	0	0	0	0	1
Boophis sp Ca36 Andasibe	0	0	0	1	0
Boophis sp Ca37 Andasibe	0	0	0	1	0
Boophis sp Ca38 Ranomafana	0	0	0	0	1
Boophis sp Ca40 Mahasoa Forest	0	0	0	0	0
Boophis sp Ca41 Mahasoa Forest	0	0	0	0	0
Boophis sp Ca42 Ranomafana	0	0	0	0	1
Boophis sp Ca43 Toamasina Sahafina	0	0	0	1	0
Boophis sp Ca44 Marolambo	0	0	0	1	0
Boophis sp Ca46 An Ala	0	0	0	1	0
Boophis sp Ca47 Ranomafana	0	0	0	0	1
Boophis sp Ca48 Antsohihy Bealanana	0	0	0	0	1
Boophis sp Ca49 Ankijagna Lalagna	0	0	0	0	0
Boophis sp Ca50 Ambinanitelo	0	0	0	1	0
Boophis sp Ca51 Ranomafana	0	0	0	0	1
Boophis sp Ca52 Ambinanitelo	0	0	0	1	0
Boophis sp Ca52 Tsaratanana	0	0	0	0	0
Boophis sp Ca53 Tsaratanana	0	0	0	0	0
Boophis sp Ca54 Tsaratanana	0	0	0	0	0
Boophis sp Ca55 Andrevorevo	0	0	0	0	0
Boophis sp Ca68 Vohidrazana	0	0	0	1	0
Boophis aff reticulatus	0	0	0	1	1
Boophis aff picturatus	0	0	0	0	1

Table S6 part 2. The 10 biogeographic zones for the analyses presented in Figure S1 are coded here for each species in the phylogeny. Refer to Figure S1 in Appendix I for the delimited regions

Species	South East	South	Central	West	North West
Boophis albilabris	0	0	0	0	0
Boophis albipunctatus	1	0	0	0	0
Boophis andohahela	1	0	0	0	0
Boophis andrangoloaka	0	0	0	0	1
Boophis andreonei	0	0	0	0	0
Boophis anjanaharibeensis	0	0	0	0	0
Boophis ankarafensis	0	0	0	0	1
Boophis ankaratra	0	0	1	0	0
Boophis arcanus	0	0	0	0	0
Boophis axelmeyeri	0	0	0	0	0
Boophis baetkei	0	0	0	0	0
Boophis blommersae	0	0	0	0	1
Boophis boehmei	1	0	0	0	0
Boophis boppa	0	0	0	0	0
Boophis bottae	0	0	0	0	0
Boophis brachychir	0	0	1	0	1
Boophis burgeri	0	0	0	0	0
Boophis calcaratus	0	0	0	0	0
Boophis doulioti	0	1	1	1	0
Boophis elenae	0	0	0	0	0
Boophis englaenderi	0	0	0	0	0
Boophis entingae	0	0	0	0	0
Boophis erythrodactylus	0	0	1	0	0
Boophis fayi	0	0	0	0	0
Boophis feonnyala	0	0	0	0	0
Boophis goudotii	0	0	1	0	0
Boophis guibei	0	0	0	0	0
Boophis haematopus	1	0	0	0	0
Boophis haingana	1	0	0	0	0
Boophis idae	0	0	0	0	0
Boophis jaegeri	0	0	0	0	1
Boophis laurenti	1	0	0	0	0
Boophis liami	0	0	0	0	0
Boophis lichenoides	0	0	0	0	0
Boophis lilianae	0	0	0	0	0
Boophis luciae	1	0	0	0	0

Boophis luteus	1	0	0	0	0
Boophis madagascariensis	1	0	0	0	0
Boophis majori	0	0	0	0	0
Boophis mandraka	0	0	0	0	0
Boophis marojezensis	0	0	0	0	0
Boophis miadana	1	0	0	0	0
Boophis microtympanum	0	0	0	0	0
Boophis miniatus	1	0	0	0	0
Boophis narinsi	0	0	0	0	0
Boophis obscurus	0	0	1	0	0
Boophis occidentalis	0	0	1	1	0
Boophis opisthodon	1	0	0	0	0
Boophis pauliani	1	0	0	0	0
Boophis periegetes	1	0	0	0	0
Boophis picturatus	0	0	0	0	0
Boophis piperatus	0	0	0	0	0
Boophis popi	0	0	0	0	0
Boophis praedictus	0	0	0	0	0
Boophis pyrrhus	0	0	0	0	0
Boophis quasiboehmei	1	0	0	0	0
Boophis rappiodes	1	0	0	0	0
Boophis reticulatus	0	0	0	0	0
Boophis rhodoscelis	0	0	0	0	0
Boophis roseipalmatus	0	0	0	0	0
Boophis rufioculis	0	0	0	0	0
Boophis sambirano	0	0	0	0	0
Boophis sandrae	0	0	0	0	0
Boophis schuboeae	0	0	0	0	0
Boophis septentrionalis	0	0	0	0	0
Boophis sibilans	0	0	0	0	0
Boophis solomaso	0	0	0	0	0
Boophis spinophis	0	0	0	0	0
Boophis tampoka	0	0	0	1	0
Boophis tasymena	1	0	0	0	0
Boophis tephraeomystax	0	0	0	0	0
Boophis tsilomaro	0	0	0	0	0
Boophis ulftunni	0	0	0	0	0
Boophis viridis	0	0	0	0	0
Boophis vittatus	0	0	0	0	0
Boophis williamsi	0	0	1	0	0

Boophis xerophilus	0	1	1	1	0
Boophis sp Ca01 Mayotte	0	0	0	0	1
Boophis sp Ca07 Marojejy	0	0	0	0	0
Boophis sp Ca10 Ambolokopatrika	0	0	0	0	0
Boophis sp Ca21 Ambohitantely	0	0	0	0	0
Boophis sp Ca23 Marojejy	0	0	0	0	0
Boophis sp Ca24 Sahavontsira	0	0	0	0	0
Boophis sp Ca25 Marojejy	0	0	0	0	0
Boophis sp Ca26 Marojejy	0	0	0	0	0
Boophis sp Ca27 Masoala	0	0	0	0	0
Boophis sp Ca28 Marojejy	0	0	0	0	0
Boophis sp Ca33 Andringitra Antoetra	1	0	0	0	0
Boophis sp Ca36 Andasibe	0	0	0	0	0
Boophis sp Ca37 Andasibe	0	0	0	0	0
Boophis sp Ca38 Ranomafana	0	0	0	0	0
Boophis sp Ca40 Mahasoa Forest	0	1	0	0	0
Boophis sp Ca41 Mahasoa Forest	0	1	0	0	0
Boophis sp Ca42 Ranomafana	0	0	0	0	0
Boophis sp Ca43 Toamasina Sahafina	0	0	0	0	0
Boophis sp Ca44 Marolambo	0	0	0	0	0
Boophis sp Ca46 An Ala	0	0	0	0	0
Boophis sp Ca47 Ranomafana	0	0	0	0	0
Boophis sp Ca48 Antsohihy Bealanana	0	0	0	0	0
Boophis sp Ca49 Ankijagna Lalagna	0	0	0	0	1
Boophis sp Ca50 Ambinanitelo	0	0	0	0	0
Boophis sp Ca51 Ranomafana	0	0	0	0	0
Boophis sp Ca52 Ambinanitelo	0	0	0	0	0
Boophis sp Ca52 Tsaratanana	0	0	0	0	1
Boophis sp Ca53 Tsaratanana	0	0	0	0	1
Boophis sp Ca54 Tsaratanana	0	0	0	0	1
Boophis sp Ca55 Andrevorevo	0	0	0	0	1
Boophis sp Ca68 Vohidrazana	0	0	0	0	0
Boophis aff reticulatus	0	0	0	0	0
Boophis aff picturatus	0	0	0	0	0

Table S7. The four biogeographic zones for the analyses presented in the main text are coded for each species in the phylogeny. Refer to Figure 3 in Chapter 2 for the delimited regions.

Species	North	North Central East	South East	Central
Boophis albilabris	0	1	1	0
Boophis albipunctatus	0	1	1	0
Boophis andohahela	0	0	1	0
Boophis andrangoloaka	1	0	0	0
Boophis andreonei	1	0	0	0
Boophis anjanaharibeensis	1	0	0	0
Boophis ankarafensis	1	0	0	0
Boophis ankaratra	0	1	1	0
Boophis arcanus	0	0	1	0
Boophis axelmeyeri	1	0	0	0
Boophis baetkei	1	0	0	0
Boophis blommersae	1	0	0	0
Boophis boehmei	0	1	1	0
Boophis boppa	0	0	1	0
Boophis bottae	0	1	1	0
Boophis brachychir	1	0	0	1
Boophis burgeri	0	1	0	0
Boophis calcaratus	0	1	1	0
Boophis doulioti	0	0	0	1
Boophis elenae	0	1	1	0
Boophis englaenderi	0	1	0	0
Boophis entingae	1	0	0	0
Boophis erythrodactylus	0	1	0	1
Boophis fayi	0	1	0	0
Boophis feonnyala	0	1	0	0
Boophis goudotii	0	1	0	1
Boophis guibei	0	1	1	0
Boophis haematopus	0	0	1	0
Boophis haingana	0	0	1	0
Boophis idae	0	1	1	0
Boophis jaegeri	1	0	0	0
Boophis laurenti	0	0	1	0
Boophis liami	0	1	0	0
Boophis lichenoides	1	1	0	0
Boophis lilianae	0	0	1	0
Boophis luciae	0	1	1	0

Boophis luteus	0	1	1	0
Boophis madagascariensis	0	1	1	0
Boophis majori	0	0	1	0
Boophis mandraka	0	1	0	0
Boophis marojezensis	1	0	0	0
Boophis miadana	0	0	1	0
Boophis microtympanum	0	1	1	0
Boophis miniatus	0	0	1	0
Boophis narinsi	0	0	1	0
Boophis obscurus	0	0	1	1
Boophis occidentalis	0	0	0	1
Boophis opisthodon	0	1	1	0
Boophis pauliani	0	0	1	0
Boophis periegetes	0	0	1	0
Boophis picturatus	0	1	1	0
Boophis piperatus	0	0	1	0
Boophis popi	0	0	1	0
Boophis praedictus	1	0	0	0
Boophis pyrrhus	0	1	0	0
Boophis quasiboehmei	0	0	1	0
Boophis rappiodes	0	1	1	0
Boophis reticulatus	1	1	0	0
Boophis rhodoscelis	0	1	1	0
Boophis roseipalmatus	1	0	0	0
Boophis rufioculis	0	1	0	0
Boophis sambirano	1	0	0	0
Boophis sandrae	0	0	1	0
Boophis schuboeae	0	0	1	0
Boophis septentrionalis	1	0	0	0
Boophis sibilans	0	1	1	0
Boophis solomaso	0	1	0	0
Boophis spinophis	0	0	1	0
Boophis tampoka	0	0	0	1
Boophis tasymena	0	1	1	0
Boophis tephraeomystax	1	1	0	0
Boophis tsilomaro	1	0	0	0
Boophis ulftunni	1	0	0	0
Boophis viridis	0	1	1	0
Boophis vittatus	1	0	0	0
Boophis williamsi	0	0	0	1

Boophis xerophilus	0	0	0	1
Boophis sp Ca01 Mayotte	0	0	0	1
Boophis sp Ca07 Marojejy	1	0	0	0
Boophis sp Ca10 Ambolokopatrika	1	0	0	0
Boophis sp Ca21 Ambohitantely	0	0	1	0
Boophis sp Ca23 Marojejy	1	0	0	0
Boophis sp Ca24 Sahavontsira	0	0	1	0
Boophis sp Ca25 Marojejy	1	0	0	0
Boophis sp Ca26 Marojejy	1	0	0	0
Boophis sp Ca27 Masoala	1	0	0	0
Boophis sp Ca28 Marojejy	1	0	0	0
Boophis sp Ca33 Andringitra Antoetra	0	0	1	0
Boophis sp Ca36 Andasibe	0	1	0	0
Boophis sp Ca37 Andasibe	0	1	0	0
Boophis sp Ca38 Ranomafana	0	0	1	0
Boophis sp Ca40 Mahasoa Forest	0	0	1	0
Boophis sp Ca41 Mahasoa Forest	0	0	1	0
Boophis sp Ca42 Ranomafana	0	0	1	0
Boophis sp Ca43 Toamasina Sahafina	0	1	0	0
Boophis sp Ca44 Marolambo	0	1	0	0
Boophis sp Ca46 An Ala	0	1	0	0
Boophis sp Ca47 Antsohihy Bealanana Ranomafana	0	0	1	0
Boophis sp Ca48 Antsohihy Bealanana	0	0	1	0
Boophis sp Ca49 Ankijagna Lalagna	1	0	0	0
Boophis sp Ca50 Ambinanitelo	0	1	0	0
Boophis sp Ca51 Ranomafana	0	0	1	0
Boophis sp Ca52 Ambinanitelo	0	1	0	0
Boophis sp Ca52 Tsaratanana	1	0	0	0
Boophis sp Ca53 Tsaratanana	1	0	0	0
Boophis sp Ca54 Tsaratanana	1	0	0	0
Boophis sp Ca55 Andrevorevo	1	0	0	0
Boophis sp Ca68 Vohidrazana	0	1	0	0
Boophis aff reticulatus	0	1	1	0
Boophis aff picturatus	0	0	1	0

Table S8. Results of the GeoSSE analyses testing for different diversification rates between highland and lowland regions in Madagascar, using the chronogram calibrated with a secondary calibration from Feng et al. (2017). We also tested models constraining between-region speciation to be zero. The most strongly supported models are boldfaced. S = speciation rate. E = extinction rate. D = dispersal rate between regions. Df = number of parameters. lnLik = log likelihood. AIC = Akaike Information Criterion.

				Speciation			Extinction		Dispersal	
Model	Df	lnLik	AIC	Lowland	Highland	Both	Lowland	Highland	To highland	To lowland
Full	**7**	**-475.9**	**965.9**	**0.007**	**0.086**	**0.052**	**0**	**0**	**0**	**0.057**
Equal S	6	-480.3	972.6	0.062	0.062	0.051	0	0	0.094	0.026
Equal E	**6**	**-475.9**	**963.9**	**0.007**	**0.086**	**0.039**	**0**	**0**	**0**	**0.057**
Equal D	**6**	**-477.2**	**966.5**	**0.024**	**0.082**	**0.053**	**0**	**0.002**	**0.048**	**0.048**
Equal S / E	5	-480.3	970.6	0.062	0.062	0.051	0	0	0.094	0.026
Equal S / D	5	-481.9	973.9	0.069	0.069	0.033	0.033	0	0.053	0.053
Equal E / D	**5**	**-477.2**	**964.5**	**0.025**	**0.081**	**0.055**	**0**	**0**	**0.048**	**0.048**
Equal All	4	-483.4	974.8	0.065	0.065	0.046	0	0	0.045	0.045

Table S9. Results of the GeoSSE analyses testing for different diversification rates between highland and lowland regions in Madagascar, using the alternative fossil calibrated tree. We also tested models constraining between-region speciation to be zero. The most strongly supported models are boldfaced. S = speciation rate. E = extinction rate. D = dispersal rate between regions. Df = number of parameters. lnLik = log likelihood. AIC = Akaike Information Criterion.

				Speciation			Extinction		Dispersal	
Model	Df	lnLik	AIC	Lowland	Highland	Both	Lowland	Highland	To highland	To lowland
Full	**7**	**-343.9**	**701.8**	**0**	**0.065**	**0.039**	**0**	**0**	**0**	**0.056**
Equal S	6	-346.6	705.2	0.047	0.047	0.024	0	0	0.079	0.024
Equal E	**6**	**-343.9**	**699.8**	**0**	**0.065**	**0.039**	**0**	**0**	**0**	**0.056**
Equal D	**6**	**-345.0**	**702.1**	**0.018**	**0.069**	**0.013**	**0**	**0.011**	**0.044**	**0.044**
Equal S / E	**5**	**-346.6**	**703.2**	**0.047**	**0.047**	**0.024**	**0**	**0**	**0.079**	**0.024**
Equal S / D	5	-347.9	705.9	0.051	0.051	0.013	0.019	0	0.046	0.046
Equal E / D	**5**	**-346.6**	**703.2**	**0.024**	**0.061**	**0.025**	**0**	**0**	**0.042**	**0.042**
Equal All	3	-349.6	705.3	0.054	0.054	0	0.010	0.010	0.044	0.044

Appendix III.

From:

CHAPTER 3

FrogCap: a modular sequence capture probe set for phylogenomics and population genetics for all frogs, assessed across multiple phylogenetic scales

Hutter CR, Cobb KA, Portik DM, Travers S, and Brown RM; Not yet published.

Table S1. The transcriptomes and their associated GenBank ID used in this study are shown.

ID	SuperFamily	Family	Species	GenBank ID
agaCal	Hyloidea	Hylidae	*Agalychnis callidryas*	PRJNA259743
atelgly	Hyloidea	Bufonidae	*Atelopus glyphus*	PRJNA259720
atezet	Hyloidea	Bufonidae	*Atelopus zeteki*	PRJNA216050
bomMax	Basal	Bombinatoridae	*Bombina maxima*	PRJNA174732
bufMar	Hyloidea	Bufonidae	*Bufo marinus*	PRJNA395127
bufSch	Hyloidea	Bufonidae	*Bufo schneideri*	PRJNA255079
bufSpin	Hyloidea	Bufonidae	*Bufo spinulosus*	PRJNA236569
craufit	Hyloidea	Craugastoridae	*Craugastor fitzingeri*	PRJNA259742
cycAlb	Hyloidea	Hylidae	*Cyclorana alboguttata*	PRJNA177363
espProb	Hyloidea	Centrolenidae	*Espadarana prosoblepon*	PRJNA237648
hylArb	Hyloidea	Hylidae	*Hyla arborea*	PRJNA196399
kasDec	Ranoidea	Hyperoliidae	*Kassina decorata*	Unpublished
leptOva	Ranoidea	Arthroleptidae	*Leptodactylodon ovatus*	Unpublished
leptBou	Ranoidea	Arthroleptidae	*Leptopelis boulengeri*	Unpublished
nanPar	Target	Dicroglossidae	*Nanorana parkeri*	PRJNA344660
pelLes	Ranoidea	Ranidae	*Pelophylax lessonae*	PRJNA230915
pelNig	Ranoidea	Ranidae	*Pelophylax nigromaculatus*	PRJNA299518
polMeg	Ranoidea	Rhacophoridae	*Polypedates megacephalus*	PRJNA299518
pseReg	Ranoidea	Hylidae	*Pseudacris regilla*	PRJNA163143
quaBou	Ranoidea	Dicroglossidae	*Quasipaa boulengeri*	PRJNA304335
ranChen	Ranoidea	Ranidae	*Rana chensinensis*	PRJNA178186
ranCla	Ranoidea	Ranidae	*Rana clamitans*	PRJNA162931
ranPip	Ranoidea	Ranidae	*Rana clamitans*	PRJNA240240
ranKuk	Ranoidea	Ranidae	*Rana kukunoris*	PRJNA178186
ranMar	Ranoidea	Ranidae	*Rana margaretae*	PRJNA299518
ranSyl	Ranoidea	Ranidae	*Rana sylvatica*	PRJNA392411
ranTem	Ranoidea	Ranidae	*Rana temporaria*	PRJEB9622
ranYav	Ranoidea	Ranidae	*Rana yavapaiensis*	PRJNA232044
rhaDen	Ranoidea	Rhacophoridae	*Rhacophorus dennysi*	PRJNA299518
xenLae	Basal	Pipidae	*Xenopus laevis*	PRJNA338693
xenTro	Basal	Pipidae	*Xenopus tropicalis*	PRJNA205740

Table S2 part 1. The samples and their associated collection ID used in this study are shown. Each samples' summary statistics are shown, where orthologs and paralogs are discovered during probe matching. The length statistics are calculated from the orthologous contigs.

Probe Set	Scale	Sample	N contigs	N orthologs	N paralogs
Ranoidea	Species	Cornufer vertebralis A 24L	17583	11181	442
Ranoidea	Species	Cornufer vertebralis A168972	12690	11096	542
Ranoidea	Species	Cornufer vertebralis JLW 173	14253	11088	594
Ranoidea	Species	Cornufer vertebralis JLW 343	16767	11557	692
Ranoidea	Species	Cornufer vertebralis JQR 1793	14248	11018	640
Ranoidea	Species	Cornufer vertebralis JQR 1868	16580	10736	509
Ranoidea	Species	Cornufer vertebralis JQR 1869	11098	10010	314
Ranoidea	Species	Cornufer vertebralis JQR2001	13788	11026	585
Ranoidea	Species	Cornufer vertebralis RMB 7128	16344	9666	271
Ranoidea	Species	Cornufer vertebralis SLT 179	12983	11010	496
Ranoidea	Species	Cornufer vertebralis SLT 200	12080	10798	393
Ranoidea	Species	Cornufer vertebralis SLT 203	16007	9692	299
Ranoidea	Species	Cornufer vertebralis SLT 268	12655	10066	325
Ranoidea	Species	Cornufer vertebralis SLT 280	14160	11106	640
Ranoidea	Species	Cornufer vertebralis SLT 524	11810	10538	350
Ranoidea	Species	Cornufer vertebralis SLT 674	14742	10823	539
Ranoidea	Superfamily	Aglyptodactylus securifer CRH1644	12005	11118	453
Ranoidea	Superfamily	Amietia angolensis CAS254876	13943	11989	647
Ranoidea	Superfamily	Amolops ricketti KUFS65	9527	8628	329
Ranoidea	Superfamily	Anodontohyla boulengeri CRH1898	9516	7111	284
Ranoidea	Superfamily	Arthroleptis variabilis RMB19372	8530	6147	267
Ranoidea	Superfamily	Boophis tephraeomystax CRH1675	14168	11198	405
Ranoidea	Superfamily	Cardioglossa leucomystax RMB19294	9117	6430	248
Ranoidea	Superfamily	Ceratobatrachus guentheri SLT345	13498	11695	470
Ranoidea	Superfamily	Cornufer gilliardi JF112	15155	11752	723
Ranoidea	Superfamily	Gastrophyrne olivacae KUFS914	8949	6026	172
Ranoidea	Superfamily	Heterixalus punctatus CRH1685	15189	8681	356
Ranoidea	Superfamily	Hylarana erythraea RMB4300	12230	10783	640
Ranoidea	Superfamily	Ingerana mariae RMB7803	12329	11311	473
Ranoidea	Superfamily	Kassina senegalensis KU290414	8562	6986	257
Ranoidea	Superfamily	Leptodactylodon ovatus CAS253933	9873	8276	284
Ranoidea	Superfamily	Limnonectes kuhlii RMB2127	15648	12235	865
Ranoidea	Superfamily	Microhyla heymonsi KUFS265	8023	5225	198
Ranoidea	Superfamily	Nyctixalus pictus 239460	14308	11710	560
Ranoidea	Superfamily	Odontobatrachus natator CAS230052	12659	11865	403

Ranoidea	Superfamily	Oreophryne annulata RMB10029	6968	5050	85
Ranoidea	Superfamily	Platymantis corrugatus RMB15045	11706	10571	333
Ranoidea	Superfamily	Pulchrana moellendorffi KU 327049	18062	11770	911
Ranoidea	Superfamily	Rhacophorus bipunctatus 221351	16015	11745	777
Ranoidea	Superfamily	Scaphiophryne marmorata CRH920	14222	9007	651
Ranoidea	Superfamily	Aglyptodactylus securifer CRH1644	12005	11118	453
Ranoidea	Superfamily	Blommersia grandisonae CRH792	12170	10697	515
Ranoidea	Superfamily	Boophis tephraeomystax CRH1675	14168	11198	405
Ranoidea	Superfamily	Gephyromantis redimitus CRH1628	14178	11259	1042
Ranoidea	Superfamily	Guibemantis depressiceps CRH535	12747	11017	503
Ranoidea	Superfamily	Mantella baroni CRH1027	12099	9428	347
Ranoidea	Superfamily	Mantidactylus melanopleura CRH1998	12865	10928	899
Ranoidea	Superfamily	Spinomantis bertini CRH726	13326	11920	630
Ranoidea	Genus	Cornufer batantae SJR 7502	12575	9783	292
Ranoidea	Genus	Cornufer boulengeri FK 10744	14132	10440	326
Ranoidea	Genus	Cornufer bufoniformis SJR 5475	13601	11066	418
Ranoidea	Genus	Cornufer cryptotis yapeni RG 7979	13980	10970	396
Ranoidea	Genus	Cornufer custos ABTC 136625	19919	11064	447
Ranoidea	Genus	Cornufer exedrus SJR 10784	10062	8356	223
Ranoidea	Genus	Cornufer gilliardi JF 112	15111	11913	622
Ranoidea	Genus	Cornufer guentheri SLT 345	13770	11569	603
Ranoidea	Genus	Cornufer guppyi SLT 679	12322	11320	596
Ranoidea	Genus	Cornufer hedigeri SLT 710	12670	11542	511
Ranoidea	Genus	Cornufer heffernani 5303 5316	11591	9772	319
Ranoidea	Genus	Cornufer latro SR 2145	13005	10862	445
Ranoidea	Genus	Cornufer magnus 5220 5252	12439	11018	412
Ranoidea	Genus	Cornufer minutus SLT 202	12495	10831	457
Ranoidea	Genus	Cornufer papuensis RG 7373	11936	10954	491
Ranoidea	Genus	Cornufer parkeri CCA 2644	13333	10288	523
Ranoidea	Genus	Cornufer punctatus RG 7970	12013	10973	386
Ranoidea	Genus	Cornufer schmidti CCA 1583	11540	10500	350
Ranoidea	Genus	Cornufer solomonis RMB 6960	35201	11388	538
Ranoidea	Genus	Cornufer trossulus SLT 262	12253	10168	295
Ranoidea	Genus	Cornufer vertebralis JLW 343	16767	11557	692
Ranoidea	Genus	Cornufer vitianus CM 1498	12220	9271	332
Ranoidea	Genus	Cornufer weberi SLT 269	13207	10678	371
Ranoidea	Genus	Cornufer wuenscheorum RG 7751	11456	9364	267
Reduced	Reduced	Occidozyga sp CDS 2282	13450	2718	70
Reduced	Reduced	Occidozyga sp CDS1257	13736	2787	106
Reduced	Reduced	Occidozyga sp CDS1808	16694	2853	111

Reduced	Reduced	Occidozyga sp CDS2026	17525	2875	110
Reduced	Reduced	Occidozyga sp CDS2045	19231	2870	116
Reduced	Reduced	Occidozyga sp CDS270	19332	2832	123
Reduced	Reduced	Occidozyga sp CDS3582	15784	2807	88
Reduced	Reduced	Occidozyga sp CDS487	20810	2953	122
Reduced	Reduced	Occidozyga sp CDS543	21314	2938	134
Reduced	Reduced	Occidozyga sp RMB11020	16437	2862	74
Reduced	Reduced	Occidozyga sp RMB15467	14586	2847	94
Reduced	Reduced	Occidozyga sp RMB16321	23856	2935	123
Reduced	Reduced	Occidozyga sp RMB16436	20593	2891	118
Reduced	Reduced	Occidozyga sp RMB17235	25179	2983	125
Reduced	Reduced	Occidozyga sp RMB20282	25553	2868	128
Reduced	Reduced	Occidozyga sp RMB20559	13377	2769	91
Reduced	Reduced	Occidozyga sp RMB2133	11852	2747	84
Reduced	Reduced	Occidozyga sp RMB2542	7766	2299	50
Reduced	Reduced	Occidozyga sp RMB3068	20096	2942	132
Reduced	Reduced	Occidozyga sp RMB3127	17714	2829	99
Reduced	Reduced	Occidozyga sp RMB4318	18594	2904	118
Reduced	Reduced	Occidozyga sp RMB4468	25764	2933	115
Reduced	Reduced	Occidozyga sp RMB5396	19282	2865	108
Reduced	Reduced	Occidozyga sp RMB6117	18603	2910	96
Reduced	Reduced	Occidozyga sp RMB6411	13723	2804	101
Reduced	Reduced	Occidozyga sp RMB7686	11193	2826	91
Reduced	Reduced	Occidozyga sp RMB819	12873	2790	90
Reduced	Reduced	Occidozyga sp RMB8750	21191	2894	119
Reduced	Reduced	Occidozyga sp RMB8900	15194	2910	103
Reduced	Reduced	Occidozyga sp RMB9600	25680	2974	119
Hyloidea	Superfamily	Allobates femoralis WED 55592	24894	5662	372
Hyloidea	Superfamily	Anaryxus woodhousii RMB 19577	22188	7699	1750
Hyloidea	Superfamily	Ansonia sp RMB 10371	24794	7810	2718
Hyloidea	Superfamily	Barycholos pulcher LAC 692	16724	5907	451
Hyloidea	Superfamily	Bolitaglossa palmata LAC 1154	13790	535	20
Hyloidea	Superfamily	Bufo valliceps KU 203846	43113	8232	3475
Hyloidea	Superfamily	Ceratophrys cornuta WED 57689	20379	7889	1073
Hyloidea	Superfamily	Craugastor rupinius JES 2401	19238	6570	1288
Hyloidea	Superfamily	Dendrobates histrionicus LAC 2539	11997	5459	343
Hyloidea	Superfamily	Eluetherodactylus sp GLOR 6202	17099	6733	963
Hyloidea	Superfamily	Gastrotheca marsupiata WED 58521	13538	6559	797
Hyloidea	Superfamily	Hyalinobatrachium fleischmanni MZUTI 3621	17393	6705	1316
Hyloidea	Superfamily	Hyloscirtus phyllognathus WED 58378	16567	7157	809

Hyloidea	Superfamily	Leptobrachium hainensis KUFS 194	8193	2418	75
Hyloidea	Superfamily	Leptodactylus pentadactylus WED 55494	22665	7677	864
Hyloidea	Superfamily	Nyctimystes infrafrenatus SLT 771	25534	7940	978
Hyloidea	Superfamily	Oreobates quizensis WED 59885	12446	5870	953
Hyloidea	Superfamily	Phyrnohyas venulosa WED 55450	20170	7320	859
Hyloidea	Superfamily	Physalamus pustulatus LAC 1642	25150	7259	969
Hyloidea	Superfamily	Pristimantis w-nigrum WED 53045	26099	7576	1521
Hyloidea	Superfamily	Spea bombifrons RMB 19586	21131	4328	246
Hyloidea	Superfamily	Strabomantis sulcatus LAC 841	17898	6754	1459
Hyloidea	Superfamily	Telmatobius truebae WED 56933	28122	8337	1916
Hyloidea	Superfamily	Vitreorana castroviejoi JMG 33	22072	7183	2434

Table S2 part 2. The samples and their associated collection ID used in this study are shown. Each samples' summary statistics are shown, where orthologs and paralogs are discovered during probe matching. The length statistics are calculated from the orthologous contigs.

Probe Set	Scale	Sample	Min length	Max length	Mean length	Median length
Ranoidea	Species	Cornufer vertebralis A 24L	125	5840	845.7	795
Ranoidea	Species	Cornufer vertebralis A168972	129	5653	921.9	894
Ranoidea	Species	Cornufer vertebralis JLW 173	104	4892	827.9	787.5
Ranoidea	Species	Cornufer vertebralis JLW 343	167	7547	912.0	874
Ranoidea	Species	Cornufer vertebralis JQR 1793	84	5728	811.4	767
Ranoidea	Species	Cornufer vertebralis JQR 1868	93	7339	773.6	730
Ranoidea	Species	Cornufer vertebralis JQR 1869	116	9788	803.7	761
Ranoidea	Species	Cornufer vertebralis JQR2001	101	4236	835.8	791
Ranoidea	Species	Cornufer vertebralis RMB 7128	118	7266	784.1	724.5
Ranoidea	Species	Cornufer vertebralis SLT 179	109	12413	850.4	808
Ranoidea	Species	Cornufer vertebralis SLT 200	117	12118	810.8	771
Ranoidea	Species	Cornufer vertebralis SLT 203	93	4517	767.2	716
Ranoidea	Species	Cornufer vertebralis SLT 268	129	12173	829.8	782
Ranoidea	Species	Cornufer vertebralis SLT 280	107	7124	845.1	807
Ranoidea	Species	Cornufer vertebralis SLT 524	61	12309	825.9	787
Ranoidea	Species	Cornufer vertebralis SLT 674	120	12713	875.7	832
Ranoidea	Superfamily	Aglyptodactylus securifer CRH1644	76	12498	965.6	936
Ranoidea	Superfamily	Amietia angolensis CAS254876	138	9433	944.8	919
Ranoidea	Superfamily	Amolops ricketti KUFS65	92	12583	767.1	699
Ranoidea	Superfamily	Anodontohyla boulengeri CRH1898	106	23144	815.2	765
Ranoidea	Superfamily	Arthroleptis variabilis RMB19372	111	6045	821.7	776
Ranoidea	Superfamily	Boophis tephraeomystax CRH1675	129	15946	1114.2	1082
Ranoidea	Superfamily	Cardioglossa leucomystax RMB19294	98	12048	819.9	775
Ranoidea	Superfamily	Ceratobatrachus guentheri SLT345	147	6840	930.6	899
Ranoidea	Superfamily	Cornufer gilliardi JF112	79	12400	957.9	921
Ranoidea	Superfamily	Gastrophyrne olivacae KUFS914	112	11909	848.8	802
Ranoidea	Superfamily	Heterixalus punctatus CRH1685	110	6692	908.2	869
Ranoidea	Superfamily	Hylarana erythraea RMB4300	101	12268	929.5	902
Ranoidea	Superfamily	Ingerana mariae RMB7803	145	18047	958.0	928
Ranoidea	Superfamily	Kassina senegalensis KU290414	110	12075	811.2	772
Ranoidea	Superfamily	Leptodactylodon ovatus CAS253933	81	5529	875.5	830
Ranoidea	Superfamily	Limnonectes kuhlii RMB2127	156	10844	1005.6	981
Ranoidea	Superfamily	Microhyla heymonsi KUFS265	80	11467	838.2	784
Ranoidea	Superfamily	Nyctixalus pictus 239460	115	8314	1003.5	962
Ranoidea	Superfamily	Odontobatrachus natator CAS230052	122	12170	892.2	862

Ranoidea	Superfamily	Oreophryne annulata RMB10029	102	12605	791.3	742
Ranoidea	Superfamily	Platymantis corrugatus RMB15045	106	10810	858.5	826
Ranoidea	Superfamily	Pulchrana moellendorffi KU 327049	103	12633	998.9	970
Ranoidea	Superfamily	Rhacophorus bipunctatus 221351	114	9515	982.9	947
Ranoidea	Superfamily	Scaphiophryne marmorata CRH920	111	22883	868.4	831
Ranoidea	Superfamily	Aglyptodactylus securifer CRH1644	76	12498	965.6	936
Ranoidea	Superfamily	Blommersia grandisonae CRH792	125	5288	895.8	858
Ranoidea	Superfamily	Boophis tephraeomystax CRH1675	129	15946	1114.2	1082
Ranoidea	Superfamily	Gephyromantis redimitus CRH1628	96	10021	901.1	872
Ranoidea	Superfamily	Guibemantis depressiceps CRH535	119	9668	1044.5	1011
Ranoidea	Superfamily	Mantella baroni CRH1027	122	12213	964.5	919
Ranoidea	Superfamily	Mantidactylus melanopleura CRH1998	101	16850	917.5	882
Ranoidea	Superfamily	Spinomantis bertini CRH726	129	12744	1107.9	1084
Ranoidea	Genus	Cornufer batantae SJR 7502	101	12727	881.6	824
Ranoidea	Genus	Cornufer boulengeri FK 10744	94	12322	889.0	826
Ranoidea	Genus	Cornufer bufoniformis SJR 5475	97	12190	1006.2	971
Ranoidea	Genus	Cornufer cryptotis yapeni RG 7979	146	7935	1032.1	987
Ranoidea	Genus	Cornufer custos ABTC 136625	142	12217	1017.9	964
Ranoidea	Genus	Cornufer exedrus SJR 10784	61	12265	782.1	719
Ranoidea	Genus	Cornufer gilliardi JF 112	144	12400	974.3	942
Ranoidea	Genus	Cornufer guentheri SLT 345	143	14988	889.3	861
Ranoidea	Genus	Cornufer guppyi SLT 679	142	4943	1001.6	976
Ranoidea	Genus	Cornufer hedigeri SLT 710	62	8940	947.1	916
Ranoidea	Genus	Cornufer heffernani 5303 5316	122	12134	881.2	823
Ranoidea	Genus	Cornufer latro SR 2145	124	6006	828.4	790
Ranoidea	Genus	Cornufer magnus 5220 5252	129	12326	879.8	838
Ranoidea	Genus	Cornufer minutus SLT 202	119	8937	801.6	763
Ranoidea	Genus	Cornufer papuensis RG 7373	116	5854	884.6	855
Ranoidea	Genus	Cornufer parkeri CCA 2644	69	5899	814.5	764
Ranoidea	Genus	Cornufer punctatus RG 7970	166	12435	933.2	897
Ranoidea	Genus	Cornufer schmidti CCA 1583	115	5928	887.0	854
Ranoidea	Genus	Cornufer solomonis RMB 6960	186	15024	1206.4	1150
Ranoidea	Genus	Cornufer trossulus SLT 262	144	14170	805.7	749
Ranoidea	Genus	Cornufer vertebralis JLW 343	167	7547	912.0	874
Ranoidea	Genus	Cornufer vitianus CM 1498	78	12371	848.8	793
Ranoidea	Genus	Cornufer weberi SLT 269	139	12594	1054.3	1020
Ranoidea	Genus	Cornufer wuenscheorum RG 7751	108	12181	799.4	746
Reduced	Reduced	Occidozyga sp CDS 2282	255	8032	961.3	817.5
Reduced	Reduced	Occidozyga sp CDS1257	376	8762	1045.2	861
Reduced	Reduced	Occidozyga sp CDS1808	337	12094	1035.8	844

Reduced	Reduced	Occidozyga sp CDS2026	188	20351	1055.6	864
Reduced	Reduced	Occidozyga sp CDS2045	152	12048	1044.3	857
Reduced	Reduced	Occidozyga sp CDS270	379	11986	1080.9	890.5
Reduced	Reduced	Occidozyga sp CDS3582	186	12054	1036.7	829
Reduced	Reduced	Occidozyga sp CDS487	446	8110	1050.5	884
Reduced	Reduced	Occidozyga sp CDS543	251	7344	998.1	861
Reduced	Reduced	Occidozyga sp RMB11020	287	8238	1068.1	908
Reduced	Reduced	Occidozyga sp RMB15467	227	11997	991.8	820
Reduced	Reduced	Occidozyga sp RMB16321	336	12276	1103.0	908
Reduced	Reduced	Occidozyga sp RMB16436	253	12134	1080.2	883
Reduced	Reduced	Occidozyga sp RMB17235	431	12180	1140.9	950
Reduced	Reduced	Occidozyga sp RMB20282	352	12774	1088.1	887
Reduced	Reduced	Occidozyga sp RMB20559	359	12118	1038.5	861
Reduced	Reduced	Occidozyga sp RMB2133	351	12085	1057.8	876
Reduced	Reduced	Occidozyga sp RMB2542	154	11768	945.4	735
Reduced	Reduced	Occidozyga sp RMB3068	297	12079	1095.4	910
Reduced	Reduced	Occidozyga sp RMB3127	215	12132	1056.0	874
Reduced	Reduced	Occidozyga sp RMB4318	242	13443	984.3	847
Reduced	Reduced	Occidozyga sp RMB4468	309	12153	1098.9	906
Reduced	Reduced	Occidozyga sp RMB5396	326	12250	1058.8	874
Reduced	Reduced	Occidozyga sp RMB6117	247	8569	1025.1	865
Reduced	Reduced	Occidozyga sp RMB6411	434	12016	1055.3	868
Reduced	Reduced	Occidozyga sp RMB7686	272	7881	1008.0	871
Reduced	Reduced	Occidozyga sp RMB819	319	12105	1080.2	887
Reduced	Reduced	Occidozyga sp RMB8750	226	12641	1067.0	874
Reduced	Reduced	Occidozyga sp RMB8900	403	12119	1095.2	908
Reduced	Reduced	Occidozyga sp RMB9600	172	12100	1097.2	910
Hyloidea	Superfamily	Allobates femoralis WED 55592	163	9924	852.3	781.5
Hyloidea	Superfamily	Anaryxus woodhousii RMB 19577	73	10914	1019.8	962
Hyloidea	Superfamily	Ansonia sp RMB 10371	180	8799	1103.4	1055
Hyloidea	Superfamily	Barycholos pulcher LAC 692	122	11654	1014.0	954
Hyloidea	Superfamily	Bolitaglossa palmata LAC 1154	88	3642	762.6	720
Hyloidea	Superfamily	Bufo valliceps KU 203846	100	8605	1244.2	1178
Hyloidea	Superfamily	Ceratophrys cornuta WED 57689	84	10112	1054.4	994
Hyloidea	Superfamily	Craugastor rupinius JES 2401	167	8343	1135.3	1058
Hyloidea	Superfamily	Dendrobates histrionicus LAC 2539	120	8204	851.2	788
Hyloidea	Superfamily	Eluetherodactylus sp GLOR 6202	139	11649	1163.2	1102
Hyloidea	Superfamily	Gastrotheca marsupiata WED 58521	108	7923	865.5	800
Hyloidea	Superfamily	Hyalinobatrachium fleischmanni MZUTI 3621	201	8343	1059.0	989
Hyloidea	Superfamily	Hyloscirtus phyllognathus WED 58378	98	13871	1058.8	1006

Hyloidea	Superfamily	Leptobrachium hainensis KUFS 194	104	6717	828.8	785
Hyloidea	Superfamily	Leptodactylus pentadactylus WED 55494	79	16967	1078.1	1029
Hyloidea	Superfamily	Nyctimystes infrafrenatus SLT 771	83	11291	1105.6	1047
Hyloidea	Superfamily	Oreobates quizensis WED 59885	112	8416	913.2	842
Hyloidea	Superfamily	Phyrnohyas venulosa WED 55450	157	9389	1081.0	1023
Hyloidea	Superfamily	Physalamus pustulatus LAC 1642	102	7745	1033.5	982
Hyloidea	Superfamily	Pristimantis w-nigrum WED 53045	107	11463	1101.7	1040
Hyloidea	Superfamily	Spea bombifrons RMB 19586	88	7441	1067.5	1016
Hyloidea	Superfamily	Strabomantis sulcatus LAC 841	121	8466	1002.3	931
Hyloidea	Superfamily	Telmatobius truebae WED 56933	195	8743	1282.1	1226
Hyloidea	Superfamily	Vitreorana castroviejoi JMG 33	78	8044	1059.6	999

Figure S1. The samples and their associated collection ID

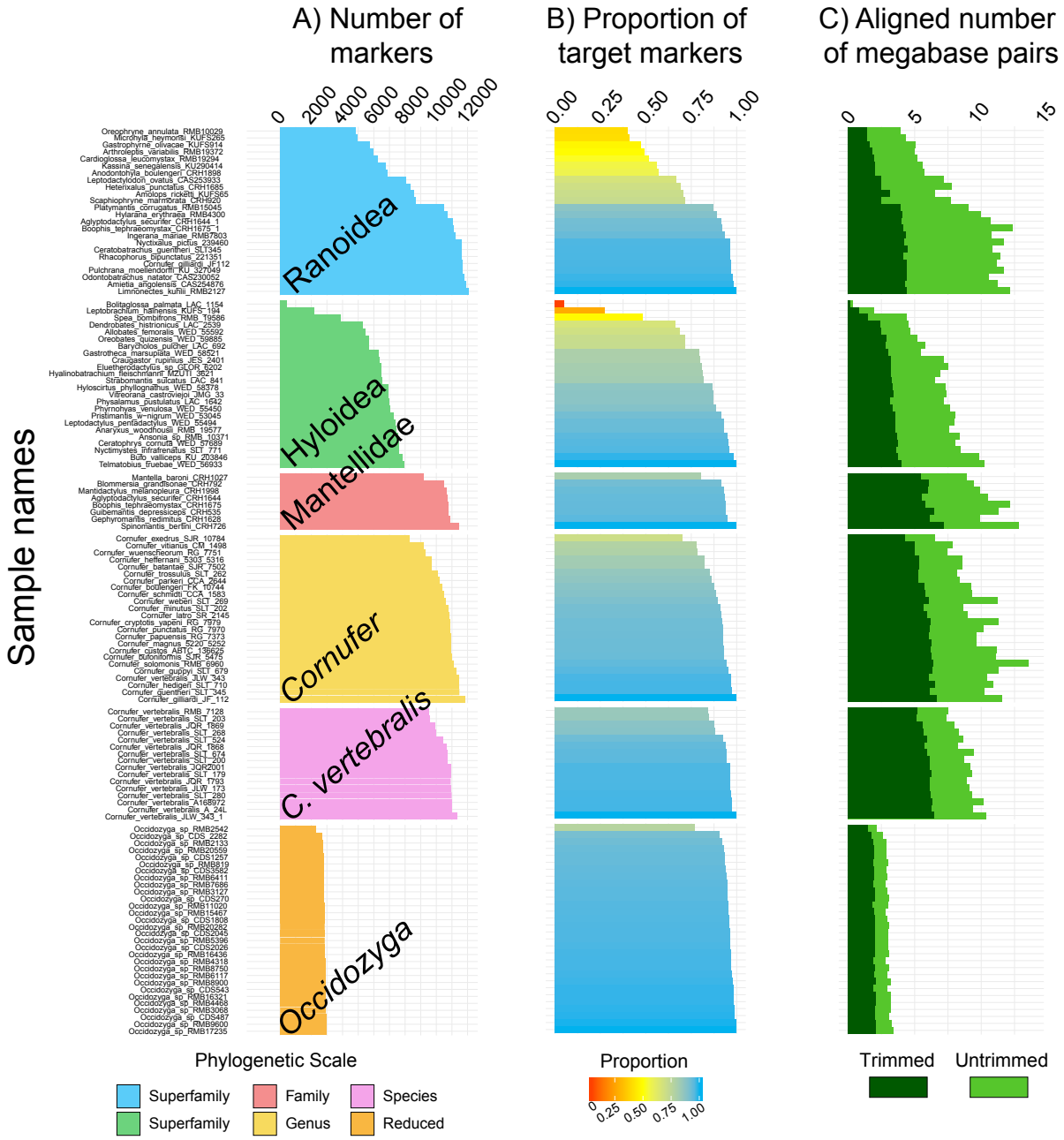

Appendix IV.

From:

CHAPTER 4

Transcriptomes or sequence capture for phylogenomics? A comparison of their efficacy and gene tree discordance in the frog family Mantellidae from Madagascar

Carl R. Hutter, Iker Irisarri, Loïs Rancilhac, Frank Glaw, Walter Cocca, Angelica Crottini, Sven Künzel, Andolalao Rakotoarison, Mark Scherz, Hervé Philippe, Miguel Vences; unpublished

Table S1 part 1. The samples and their associated collection ID used in this study are shown. Each samples' summary statistics are shown, where orthologs and paralogs are discovered during probe matching. The length statistics are calculated from the orthologous contigs.

Sample	N contigs	N orthologs	N paralogs
Aglyptodactylus securifer CRH1644	12255	11069	599
Blommersia grandisonae CRH792	12622	10667	976
Boehmantis microtympanum FGZC132	13212	11928	619
Boophis tephraeomystax CRH1675	14596	11663	559
Gephyromantis redimitus CRH1628	14217	11349	976
Guibemantis depressiceps CRH535	12810	11171	622
Laliostoma labrosum ZCMV5617	12516	10571	1657
Mantella baroni CRH1027	13364	10755	495
Mantidactylus melanopleura CRH1998	12634	11079	857
Spinomantis aglavei JJW2354	14500	11737	633
Tsingymantis antitra FGZC1128	12307	11519	616
Wakea madinika 2001F54	10967	10208	427

Table S1 part 2. The samples and their associated collection ID used in this study are shown. Each samples' summary statistics are shown, where orthologs and paralogs are discovered during probe matching. The length statistics are calculated from the orthologous contigs.

Sample	Min length	Max length	Mean length	Median length
Aglyptodactylus securifer CRH1644	76	12593	945.6	901
Blommersia grandisonae CRH792	129	5911	886.7	846
Boehmantis microtympanum FGZC132	127	23479	938.7	906
Boophis tephraeomystax CRH1675	104	12154	1101.1	1055
Gephyromantis redimitus CRH1628	70	23642	916.4	873
Guibemantis depressiceps CRH535	115	10271	1049.7	1006
Laliostoma labrosum ZCMV5617	103	7750	857.2	822
Mantella baroni CRH1027	88	7139	983.1	939
Mantidactylus melanopleura CRH1998	101	16666	935.0	900
Spinomantis aglavei JJW2354	111	12320	871.2	835
Tsingymantis antitra FGZC1128	103	10827	874.3	844
Wakea madinika 2001F54	125	7245	840.0	805

Appendix V.

From:

CHAPTER 5

Environmental acoustic interference from loud streams drives the evolution of higher frequency signals in Malagasy tree frogs (Mantellidae: *Boophis*)

Carl R. Hutter, Daniel Paluh, Frank Glaw, Miguel Vences; not yet published

Table S1. Acoustic data measured from *Boophis* recorded in the field is shown. The mean DF is the mean dominant frequency across all individuals recorded in the genus, while the lower and higher DF represent the minimum and maximum bounds of the dominant frequency used to measure frequency bandwidth. The abbreviation BW indicates the Bandwidth.

Species	Mean DF	Lower DF	Higher DF	BW	Hutter samples	Vences samples	Total samples	N calls
Boophis vittatus	7791	7500	8250	2000		2	2	213
Boophis jaegeri	4300	3000	7000	4000		1	1	146
Boophis sp Ca46 Vohimana	6000	5250	6750	1500	2		2	20
Boophis feonnyala	4800	3450	5550	2200		2	2	57
Boophis liami	5460	5300	6400	1700	6	1	7	31
Boophis ulftunni	5800	5200	6400	1200		3	3	13
Boophis solomaso	5700	5600	6350	550	7	1	8	27
Boophis marojezensis	5172	5122	6250	1550		1	1	34
Boophis tasymena	5400	5200	6100	2400	9	2	11	33
Boophis sp CaNew Vohidrazana	5857	5340	6029	689	7		7	34
Boophis sp Ca62NEW	5776	5600	5951	352	3		3	43
Boophis lilianae	5700	5600	5800	200	3		3	29
Boophis haematopus	4505	3600	5000	2100		1	1	25
Boophis sp Ca38 Ranomafana	5600	5500	5700	200	10		10	12
Boophis sp Ca60NEW	5259	4867	5650	784	3		3	23
Boophis sp Ca07 Marojejy	5081	4737	5512	775		1	1	98
Boophis sp Ca51 Ranomafana	5340	4823	5512	689	12		12	34
Boophis picturatus	4400	3900	5500	1900	5	1	6	42
Boophis sp CaNew Andasibe	5250	4875	5437	563	3		3	45
Boophis sp Ca56NEW	5278	5122	5434	312	3		3	12
Boophis miniatus	4399	3200	5350	2150		1	1	84
Boophis mandraka	4800	4000	5300	1300	2	1	3	12
Boophis piperatus	4450	2870	5300	2500		2	2	126
Boophis pyrrhus	4080	4022	5300	1800	7	2	9	23
Boophis blommersae	4770	4450	5200	750		2	2	10
Boophis sp CaNEW Vohidrazana	4875	4312	5062	750	1		1	23
Boophis arcanus	4000	3000	5000	2000		1	1	12
Boophis andohahela	4500	3600	4900	1300	1	1	2	13
Boophis bottae	4300	4100	4900	1300	2	3	5	58
Boophis sambirano	4150	4100	4800	900		1	1	14
Boophis sp Ca25 Marojejy	4750	4700	4800	100	3		3	23
Boophis sp Ca28 Marojejy	4475	4400	4550	150	2		2	11
Boophis sp Ca47 Ranomafana	4392	4100	4514	415	6		6	2
Boophis andreonei	4100	4000	4500	500		2	2	24

Boophis anjanaharibeensis	3750	3000	4500	1500	2	1	3	2
Boophis englaenderi	4000	3378	4500	1000	2	2	4	45
Boophis luciae	3127	3600	4500	1500	6	2	8	122
Boophis ankarafensis	4155	4000	4310	310		1	1	8
Boophis aff picturatus	3963	3617	4306	689	3	1	4	1
Boophis majori	3483	3200	4050	1350	6	2	8	102
Boophis doulioti	3130	3100	4000	3000		2	2	150
Boophis baetkei	3500	3100	3900	800		1	1	3
Boophis schuboeae	3300	3350	3900	1050	2	1	3	105
Boophis entingae	2253	2100	3800	2000	4	1	5	14
Boophis tampoka	3446	3000	3800	800		1	1	3
Boophis septentrionalis	3400	3000	3700	1200	2	2	4	164
Boophis burgeri	2212	1750	3500	1750	3	2	5	10
Boophis erythrodactylus	2800	2800	3500	1650	12	2	14	75
Boophis rappiodes	2900	2800	3500	1000	4	1	5	11
Boophis ankaratra	2800	1750	3400	1650	7	3	10	54
Boophis boehmei	2681	2500	3400	1400	6	2	8	22
Boophis nautilus	1800	1200	3400	2200		1	1	2
Boophis sibilans	3000	2700	3400	800	2	1	3	95
Boophis sp CaNew Tavalobe	2812	2250	3375	1125	4		4	23
Boophis tephraeomystax	3445	3014	3359	3400		2	2	45
Boophis boppa	3100	2800	3359	559	14	2	16	13
Boophis microtympanum	2567	2507	3350	1800		1	1	12
Boophis luteus	3000	3000	3300	600		2	2	403
Boophis viridis	2900	2899	3222	1150		2	2	77
Boophis brachychir	2750	2600	3100	600		3	3	45
Boophis sp Ca33 Andringitra Antoetra	2500	1800	3100	1300		1	1	20
Boophis rhodoscelis	2700	2490	3060	2200	2	2	4	231
Boophis albipunctatus	2700	2000	3000	1000		1	1	9
Boophis andrangoloaka	2473	1750	3000	1250		2	2	15
Boophis axelmeyeri	2073	1500	3000	1500		1	1	2
Boophis laurenti	2600	2600	3000	1200		1	1	10
Boophis narinsi	2970	2900	3000	3000	2		2	37
Boophis sandrae	2920	2870	2970	100	3	2	5	861
Boophis sp CaNEW Elenae	2756	2584	2928	345	5		5	234
Boophis miadana	2700	2720	2900	700		2	2	96
Boophis sp Ca10 Ambolokopatrika	2850	2800	2900	100		1	1	15
Boophis haingana	2800	2680	2880	100		2	2	200
Boophis popi	2120	2100	2850	1100	1	1	2	5
Boophis pauliani	2700	2600	2800	200		1	1	18

Boophis quasiboehmei	2774	2600	2800	1800	4	1	5	4
Boophis sp CaNew Anjaraharibe	2411	1894	2756	861	5		5	26
Boophis elenae	2700	2510	2705	900	5	1	6	115
Boophis reticulatus	2635	2600	2700	1600	4	2	6	49
Boophis xerophilus	2619	2400	2600	400		2	2	74
Boophis rufioculis	2466	2100	2500	3100		1	1	14
Boophis sp Ca37 Andasibe	2600	1600	2500	900	3	1	4	53
Boophis aff reticulatus	2062	1687	2437	750	3		3	8
Boophis fayi	2075	1950	2200	250		2	2	9
Boophis calcaratus	1375	750	2000	1250		2	2	34
Boophis idae	1937	1750	2000	1250		2	2	92
Boophis lichenoides	1120	900	2000	3400		1	1	57
Boophis opisthodon	1800	1000	1800	1500		1	1	21
Boophis sp Ca42 Ranomafana	1312	937	1687	750	5		5	3
Boophis pereigetes	1371	1320	1510	1800	1	3	4	149
Boophis goudotii	707	700	1300	2000		2	2	287
Boophis guibei	1060	1000	1200	2800		3	3	113
Boophis tsilomaro	1100	1000	1200	1100		2	2	3
Boophis albilabris	750	700	947	3000		2	2	38
Boophis obscurus	915	550	915	1900		1	1	34
Boophis madagascariensis	866	800	900	2400		1	1	58
Boophis occidentalis	655	560	750	190		2	2	311

Table S2. Measurements from Diffusible Iodine-based Contrast-enhanced Computed Tomography (DiceCT) for each specimen is shown. The SVL is the snout-vent length of the specimen, while the remaining measures were measured from the larynges of specimens. The abbreviations PO and AO indicate the posterior and anterior openings, respectively.

Species	KU#	Field#	SVL	Height	Width	Length	PO	AO
Boophis boppa	KU336825	CRH180	18.35	2.44	1.63	1.75	1.04	0.3
Boophis majori	KU336856	CRH128	23.83	2.07	1.99	2.68	1.14	0.31
Boophis aff picturatus	KU336861	CRH97	20.01	2.43	1.78	1.82	1.23	0.31
Boophis rhodoscelis	KU336865	CRH2372	26.97	2.43	1.81	2.24	1.26	0.2
Boophis sp Ca38 Ranomafana	KU336892	CRH004	24.15	2.87	2.54	1.84	1.27	0.31
Boophis luteus	KU340633	CRH264	35.61	2.03	1.41	2.89	1.03	0.13
Boophis bottae	KU340699	CRH386	23.62	2.26	1.66	1.91	1.13	0.13
Boophis sp CaNEW Elenae	KU340718	CRH427	35.38	2.51	1.69	2.72	1.07	0.29
Boophis sp Ca42 Ranomafana	KU340729	CRH453	56.12	3.49	2.68	3.81	1.59	0.78
Boophis sp Ca51 Ranomafana	KU340730	CRH455	23.39	3.08	2.42	2.24	1.29	0.14
Boophis lilianae	KU340865	CRH749	21.74	1.9	1.42	2.13	0.88	0.21
Boophis guibei	KU342885	CRH1193	38.6	1.85	2.17	2.32	1.52	0.43
Boophis sp CaNew Vohidrazana	KU342894	CRH989	25.9	2.58	2.29	2.29	1.44	0.1
Boophis sp CaNew Andasibe	KU342939	CRH971	22.27	1.07	0.89	1.32	0.51	0.1
Boophis sp CaNEW Vohidrazana	KU342970	CRH1097	21.5	2.88	1.96	1.95	1.12	0.36
Boophis picturatus	KU342989	CRH1297	28.05	2.08	1.95	2.3	1.34	0.37
Boophis pyrrhus	KU343021	CRH1179	27.04	2.22	1.93	2.79	1.3	0.29
Boophis sp Ca37 Andasibe	KU343036	CRH1023	40.62	2.47	3.26	3.05	1.41	0.55
Boophis solomaso	KU343065	CRH1382	23.17	2.54	1.95	2.01	0.97	0.4
Boophis sp Ca07 Marojejy	KU347240	CRH1691	46.4	3.26	3.09	5.32	2.26	0.6
Boophis sp Ca46 Vohimana	KU347259	CRH2059	22.7	2.15	2.01	2.4	1.21	0.11
Boophis anjanaharibeensis	KU347263	CRH1572	33.73	2.42	1.68	2.73	1.12	0.65
Boophis sp CaNew Anjaraharibe	KU347268	CRH1753	31	2.22	2.43	2.53	1.66	0.2
Boophis entingae	KU347278	CRH1601	55.44	3.9	2.83	3.95	1.71	0.6
Boophis erythrodactylus	KU347280	CRH1908	22.65	2.47	1.83	2.1	1.03	0.11
Boophis tasymena	KU347318	CRH1909	17.25	0.7	0.87	0.85	0.46	0.09
Boophis tephraeomystax	KU347320	CRH1675	43.01	1.93	2.12	3.48	1.54	0.58

Table S3 part 1. The samples and their associated collection ID used in this study are shown. Each samples' summary statistics are shown, where orthologs and paralogs are discovered during probe matching. The length statistics are calculated from the orthologous contigs.

Sample	N contigs	N orthologs	N paralogs
Aglyptodactylus securifer CRH1644	11613	10814	401
Amnirana sp C70 057	11236	9113	247
Amolops ricketti KUFS65	9527	8618	322
Blommersia blommersae CRH523	11978	10792	809
Boehmantis microtympanum FGZC132	12977	11847	559
Boophis aff marojezensis CRH1932	17618	11154	382
Boophis aff williamsi CRH060	13285	11150	276
Boophis albilabris CRH1862	13201	11058	781
Boophis andohahela CRH0491	14342	11069	966
Boophis anjanaharibeensis CRH1572	14228	11369	350
Boophis ankaratra CRH1811	15169	10590	399
Boophis baetkei FGZC 1391	13708	11155	211
Boophis blommersae FGZC 0421	14313	11773	248
Boophis boehmei CRH1753	13876	11017	613
Boophis aff brachychir CRH453	12873	11363	404
Boophis burgeri CRH461	11849	10856	247
Boophis douloti ZCMV 5607	13352	11543	338
Boophis entingae CRH1601	13178	11693	264
Boophis aff majori CRH1087	12283	11170	183
Boophis liami CRH0271	14598	11523	395
Boophis lichenoides CRH1643	13579	10426	377
Boophis lilianae CRH0750	13612	11319	325
Boophis luciae CRH0814	17864	10891	217
Boophis luteus CRH1830	14364	11079	967
Boophis madagascariensis CRH1295	13168	11509	624
Boophis majori CRH0828	15004	9988	139
Boophis maosala FGZC 5428	14048	10069	140
Boophis microtympanum ZCMV 988	13984	10029	146
Boophis nautilus MV2000F50	18752	11330	182
Boophis opistodon ZCMV462	17006	10906	190
Boophis pauliani CRH926	16838	10776	168
Boophis pereigetes CRH065	15620	10515	171
Boophis praedictus ZCMV678	13684	10468	186
Boophis pyrrhus CRH1176	12917	10065	320
Boophis rhodoscelis CRH863	16362	10720	404

Boophis solomaso CRH0988	14336	11023	404
Boophis solomaso CRH1102	11835	10381	287
Boophis tasymena CRH1714	12505	10456	385
Boophis tephraeomystax CRH1675	14292	11285	410
Boophis ulftunni FGZC 2879	13095	10204	197
Boophis viridis CRH0392	13905	10692	178
Boophis vittatus ZCMV 842	14233	10852	171
Boophis williamsi MV 2001G62	13660	10470	128
Buergeria oxycephalus MVZ241443	17202	12122	336
Gephyromantis redimitus CRH1628	14087	11511	936
Guibemantis depressiceps CRH535	13268	11110	696
Laliostoma labrosum ZCMV5617	12066	11134	825
Mantella crocea DSM1076	14532	11199	512
Mantidactylus melanopleura CRH1998	12036	11092	513
Nyctixalus pictus KU239460	14308	11734	590
Pulchrana moellendorffi KU327049	18062	11808	906
*Rhacophorus bipunctatus KU*221351	16015	11762	786
Spinomantis bertini CRH726	13448	11941	586
Tsingymantis antitra FGZC1128	12180	11517	599
Wakea madinika 2001F54	10891	10047	490

Table S3 part 2. The samples and their associated collection ID used in this study are shown. Each samples' summary statistics are shown, where orthologs and paralogs are discovered during probe matching. The length statistics are calculated from the orthologous contigs.

Sample	Min length	Max length	Mean length	Median length
Aglyptodactylus securifer CRH1644	68	12498	972.9	945
Amnirana sp C70 057	65	12014	772.4	709
Amolops ricketti KUFS65	97	12583	768.2	700
Blommersia blommersae CRH523	67	12555	954.7	908
Boehmantis microtympanum FGZC132	113	12363	923.4	893
Boophis aff marojezensis CRH1932	105	11609	1012.1	975
Boophis aff williamsi CRH060	112	10191	799.1	756
Boophis albilabris CRH1862	122	7235	1026.3	989
Boophis andohahela CRH0491	105	9447	838.1	811
Boophis anjanaharibeensis CRH1572	103	7685	853.4	827
Boophis ankaratra CRH1811	71	9496	1079.1	1045
Boophis baetkei FGZC 1391	90	12149	860.1	823
Boophis blommersae FGZC 0421	97	12329	894.4	854
Boophis boehmei CRH1753	100	8848	777.1	751
Boophis aff brachychir CRH453	112	7685	831.3	804
Boophis burgeri CRH461	93	12119	796.2	752
Boophis douloti ZCMV 5607	101	12146	868.9	835
Boophis entingae CRH1601	83	9036	898.3	873
Boophis aff majori CRH1087	74	12071	832.4	794
Boophis liami CRH0271	97	7192	846.1	826
Boophis lichenoides CRH1643	77	12415	929.9	882
Boophis lilianae CRH0750	105	12150	821.0	782
Boophis luciae CRH0814	102	7674	785.2	749
Boophis luteus CRH1830	126	4584	819.2	778
Boophis madagascariensis CRH1295	92	5397	851.1	827
Boophis majori CRH0828	76	7457	767.9	724
Boophis maosala FGZC 5428	113	12234	845.7	794
Boophis microtympanum ZCMV 988	77	12060	830.7	774
Boophis nautilus MV2000F50	102	12616	934.4	892.5
Boophis opistodon ZCMV462	62	11944	862.8	810
Boophis pauliani CRH926	73	25265	906.9	851
Boophis pereigetes CRH065	94	12054	856.3	797
Boophis praedictus ZCMV678	100	12113	875.1	832
Boophis pyrrhus CRH1176	71	12638	1062.5	1017
Boophis rhodoscelis CRH863	77	13226	1102.0	1053

Boophis solomaso CRH0988	74	5655	743.3	716
Boophis solomaso CRH1102	97	7266	815.3	783
Boophis tasymena CRH1714	104	12413	1128.4	1095.5
Boophis tephraeomystax CRH1675	112	15998	1107.6	1078
Boophis ulftunni FGZC 2879	85	12134	797.0	737
Boophis viridis CRH0392	72	12121	826.3	775
Boophis vittatus ZCMV 842	81	17264	827.8	773
Boophis williamsi MV 2001G62	112	12239	849.7	800
Buergeria oxycephalus MVZ241443	104	9629	927.7	901
Gephyromantis redimitus CRH1628	89	5601	920.3	894
Guibemantis depressiceps CRH535	105	7867	1003.1	967
Laliostoma labrosum ZCMV5617	101	12246	903.8	874
Mantella crocea DSM1076	107	8029	831.9	801
Mantidactylus melanopleura CRH1998	115	7414	952.1	911
Nyctixalus pictus KU239460	60	8305	1000.7	961
Pulchrana moellendorffi KU327049	129	12633	996.5	969
*Rhacophorus bipunctatus KU*221351	91	9515	981.8	946
Spinomantis bertini CRH726	128	12744	1104.8	1083
Tsingymantis antitra FGZC1128	103	6787	867.4	838
Wakea madinika 2001F54	104	5010	828.9	794

Figure S1. An example oscillogram and spectrogram and the measurements taken. The frequencies shown in B were used in analyses.

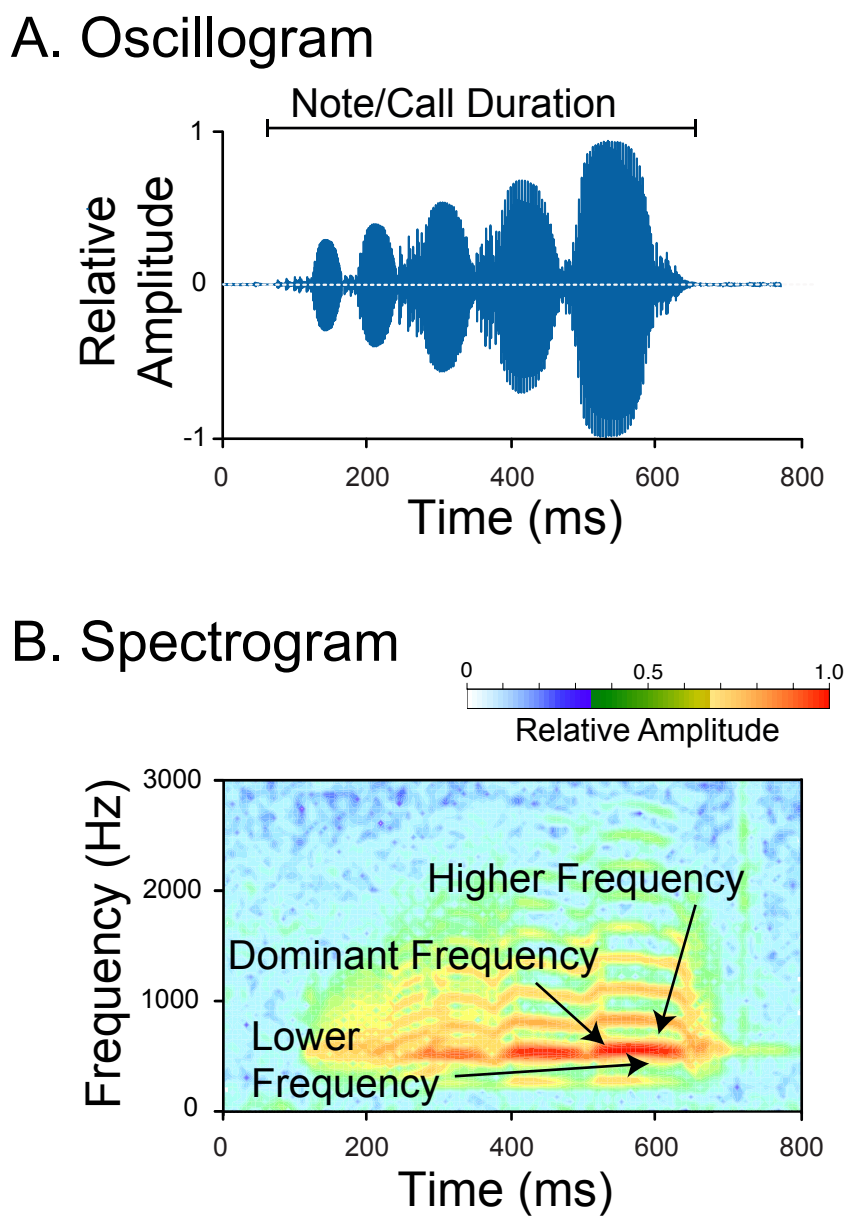

Figure S2. Extracted larynx and the measurements taken. The measurements were next combined into a principal component analysis where the first PC axis was used for analyses.

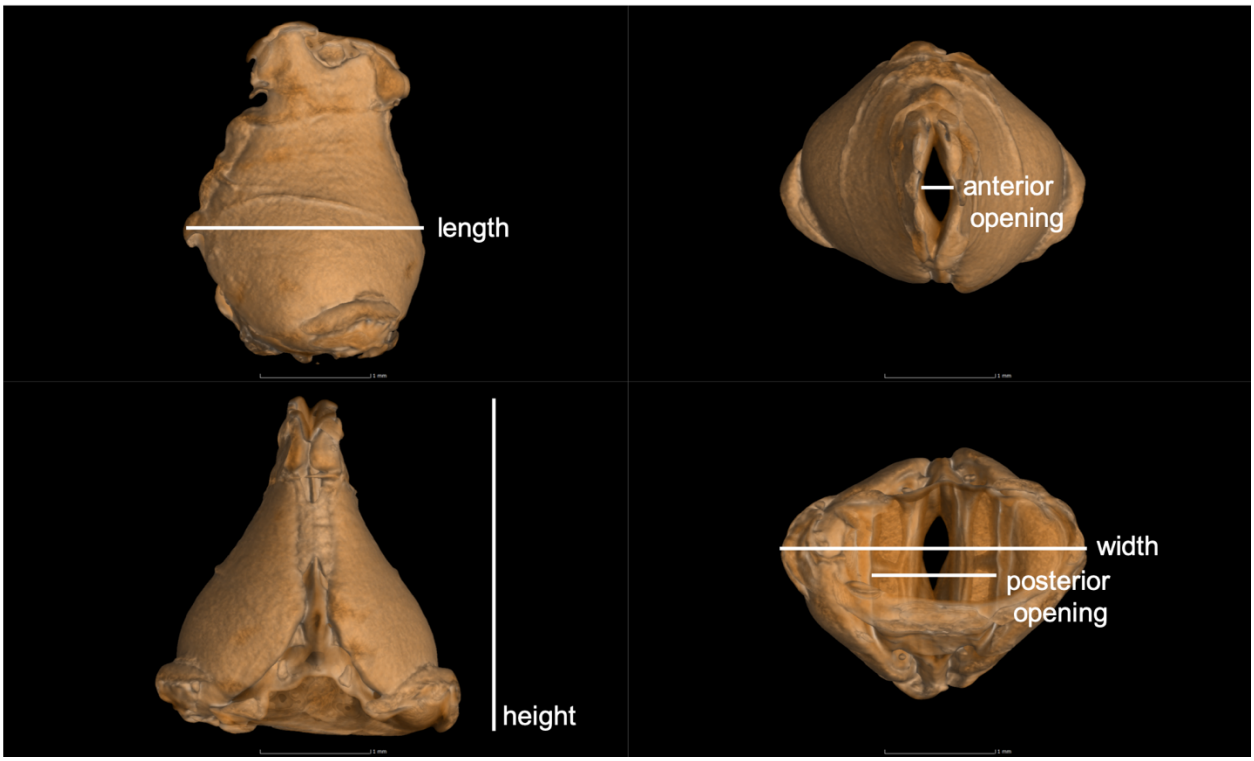

Figure S3. MCMCTree preferred analysis that includes the 95% confidence intervals for each node.

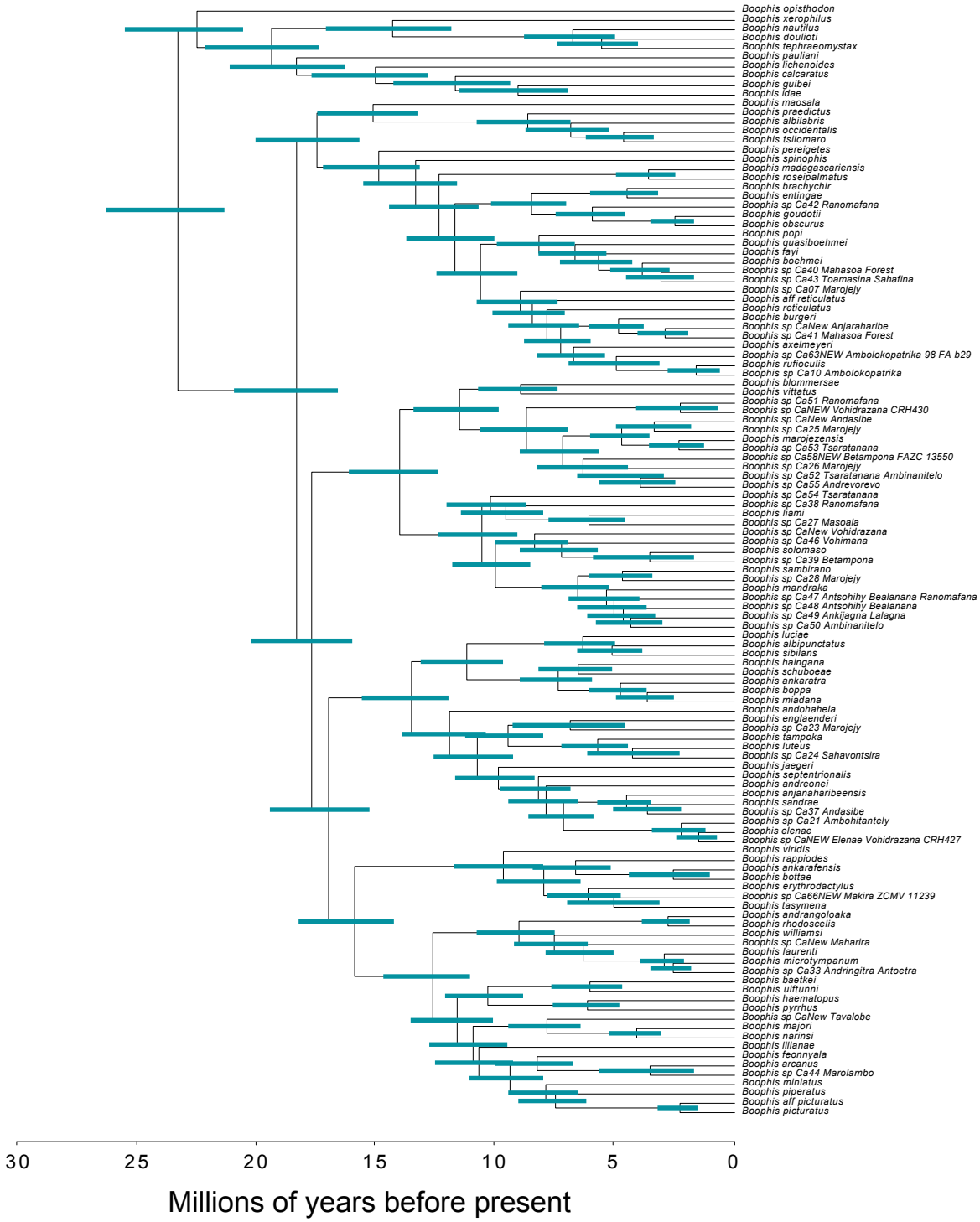

Figure S4. Comparison of larynx size variation in loud stream CT scanned specimens. Specimens are scaled to their relative body sizes.